
Adaptive Model Predictive Control of Renewable Energy-Based Micro-grid



UNIVERSITY OF
KWAZULU-NATAL
INYUVESI
YAKWAZULU-NATALI

By:

Peter Anuoluwapo Gbadega (BScEng [UNILAG], MScEng [UKZN])

217071302

Supervised by:

Professor Akshay Kumar Saha

A doctoral research thesis submitted in fulfilment of the
requirements for the degree of

DOCTOR OF PHILOSOPHY IN ENGINEERING (PhD)
(ELECTRICAL ENGINEERING)

Discipline of Electrical, Electronic and Computer Engineering,

School of Engineering, Howard College Campus,

College of Agriculture, Engineering and Science,

University of KwaZulu-Natal, Durban, South Africa

25th March, 2021

CERTIFICATION

As the candidate's Supervisor, I agree to the submission of this thesis.

Signed: **Professor Akshay Kumar Saha.**

Date: **25th March 2021**

DECLARATION 1 - PLAGIARISM

I, **Peter Anuoluwapo Gbadega**, with Student Number 217071302, with the thesis entitled “Adaptive Model Predictive Control of a Renewable Energy-Based Micro-grid,” declare that:

1. The research reported in this thesis, except where otherwise indicated, is my original research.
2. This thesis has not been submitted for any degree or examination at any other university.
3. This thesis does not contain other persons’ data, pictures, graphs or other information, unless specifically acknowledged as being sourced from other persons.
4. This thesis does not contain other persons' writing, unless specifically acknowledged as being sourced from other researchers. Where other written sources have been quoted, then:
 - a. Their words have been re-written but the general information attributed to them has been referenced
 - b. Where their exact words have been used, then their writing has been placed in italics and inside quotation marks, and referenced.
5. This thesis does not contain texts, graphics or tables copied and pasted from the internet, unless specifically acknowledged, and the source being detailed in the thesis and in the reference section.

Signed: **Peter. A Gbadega**

Date: **25th March 2021**

DECLARATION 2 - PUBLICATIONS

DETAILS OF CONTRIBUTION TO PUBLICATIONS AND CONFERENCE PRESENTATIONS that form part and/or include research presented in this thesis (include publications in preparation, submitted, *in press* and published and give details of the contributions of each author to the experimental work and writing of each publication).

The following articles stemming from this research work have either been published or accepted for publication (in press):

ISI/SCOPUS/DoHET Accredited Journals and Conferences

Publication 1

P. A. Gbadega and A. K. Saha, "Impact of Incorporating Disturbance Prediction on the Performance of Energy Management Systems in Micro-Grid," in IEEE Access, vol. 8, pp. 162855-162879, 2020, doi: 10.1109/ACCESS.2020.3021598. **Status: (Published)**

Publication 2

P. A. Gbadega and A. K. Saha, "Load Frequency Control of a Two-Area Power System with a Stand-Alone Micro-grid based on Adaptive Model Predictive Control," in IEEE Journal of Emerging and Selected Topics in Power Electronics, doi: 10.1109/JESTPE.2020.3012659. **Status: (Published)**

Publication 3

Gbadega, Peter Anuoluwapo, and Akshay Kumar Saha. "Model Predictive Controller Design of a Wavelength-Based Thermo-Electrical Model of a Photovoltaic (PV) Module for Optimal Output Power." International Journal of Engineering Research in Africa, vol. 48, Trans Tech Publications, Ltd., May 2020, pp. 133–148. Crossref, doi:10.4028/www.scientific.net/jera.48.133. **Status: (Published)**

Publication 4

Gbadega, Peter Anuoluwapo, and Akshay Kumar Saha. "Dynamic Tuning of the Controller Parameters in a Two-Area Multi-Source Power System for Optimal Load Frequency Control Performance." International Journal of Engineering Research in Africa, vol. 51, Trans Tech Publications, Ltd., Nov. 2020, pp. 111–129. Crossref, doi:10.4028/www.scientific.net/jera.51.111. **Status: (Published)**

Publication 5

P. A. Gbadega and A. K. Saha, "Adaptive Model-Based Receding Horizon Control of Interconnected Renewable-Based Power Micro-grids for Effective Control and Optimal Power Exchanges," 2020 International SAUPEC/RobMech/PRASA Conference, Cape Town, South Africa, 2020, pp. 1-6, doi: 10.1109/SAUPEC/RobMech/PRASA48453.2020.9041136. **Status: (Published)**

Publication 6

P. A. Gbadega and A. K. Saha, "Electrical Characteristics Improvement of Photovoltaic Modules Using Two-Diode Model and its Application Under Mismatch Conditions," 2019 Southern African Universities Power Engineering Conference/Robotics and Mechatronics/Pattern Recognition Association of South Africa (SAUPEC/RobMech/PRASA), Bloemfontein, South Africa, 2019, pp. 328-333, doi: 10.1109/RoboMech.2019.8704846. **Status: (Published)**

Publication 7

P. A. Gbadega and A. K. Saha, "Effects and Performance Indicators Evaluation of PV Array Topologies on PV Systems Operation Under Partial Shading Conditions," 2019 Southern African Universities Power Engineering Conference/Robotics and Mechatronics/Pattern Recognition Association of South Africa (SAUPEC/RobMech/PRASA), Bloemfontein, South Africa, 2019, pp. 322-327, doi:10.1109/RoboMech.2019.8704823. **Status: (Published)**

The candidate is the main and corresponding author respectively for all the publications and conference presentations whilst Professor Akshay Kumar Saha is the co-author and my research supervisor. All the sections of the aforementioned publications are the original research works of Mr. Peter Anuoluwapo Gbadega. Professor Akshay Kumar Saha provided adequate guidance in various sections of the research works, which brings the research publications to fruition.

ACKNOWLEDGEMENTS

I want to give all the glory to God for the gift of life and the strength granted to me in the course of this research and for making it a possibility. Most importantly, I thank God Almighty for giving me the strength to overcome the challenges I faced, and for blessing me in ways that is beyond my imagination.

I would also like to appreciate my supervisor the person of Professor Akshay Kumar Saha, for all his contributions, supports and for his prompt reply to my mails. I cannot imagine the success of this degree without his inputs. His criticism and scrutiny have thus helped me a lot. You did turn a better person out of me through your generous support and guidance.

My sincere appreciation goes to National Research Foundation (NRF) South Africa for the NRF block grant award. This bursary went a long way in the provision of adequate support to this doctoral programme.

I would also like to express my beloved gratitude to my parents Late Mr. Sunday Michael Gbadega and Mrs. Elizabeth Gbadega (nee Olorunshola) for their advice, encouragement and prayers throughout my study period. My profound gratitude also goes to my siblings: Mr. Emmanuel, Mr. Samuel, Mrs. Deborah Oyedele (nee Gbadega), Miss Favour and little Mr. Jomiloju for their relentless supports.

I would also appreciate the person of Dr. Awogbemi Omojola for his motivations, encouragement and support throughout my stay here in South Africa, may God raise help for you in all your endeavors.

I would also show my profound gratitude to the person of Dr. Babatunde Olubayo Moses, who was encouraging and mentoring me on what is expected of me as a researcher, I really do appreciate his relentless efforts throughout the tenure of this research work.

I am truly indebted to my lovely wife (Mrs. Olufunke Abolaji Gbadega (nee Balogun)) for her encouragement, support and prayers. I will be eternally grateful to my wonderful wife for her incredible patience and cooperation while I was away most of the times throughout the duration of this research.

I cannot forget in a haste the support and prayers from Late Pastor Abiola Henry Ishola and Mrs. Folakemi Ishola (nee Osikoya) and the entire family of Osikoya for their immense supports.

I also wish to express my heartfelt appreciation to my father-in-law (Mr. Olubunmi Balogun), mother in-law (Late Mrs. Olufunmilayo Balogun (nee Osikoya)), brother-in-laws (Mr. Olukayode and Mr. Olubodun Balogun, and Mr. Olanrewaju Oyedele) and sister-in-law (Yetunde Balogun).

Space will not permit me to start mentioning names of everyone who helped make the study and my stay at UKZN a success. I owe you all my gratitude.

ABSTRACT

Energy sector is facing a shift from a fossil-fuel energy system to a modern energy system focused on renewable energy and electric transport systems. New control algorithms are required to deal with the intermittent, stochastic, and distributed nature of the generation and with the new patterns of consumption. Firstly, this study proposes an adaptive model-based receding horizon control technique to address the issues associated with the energy management system (EMS) in micro-grid operations. The essential objective of the EMS is to balance power generation and demand through energy storage for optimal operation of the renewable energy-based micro-grid. At each sampling point, the proposed control system compares the expected power produced by the renewable generators with the expected load demand and determines the scheduling of the different energy storage devices and generators for the next few hours. The control technique solves the optimization problem in order to minimize or determines the minimum running cost of the overall micro-grid operations, while satisfying the demand and taking into account technical and physical constraints. Micro-grid, as any other systems are subject to disturbances during their normal operation. Hence, the power generated by the renewable energy sources (RESs) and the demanded power are the main disturbances acting on the micro-grid. As renewable sources are used for the generation, their time-varying nature, their difficulty in predicting, and their lack of ability to manipulate make them a problem for the control system to solve. In view of this, the study investigates the impacts of considering the prediction of disturbances on the performance of the energy management system (EMS) based on the adaptive model predictive control (AMPC) algorithm in order to improve the operating costs of the micro-grid with hybrid-energy storage systems. Furthermore, adequate management of loads and electric vehicle (EV) charging can help enhance the micro-grid operation. This study also introduced the concept of demand-side management (DSM), which allows the customers to make decisions regarding their energy consumption and also help to reduce the peak load demand and to reshape the load profile so as to improve the efficiency of the system, environmental impacts, and reduction in the overall operational costs. More so, the intermittent nature of renewable energy and consumer random behavior introduces a stochastic component to the problem of control. Therefore, in order to solve this problem, this study utilizes an AMPC control technique, which provides some robustness to the control of systems with uncertainties. Lastly, the performances of the micro-grids used as a case study are evaluated through simulation modeling, implemented in MATLAB/Simulink environment, and the simulation results show the accuracy and efficiency of the proposed control technique. More so, the results also show how the AMPC can adapt to various generation scenarios, providing an optimal solution to power-sharing among the distributed energy resources (DERs) and taking into consideration both the physical and operational constraints and similarly, the optimization of the imposed operational criteria.

TABLE OF CONTENTS

CERTIFICATION	i
DECLARATION 1 - PLAGIARISM	ii
DECLARATION 2 - PUBLICATIONS	iii
ACKNOWLEDGEMENTS	v
ABSTRACT	vi
TABLE OF CONTENTS	vii
LIST OF FIGURES	xiii
LIST OF TABLES	xvii
LISTS OF ACRONYMS/SYMBOLS/TERMS	xix
CHAPTER ONE	1
INTRODUCTION	1
1.1 General Background	1
1.1.1 Wavelength-Based Thermo-Electrical Model of a Photovoltaic (PV) Module	2
1.1.2 Energy Management System in Microgrids.....	3
1.1.3 Management of Hybrid Energy Storage Systems in micro-grids	3
1.1.4 The Concept of Demand Side Management and Demand Response Techniques in Micro-grids	4
1.1.5 Electric Vehicle Integration in Micro-grids	4
1.1.6 Load Frequency Control Model with Renewable Energy Sources	5
1.1.7 The Model Predictive Control Concept	6
1.2 Research Motivation and Problem Statement	6
1.3 Research Questions	7
1.4 Research Aims and Objectives	8
1.5 Main Findings and Contributions of the Thesis.....	9

1.6 Thesis Layout.....	10
1.7 Chapter Summary	12
CHAPTER TWO	13
CONTEXT AND LITERATURE REVIEW	13
2.1 Introduction.....	13
2.2 Energy Management System of Renewable Energy-Based Microgrids	14
2.3 Control Architectures of Micro-grid Energy Management System	18
2.3.1 Centralized EMS Control Structure	18
2.3.2 Decentralized EMS Control Structure	19
2.3.3 Hierarchical EMS Control Structure.....	20
2.4 Energy Storage Technologies of Micro-grid Systems	22
2.5 Mathematical Formulations of Micro-grid Energy Management	24
2.5.1 Objective Functions of Energy Management Problem	24
2.5.2 Constraints in Energy Management Problem	26
2.6 Optimization Techniques used in Micro-grid Energy Management Problem	27
2.6.1 Energy Management Based on Linear and Non-Linear Programming Techniques	28
2.6.2 Energy Management Based on Dynamic Programming Techniques.....	28
2.6.3 Energy Management Based on Stochastic and Robust Programming	29
2.7 Solution Approaches for the Energy Management Problem.....	29
2.7.1 Heuristic and Metaheuristic Solution Approaches.....	30
2.7.2 Agent-Based Solution Approaches	30
2.7.3 Artificial Intelligence Solution Approaches.....	31
2.7.4 Model Predictive Control Solution Approaches	31
2.8 Simulation Software and Tools used to Solve Micro-grid Energy Management Problem	33
2.9 Demand Response Techniques for Micro-grid Energy Management System	34
2.10 Micro-grid Energy Management System with Electric Vehicles Integration	35
2.11 Load Frequency Control of a Stand-Alone Micro-grid.....	35
2.12 Chapter Summary	37

CHAPTER THREE	39
MATHEMATICAL MODELING AND METHODOLOGY	39
3.1 Introduction.....	39
3.2 Derivation of the Wavelength-Based Thermo-Electrical Model of PV Module	40
3.2.1 Shortwave Radiation	40
3.2.2 Longwave Radiation	40
3.2.3 Convection Heat Transfer	41
3.2.4 Output Power	41
3.2.5 Heat Capacity.....	43
3.2.6 Integration of the Thermo-Electrical Model of PV Module	43
3.2.7 Generation of Controller Reference	43
3.3 System Model Development of the Stand-alone Micro-grid	44
3.3.1 Diesel Generator	44
3.3.2 Storage System Power	45
3.3.3 Storage System.....	45
3.3.4 Description of the Control Scheme	45
3.3.5 Formulations of the AMPC Optimization Problem	46
3.3.5.1 Assumptions.....	46
3.3.5.2 System Dynamics.....	46
3.3.5.3 Cost Function	47
3.3.5.4 State Constraints	47
3.4 Dynamic Modeling of the Renewable-based Micro-grid Components	48
3.4.1 Modeling of the Distributed Energy Resources	49
3.4.1.1 Photovoltaic System Modeling	49
3.4.1.2 Wind Turbine System Modeling.....	51
3.4.2 Modeling of the Distributed Energy Storage System	52
3.4.2.1 Battery Storage System Modeling	53
3.4.2.2 Ultracapacitor Dynamical Modeling.....	54
3.4.3 Modeling of the Hydrogen Storage System	55
3.4.3.1 Mathematical Modeling of Electrolyser.....	55
3.4.3.2 Mathematical Modeling of Metal Hydride	56
3.4.3.3 Mathematical Modeling of Fuel Cell	56

3.4.4 Dynamic Modeling of the Load	57
3.4.5 Main Grid.....	58
3.5 Formulations of EMS-Based AMPC Optimization Problem.....	58
3.5.1 Cost Function Formulations.....	58
3.5.2 Dynamic System Constraints Formulations.....	60
3.5.2.1 Inequality Constraints	60
3.5.2.2 Energy Balance Constraints	61
3.6 Formulations of DR-Based AMPC Optimization Problem	61
3.6.1 DR-Based Cost Function Formulations	61
3.6.2 DR-Based System constraints Formulations.....	62
3.7 Formulations of EMS-Based AMPC Optimization Problem with EV Integration	62
3.8 Control Oriented Linear Model.....	66
3.9 System Modeling of the Two-Area Power System with a Stand-Alone Micro-grid	67
3.10 Adaptive MPC-Based Power Scheduling of Renewable Energy-Based Micro-grid	68
3.11 Adaptive MPC Controller Design of Two-Area Power System with a Stand-Alone Micro-grid...	71
3.12 Chapter Summary	73
CHAPTER FOUR.....	74
OPTIMAL CONTROL STRATEGY FOR ENERGY MANAGEMENT IN A STAND-ALONE MICRO-GRID.....	74
4.1 Introduction.....	74
4.2 Description of the System Models	75
4.3 Simulations, Results, and Discussions	76
4.3.1 Scenario 1: Location of the Optimal Power at Each Ambient Temperature.....	76
4.3.2 Scenario 2: Generation of data required for system linearization from the PV module	78
4.3.3 MPC Controller Tracking Performance of the PV Module Temperature	80
4.3.4 Reference Power Profile	86
4.4 Chapter Summary	94
CHAPTER FIVE	96

ENERGY MANAGEMENT SYSTEMS IN A RENEWABLE ENERGY-BASED MICRO-GRID	96
5.1 Introduction.....	96
5.2 Description of the System Model under Study	97
5.3 Simulations, Results, and Discussions	99
5.3.1 Micro-Grid Operation with Generation Sources and the Lead-Acid Battery Storage	99
5.3.1.1 Scenario 1: The AMPC formulation without integrating disturbances prediction.....	100
5.3.1.2 Scenario 2: The AMPC formulation with the integration of both constant and perfect disturbances predictions	104
5.3.2 Micro-Grid Operation with Generation Sources and Hybrid Storage Systems (Lead Acid and Lithium-ion Batteries).....	107
5.3.2.1 Scenario 1: The AMPC formulation without including disturbances prediction	107
5.3.2.2 Scenario 2: The AMPC formulation with the integration of both constant and perfect disturbances predictions	109
5.4 Chapter Summary	110
CHAPTER SIX.....	112
DEMAND RESPONSE TECHNIQUES FOR ENERGY MANAGEMENT SYSTEM IN A STAND-ALONE MICRO-GRID	112
6.1 Introduction.....	112
6.2 Description of the System Model under Study	113
6.3 Simulations, Results, and Discussions	116
6.4 Chapter Summary	127
CHAPTER SEVEN	129
ENERGY MANAGEMENT SYSTEM OF A MICRO-GRID WITH THE INTEGRATION OF ELECTRIC VEHICLES	129
7.1 Introduction.....	129
7.2 Description of the Dynamic Modeling of the micro-grid System.....	130
7.3 Simulations, Results, and Discussions	132
7.4 Chapter Summary	145

CHAPTER EIGHT	146
LOAD FREQUENCY CONTROL OF A TWO-AREA POWER SYSTEM WITH A STAND-ALONE MICRO-GRID	146
8.1 Introduction.....	146
8.2 Description of the Dynamic Modeling of the Stand-Alone Micro-grid.....	147
8.3 Simulations, Results, and Discussions.....	149
8.3.1 Case 1: Step load variation and dynamic system response	151
8.3.2 Case 2: System dynamic response with dispatchable DERs.....	154
8.3.3 Case 3: System dynamic response with wind speed fluctuation of 2m/s.....	155
8.3.4 Case 4: System dynamic response with series step changes in solar power	156
8.3.5 Case 5: System dynamic response with all the disturbances in the system (ΔPL , ΔPW , and ΔPS)	157
8.3.6 Case 6: Robustness Analysis for Parametric Uncertainties	161
8.3.7 Impacts of the WTG Based on DFIG on the Performance of the Proposed Control Algorithms	164
8.4 Chapter Summary	166
CHAPTER NINE.....	168
CONCLUSION AND FUTURE STUDIES	168
9.1 Closing Remarks	168
9.2 Recommendation for Future Studies.....	169
REFERENCES	171
APPENDICES	193
Appendix A.....	193
Appendix B.....	195
Appendix C.....	196
Appendix D.....	198

LIST OF FIGURES

Figure 2-1: Centralized EMS control structure [55]	18
Figure 2-2: Control structure for energy management in micro-grid systems [74]	19
Figure 2-3: Decentralized EMS control structure [55]	19
Figure 2-4: The requirements at each hierarchical control level.....	20
Figure 2-5: Classification of EMS mathematical formulation and optimization techniques [30]	24
Figure 2-6: Optimization techniques used in micro-grid energy management [54]	27
Figure 2-7: Solution approaches for energy management problem [54]	30
Figure 4-1: Heat transfer and exchange of energy in the PV module.....	75
Figure 4-2: The model-based design description of the micro-grid under study	76
Figure 4-3: System model for the Design of Experiment (DOE)	77
Figure 4-4: The output power and temperature of a PV module against the ambient temperature	78
Figure 4-5: System linearization from the PV module	79
Figure 4-6: System identification of the input and output parameters of the PV module.....	79
Figure 4-7: Simulated response comparison of the Linearized and actual plant model data.....	80
Figure 4-8: The simulation of the MPC controller.....	81
Figure 4-9: Overall simulation of MPC controller with the PV model.....	81
Figure 4-10: MPC controller performance for the first 2160 seconds of the simulation	82
Figure 4-11: MPC controller performance for the first 1:40 hours of the simulation.....	82
Figure 4-12: MPC controller performance for 3 hours of the simulation	83
Figure 4-13: MPC controller performance for 9 hours of the simulation	83
Figure 4-14: MPC controller performance for 12 hours of the simulation	84
Figure 4-15: MPC controller performance for 14 hours of the simulation	84
Figure 4-16: MPC controller performance for 18 hours of the simulation	85
Figure 4-17: MPC controller performance for 24 hours of the simulation	85
Figure 4-18: Consumer Load Power.....	86
Figure 4-19: Optimal control inputs for tracking a 50-kW constant load.....	87
Figure 4-20: Trajectory followed by the state variables with a 50-kW constant load	87
Figure 4-21: The load power and cost value with a 50-kW constant load.....	88
Figure 4-22: Optimal control inputs for tracking a 50-kW constant load.....	88
Figure 4-23: Trajectory followed by the state variables with a 50-kW constant load	88
Figure 4-24: The load power and cost value with a 50-kW constant load.....	89
Figure 4-25: Optimal control inputs for tracking a load-varying profile reference ($W \times 2,5,10$).....	90

Figure 4-26: Trajectory followed by the state variables with a load-varying profile reference ($Wx2,5,10$)	90
Figure 4-27: The load power and cost value with a load-varying profile reference ($Wx2,5,10$)	91
Figure 4-28: Optimal control inputs for tracking a load-varying profile reference ($Wx5,2,20$)	91
Figure 4-29: Trajectory followed by the state variables with a load-varying profile reference ($Wx5,2,20$)	92
Figure 4-30: The load power and cost value with a load-varying profile reference ($Wx5,2,20$)	92
Figure 4-31: Optimal control inputs for tracking a load-varying profile reference ($Wx5,2,40$)	93
Figure 4-32: Trajectory followed by the state variables with a load-varying profile reference ($Wx5,2,40$)	93
Figure 4-33: The load power and cost value with a load-varying profile reference ($Wx5,2,40$)	94
Figure 5-1: The model-based design description of the proposed micro-grid system for case 1	98
Figure 5-2: The model-based design description of the proposed micro-grid system for case 2	98
Figure 5-3: MATLAB/Simulink representation of scenario 1 without disturbance prediction (Sunny, windy, and cloudy)	100
Figure 5-4: The power flow profile during the sunny day (scenario 1) without disturbances	101
Figure 5-5: The level of storage during the sunny day (scenario 1) without disturbances	101
Figure 5-6: The power flow profile during the cloudy day (scenario 1) without disturbances	102
Figure 5-7: The level of storage during the cloudy day (scenario 1) without disturbances	102
Figure 5-8: The power flow profile during the windy day (scenario 1) without disturbances	103
Figure 5-9: The level of storage during the windy day (case 1) without disturbances	103
Figure 5-10: MATLAB/Simulink representation of scenario 2 with constant and perfect disturbance predictions	105
Figure 5-11: The power flow profile (scenario 2) for constant disturbances prediction	105
Figure 5-12: Storage levels (scenario 2) for constant disturbances prediction	106
Figure 5-13: The power flow profile (scenario 2) for perfect disturbances prediction	106
Figure 5-14: Storage levels (scenario 2) for perfect disturbances prediction	106
Figure 5-15: MATLAB/Simulink representation of scenario 1 without disturbance predictions	108
Figure 5-16: The power flow profile with hybrid storage system (scenario 1) without disturbances	108
Figure 5-17: The level of storage with hybrid storage system (scenario 1) without disturbances	109
Figure 5-18: MATLAB/Simulink representation of scenario 2 with Perfect disturbances predictions	109
Figure 5-19: Power flows for perfect disturbance prediction with hybrid storage system (scenario 2)	110
Figure 5-20: Storage levels for perfect disturbance prediction with hybrid storage system (scenario 2)	110

Figure 6-1: The model-based design description of the DR technique in the micro-grid system for case 1	115
Figure 6-2: The model-based design description of the DR technique in the micro-grid system for case 2	115
Figure 6-3: MATLAB/Simulink representation of scenario 1 with load curtailment (Sunny, windy, and cloudy).	117
Figure 6-4: The power flow profile during the sunny day with load curtailment (scenario 1).....	117
Figure 6-5: The level of storage during the sunny day with load curtailment (scenario 1).....	118
Figure 6-6: The power flow profile during the cloudy day with load curtailment (scenario 1).....	119
Figure 6-7: The level of storage during the cloudy day with load curtailment (scenario 1).....	119
Figure 6-8: The power flow profile during the windy day with load curtailment (scenario 1).....	120
Figure 6-9: The level of storage during the windy day with load curtailment (scenario 1).....	121
Figure 6-10: MATLAB/Simulink representation of scenario 2 with load curtailment (Sunny, windy, and cloudy).	122
Figure 6-11: The power flow profile during the sunny day with load curtailment (scenario 2).....	123
Figure 6-12: The level of storage during the sunny day with load curtailment (scenario 2).....	123
Figure 6-13: The power flow profile during the cloudy day with load curtailment (scenario 2).....	124
Figure 6-14: The level of storage during the cloudy day with load curtailment (scenario 2).....	124
Figure 6-15: The power flow profile during the windy day with load curtailment (scenario 2).....	125
Figure 6-16: The level of storage during the windy day with load curtailment (scenario 2).....	126
Figure 7-1: The model-based design description of the micro-grid with electric vehicles.....	131
Figure 7-2: MATLAB/Simulink representation of a micro-grid with Electric Vehicle Integration.....	133
Figure 7-3: Power flows in the micro-grid without EV charge during a sunny day.....	134
Figure 7-4: Power flows in the micro-grid with EVs mid-night charge during a sunny day.....	135
Figure 7-5: Power flows in the micro-grid with flexible EVs charge during a sunny day.....	136
Figure 7-6: 24 hours demand vector.....	137
Figure 7-7: Power flow profile of the energy sources during a sunny day.....	138
Figure 7-8: Level of storage during a sunny day.....	138
Figure 7-9: Power flow profile of the EVs charging management during a sunny day.....	139
Figure 7-10: Level of storage of the EVs charging management during a sunny day.....	139
Figure 7-11: Power flow profile of the energy sources during a cloudy day.....	140
Figure 7-12: Level of storage during a cloudy day.....	140
Figure 7-13: Power flow profile of the EVs charging management during a cloudy day.....	141
Figure 7-14: Level of storage of the EVs charging management during a cloudy day.....	141

Figure 7-15: Power flow profile of the energy sources during a windy day.....	142
Figure 7-16: Level of storage during a windy day.....	142
Figure 7-17: Power flow profile of the EVs charging management during a windy day	143
Figure 7-18: Level of storage of the EVs charging management during a windy day	143
Figure 7-19: System frequency without EVs.....	144
Figure 7-20: System frequency with EVs	144
Figure 8-1: The model-based design description of the stand-alone micro-grid	148
Figure 8-2: Transfer function model of a two-area multi-renewable energy sources-based autonomous micro-grid.	149
Figure 8-3: Two-area multi-renewable sources isolated micro-grid with UPFC.....	150
Figure 8-4: Dynamic response of the system for 2% step increase in load with AC tie-line: (a) Load disturbance (b) Area 1 frequency deviation (c) Area 2 frequency deviation (d) Tie-line power deviation	153
Figure 8-5: Dynamic response of the system for 2% step increase in load with AC-DC tie-line: (a) Load disturbance (b) Area 1 frequency deviation (c) Area 2 frequency deviation (d) Tie-line power deviation	154
Figure 8-6: Dynamic response of the system with only dispatchable DERs (a) Area 1 frequency deviation (b) Area 2 frequency deviation (c) Tie-line power deviation	155
Figure 8-7: Dynamic response of the system with wind perturbation of 2 m/s (a) Wind perturbation (b) Area 1 frequency deviation (c) Area 2 frequency deviation (d) Tie-line power deviation.....	156
Figure 8-8: Dynamic response of the system with series of step changes in solar power (a) solar perturbation (b) Area 1 frequency deviation (c) Area 2 frequency deviation (d) Tie-line power deviation	157
Figure 8-9: Dynamic response of the system with all the disturbances (a) Area 1 frequency deviation (b) Area 2 frequency deviation (c) Tie-line power deviation.	158
Figure 8-10: Dynamic response of the system with parametric variations (a) Area 1 frequency deviation (b) Area 2 frequency deviation (c) Tie-line power deviation	162
Figure 8-11: Block representation of the generator and windmill characteristics	165
Figure 8-12: Dynamic response of the system with wind perturbation of 2 m/s (a) Area 1 frequency deviation (b) Area 2 frequency deviation (c) Tie-line power deviation.....	166

LIST OF TABLES

Table 2-1: Renewable energy technologies used for energy management operation of micro-grids	14
Table 2-2: Recent literature reviews on energy management of hybrid micro-grid systems.....	15
Table 2-3: Reviews of existing literature on energy management system of micro-grids.....	17
Table 2-4: Merits and demerits of the control architectures for hybrid systems [55].....	21
Table 2-5: Energy storage technologies and their applications [93].....	23
Table 2-6: Collection of utilized EMS objective functions in the literature [54]	25
Table 2-7: Collection of utilized micro-grid EMS constraints in the literature [30].....	27
Table 2-8: Simulation software and tools used to address micro-grid EM problems	33
Table 7-1: Characteristics and the simulation results of different case studies.	136
Table 8-1: The parameter settings of the AMPC and conventional MPC control schemes.....	151
Table 8-2: Comparison of the system performance of the control techniques using the performance indices in CASE 1-A.....	158
Table 8-3: Comparison of the system performance of the control techniques using the performance indices in CASE 1-B	158
Table 8-4: Comparison of the system performance of the control techniques using the performance indices in CASE 2	159
Table 8-5: Comparison of the system performance of the control techniques using the performance indices in CASE 3	159
Table 8-6: Comparison of the system performance of the control techniques using the performance indices in CASE 4	159
Table 8-7: Comparison of the system performance of the control techniques using the performance indices in CASE 5	160
Table 8-8: Comparison of the system performance of the control techniques using the performance indices in CASE 6	160
Table 8-9: Comparison of simulation results for different control techniques over 30 independent runs without physical constraints and UPFC	162
Table 8-10: Comparison of simulation results for different control techniques over 30 independent runs with physical constraints and UPFC	162
Table 8-11: The system eigenvalues and minimum damping ratios with and without the proposed controller (AMPC) and UPFC.....	163
Table 8-12: The configuration parameters of the wind turbine generator [256].....	165

Table D-1: System parameters used in chapter 4.....	198
Table D-2: System parameters used in case 2 of chapter 4.....	198
Table D-3: Main components and the micro-grid characteristics used in chapter 5, 6 and 7	199
Table D-4: Constraints imposed on the energy resources for safe operation used in chapter 5, 6 and 7..	200
Table D-5: Weight values imposed on the multi-objective function to be solved by AMPC control Algorithm used in chapter 5, 6 and 7	200
Table D-6: System model parameters used in chapter 8.....	200

LISTS OF ACRONYMS/SYMBOLS/TERMS

Acronyms/Symbols/Terms	Descriptions
AGC	Automatic generation control
AMPC	Adaptive model predictive control
BESS	Battery energy storage system
CAES	Compressed-air energy storage
ESSs	Energy storage systems
EMS	Energy management system
EV	Electric vehicles
DSM	Demand-side management
DR	Demand response
HVAC	Heating ventilating and air conditioning
HESSs	Hybrid energy storage systems
V2G	Vehicle-to-grid
RESs	Renewable energy sources
LFC	Load frequency control
DG	Distributed generation
DERs	Distributed energy resources
EDS	Electrical distribution system
MGCC	Micro-grid central controller
PV	Photovoltaic
PEM	polymer electrolyte membrane
MILP	Mixed-integer linear programming
GAMS	General algebraic modeling system
PDF	Probability distribution function
SRHC	Stochastic receding-horizon control
SMPC	Stochastic model predictive control
SOC	State of charge
LOH	Level of hydrogen
DB	Dead band
TD	Time delay
GRC	Generation rate constraint
MLD	Mixed logic dynamic
elz	Electrolyser
$T_{elz}(t)$	Electrolyser temperature

$K_{1,elz}^{conc}$	Concentration-losses factors of the electrolyser
$V_{elz,act}^{cell}$	Activation overpotential
$V_{elz,0}^{cell}$	Nernst voltage or reversible potential
$\Delta P_{PV1}(t)$	Power deviation of PV
$\Delta P_1(t)$	The intermediate power deviation of PV
ΔF_i	Frequency deviation of area i
B	Frequency bias factor
P_{H_2}	The power of the hydrogen storage
P_{grid}	The grid power
P_{bat}	The battery bank power
MIQP	Mixed Integer Quadratic Programming
δ_{elz}	The activation signals for the electrolyser
δ_{fc}	the activation signals for the fuel cell
P	Prediction horizon
$t_{s1}(t_{s2})$	Settling time of $\Delta F_1(\Delta F_2)$
T_s	Sampling time
$t_{r1}(t_{r2})$	Rising time of $\Delta F_1(\Delta F_2)$
T_{12}	Synchronizing coefficient of tie – line
ΔP_{Li}	Load change
ΔP_{tie}	Power deviation of tie – lines

NB: All other parameters not defined on the list of Acronyms/Symbols/Terms have been defined at the first instance of use

CHAPTER ONE

INTRODUCTION

1.1 General Background

The aim of reducing greenhouse gas emissions is to focus more on environmentally friendly and renewable energy sources. Renewable energy technology now plays a significant role in a society that is becoming highly energy-intensive while still becoming more conscious of environmental issues. In reality, the penetration of renewable energy sources (RESs) into the electrical network poses many challenges arising from their inherent intermittent nature and the need to satisfy unpredictable consumer demand [1]. More so, several uncertainties have been imposed on the modern operation of the distribution network by integrating large-scale distributed renewable energy. It is necessary to determine the economic and reliable control strategies against fluctuating generation outputs and unpredictable weather conditions. In addition, the stochastic characteristics of the load profiles are exacerbated by increasingly complicated end-users [2], [3]. Conversely, while the traditional, source-controllable method of generating energy enables generation to balance the demand, incorporating new renewable-based technology with an unpredictable and variable profile makes it imperative to provide unique solutions to the problems that have not previously emerged. It is essential to realize that the energy imbalances in the grid, associated with the issues of reliability, stability, and power quality, result from the high penetration of the RESs in the electrical network. The inclusion of energy storage systems (ESSs) such as hydrogen, batteries, flywheels, ultracapacitors, etc., is a one-way approach to addressing these issues [4]. Meanwhile, due to its inherent predictive difficulties and variability, consideration of renewable sources, such as the un-dispatchable unit, can be avoided with the help of the ESS buffering capability. Therefore, the discontinuous nature of renewable generation and the randomness of the consumer's behavior are compensated by the stored energy in these units [5]. The outlined problems can be solved by redesigning the grid into smaller, more functional components. In addition, the imbalances introduced by the fluctuation of the RESs in the grid are compensated by the use of energy storage technologies, thus ensuring the appropriate quality of the power supplied to the local loads. However, storage concerns are a technical solution for energy management in the electrical network and a way of effectively using sustainable resources by averting the shedding of generation amid overproduction and, similarly, shedding of loads in the event of generation deficit. Meanwhile, the design and implementation of an advanced control system are vital for the convenient operation of hybrid ESSs. More so, the control technique will manipulate the characteristics of the individual ESS, taking into account degradation problems and operational constraints; thus, it appears as a technical solution to improve flexibility, performance, and lifespan [6], [7]. The development of micro-grids comes as a necessity for

integrating renewable energy sources into remote communities and as an intermediate milestone towards the realization of the Smart Grid. The microgrid system, which has its own control, allows for the scalable integration of local generation and loads in existing electrical networks, allowing for greater penetration of DG and RESs. The design, operation, and control of microgrids pose significant technical challenges, which must be addressed by appropriate advanced control techniques [8]. The design and implementation of appropriate advanced control strategies is a key factor for the effective integration of micro-grids into the electrical network.

1.1.1 Wavelength-Based Thermo-Electrical Model of a Photovoltaic (PV) Module

Solar energy is one of the most essential sustainable energy sources in the universe, and as such, it is increasingly becoming more efficient to produce electricity using photovoltaic effect, which can be obtained, by photovoltaic (PV) cells [9], [10]. As it stands, in terms of environmental impact and performance, photovoltaic energy appears to be a potential source of renewable energy, especially in the context of conventional power generation schemes. The PV module temperature, in particular, is a noteworthy factor that has a negative impact on PV module performance. Therefore, the more the PV module temperature increases, the lesser the PV module efficiency. Consequently, in order to enhance the design, development, and optimization of the photovoltaic module, it is essential to have a good comprehension of the factors that influence the PV modules' performance. Recently, thermal models have been introduced to predict the module's temperatures, and likewise, the thermo-electrical models to investigate the interaction of electrical and thermal module characteristics. Therefore, in the bid to fully understand how MPC is designed and implemented in an electrical network, the MPC controller is used in a wavelength-based thermo-electrical model of a photovoltaic module [11], [12].

The essence of this model is mainly to predict the impact of each module wavelength on both the temperature and the output power of the PV module. More so, since the output power is affected by the module temperature, it is expedient to design a controller that locates the optimal cut-off spectral wavelength to lessen the module temperature, therefore, getting the most out of the output power over a period of time. In this vein, a model predictive controller whose objective is to maximize the output power by simply controlling the input power through filtering the spectrum wavelength is designed for a photovoltaic system. The main objective of this case study is to improve the PV module efficiency by using an optimal control scheme to design an active filtering process that enhances the output power through controlling the input power [13], [14]. The design and simulation of the plant model and the MPC controller were carried-out on MATLAB/Simulink environment in chapter 4 of this thesis.

1.1.2 Energy Management System in Microgrids

The energy management system (EMS) is responsible for the most efficient means of maintaining the energy balance in the micro-grid. Hence, the primary objective is to ensure a reliable supply of electrical power to its local load consumers. This could involve simply handling the surplus/shortage of energy or considering certain functionalities based on economic or operational parameters. EMS objective is located at the tertiary level and, if necessary, must balance power generation and demand through energy storage, dispatch-able generators, and demand management. The EMS can also maximize system efficiency and reduce running costs. The power generated by the renewable energy sources and the power demanded are the two major disturbances (sources of uncertainty) that operate on a micro-grid that could positively impact its EMS and economic performances [15], [16]. The challenges emerge from the inherent intermittent nature of renewable energy sources and the criteria for satisfying the variable demand for energy. While renewable sources are used for the generation, the control system makes them a problem due to their time-varying nature, difficulty in predicting, and lack of manipulative capability. The EMS controls the surplus or shortfall of energy from renewable sources; where possible, electricity from renewable sources is supplied directly to loads. Any surplus power is transferred to storage units or grids and, if power is not available from renewable sources, it must be provided by storage units or grids. The EMS's primary goal is to balance power in the micro-grid efficiently, but depending on the control algorithm, the EMS can also attempt to maximize output against predetermined goals. The required amount of energy to be exchanged between generators, storage units, loads, and external grids will be determined by the control policy used, which can vary from basic heuristic principles to complex optimization algorithms [4], [17].

1.1.3 Management of Hybrid Energy Storage Systems in micro-grids

The use of ESSs provides an ability to choose the appropriate micro-grid operating approach for both islanded and grid-connected modes and control the appropriate means of exchanging energy between microgrid components and the external network. There are several energy storage technologies, such as batteries, ultracapacitor, hydrogen, etc. Storage problems in micro-grids can be solved by combining various types of ESSs in one hybrid structure. Each energy storage system has its benefits and drawbacks, taking into account energy and power rating, economic cost, autonomy, time response, lifespan, and degradation issues. The use of hybrid energy storage systems (HESSs), i.e., incorporating several storage technologies, emerges as a way to mitigate the drawbacks of these technologies. Therefore, to minimize the overall costs, the control technique must have the ability to determine which ESS can be used at any moment. In recent years, the hybridization of energy storage systems has created considerable interest. The efficient management of multiple technologies in a single ESS necessitates an optimized algorithm for distributing power, reducing total cost, and handling various timescales. When multiple ESSs are combined

to form a hybrid scheme, the issue of power-sharing must be addressed. Several studies have addressed the importance of power-sharing in hybrid ESSs, taking advantage of each technology's transient response and autonomy and respecting degradation causes [18], [19]. Adequate use of the hybrid ESS demands the implementation of a controller that considers all the constraints, limitations, degradation issues, and economic costs of each ESS. A large number of constraints and variables to be optimized complicates the control problem, necessitating the use of advanced control algorithms. A large number of constraints and variables to be optimized increases the difficulty of the related control problem, making conventional heuristic approaches difficult to find an optimal solution. Hence, the use of the multi-objective cost function in MPC also enables the controller to measure the ESS operating costs according to their number of life cycles or hours, taking into account their degradation mechanisms [4].

1.1.4 The Concept of Demand Side Management and Demand Response Techniques in Micro-grids

Demand-side management (DSM) is an essential feature in electrical networks that helps consumers to make decisions on their energy usage while also assisting operators in reducing peak load demand and reshaping the load profile. DSM covers everything that concerns the demand side of the energy system. It consists of measures introduced by power utilities to regulate electricity use at the consumer level and are used to allow optimal use of the existing energy without the need for additional facilities [20]. The adoption of the DSM technique has a range of advantages, including improved system performance, reduced overall operational costs, supply protection, and decreased environmental effects. Demand response (DR) refers to consumers' actions using information (mainly prices) to adjust their loads in the DSM context. This type of scheme can be used to avoid unwanted peaks in the demand curve that arise at certain times throughout the day, culminating in a more beneficial rearrangement, in addition to saving money on energy bills [4], [20]. The primary aim of the DR strategies mentioned in the literature is to lower system peak load demand and running costs. The demand-side management module gives the EMS and the micro-grid more flexibility, particularly when operating in a stand-alone mode [21]. Loads may be manipulated to a certain extent in a microgrid. There are certain critical loads that must be met at all times. These uncontrollable loads must be operated at a certain power and cannot be deferred at a certain time. Conversely, controllable loads with total consumption or duration of time can be modified, such as heating ventilating and air conditioning (HVAC) and electric vehicles (EV). Any loads can then be decreased, shed, or deferred during supply shortages or emergency conditions or simply to maximize the micro-grid output [22].

1.1.5 Electric Vehicle Integration in Micro-grids

Electric vehicles will increasingly be connected to the grid in the immediate future. Consequently, the development of an energy management system for managing the use of electric vehicle batteries is a core

area of research. Electric vehicle charging may be used in DSM strategies (since EVs are microgrid loads), but because of their storage capacity, EVs can still supply energy to the grid when required, making them prosumers. Vehicle-to-grid (V2G) systems use the batteries in electric vehicles to store energy for an electrical network when they are not in use. Therefore, it is reported that a vehicle is only in motion for 4% of the time [23], leaving the majority of the time for it to function as an electrical energy storage facility. Furthermore, in regular operation, the batteries are recharged overnight (during times of low electricity demand) and parked in the workplace during high electricity demand, allowing the generated energy to be used to satisfy peak demand. The incorporation of V2G networks can be a crucial component of microgrid reliability, ensuring that demand and generation variations are mitigated [4].

1.1.6 Load Frequency Control Model with Renewable Energy Sources

One of the power system utility goals is to maintain continuity of electrical supply with its desired quality [24]. The power system assumes continuous equilibrium as long as there is a balance between the generation and demand for electrical energy. In an interconnected power system, the main objective of automatic generation control (AGC) is to reduce the deviation in the transient response in the area frequency, tie-line power interchange. AGC has been developed to compensate for the steady-state error caused by primary frequency control. Frequency is a significant stability criterion for large-scale stability in multi-area power systems [25]. Load frequency control (LFC) problem of a multi-area interconnected power system with a stand-alone micro-grid is more challenging as the penetration level of renewable distribution generations with the major issues of variability and uncertainty continue to increase. Therefore, to ensure stand-alone micro-grid stability, the frequency controller should be appropriately designed with due importance [26]. More importantly, the load frequency control for micro-grid operations in the distribution network requires more attention, particularly off-grid remote micro-grid operation. Consequently, significant challenges emerge due to low inertia, converter-based, and intermittent generation of renewable and distributed energy resources common to micro-grid. Therefore, it calls for advanced control techniques to ensure a consistent supply of loads and further reduce the system's frequency deviation [27]. Frequency and voltage regulation within specified nominal values in autonomous micro-grid operation is essential for reliable system operation and has received sufficient considerations. The battery energy storage system (BESS) used in the stand-alone micro-grid system with a secondary frequency control function enhances the frequency control performance. As renewable distributed generations such as wind turbine generators and photovoltaic stations have increased penetration levels, these renewable generations have a huge impact on the LFC problem of the multi-area power system with a stand-alone micro-grid [26].

1.1.7 The Model Predictive Control Concept

The microgrid control system is capable of dealing with a wide variety of problems. The model predictive control offers an intuitive approach to the optimal control of systems subject to constraints. This factor demonstrates why MPC is the most widely used advanced control technique in the industry. The term model predictive control does not apply to a specific control technique but rather to a group of control methods that use a system model to measure the control signal by minimizing a cost function [28]. The first input of this sequence is applied to the system using the receding horizon principle, and the scheme is replicated at the next sampling time as new state information becomes available. MPC addresses a constrained hierarchical optimal control problem by repeatedly optimizing the open-loop problem online rather than relying on time-consuming offline control law computation. MPC has several characteristics that make it a viable microgrid control technique. Aside from its intuitive formulation, the approach is simple to comprehend, and it can handle multivariable and distributed cases when taking into account constraints and nonlinearities. The main differences between the MPC algorithms are the model used to represent the system, the cost function to be minimized, and how the optimization is carried out. The MPC-based control scheme's advantages over other control schemes are not limited to the following criteria [29]. It focuses on the future behavior and predictions of the system and is therefore extremely appealing to systems that are inherently dependent on forecasting energy demand and the production of renewable energy, and offers a feedback mechanism that makes the system more sensitive to uncertainty and disturbance [1], [30]. Moreover, this control strategy can address complex system constraints, integrate generation and demand projections, and finally, manage physical and operational constraints such as storage capacity or generator slew-rate power limits [31].

1.2 Research Motivation and Problem Statement

Our sector is facing a shift from a fossil-fuel energy system to a modern energy system focused on renewable energy and electric transport systems. New control algorithms are required to deal with the intermittent, stochastic, and distributed nature of the generation and new consumption patterns. The transition from a fossil-fuel-based electricity infrastructure to one with a significant proportion of clean energy and electric transportation systems poses new problems in the electrical grid's design, control, and management. This scenario necessitates new schemes for future power grids that allow for the easy integration of distributed generation, demand response, and energy storage systems. Microgrids are attracting a lot of attention in the scientific community because they can play a significant role in this transition. Microgrid energy management poses significant problems which need to be solved by advanced control techniques. This study provides a current and broad view of the key issues that arise when managing microgrids and how adaptive model predictive control (AMPC) can provide effective solutions. Despite the

fact that there are several methods for controlling microgrids, MPC is one of the most interesting technologies to use in this context because it can provide solutions at all levels. More so, frequency control as a key feature of automatic generation control is one of the main control problems in the design and operation of electrical power systems and is becoming increasingly relevant today due to the growing scale, evolving configuration, developing new uncertainties, environmental limitations, and complexity of power systems. There are a number of issues that are currently prevalent and need to be addressed with appropriate research and establish the methodologies that are capable of handling and sorting out, if possible, all of them. Model predictive control is a powerful tool compared to other conventional control applied for various purposes in power systems applications. The application of predictive model control can be furthered to adaptive mode would possibly bring a lot of solutions to the control of micro-grid following IEEE standard 1547.4 through the dynamic model of micro-grid components, controller strategies, optimal operation through mathematical modeling, including economic impacts. Moreover, several control techniques in micro-grid such as droop characteristics-based and communication-based offer excellent voltage and frequency regulation and adequate power-sharing among the DG inverters but with the drawback of prediction precision. MPC corrects this drawback, and to obtain reliable, flexible, stable, and better performance of the microgrid operation, the MPC is furthered to the adaptive MPC mode.

1.3 Research Questions

Micro-grids need a certain degree of coordination among various DERs to operate cost-effectively and reliably. This coordination is becoming more difficult in island micro-grids, where critical demand-supply balancing and generally higher component failure rates need a highly coupled problem to be resolved over the extended horizon, considering the volatility of parameters such as load profile and weather forecasting. The Micro-grid control mechanism must ensure the efficient and economical operation of the micro-grid while solving any control problems. The following research questions would be addressed in the subsequent chapters to achieve a reliable, efficient, scalable, and cost-effective operation of the micro-grid controller to harness the application of DERs using the AMPC algorithm completely:

- How can the utilization rate of the integrated renewable and distribution energy resources for local use with a consequence of the consumers' independence from the external grid be increased?
- How can the optimal power reference tracking problem be solved, where the energy consumption from the diesel generator is minimized while maximizing the efficiency of the storage bank?
- How can the AMPC optimization problem cost function, dynamic system constraints, and the control-oriented linear model used to solve the micro-grid energy management problem be formulated?

- How can the EMS-based energy optimization problem be solved in an optimal way using an AMPC algorithm in a renewable-based micro-grid?
- What are the impacts of integrating disturbance predictions on the energy management system performance based on the proposed control technique?
- What are the benefits of adopting the concept of demand response technique for EMS in micro-grids?
- How can the effectiveness of the AMPC strategy from other control strategies be demonstrated, with the help of a simulation-based model, in addressing economic dispatch problems for micro-grids with a strong presence of intermittent resources (DGs)?
- How can frequency deviation problems against variations in system parameters and load disturbance of a typical micro-grid system be solved with appropriate advanced control techniques?

1.4 Research Aims and Objectives

Microgrid control has advanced significantly in recent years. Microgrids, which are small-scale power systems with a cluster of loads, distributed generators, and storage units that work together, is the most innovative sector of the electric power field today, and as a result, new control problems are emerging. This study aims to use adaptive model predictive control (AMPC) to provide solutions for renewable energy-based microgrids' operation. Although several approaches can be used to manage microgrids, AMPC offers a general method for addressing most problems using certain basic concepts in an organized manner. AMPC solves an optimization problem incorporating a feedback mechanism, which allows the system to face uncertainty and disturbances. It can handle physical constraints and incorporate the system's future behavior, which is vital for micro-grid. AMPC has been successfully applied in the industry, but in this context, it can add solutions to problems derived from the nature of the generation and demand and also to the need to operate with equipment from different nature such as geographically distributed energy resources. This research aims to develop an AMPC algorithm to regulate the power flow among the integrated DERs to maintain quality, reliable, and economic power supply. This work has a general objective to develop an AMPC algorithm to solve the energy management problem of hybrid energy systems based on the renewable energy sources. Therefore, to achieve this aim, the following objectives shall be accomplished, namely:

- Dynamic modeling of the micro-grid components (hybrid energy system, integrating energy sources, i.e., solar and wind, hybrid storage unit (battery and hydrogen), and electric vehicles (V2G)).

- Development of the mathematical model for the micro-grid optimal operation and subsequently formulate an optimization problem (cost or objective function and constraints) which are solved using the AMPC algorithm.
- Investigation of the optimal control strategy that efficiently manages a stand-alone residential micro-grid comprising of renewable and non-renewable energy sources. The objective of the optimal control scheme is for the generation to meet the demand, minimize the use of fossil fuels and ensure the energy storage is always maintained around a nominal point such that it is not over-depleted.
- Investigation of the impact of integrating the disturbance prediction on the energy management system's performance (EMS) based on the adaptive model predictive control (AMPC) algorithm to improve the operating costs of the micro-grid with hybrid-energy storage systems.
- Investigation of the benefits of adopting the concept of DR technique for energy management system in a stand-alone micro-grid with both critical and curtailable loads connected.
- Investigation and solution to the problems of control and energy management in micro-grid with the incorporation of renewable energy generation, hybrid storage technologies, and integrating the EVs with V2G technology.
- Development of load controllers' strategies and management of the electric vehicle batteries usage as energy storage connected to micro-grid in the context of V2G systems.
- The development of an adaptive model predictive control (AMPC) technique for load frequency control of a two-area interconnected power system with a stand-alone micro-grid.

1.5 Main Findings and Contributions of the Thesis

The main findings and contributions of the thesis are summarized as follows:

- An advanced control strategy was proposed in this thesis, i.e., an adaptive model-based receding horizon control technique, mainly for the effective integration of micro-grids into the electrical network; permits the integration of the information on the disturbances prediction, improves the system flexibility and operational reliability and address issues related to the energy management system (EMS) in micro-grid operations.
- The impact of considering the prediction of disturbances on the performance of the energy management system based on the adaptive model predictive control (AMPC) algorithm to improve the operating costs of the micro-grid with hybrid-energy storage systems was also investigated.

- The Effectiveness and superiority of the proposed AMPC technique in terms of control performance, optimization of the system efficiency, and minimization of the operational costs are investigated.
- A comprehensive multi-objective formulation is developed, which weighs the usage of manipulated variables, penalizes the rate, and keeps the stored energy around an operating point.
- Comprehensive case studies with single and hybrid storage systems are presented to provide insights on the significant effects of introducing more battery storage into the micro-grid on the system efficiency and cost function minimization.
- An AMPC technique with an extended state vector is proposed for the optimal LFC problem of a multi-area interconnected power system with a standalone micro-grid.
- Since the control performance of AMPC is dependent on the micro-grid system parameters, understanding the most sensitive parameters to the AMPC could be useful for the designing process to achieve better performance. Therefore, the effects of the system parameters on the control performance of the control techniques were evaluated. More so, a comparative study of AMPC and MPC control for frequency control is investigated to show the effectiveness of the AMPC based frequency control.

1.6 Thesis Layout

This research project describes “micro-grid and its operational aspects.” More specifically, it further explains the steady-state operations of a micro-grid consisting of various distributed energy resources (which provides a number of advantages on top of the existing grid, including dwindling primary resources, application of renewable energy resources such as sun, wind, and water together with storage concerns considering the intermittency of power available from such sources). This thesis is structured in nine chapters. A brief description of each chapter is arranged as follows:

In the **first chapter**, an introduction to energy management in micro-grids, management of hybrid energy storage systems in micro-grid, the concept of demand-side management and demand techniques in micro-grids, electric vehicle integration in micro-grids, load frequency control model with renewable energy sources, and model predictive control concept is explained. The chapter also presents the research motivation and problem statement, research questions, and research aim and objectives.

A comprehensive state-of-the-art overview of energy management in microgrid systems with renewable energy generations is presented in the **second chapter**. It also reviews the main concepts and modules of the control structures of a generalized energy management system. This chapter also summarizes the most common optimization techniques, solution algorithms, software, and the mathematical formulations used

in the specialized literature to solve energy management problems. More so, recent studies on the integration of EVs in microgrids are summarized.

The **third chapter** presents the various optimization techniques and solution approaches to solve the EMS-based optimization problem in the micro-grid systems. It further focuses on the model and analysis of the micro-grid components. This chapter describes in detail the formulations of the proposed control algorithm (AMPC) used to solve the control and EMS problems in the micro-grid system throughout this thesis.

The **fourth chapter** investigates an optimal control strategy that efficiently manages a stand-alone residential micro-grid comprising renewable and non-renewable energy sources. It also implemented an adaptive model predictive control (AMPC) algorithm for choosing an optimal mode and set of inputs for the system to track both a constant and load-varying power demand profile. The objective of the optimal control scheme is for the generation to meet the demand, minimize the use of fossil fuels and ensure the energy storage is always maintained around a nominal point such that it is not over-depleted.

The **fifth chapter** investigates the impact of integrating the disturbance prediction on the performance of the energy management system (EMS) based on the adaptive model predictive control (AMPC) algorithm to improve the operating costs of the micro-grid with hybrid-energy storage systems. Additionally, this chapter studies the proposed controller's behavior under various external conditions, such as weather and demand changes.

In the **sixth chapter**, the benefits of adopting the concept of DR technique for energy management system in a renewable energy-based stand-alone micro-grid with both critical and curtailable loads connected are investigated. The aim of the demand response technique in the energy management system is to use the diversity of the load consumption patterns and the energy available from the distributed energy resources, the demand response, and the energy storage system (ESS) to reduce the peak load demand and minimize the operating/electricity costs of the micro-grid system.

The **seventh chapter** addresses the problems of control and energy management in micro-grid with the incorporation of renewable energy generation, hybrid storage technologies, and integrating the EVs with V2G technology. The AMPC technique is used to optimize the charge/discharge of the EVs in a receding horizon manner in order to reduce operational cost in a renewable energy-based micro-grid.

The **eighth chapter** uses the adaptive model predictive control (AMPC) technique for load frequency control of a two-area interconnected power system with a stand-alone micro-grid. Hence, the effects of system parameters variation on the control performance of the AMPC technique for frequency control in a stand-alone micro-grid are investigated. The purpose of this chapter is to solve the problems of frequency deviation against variations in system parameters and load disturbance of a typical stand-alone micro-grid.

The **final chapter** of this thesis outlines the findings of the work under investigation. Conclusions have been based on these findings, and recommendations for further studies have also been proposed.

1.7 Chapter Summary

This chapter presents an introduction to energy management in micro-grids, management of hybrid energy storage systems in micro-grid, the concept of demand-side management and demand techniques in micro-grids, electric vehicle integration in micro-grids, load frequency control model with renewable energy sources, and model predictive control concept. This section of the thesis also presents the research motivation and problem statement, research questions, research aim and objectives, research findings and the contributions of the thesis, and finally, the thesis outline.

CHAPTER TWO

CONTEXT AND LITERATURE REVIEW

2.1 Introduction

The erratic nature of renewable energy resources (RERs) such as wind and photovoltaic generations, market (energy) prices, and the randomness of the load profile has contributed to difficulties in maintaining the power quality and generation-consumption balance. Hence, microgrids can be managed by an energy management system (EMS) to solve these issues, enabling the minimization of running costs, emissions, and peak loads while respecting the microgrids' technical and physical constraints [32]. Several issues are currently prevalent and need to be addressed with appropriate research and establish the methodologies that are capable of handling and sorting out, if possible, all of them. Microgrids' energy management system has been researched from numerous perspectives over the past few years and has recently gained significant interest from researchers. To this end, this chapter presents a comprehensive state-of-the-art overview of energy management in microgrid systems with renewable energy generations. It also reviews the main concepts and modules of the control structures of a generalized energy management system [32], [33]. Energy storage technologies are considered an attractive option for managing the fluctuant renewable energy generation profiles due to increased technological maturity, energy density, and the ability to provide grid services, such as frequency response. Hence, a survey on the main energy storage technologies, which is one way to get over the energy imbalance problem due to the high penetration of RERs, is presented [4]. Meanwhile, many researchers have solved these energy management problems using various optimization techniques and solution approaches to achieve the optimal microgrid operation. Therefore, this chapter further summarizes the most common optimization techniques, solution algorithms, software, and the mathematical formulations used in the specialized literature to solve energy management problems. More so, appropriate management of loads and electric vehicles (EVs) charging can help improve microgrid operation. Therefore, this chapter presents an overview of the key concepts of demand side management (DSM) and demand response technique (DRT) for energy management in microgrid systems [17]. Incorporating the vehicle-to-grid system can be crucial in the microgrid's reliability to protect against load and generation variability. The development of an energy management system for managing the use of electric vehicle batteries is a core area of research, which has been reviewed in the literature. Hence, recent studies on the integration of EVs in microgrids are summarized. Lastly, the system's dynamics under various system disturbances, various control strategies, and techniques in the area of load frequency control (LFC) in micro-grids are also reviewed [26]. The essence of this chapter is to provide a basis for an in-depth study in the field of microgrid control approaches and structure, with particular emphasis on energy management

systems. In addition, to put some perspective on the need for predictive control for energy management in microgrids, different classifications of control techniques are reviewed [34], [35].

2.2 Energy Management System of Renewable Energy-Based Microgrids

Microgrids composed of distributed energy resources (DERs), such as distributed generation systems (DGSs), energy storage systems (ESSs), and loads (controllable and uncontrollable loads), necessitate a management system capable of controlling, monitoring, and planning its operation while ensuring efficient, cost-effective and reliable performance [36], [37]. It is worth mentioning that the most important procedure in microgrids' operation is the energy management process [38]. An EMS can be described as a comprehensive automated and real-time system operating within an electrical distribution system (EDS) used for optimal scheduling and management of DERs and controllable loads. The EMS balances the power generation and demand through dispatchable generators, energy storage, demand management, etc. More so, the EMS improves the system performance and minimizes the operating costs [4]. The key objective of the energy management problem is to determine an optimal schedule to achieve a predefined goal for all dispatchable DGS, energy storage systems, and controllable loads. The optimization of the EDS's running costs, including the generation and operation of both DGS and ESS, is a more popular objective of the energy management problem [33], [4]. Moreover, the required amount of energy to be exchanged among generators, storage units, loads, and external grids will be determined by the control mechanism used, which can vary from basic heuristic principles to sophisticated optimization algorithms. Therefore, in this context, the key functions of an energy management system are as follows; It maximizes the use of renewable energy resources; It maximizes the energy purchased outside the micro-grid; It minimizes operational costs, energy losses, fuel consumption and gas emissions; It manages all the DGS, ESS and controllable loads in case of resynchronization with the main grid; It increases system reliability by simply maximizing each customer energy availability [39], [40]. Few examples of renewable energy technologies that are used in the literature for energy management operation of micro-grids are presented in Table 2-1.

Table 2-1: Renewable energy technologies used for energy management operation of micro-grids

Solar	Wind	Fuel cell	Hydro	Biomass	Combined heat & power	Tidal	Ref.
✓		✓				✓	[41]
✓	✓		✓				[42]
	✓			✓			[43]
✓	✓				✓		[44]
✓			✓				[45]

✓	✓				✓		[46]
✓		✓				✓	[47]
	✓	✓					[48]
✓	✓				✓		[49]
✓	✓	✓			✓		[50]

The contributions of the existing review papers related to the energy management system of microgrids are summarized as follows. Ref [51] presented a comprehensive review on standalone renewable energy systems. The review topics were hybrid system configurations, sizing methodologies, storage options, and control strategies. Three types of control for the flow of energy management were addressed in this review: the centralized, the distributed, and the hybrid of centralized and distributed controls. Ref [52] presented an overview of various distributed generation technologies and reviewed sizing, energy flow management, and hybrid systems construction. The feasibility of various types of controllers was also discussed in this paper. The authors in [53] reviewed strategies and approaches used to implement energy management in stand-alone and grid-connected hybrid renewable energy systems. The authors in [54] presented a summary of recent research advances using optimization algorithms in microgrid planning and methodologies. Ref [55] presented an overview of current hybrid microgrids and optimization methods and applications. Additionally, the authors in [56] demonstrated an extensive review of energy management methodologies applied in microgrids. It reviews EMS for real-time electricity control and short-/long-term energy management. Ref [57] conducted a comprehensive review on energy management in micro-grids. The review topics are optimization objectives, constraints, algorithm types, and software tools. The authors in [58] briefly explained the modeling of RERs and ESSs. This review also discusses meta-heuristic optimization methods and software tools for energy management and control of hybrid RERs, sizing objectives, ESS management, power quality, and energy dispatch-related problems.

More so, recent literature surveys regarding the implementation of hybrid systems are summarized in Table 2-2. As illustrated in Table 2-2, the most widely used energy storage devices are batteries.

Table 2-2: Recent literature reviews on energy management of hybrid micro-grid systems

Grid	DG	PV	WT	Fuel Cell	Biomass	Diesel	Hydrogen	Battery	SC	EV	Performance Evaluation	Ref.
✓		✓	✓					✓			The authors presented the experimental investigations of the operation of a grid-	[59]

											connected hybrid PV-wind system using a standalone inverter capable of operating in both standalone and grid-connection modes.	
✓	✓	✓	✓					✓			The authors presented a multi-objective optimization problem over a receding control horizon used for energy storage dispatch and sharing of renewable energy resources in a network of grid-connected micro-grid. The formulation of the multi-objective optimization is implemented as a lexicographic program to ensure preferential treatment of multiple micro-grids.	[60]
								✓	✓	✓	A real-time EM control technique incorporating wavelet transformation, neural network, and fuzzy logic methods was proposed for the work. Experimental findings showed that the battery pack's power variance and peak strength were successfully suppressed.	[58]
				✓				✓	✓	✓	The authors developed an intelligent control strategy for a hybrid energy storage system composed of the battery, fuel cell, and supercapacitor. A multi-input/multi-output state-space model is used to implement the system model in the study.	[61]
✓	✓	✓	✓		✓			✓			The authors developed an economical linear programming model with a sliding-time-window to assess the design and scheduling of biomass, combined heat, and power-based micro-grid systems.	[62]

		✓		✓			✓	✓			The authors proposed a combined sizing and EM methodology and formulated it as a leader-follower problem. The leader problem focuses on sizing and aims at selecting the optimal size for the micro-grid components. It is solved using a genetic algorithm.	[63]
	✓	✓		✓		✓	✓				The authors used the crow search algorithm to optimize and size a hybrid system. The study considered two constraints to minimize the total net cost: Renewable energy portion and loss of power supply probability.	[64]

Furthermore, review papers in the literature on microgrid energy management systems from different aspects are summarized in Table 2-3.

Table 2-3: Reviews of existing literature on energy management system of micro-grids

Objective Function	Constraints	Flexible Resources		Optimization Strategies	Micro-grid Operational Mode		Ref.
		DR	ESS		Islanded	Grid-Connected	
✓	✓			✓	✓		[65]
		✓		✓	✓		[66]
✓	✓		✓	✓	✓		[57]
✓			✓	✓	✓	✓	[55]
				✓	✓	✓	[56]
			✓		✓	✓	[67]
			✓	✓	✓	✓	[54]
✓	✓		✓	✓	✓	✓	[17]
✓	✓		✓	✓		✓	[68]

Tables 2-2 and 2-3 presented several literature surveys that reviewed the energy management strategies used for special cases of hybrid systems. Moreover, the literature includes many papers that conducted reviews for various aspects related to hybrid renewable energy systems [69], [70].

2.3 Control Architectures of Micro-grid Energy Management System

Several authors in the literature have reviewed the various control structures for micro-grid EMS to control and intelligently co-ordinate the DERs. The three EMS control structures commonly used in practical application are as follows; Centralized, decentralized, and hierarchical control structures. These control structures of micro-grid EMS are briefly discussed in the following subsection [71].

2.3.1 Centralized EMS Control Structure

In a centralized EMS control structure, the central controller gathers all the relevant information such as power generation of DERs, energy consumption pattern of each consumer, meteorological data, cost-function, etc., as the information related to the operating point of the EDS. These data are used in conjunction with the renewable generation forecasting and the load consumption to schedule the operation of the DERs and determine the optimal energy scheduling of micro-grid and sends these decisions to all local controllers (LCs). The micro-grid central controller (MGCC) has the primary responsibility for the optimization procedure for microgrid energy management. Several research papers have developed and implemented centralized EM control approaches. For example, the authors of [72] proposed a centralized controller to optimize micro-grid operation by maximizing the production of distributed RESs generators while establishing back-and-forth energy transfer with the main utility grid. The efficiency of the proposed solution on a micro-grid system was investigated by considering a typical case network operating under various market policies and spot market prices. Additionally, ref [73] developed a centralized EM system for a standalone micro-grid system based on the model predictive control method to reduce computational loads. Hence, the studied problem was solved iteratively by nonlinear programming (NLP) and mixed-integer linear programming (MILP) techniques. A typical structure of a centralized EMS is shown in Figure 2-1.

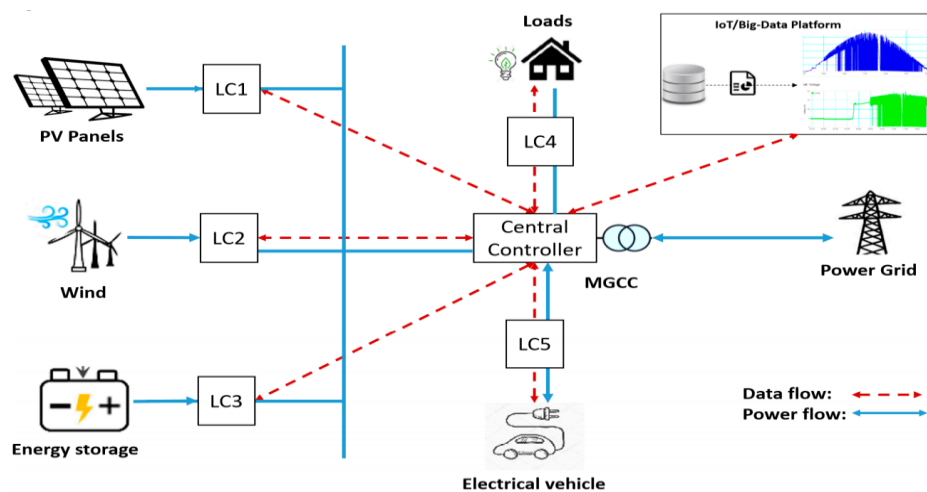


Figure 2-1: Centralized EMS control structure [58]

2.3.2 Decentralized EMS Control Structure

In a decentralized EMS control structure, local controllers (LCs) are mainly responsible for maximizing their operations in a dynamic environment. More so, all decisions are made on a distributional basis until the DGS, the ESS, and the controllable loads have reached a shared agreement to operate the microgrid. In literature, the terms decentralized and distributed EMS controls are often used interchangeably [74], [75]. For distributed control, local controllers use local measurements and can send and receive the necessary information to other LCs [76]. Figure 2-2 depicts the Control structure for energy management in micro-grid systems. Similarly, several literature papers have deployed decentralized EM control approaches. For instance, the authors of [15] used a robust optimization to analyze decentralized microgrid energy management, taking the uncertainties of wind power and solar power generations and energy consumption into consideration [77]. In addition, the authors of [62] proposed deterministic constrained optimization and stochastic optimization approaches to estimate the uncertainties in biomass-integrated micro-grid supplying both heat and electricity. The work developed an economical linear programming model with a sliding time window to assess the design, scheduling biomass-combined power, and heat-based micro-grid systems. A typical structure of this approach is shown in Figure 2-3.

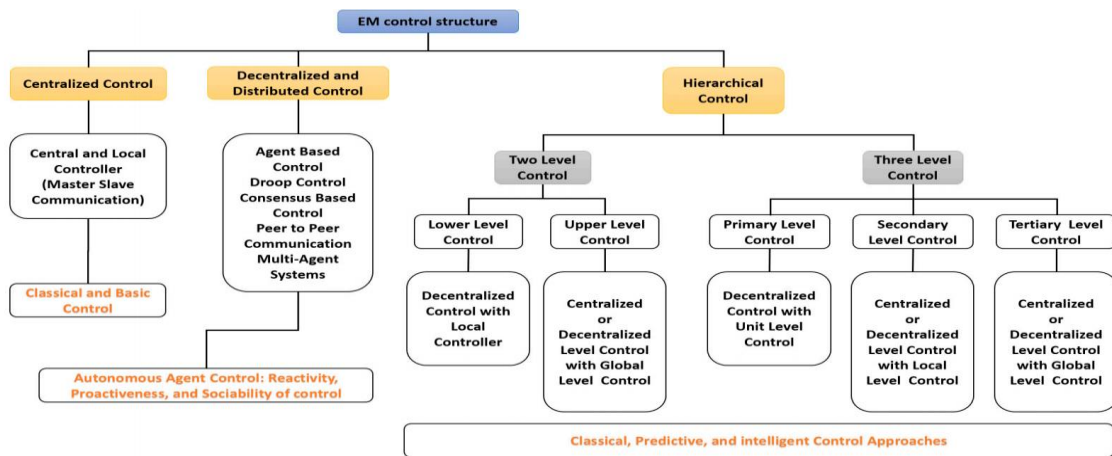


Figure 2-2: Control structure for energy management in micro-grid systems [78]

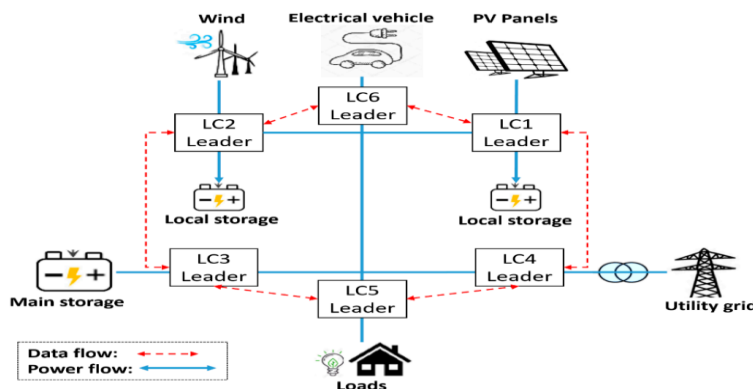


Figure 2-3: Decentralized EMS control structure [58]

2.3.3 Hierarchical EMS Control Structure

It is worth mentioning that the centralized control approach is challenging to implement due to the extended geographic areas of the systems and the extensive communication and computation requirements. Similarly, a higher degree of coordination, which decentralized control systems cannot accomplish, is needed for greater coupling between the various LCs. Nonetheless, a compromise between the fully centralized and decentralized control structures is accomplished by having hierarchical control structures [79], [80] on three layers of control: primary, secondary, and tertiary [81], [82]. The primary level operates on a fast timescale. It maintains the voltage and frequency stability generated from each source during changes in the generation or demand and after switching to islanded mode [58],[83]. Additionally, the primary control level detects the operating mode of micro-grid systems, offering the ability to operate in grid-connected and standalone modes [84]. During a load or generation adjustment, the secondary level is committed to ensuring that the voltage and frequency differences are restored to zero. It is responsible for mitigating any steady-state error introduced by the primary control, as well as synchronizing with the grid during the transition from islanded to grid-connected mode. This control level aims to ensure and enhance the power quality within the required standards values, allowing the synchronization between the micro-grid systems and the main electrical network [85]. The tertiary control level's main objective is to control the power flow between the microgrid and the main grid (or other microgrids) and for the optimal operation on large timescales (planning and scheduling). Hence, this level may include several optimization strategies, according to the timescales [86], [87]. The hierarchical control can be implemented in parallel in both centralized and distributed structure. The requirements at each hierarchical control level are shown in Figure 2-4.

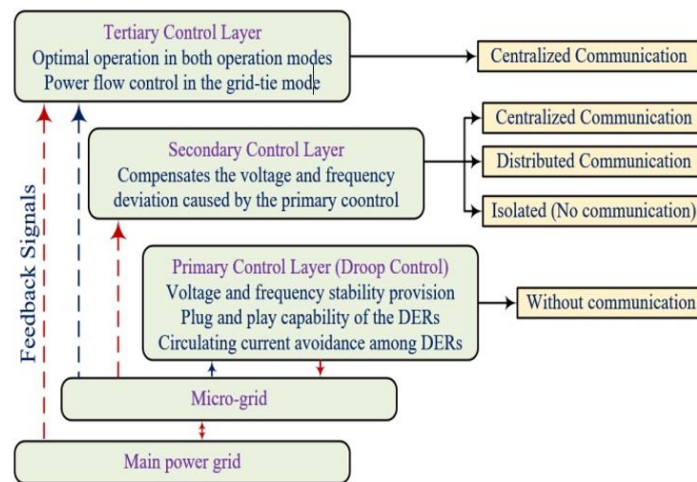


Figure 2-4: The requirements at each hierarchical control level

The authors in [88] presented a hierarchical EMS control system to minimize the daily operating cost of a micro-grid and maximize the Implemented RES's self-consumption by selecting the best setting for a central battery storage system based on a defined cost function. Ghaffari et al. [64] developed a method to size an

off-grid PV/diesel/FC hybrid energy system to optimize the number of system components with respect to the installation's cost minimization. Table 2-4 shows the merits and demerits of each control structure.

Table 2-4: Merits and demerits of the control architectures for hybrid systems [58]

EM	Merits	Demerits
Centralized	<ul style="list-style-type: none"> ▪ Suitable for small size micro-grid systems where the collected information is performed by low bandwidths communication [89] 	<ul style="list-style-type: none"> ▪ A high level of connectivity is needed due to the direct interaction of each entity with the central.
	<ul style="list-style-type: none"> ▪ Provides intense supervision and wide control of the whole system. 	<ul style="list-style-type: none"> ▪ Heavy computation burden is a technical barrier for the deployment.
	<ul style="list-style-type: none"> ▪ The optimal decision is guaranteed. 	<ul style="list-style-type: none"> ▪ Reliability is degraded for the whole system.
	<ul style="list-style-type: none"> ▪ Strong controllability and real-time observability of the whole micro-grid system. 	<ul style="list-style-type: none"> ▪ The failure of the centralized control affects the whole system operation.
	<ul style="list-style-type: none"> ▪ Straightforward implementation, the centralized control allows economic implementation, and it is easy to maintain. 	<ul style="list-style-type: none"> ▪ More prone to failures since only one unit regulates the voltage and reduces the life span of the battery bank stack [90].
Decentralized	<ul style="list-style-type: none"> ▪ Easy realization of plug-and-play functionality. 	<ul style="list-style-type: none"> ▪ Requires fast periodical reconfiguration.
	<ul style="list-style-type: none"> ▪ Reduces computational burden and increases reliability and robustness. 	<ul style="list-style-type: none"> ▪ Requires effective synchronization and strong communication to achieve synchronicity.
	<ul style="list-style-type: none"> ▪ Higher reliability due to the redundancy of controllers and communication 	<ul style="list-style-type: none"> ▪ Has high complexity of implementation compared to centralized and hierarchical control.
	<ul style="list-style-type: none"> ▪ Peer-to-peer node communication, allowing greater flexibility of operation and avoiding single-point failure. 	<ul style="list-style-type: none"> ▪ Incomplete information about the overall micro-grid status.
	<ul style="list-style-type: none"> ▪ Droop control strategy is usually used to avoid circulating currents between the converters without using a digital communication link. 	<ul style="list-style-type: none"> ▪ Local optimization in EMS cannot provide a global solution for operating cost minimization of the total micro-grid.

Hierarchical	<ul style="list-style-type: none"> ▪ More suitable for DC micro-grid systems. 	<ul style="list-style-type: none"> ▪ Fewer computation burdens.
	<ul style="list-style-type: none"> ▪ The optimal decision is possible. 	<ul style="list-style-type: none"> ▪ There is no transfer of information and energy if there is a communication fault in the upper layer.
	<ul style="list-style-type: none"> ▪ The voltage and the current are regulated locally by the source converters. 	<ul style="list-style-type: none"> ▪ The distributed generators should participate in voltage regulation and frequency control.
	<ul style="list-style-type: none"> ▪ Flexible regulation of the system voltage within acceptable intervals. 	<ul style="list-style-type: none"> ▪ Adjacent layers coordination is required.
	<ul style="list-style-type: none"> ▪ Improving the current mismatches among the controllers; 	<ul style="list-style-type: none"> ▪ Some generators operate in limited power mode while supplying only the power planned by the electricity market.

2.4 Energy Storage Technologies of Micro-grid Systems

Energy management systems of micro-grid encounter difficulties in managing renewable energy sources such as wind and solar energy. This issue is due to the unpredictable existence of the renewable energy available, which is exacerbated by the disparity between real-time and forecasted power generation. Therefore, ESSs are solutions to resolve this problem [91], [92]. Energy storage technologies compensate for the imbalances between generation and consumption by storing power during low-cost or off-peak hours and discharging it during high-cost or peak hours induced by RESs fluctuations in the grid, ensuring that the power supplied to the end loads is of sufficient quality [93]. In addition, the optimum use of RES is possible by the use of ESSs across a wide variety of applications (i.e., from remote user level (stand-alone microgrids) to large-scale RES systems). The benefits resulting from the introduction of energy storage systems can be summarized as the possibility to minimize energy losses, to increase the reliability and quality of energy supply to consumers (since an additional power source is available), and to boost the operation of the power grid (e.g., operation of conventional units at an optimum point) [94]. There are several energy storage technologies. Each energy storage system has its benefits and drawbacks, taking into account energy and power rating, economic cost, autonomy, time response, lifespan, and degradation issues. The use of hybrid energy storage systems (HESSs), i.e., incorporating several storage technologies, emerges as a way to mitigate the drawbacks of these technologies. Therefore, to minimize the overall costs, the control technique must have the ability to determine which ESS can be used at any moment. In recent years, the hybridization of energy storage systems has created considerable interest [95], [96]. The integration of hydrogen storage along with electrochemical batteries and ultracapacitors, in particular, seems like an

effective combination for renewable generation [97]. Energy storage is a technological solution for network management and a way to allow effective renewable energy use by avoiding generation shedding in periods of overproduction and load shedding while generation is insufficient. For the convenient operation of hybrid ESSs, the design and implementation of an advanced control system are essential. Table 2-5 shows the comparison of technical features of different ESS technologies. According to this, various fields of application and implementation of the different energy storage systems can be seen. Systems with very low storage periods (seconds) and high specific power, such as ultracapacitors, are used for grid stability in power quality problems. On the other hand, there are ESSs with the ability to store large quantities of energy e.g., hydrogen systems. They can be used to compensate for the fluctuations in electricity generation from renewable sources and the smooth peaks in demand for energy. The other ESSs can be used to ensure uninterrupted power supply, black start and spinning reserve [98].

Table 2-5: Energy storage technologies and their applications [99]

Full power duration of storage	Application of storage and possible replacement of conventional electricity system control	Batteries	H2 Storage System	CAES	Large hydro	Pumped hydro	Supercapacitor	Flywheel
20 s	Line or local faults, Voltage and frequency control	✓					✓	✓
3 min	Spinning reserve, wind power smoothing of gusts	✓	✓			✓		✓
20 min	Spinning reserve, wind power smoothing, clouds on PV	✓	✓	✓	✓	✓		✓
2 h	Peak load looping, wind power smoothing etc.	✓	✓	✓	✓	✓		
8 h	Daily load cycle, PV, wind, transmission line repair	✓	✓	✓	✓	✓		
3 days	Weekly smoothing of loads and most weather variations		✓	✓	✓	✓		
4 Months	Annual smoothing of loads, PV, wind, and small hydro		✓		✓			

Several research studies have concentrated on the utilization of ESSs in microgrids [100]. Karavas et al. [101] have studied the microgrid EMS considering a battery as ESS and solved the optimization problem based on distributed intelligence and MAS. Alavi et al. [102] solved the microgrid energy management problem by considering a battery as a reserve energy source. The polymer electrolyte membrane (PEM) was used to cover wind and solar power uncertainties. Authors [97, 103] applied the MPC in their studies to control the load sharing of a hybrid ESS composed of a fuel cell and an ultracapacitor, including some degradation issues. However, these studies do not include connecting to the grid, or the startup/shut down degradation issues associated with the fuel cell. Arce et al. and Bordons et al. in [104], [105] have advanced similar developments in the hybridization of a fuel cell and a battery.

2.5 Mathematical Formulations of Micro-grid Energy Management

Microgrid energy management is an optimization problem aimed at efficiently scheduling the short-term operation of DGs, ESSs, and controllable loads with respect to different objective functions and constraints [32], [106]. A literature review of existing objective functions and constraints considered by the EMS has been developed in this section. More so, the classification of objective functions utilized by the EMSs along with their constraints are shown in Figure 2-5.

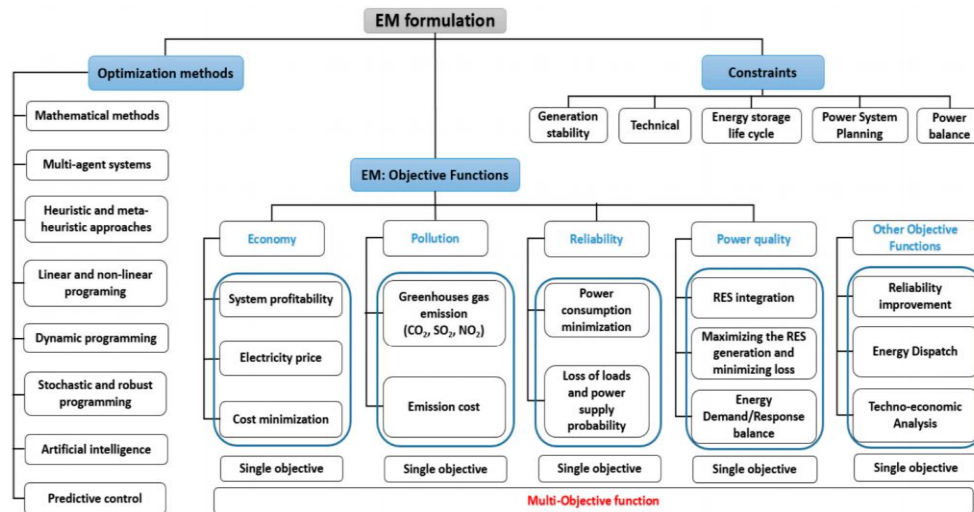


Figure 2-5: Classification of EMS mathematical formulation and optimization techniques [32]

2.5.1 Objective Functions of Energy Management Problem

The energy management of a renewable-based micro-grid can have different objective functions. Thus, the micro-grid system can be managed by the EMS simply by solving various objective functions. Hence, these objective functions are based on the geographical area, user preferences, microgrid capacity, equipment installed in the microgrid, types of tariff, energy generation, energy storage, and government regulations. The capital or operational costs of the microgrid is an excellent example of objective functions. Therefore,

some examples of operational or capital costs are costs related to fuel, start-up and shut-down, maintenance, degradation, and procurement from the utility in case of power deficiency [107]. Some of the collection of utilized EMS objective functions in the literature are stipulated in Table 2-6. The objective functions are reviewed from being single objective and multi-objective perspectives, as shown in Table 2-6.

Table 2-6: Collection of utilized EMS objective functions in the literature [57]

Objective Function Equations	Descriptions	Single	Multi	Ref.
$F = CF_t^{OPR} + CF_t^{EMI} + CF_t^{RLB} \quad (2-1)$	CF_t^{OPR} , CF_t^{EMI} and CF_t^{RLB} represent the operation, emission, and reliability costs of micro-grid, respectively.	✓		[102]
$F = Cost^{Operating} + Cost^{Emission}$ $Cost^{Operating} = \sum_{t=1}^T (cost_{DG}(t) + ST_{DG}(t) + cost_s(t) + cost_{Grid}(t) + cost_{DR}(t)) \quad (2-2)$ $Cost^{Emission} = \sum_{t=1}^T \{emission_{DG}(t) + emission_s(t) + emission_{Grid}(t)\}$	The objective function is taken as the operating and emission cost. $cost_{DG}(t)$, $ST_{DG}(t)$, $cost_s(t)$, $cost_{Grid}(t)$, $cost_{DR}(t)$ represent DG cost, start-up and shut-down costs, reserve cost, and cost of exchanging power with the grid.		✓	[108]
$F = F_{Cost}^{start-up} + F_{Cost}^{generation} + F_{Cost}^{reserve} + F_{Cost}^{DR} + F_{Emission} \quad (2-3)$	The objective function is composed of overall cost and emission functions.	✓	✓	[109]
$F = F_t^{DEG} + F_t^{MT} + F_t^{OP} + SC_t \quad (2-4)$	The objective function is considered as the operation, maintenance, and start-up costs of the DEG. F_t^{DEG} , F_t^{MT} , F_t^{OP} , and SC_t represent DEG, maintenance, operation, and start-up costs of the micro-grid, respectively.		✓	[110]
$F = C_{INV} + C_{OP} + C_{GRID}^{PUR} + C_{CARBTAX} - C_{GRID}^{SAL} \quad (2-5)$	C_{INV} , C_{OP} , C_{GRID}^{PUR} , $C_{CARBTAX}$, C_{GRID}^{SAL} represent investment cost, operating cost, purchase cost from the grid, penalty cost for carbon emissions, and sale cost to the main grid, respectively.		✓	[111]

$F = NPC + \sum_{t=1}^{8760} P_b(t) + \sum_{t=1}^{8760} P_{H_2}(t) + \sum_{t=1}^{8760} P_w(t) + P_{wt} + P_{H_2T} \quad (2-6)$	<p>NPC, $P_b(t)$, $P_{H_2}(t)$, $P_w(t)$, P_{wt}, P_{H_2T} represent the net present cost for 20 operating years, the battery, hydrogen, water, water tank, and metal hydride tank penalty, respectively.</p>	✓		[101]
$F = C_{in}^{MG} + C_{op}^{MG} \quad (2-7)$ $C_{op}^{MG} = \sum_{i=1}^L (C_{Fi} + C_{OMi} + C_{Si} + C_{Ei}) + \sum_{j=1}^M C_{OMj}^{ESS} - C_G^{MG}$	<p>The EMS cost is taken as C_{in}^{MG} (investment cost) and C_{op}^{MG} (operation cost)</p>	✓		[112]

2.5.2 Constraints in Energy Management Problem

Various constraints in applications influence the optimum microgrid energy management system, i.e., various constraints can affect the microgrid's energy management. For example, maximum and minimum limits of power generation units must be fulfilled to ensure their stability and economic performance [78], [113]. It is worth noting that another necessity of the system is the balance between generation and consumption. Residential, commercial, and industrial loads consume electric power according to their operating limits, which is an example of load or consumption constraints. The charge and discharge rates of ESSs, such as the battery, hydrogen, ultra-capacitors, etc., are also constrained. Violation of the storage constraints can affect the lifetime and efficiency of the ESSs. Operational constraints are used for ramping limits, start-up and shut-down rates of generating units, spinning, and non-spinning reserves. Microgrids rely more on renewable energy resources such as Wind, solar, and fuel cell energy resources which have been integrated to reduce carbon emissions. Solar and wind energies are stochastic in nature and have specific output limits which must be met. Similarly, the fuel cell also has specific operating limits. Therefore, while solving the optimization formulations related to the energy management for microgrids utilizing renewable resources, these operating conditions are considered constraints [57], [58]. Furthermore, micro-grid technical constraints include feeder currents, the voltage at buses, start-up and shut-down reserve constraints, frequency security aspects, and ramping limits. In some of the studies that often consider responsive loads, DR program-related constraints need to be fulfilled [32], [114]. A summary of the considered constraints used in the formulation of microgrid EMS in various literature is shown in Table 2-7.

Table 2-7: Collection of utilized micro-grid EMS constraints in the literature [32]

Supply	Demand	Generations							ESS	DR	Prices	Technical	Carbon emns.	Ref.
		MT	Solar PV	Wind	FC	EV	Grid	Biomass						
✓	✓	✓		✓					✓	✓				[115]
✓	✓			✓					✓				✓	[116]
✓	✓	✓	✓	✓	✓		✓		✓	✓	✓			[108]
✓	✓		✓	✓				✓	✓			✓		[117]
	✓		✓	✓					✓					[118]
✓	✓	✓	✓	✓	✓	✓	✓			✓	✓			[119]
✓	✓	✓	✓	✓	✓				✓	✓		✓		[120]

2.6 Optimization Techniques used in Micro-grid Energy Management Problem

Many researchers have addressed energy management problems by implementing various optimization techniques to achieve the optimal and efficient operation of micro-grid. The literature reviews show that researchers have used different approaches in order to solve the optimization problems [121]. The optimization techniques used in solving the energy management problem are shown in Figure 2-6.

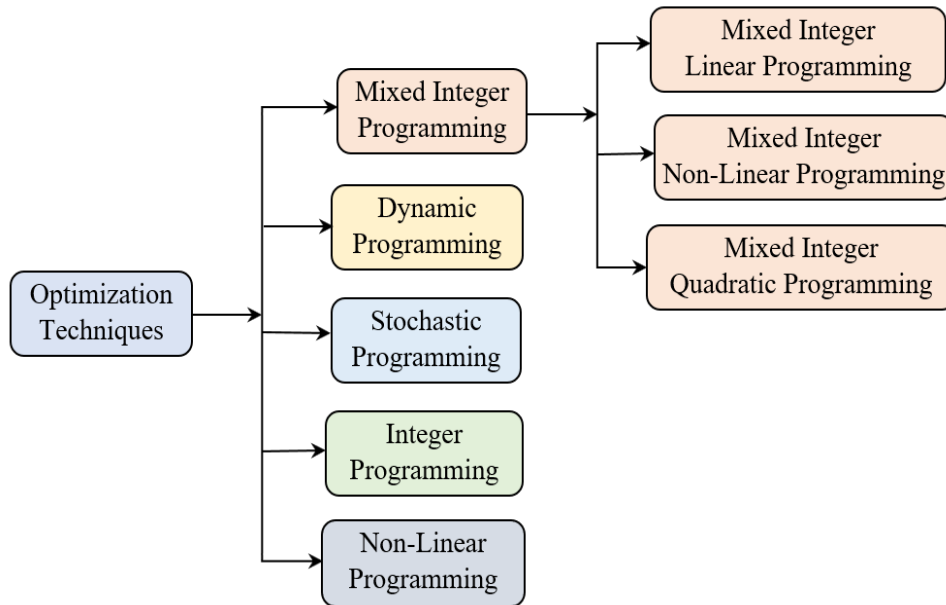


Figure 2-6: Optimization techniques used in micro-grid energy management [57]

The following sub-section discusses the relevant works related to each particular technique.

2.6.1 Energy Management Based on Linear and Non-Linear Programming Techniques

The objective functions and constraints used in linear and non-linear programming are linear functions and non-linear functions, respectively, with real-valued and whole-valued decision variables. Mixed-integer linear programming (MILP) has been suggested in various publications to address different energy-related problems. Mehleri et al. [57] minimized the total annualized cost by optimally selecting different system components and renewable resources for the smart grid. In [122], the authors presented a technical and economic approach to optimize a micro-grid based on mixed-integer linear programming (MILP). The work further presented the merits of programming the generation of distributed sources, managing the intermittency and volatility of this type of generation, and reducing load peaks. The authors solved the cost function through linear programming based on a general algebraic modeling system (GAMS). Wakui et al. [123] solved the multi-objective framework using the MILP. The framework facilitates an optimal tradeoff between low running costs and decent energy services to the end consumers. The objective includes the operating cost of distributed generators, the cost of power exchange with the main grid, the payment for demand response load, the startup and shutdown costs, the penalty costs for involuntary load curtailment, and renewable energy spillage. Manjili et al. [124] adopted a non-linear programming-based approach to optimize the system with the objective function of maximizing the revenue due to power exchange between the micro-grid and the utility grid. Comodi et al. [125] proposed a mixed-integer non-linear programming-based computational framework to evaluate the performance of a hybrid renewable energy system.

2.6.2 Energy Management Based on Dynamic Programming Techniques

Dynamic programming techniques are used to solve more complicated optimization problems that can be sequenced and discretized. Hence, the optimization problem is typically broken down into sub-problems that are solved optimally. Therefore, these solutions are then superimposed to develop an optimal solution for the original problem. Houshmand et al. [126] used a dynamic programming technique to minimize energy cost and maximize the battery's lifetime simultaneously. In [127], dynamic programming is used to solve the energy management problem in micro-grid with renewable generation sources and batteries. The objective was to minimize the cost required to satisfy the energy demand and maximize the benefits from the sale of renewable energy. A non-regulated energy market where electricity prices vacillate is used by the author and also used dynamic programming to determine the battery control actions. An algorithm based on dynamic programming for the management and control of stand-alone micro-grids was proposed in [128]. The deep learning algorithm works in real-time, requiring intra-day scheduling to obtain a control strategy for micro-grid optimization while sending information from local controllers within a centralized

management framework. Additionally, a dynamic programming method and methodology based on the rules applied to a stand-alone micro-grid containing diesel and photovoltaic generators and a battery was presented in [129]. More so, the constraints are governed by the power balance between generation and consumption, along with each distributed generator's capacity. Hence, the dynamic programming technique is adopted in minimizing the operational and emission costs. The constraints are the power balance between the supply and demand and the operating capacity of each distributed generator.

2.6.3 Energy Management Based on Stochastic and Robust Programming

Stochastic and robust programming techniques are used to solve optimization problems when the parameters have random variables. These optimization techniques were introduced to explain parameter uncertainties using uncertain boundaries. The robust optimization technique is suitable when there is a lack of information about the probability distribution function (PDF) of parameters [130]. Samadi et al. [131] used robust and stochastic programming techniques to address the challenge of load and renewable uncertainties for energy consumption scheduling in micro-grids. As uncertainties play a significant role in the micro-grid network, Farzin et al. [132], proposed a stochastic framework for optimal energy management of micro-grids during unscheduled islanding periods, providing a cost-effective solution to this problem while capturing all the inherent uncertainties. The presented framework addresses the prevailing uncertainties of islanding duration as well as prediction errors of demand and renewable power generation. Jiang et al. [133] proposed a stochastic receding-horizon control (SRHC) technique based on modified stochastic predictive model control (SMPC) to address fluctuations in renewable energy and loads. A hierarchical control mechanism was proposed by [134] to regulate and supervise the loads and dispatchable energy inside a micro-grid. Stochastic optimization was used on a low scale to avoid errors in the forecast of renewable energies. Deterministic optimization was realized on a fast scale to update the optimal dispatch conditions. In [135], a new stochastic programming algorithm is used for reactive power scheduling of a microgrid. The authors used a multi-objective function to minimize the loss and to maximize the reactive power reserve and the security margin of voltage. The author argued that the Particle Swarm Optimization algorithm performed better compared to stochastic programming algorithm.

2.7 Solution Approaches for the Energy Management Problem

Various researchers have used diverse solution methods to address the optimization problem related to energy management in microgrids. Different solution methods used in solving energy management problems are shown in Figure 2-7. These methods are discussed below, as well as the related works [57].

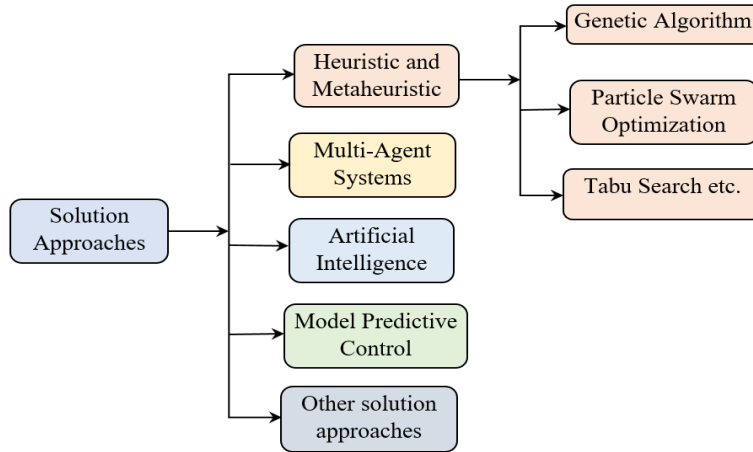


Figure 2-7: Solution approaches for energy management problem [57]

2.7.1 Heuristic and Metaheuristic Solution Approaches

Metaheuristic is a vital solution method to solve the micro-grid optimization problem. Heuristic solution methods are combined to approximate the best solution using biological evolution, genetic algorithms, and statistical mechanisms for achieving optimal operation and control of the micro-grid system. Numerous control algorithms spanning from metaheuristics and heuristics have been presented to address the problem of micro-grid power dispatch in literature. Hence, these algorithms are but are not limited to the following, genetic algorithms (GA) [136], evolutionary strategies, and algorithms for tabu searching [137]. Consequently, the emerging control methods in the literature are either computationally robust or not suitable for real-time implementation, or they may generate sub-optimal solutions. However, either the optimization problem remains non-linear in the works described above, or other essential features, such as minimum up and downtimes and demand-side programs, are overlooked [115]. Gu et al. [138] utilized heuristic algorithms to implement micro-grid electricity. Similarly, few research works [139], [140] have used the hysteresis band control (HBC) technique for energy management due to its reasonable simplicity and ease of implementation. Dufo-López et al. [141] proposed a novel control technique, optimized by genetic algorithm (GA), for the control of autonomous micro-grid consisting of renewable energy sources [PV, Wind and hydro], a fuel cell, batteries, an electrolyser, and an AC generator. This technique optimizes the hybrid system control, obtaining the values of different variables that make the system's overall net present cost (NPC) minimal.

2.7.2 Agent-Based Solution Approaches

Agent-based optimization methods used to solve micro-grid energy management problems allow decentralized management of the micro-grid and consist of sections having autonomous behavior to execute the tasks with defined objectives. Thus, these agents, including distributed generators, storage systems, and

loads, communicate with each other to achieve a minimal cost. A multi-agent system (MAS) aims to solve the optimization problems that are too difficult for a single agent [142]. Zhao et al. [143] used the multi-agent system approach to find the optimal solution by the EMS problem by assuming each member the optimal solution by the EMS problem. Karavas et al. [101] used a multi-agent system approach to the decentralized EMS problem, and optimum results were obtained. Huynh et al. [144] interconnected the multi-agent system effectively using the trust and reputation models. Logenthiran et al. [145] proposed a three-stage algorithm based on MAS to model the EMS problem in a multi-microgrid environment in which the first stage schedules each microgrid to satisfy its load. The second and third stages determine microgrid bids and export power bids, respectively.

2.7.3 Artificial Intelligence Solution Approaches

Artificial intelligence solution approaches include fuzzy logic and artificial neural networks. They are known as stochastic techniques that may solve optimization problems for the system having random variables. The dynamic nature of the RESs in micro-grid systems is caused by climatic conditions, which influence power generation. An expert system for energy management in micro-grid systems using neural networks to predict the power generation of the installed RESs was presented in [146]. Jagannathan et al. [147] developed and trained the layered ANNs strategy with Levenberg–Marquardt Back Propagation algorithm. In today's real-time energy networks, the proposed concept can be used to mitigate the risks of potential energy shortages with increased stability and seamless communication between microgrids deployed at different locations. Venayagamoorthy et al. [148] presented energy management for a micro-grid connected to the utility grid to maximize the use of renewable energies while minimizing carbon emission. The proposed energy management was modeled by two neural networks using evolutionary adaptive dynamic programming and learning concepts. The authors used one neural network to check the optimal performance of the system, while the other was used for the management strategy. Several micro-grid applications utilize fuzzy control (FC), either for tuning or supporting conventional controllers or as the central controller [149]. A fuzzy logic-based EMS for an isolated micro-grid that minimizes net present cost together with penalty cost on battery SOC, hydrogen, and water storages is proposed by [150]. The load demands are divided into three categories of electric load, transport load, and water load. Hence, hydrogen is taken as a fuel for transport load. The decision inputs for the fuzzy logic system are water, battery SOC, and system frequency.

2.7.4 Model Predictive Control Solution Approaches

The model predictive control solution approach is an optimization-based approach that can compute the control actions (i.e., set points to various units that incorporate the micro-grid) to fulfill some criteria. These

approaches are used in an application where predicting the supply and demand is essential to ensure effective management of stored energy. The main advantage of MPC is that the optimization mechanism is embedded in a control structure that integrates feedback. More so, MPC can deal with disturbances and model mismatch, re-calculating the appropriate control actions in a receding manner when new information about the microgrid state is available [4], [151]. Some of the optimization techniques (LP, QP, NLP, MILP, MIQP, metaheuristics, etc.) can be incorporated in MPC depending on the type of model used (linear, nonlinear, hybrid, etc.) and the cost function utilized in the optimization problem. The intermittent and volatile generation of renewable energy and consumers' random behavior introduces a stochastic component to the control problem. In practical applications, all of these variables are not entirely controllable. Still, knowledge of their time evolution is essential for improving micro-grid management and control, especially when using MPC approaches [15], [152]. The MPC-based optimization approach has, over time, drawn the power system network's consideration attributable to a few focal points over the Metaheuristic and Heuristic control techniques. One of the advantages of the MPC-based control scheme over other control schemes is that it focuses on the future behavior and predictions of the system and is therefore extremely appealing to systems that are inherently dependent on forecasting energy demand and the production of renewable energy, and offers a feedback mechanism that makes the system more sensitive to uncertainty and disturbance [1]. Moreover, this control strategy can address complex system constraints, integrate generation and demand projections, and finally, manage physical and operational constraints such as storage capacity or generator slew-rate power limits [31]. A model predictive control (MPC) approach has been utilized in several works on the micro-grid scheduling problem [153], [154]. The performance of deterministic and stochastic MPC in micro-grids' economic scheduling has been presented in refs [155], [156]. Zhang et al. [157] proposed a model predictive control (MPC)-based home energy management system for residential micro-grids in which all related information, such as the time-varying information of the load demand, electricity price, and renewable energy generations, are all taken into account. More so, ref [158] presented the control of a hydrogen-based domestic micro-grid by an MPC-based structure. Different works also allude to optimal generation for renewable micro-grids considering hybrid storage systems [94], [159]. Ref [160] gave an overview of the main developments in the area of stochastic model predictive control (SMPC) and further provided the various SMPC algorithms and the key theoretical challenges in stochastic predictive control without undue mathematical complexity. Ref [161] developed MPC algorithms for optimal control of distributed energy resources with a battery storage system. Ref [97] demonstrates how the MPC controller in hybrid storage systems tends to be a viable solution. MPC was also used to manage micro-networks connected to charging stations for electric vehicles [162]. Several other papers have applied the MPC controller with satisfactory results in the hybridization of ESSs. The MPC controller was used in the Vahidi and Greenwell studies [97], Del Real et al. [163], and Valverde et

al. [164]. More so, Arce et al. [104] and Bordons et al. [105] have similar technologies developed in fuel cell and battery hybridization. A careful review of the previous studies shows that, despite the use of MPCs in energy systems and industries [5], the consideration of measurable disturbance as well as an appropriate control technique, which is of great importance in addressing all the prevailing uncertainties of micro-grid operation, has not been extensively discussed. The thesis outlines a technique for considering the prediction of disturbances in the EMS while using the adaptive model predictive control (AMPC) technique. This thesis's work shows how AMPC can incorporate disturbance information to predict its effect and boost the performance of micro-grids [17].

2.8 Simulation Software and Tools used to Solve Micro-grid Energy Management Problem

The optimization algorithms used to solve the energy management problem in a micro-grid can be efficiently tested and implemented using software platforms dedicated to the modeling and simulation of the distribution systems in the presence of controllable devices, such as DGS, ESS, and controllable loads. Open-source software for static time series simulations, such as GridLAB-D [165] and OpenDSS [166], are flexible and power tools that can be used to test and analyze the performance of the energy management before its implementation into a real microgrid. The collection of simulation software and tools used to solve the micro-grid energy management problems are stipulated in Table 2-8.

Table 2-8: Simulation software and tools used to address micro-grid EM problems

Tools	Features	Ref.
MATLAB/Simulink MATPOWER	Engineers use the matrix-based programming language in power systems, telecommunications, power electronics, and control. Compatible with other programming languages such as Fortran, Java, and C++.	[167], [168]
CPLEX (IBM, Armonk, NY, USA)	CPLEX is optimization software that is compatible with Java, C++, Python, and C languages.	[169], [170]
PSCAD/EMTDC	Simulation software for power systems, HVDC, FACTS, power electronics, and control systems.	[171]
HOMER	Simulation software for modeling hybrid systems of energy generation.	[122, 172]

GAMS (GAMS Development Corp., Fairfax, VA, USA)	GAMS is a high-level language for mathematical optimization of mixed-integer linear and nonlinear systems.	[122], [173]
Dig SILENT Power Factory	The software is used for standard power system analysis and for handling wind power and distributed generation design	[174]
RSCAD (RTDS Technologies Inc., Winnipeg, MA, Canada)	RSCAD is a real-time simulator for power systems	[175]

2.9 Demand Response Techniques for Micro-grid Energy Management System

Demand-side management (DSM) is an essential feature in electrical networks that helps consumers to make decisions on their energy usage while also assisting operators in reducing peak load demand and reshaping the load profile. It consists of measures introduced by power utilities to regulate electricity use at the consumer level and are used to allow optimal use of the existing energy without the need for additional facilities [20]. The adoption of the DSM technique has a range of advantages, including improved system performance, reduced overall operational costs, supply protection, and decreased environmental effects. In the DSM context, demand response (DR) refers to consumers' actions using information (mainly prices) to adjust their loads. This type of scheme can be used to avoid unwanted peaks in the demand curve that arise at certain times throughout the day, culminating in a more beneficial rearrangement, in addition to saving money on energy bills [4], [20]. The primary aim of the DR strategies mentioned in the literature is to lower system peak load demand and running costs. Numerous research works have used DR techniques to address microgrid EM problems. Chen et al. [176] developed a scenario-based stochastic optimization approach to evaluate real-time price-based DR management of residential appliances, which can be embedded into smart meters, considering time-varying electricity price uncertainties. In [177], genetic algorithms are used for load shifting. Based on the kind of loads used in the research work, the authors modeled the inconvenience caused to the customer as a polynomial function of the shifting time. The process is aimed at minimizing the combination of generation cost and the inconvenience caused to the customer. Logenthiran et al. [20] presented a DSM technique based on load shifting technique for smart grids with many devices of various types. The day-ahead load shifting technique proposed by the authors is mathematically formulated as a minimization problem and solved with a heuristic-based evolutionary algorithm. Parisio et al. [1] formulated and solved the overall optimization problem using mixed-integer

linear programming (MILP) solver embedded in MPC. The authors integrated load curtailment into the mixed logical dynamical framework.

2.10 Micro-grid Energy Management System with Electric Vehicles Integration

The development of an energy management system for managing the use of electric vehicle batteries is a core area of research. Vehicle-to-grid (V2G) systems use the batteries in electric vehicles to store energy for an electrical network when they are not in use. Therefore, it is reported that a vehicle is only in motion for 4% of the time [23], leaving the majority of the time for it to function as an electrical energy storage facility. Furthermore, in regular operation, the batteries are recharged overnight (during times of low electricity demand) and parked in the workplace during high electricity demand, allowing the generated energy to be used to satisfy peak demand. The incorporation of V2G networks can be a crucial component of microgrid reliability, ensuring that demand and generation variations are mitigated. Hence, recent studies in the literature have based their research on optimizing the interaction between EVs and the grid [105], [5]. Wang et al. [178] formulated a stochastic optimization strategy capable of handling uncertain outputs of EVs and renewable generation. Mou et al. [179] addressed DSM for EVs by formulating the problem as convex optimization, proposing a solution by means of a decentralized algorithm. The authors also used a moving horizon approach to handle the random arrival of EVs and the inaccuracy of the forecast of non-EV load through the use of a distribution grid capacity market scheme. Mohsenian-Rad H et al. [180] proposed a closed-form solution that would allow optimal time-shifting loads with uncertain deadlines, with an emphasis on charging EVs with unpredictable departure times. The use of a game theoretical analysis was used to examine the market rivalry among electric vehicle charging stations in [181]. In the micro-grid designed by Tushar et al. [182], an electric vehicle is used as the power storage unit without a control procedure to handle the benefit of the microgrid in the case of energy exchange with an external agent. MPC was also used to manage micro-networks connected to charging stations for electric vehicles [183]. More so, in [184], the problem is solved by real-time optimization algorithms, whereas in [185], an MPC-based algorithm is presented. A multiple MPC strategy for bidirectional charging/discharging of plug-in hybrid electric vehicles are developed in [186] by regulating the batteries' SOC to control microgrid frequency stabilization. References [18] and [187] are examples of applying the interaction of microgrids with external agents.

2.11 Load Frequency Control of a Stand-Alone Micro-grid

Load frequency control (LFC) problem of a multi-area interconnected power system with a stand-alone micro-grid is more challenging as the penetration level of renewable distribution generations with the major issues of variability and uncertainty continue to increase [26]. Therefore, to ensure stand-alone micro-grid

stability, the frequency controller should be appropriately designed with due importance. Frequency and voltage regulation within specified nominal values in autonomous micro-grid operation is essential for reliable system operation and has received sufficient considerations. The battery energy storage system (BESS) used in the stand-alone micro-grid system with secondary frequency control function is to enhance the frequency control performance. Therefore, to study the system dynamics under various system disturbances, various control strategies in the area of LFC in isolated micro-grids have been reported in the literature to date. Hence, such methods range from the classical droop controls to various advanced control schemes that contribute to the secondary load frequency control of both conventional and distributed power generation systems [25]. Thus, the application of such control schemes examines various aspects of secondary load frequency control in micro-grid [188]. A fuzzy-based proportional-integral-derivative controllers (PID) controller mainly for coordinating the aqua electrolyser and fuel cell to control the micro-grid's power variation was proposed in ref [189]. Ref [188] proposes a hierarchical droop control method for the load frequency control of micro-grid. In addition, advanced control schemes based on recent LFC techniques, some of which are robust control theories [190], model predictive control (MPC) [189], sliding mode control (SMC) [191], internal mode control (IMC) [192] and neural network control (NNC) [193] have been given more considerations. It is worth noting that there are distinctive evolutionary algorithm-based proportional-integral (PI) and PID control techniques to solve multi-area power systems LFC problem [194]. Therefore, some examples of the evolutionary algorithms are differential evolution [195], firefly algorithm [196], genetic algorithm [197], hybrid-particle swarm optimization [198], and multi-objective optimization using weighted sum artificial bee colony algorithm [199] to tune the PID for the LFC problem. Recent studies did not consider physical constraints such as the DB for governor, TD at the unit control outputs, and GRC for steam turbines [200], [201]. Su et al. [202] and Han et al. [203] have proposed robust frequency control techniques taking into account the uncertainties of micro-grid system to enhance both micro-grid system robustness and its nominal performance. Hence, it is worthy of notice that MPC had recently been widely embraced due to simple and fast implementation. As a result, MPC is proven to be effective indigenously, due to its modeling flexibility, which involves a straightforward design procedure, acceptable computational time, and ease in the process-industry constraint handling. MPC also has several noteworthy points of interest, such as rapid response and stronger robustness against load disturbance and uncertainty in the parameters. One prominent feature of the MPC, is prediction of future behavior of desired control variables based on minimizing a cost function over a predefined horizon [10]. Besides, this has been a fascinating control system for LFC of power systems which can compute optimal control actions within realistic limits by simply performing an optimization procedure. Moreover, physical constraints, such as DB, TD, and GRC significantly impact the control performance of the conventional MPC algorithm [204]. As such, a more robust control scheme is needed to eliminate this drawback [205].

Besides, most of the MPCs used in load frequency control in literature are transformed from centralized to distributed/decentralized MPCs. However, just a few have presented enthusiasm in examining MPC adaptability improvements [206]. Nonetheless, little had been done recently concerning the application of the AMPC controller for optimal LFC problem of multi-area power system with renewable energy sources and practical constraints that adversely affect power system performance. The above analysis motivated the proposal for an AMPC technique for the load frequency control of a multi-area interconnected power system with renewable energy sources coupled with the addition of UPFC along both the AC tie line and the AC-DC tie line for optimal system performance.

2.12 Chapter Summary

This chapter presented a comprehensive state-of-the-art overview of energy management in microgrid systems with renewable energy generations. Hence, various control approaches for effectively operating the micro-grid systems, such as centralized, decentralized, and hierarchical management structures, were also reviewed. A concise overview of control and optimization methods was presented to define the most common and efficient EM approach in micro-grid systems. A compendium of optimization techniques, solution approaches, objectives, constraints, tools, and algorithms used to solve energy management problems in microgrids in various literature was discussed in detail. Furthermore, energy storage systems are considered an appealing choice for handling fluctuating renewable energy production trends due to improved technology sophistication, energy density, and the potential to deliver grid services, such as frequency response. Hence, a study on the key energy storage systems, which is one way to solve the energy imbalance issue due to the high penetration of RERs, is then provided. An overview of the key concepts of demand side management (DSM) and demand response technique (DRT) for energy management in microgrid systems was also presented. More so, a recent survey on the integration of EVs in microgrids, which is presently a core area of research, was summarized. A thorough review of the recent studies on the system dynamics under various system disturbances, various control strategies, and techniques in the area of LFC in isolated micro-grids has been presented in detail. Several works that adopted various control methods to solve the LFC problem in micro-grids have been reviewed. A Careful review of previous studies reveals that, despite the use of other conventional control techniques and MPCs in energy systems and industries, consideration of measurable disturbances as well as an effective control strategy, which is of great significance in resolving all the prevalent complexities of micro-grid operation, has not been thoroughly addressed. Despite the advantages of MPC over traditional control techniques and its extensive usage for most of the control aspects of micro-grid in the industrial community, some drawbacks require urgent attention as far as control performance is concerned. It is worth noticing that the conventional MPC controller is not accurate in handling varying dynamics since the internal plant model used in MPC for

prediction is constant. The optimum outcome could not be achieved by an MPC-based energy management system with the constant penalty weights when taking into account micro-grid complexities; meanwhile, the mechanism would be closed in certain outrageous circumstances. Thus, adapting the weights as indicated by the ESS state will increase the robustness of the system. The above analysis motivated the proposal for an AMPC technique, which takes the updated plant model at each time step for the current operating condition; thus, it makes accurate predictions for the new operating condition. Hence, in order to deal with changes in plant dynamics, the AMPC controller is utilized. The adaptive model predictive controller requires a discrete plant model for its control actions, which results in excellent controller performance. Thus, in terms of excellent tracking and regulating control performance, AMPC is superior to the MPC controller running in the non-adaptive mode.

CHAPTER THREE

MATHEMATICAL MODELING AND METHODOLOGY

3.1 Introduction

This chapter presents the various methods and approaches adopted in this research work. This chapter is in two folds; the first aspect discusses the mathematical modeling of the dynamic behavior of a renewable energy-based micro-grid, which is a significant concept in control engineering and, most notably, in the adaptive model predictive control scheme. A detailed derivation of a mathematical thermo-electrical model is first described, considering the wavelength-specific effects, which enhance the predictions of temperature and module performance. Subsequently, the development of the mathematical models of the renewable generation technologies (Photovoltaic system or Wind turbine generation) and energy storage system (Batteries and hydrogen-based systems) with high penetration in micro-grids are discussed in details. The state-space equations are formulated from the dynamic characteristics of the power and frequency changes in the two-area renewable energy-based micro-grid [17]. The concepts of mathematical modeling of the micro-grid system are very imperative for the design of the proposed controller (AMPC). The second part describes the research methodology used to solve different control and energy management issues in the micro-grid system of the subsequent chapters. Hence, this thesis proposed an adaptive model-based horizon control technique in the bid to addressing issues related to the control and energy management systems (EMS) in micro-grid operations. Although several techniques can be used for micro-grid control, however, AMPC offers a general framework to solve most of the problems in an integrated manner using some common ideas. The offline computation of control law is substituted with an online solution of an optimal control problem that accounts for the existing control action by the AMPC scheme [4]. This proposed algorithm is used to solve a constrained dynamic optimal control problem by repeated online optimization of the open-loop problem instead of the sophisticated offline computation of control law. The MPC offers an excellent approach to optimal control of systems subject to constraints, which justifies the reason why AMPC is referred to as an advanced control strategy with the most remarkable acceptance in the industry. Hence, the AMPC technique has some fantastic features that make it a suitable methodology for the micro-grid system used in the subsequent chapters. In addition to its logical formulation, the approach is simple to comprehend and can include constraints and nonlinearities and handle multivariate and distributed scenarios [26]. Therefore, in order to satisfy the objectives and answer the research questions stated in chapter 1 of this thesis, the AMPC algorithm is used to solve the EMS-based optimization problem in the micro-grid system in subsequent chapters. Hence, it is expedient to describe in details the fundamentals, ideas, and formulations of the AMPC technique, since it will be extensively used to solve the control and

EMS problems in the micro-grid system throughout this thesis. MATLAB/Simulink environment is the simulation tool used to model the system dynamics of the renewable energy-based micro-grids used throughout this thesis.

3.2 Derivation of the Wavelength-Based Thermo-Electrical Model of PV Module

This section describes the derivation of the mathematical model of the wavelength-based thermo-electrical model of the PV module used in chapter 4 of this thesis. The purpose of the model is to accurately predict the impact of each module wavelength on the temperature and output power of the PV module. The temperature of the PV module depends on the incident radiant power density, the electrical power output, the thermal properties of the module materials, and the heat transfer exchange with the surroundings. More so, the rate of change in the temperature of a PV module is a function of the incident light, which is said to be longwave radiation Q_{lw} , shortwave radiation Q_{sw} , output power P_{out} and heat convection to the surroundings Q_{conv} . The rate of change in the PV module temperature admits expression as [207]:

$$\Delta C_{module} \frac{dT_m}{dt} = Q_{sw} - Q_{lw} - Q_{conv} - P_{out} \quad (3-1)$$

The descriptions of all the symbols used are stipulated in the appendix section. The detailed derivations and discussions of these components are in ref [208].

3.2.1 Shortwave Radiation

The input power to the PV module through its front surface is known as shortwave radiation. The input power to the module is simply a function of the power density of the solar irradiance that is absorbed in the layers of the PV module. The detailed explanation of this component is in ref [207]. The shortwave radiation is expressed as [13], [207]:

$$Q_{sw} = \left(\int_{\lambda_1}^{\lambda_2} \alpha_{s1}(\lambda) F_{rr}(\lambda) d\lambda \right) (MA_j) + \left(\int_{\lambda_1}^{\lambda_2} \alpha_{s2}(\lambda) F_{rr}(\lambda) d\lambda \right) (A - MA_j) \quad (3-2)$$

3.2.2 Longwave Radiation

The heat exchange between the ground, the sky, and the PV module admits expression as [209]:

$$Q_{lw} = -\sigma A \left(\frac{1+\cos(\beta_{surface})}{2} \varepsilon_{sky} T_{sky}^4 + \frac{1-\cos(\beta_{surface})}{2} \varepsilon_{grd} T_{grd}^4 - \varepsilon_m T_m^4 \right) \quad (3-3)$$

The temperature of the ground is presumed to be equal to the ambient temperature due to the testing position close to the ground. Meanwhile, the tilt angle $\beta_{surface}$ is measured, the sky temperature T_{sky} is different for various sky conditions. Similarly, for a clear sky condition, the sky temperature admits expression as [209]:

$$T_{sky} = T_{amb} - \Delta T \quad (3-4)$$

Where ΔT is constant and equals 20 K. Moreover, for overcast conditions, the sky temperature is the same as the ambient temperature [209].

3.2.3 Convection Heat Transfer

The heat convection that occurs between the PV module and the air is expressed as [209]:

$$Q_{conv} = h_c A (T_m - T_{amb}) \quad (3-5)$$

Hence, the coefficients of force and free convective heat transfer are used in calculating the coefficient of heat convection, which is expressed as [210]:

$$h_c = \sqrt[3]{h_{c,free}^3 + (h_{c,forced}(WS))^3} \quad (3-6)$$

A comprehensive explanation of the computation of the convection coefficient, A , can be seen in refs [209] and [207]. Therefore, the coefficient of free heat transfer $h_{c,free}$ of the PV is expressed as:

$$h_{c,free} = \epsilon (T_m - T_{amb})^{1/3} \quad (3-7)$$

The wind speed is a significant factor that is required when estimating the value of the coefficient of forced heat transfer $h_{c,forced}$. Reference [211] presents the linear relation to compute $h_{c,forced}$ using the wind speed. It is observed in this study that utilizing a constant value of $h_{c,forced}$ over a specific time yields a large error, as a result, a formula is proposed to compute the value of $h_{c,forced}$ that put into consideration the dynamic changes of the wind speeds. The expression for computing the value of this parameter is [211]:

$$h_{c,forced} = 3.3 \left(\frac{J}{m^3 K} \right) WS + 6.5 \left(\frac{W}{m^2 K} \right) \quad (3-8)$$

Equation (3-8) is required to predict the values of $h_{c,forced}$ accurately.

3.2.4 Output Power

The temperature of a PV cell immensely influences its output power. The relation between the electrical and thermal aspects of the PV cell is mainly interactive. The M series-connected PV cells in relation to its output power admit expression as [14]:

$$P_{out} = MVI \quad (3-9)$$

This study utilized a two-diode equivalent-circuit model for an excellent PV cell performance [14]. The PV cell output current and the terminal voltage are related by the mathematical formulation, which admits expression as [14]:

$$I = I_{ph} - I_{O1} \left[\exp\left(\frac{V+IR_s}{nKT_m}\right) - 1 \right] - I_{O2} \left[\exp\left(\frac{V+IR_s}{nKT_m}\right) - 1 \right] - \frac{V+IR_s}{R_p} \quad (3-10)$$

Therefore, in order for the last term of Equation (3-10) to be negligibly small, the shunt resistance R_p is presumed to be sufficiently large. Hence, the solar-induced or photonic current admits expression as:

$$I_{ph} = QA_j \int_{\lambda_1}^{\lambda_2} \phi_{rr}(\lambda) \alpha_c(\lambda) IQE(\lambda) d\lambda \quad (3-11)$$

The photon energy admits expression as [14]:

$$E(\lambda) = \frac{hc}{\lambda} \quad (3-12)$$

Furthermore, utilizing the irradiance at each wavelength and Equation (3-12), the photons number that travels in a similar wavelength is expressed as [209]:

$$\phi_{rr}(\lambda) = \frac{F_{rr}(\lambda)}{E(\lambda)} \quad (3-13)$$

The absorption coefficient, α_c determines the fraction of the photonic flux that the material of the PV cell absorbs per each wavelength. The internal quantum efficiency (IQE) is a property of the PV cell construction. A model is required to compute the reverse saturation current, which changes dramatically with the temperature of the PV cell. Therefore, it is expressed as [209]:

$$I_0 = I_{0r} \left(\frac{T_m}{T_r}\right)^3 \exp \left[QE_g \left(\frac{1}{T_r} - \frac{1}{T_m} \right) / (K_n) \right] \quad (3-14)$$

Therefore, the determination of this reference saturation current I_{0r} is frequently at the reference temperature T_r . Similarly, the short circuit current I_{sc} and the open-circuit voltage V_{oc} ought to be measured at the reference temperature. Hence, the reference saturation current I_{0r} admits expression as [209]:

$$I_{0r} = \frac{I_{sc}}{\left[\exp(QV_{oc}/(MK_nT_r)) - 1 \right]} \quad (3-15)$$

Furthermore, in order to track the maximum power point, Equation (3-10) is solved mathematically for the current that produces the maximum output power to compute the maximum output power of the PV cells. On the other hand, we can use empirical relations to compute the maximum output power. Therefore, the maximum output power is estimated with the following expression [14]:

$$P_{max} = F_{factor} V_{oc} I_{sc} \quad (3-16)$$

However, it is presumed that the impact of the series resistance on the short-circuit current is negligibly small, that is, $I_{sc} \approx I_{ph}$. Consequently, the open-circuit voltage admits expression as [14]:

$$V_{oc} = \frac{nKT_m}{Q} \ln \left(\frac{I_{ph}}{I_0} + 1 \right) \quad (3-17)$$

It is evident from Equation (3-17), due to the changes in the open-circuit voltage, the fill factor likewise depends on temperature. The empirical formula commonly used to estimate the fill factor is [14]:

$$F_{factor} = \frac{V_n - \ln(V_n + 0.72)}{V_n + 1} \quad (3-18)$$

Where V_n is the normalized open-circuit voltage, which is expressed as [14]:

$$V_n = \frac{q}{nKT_m} V_{oc} \quad (3-19)$$

3.2.5 Heat Capacity

The summation of the heat capacities of each layer of the PV module is the module's heat capacity. Therefore, the capacity of the module for individual component made of some material, signified by m is expressed as:

$$C_{module} = \sum C_m \rho_m A_m d_m \quad (3-20)$$

3.2.6 Integration of the Thermo-Electrical Model of PV Module

The integration of the thermo-electrical model of the PV module is implemented by substituting Equations (3-2) - (3-5), and (3-20) into Equation (3-1). The general expression for the rate of change in the module temperature for the model under study is [208]:

$$\Delta C_{module} = \left(\left(\int_{\lambda_1}^{\lambda_2} \alpha_{s1}(\lambda) F_{rr}(\lambda) d\lambda \right) (MA_j) + \left(\int_{\lambda_1}^{\lambda_2} \alpha_{s2}(\lambda) F_{rr}(\lambda) d\lambda \right) (A - MA_j) \right) - \sigma A \left(\frac{1 + \cos(\beta_{surface})}{2} \varepsilon_{sky} T_{sky}^4 + \frac{1 - \cos(\beta_{surface})}{2} \varepsilon_{grad} T_{grad}^4 - \varepsilon_m T_m^4 \right) - \left(\sqrt[3]{h_{c,free}^3 + h_{c,forced}^3} \right) A (T_m - T_{amb}) - MVI \quad (3-21)$$

Thus, this model under study is a nonlinear model, which requires numerical analysis to be estimated. For instance, in order to compute the module temperature at every time step, the Euler method is utilized, which is expressed as follows [208]:

$$T_m(t + t_{step}) = T_m(t) + t_{step} \frac{dT_m}{dt} \quad (3-22)$$

3.2.7 Generation of Controller Reference

The maximum output power signal is a function of the PV module temperature and the ambient temperature, as shown in Equation (3-21). Consequently, in order to obtain optimal output power at a given ambient temperature, the PV module temperature is used as the control signal. Hence, the block diagram for the plant model, controller, and reference generator is depicted in Figure 3-1 [212].

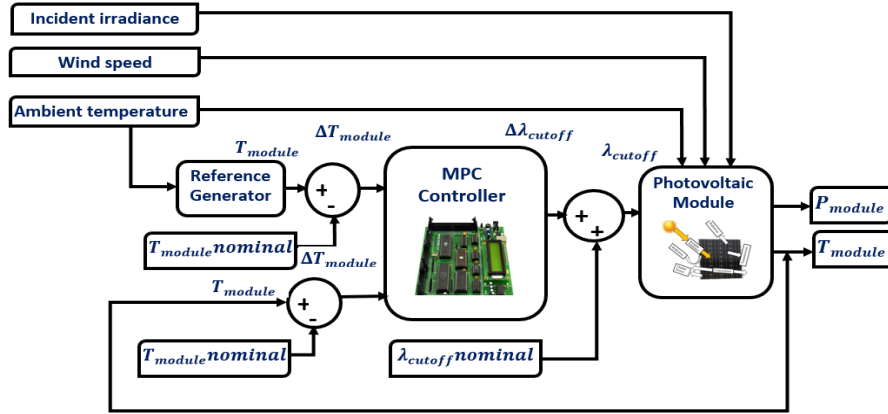


Figure 3-1: Block representation of the plant, controller, and reference generator

3.3 System Model Development of the Stand-alone Micro-grid

This section further explains the development of the system model of the stand-alone micro-grid system used in chapter 4 of this thesis. Hence, chapter 4 of this thesis is set to investigate an optimal control strategy that will efficiently manage a stand-alone residential micro-grid comprising renewable and non-renewable energy sources. The PV module described in the previous section is used as the renewable energy source of the stand-alone micro-grid investigated in this section. The variations in power output due to solar geometry, temperature changes, efficiency changes, etc. are neglected and assumed to be captured by the output power profile. This is a valid assumption for the purposes of hourly scheduling of power delivery by the AMPC controller as the solar system often contains energy storage units that can buffer energy. Such a buffering allows for minor deviations due to photovoltaic cell output, while major deviations can be readjusted in the power profile provided to the supervisory controller on a timely basis. The power output of the solar system is considered as $P_{solar}(t)$.

3.3.1 Diesel Generator

The first-order lag equation used to describe the dynamics of the diesel engine is taken from ref [213]. Since the dynamics of the generation system attached to the diesel engine is faster than the diesel engine, hence, the overall power dynamics can be assumed mostly dependent on the dynamics of the diesel engine. Hence, Equation (3-23) sufficiently describes the power output dynamics of the diesel generator at a supervisory level. The AMPC controller provides a power output command to the Diesel Generator. A local controller capable of following this commanded output is assumed and provides the required control inputs to meet the commanded power output.

$$\dot{P}_d = -\frac{1}{\tau_d} P_d + \frac{U_d}{\tau_d} \quad (3-23)$$

3.3.2 Storage System Power

The power dynamics of the storage system are modeled using first-order lag dynamics represented by Equation (3-24). The equation represents the lag between the power command and the power delivery and is modeled after the power dynamics equation presented in ref [214]. This modeling approach was considered sufficient at the supervisory level. Detailed dynamics of the storage system and its power delivery can be considered in a local-level controller.

$$\dot{P}_{SS} = -\frac{1}{\tau_{SS}}P_{SS} + \frac{U_{SS}}{\tau_{SS}} \quad (3-24)$$

Where, τ_{SS} is the average delay incurred between power command and delivery in sec, and U_{SS} is the power command by the AMPC controller in kW.

3.3.3 Storage System

The capacity of the storage system considered is 80 kWh. The storage type considered is for a battery bank; meanwhile, this can be substituted for any storage system. The battery model is obtained from ref [215], where a self-charge is also considered. The State of Charge (SOC) of the battery is the ratio of the residential energy to the total energy of the battery. It is very imperative to know the SOC of the battery for accurate control of the micro-grid. The equation for the charging dynamics of the storage system is given as:

$$\dot{E}_{SS} = -\delta_{SS}E_{SS} - \frac{P_{SS}\eta_{chrg}}{E_{SS}^{max}} \quad (3-25)$$

Where, E_{SS} is the current SOC, which is the representative of the energy content in the battery, P_{SS} is the power entering the battery in kW, η_{chrg} is the charging efficiency of the battery and E_{SS}^{max} is the maximum storage capacity of the battery in kWh. More so, the equation for the discharge dynamics of the storage system is given as:

$$\dot{E}_{SS} = -\delta_{SS}E_{SS} - \frac{P_{SS}}{E_{SS}^{max}\eta_{dis}} \quad (3-26)$$

Where, η_{dis} is the discharging efficiency of the battery.

3.3.4 Description of the Control Scheme

The AMPC technique used to solve an optimal power reference-tracking problem, where the consumption of energy from the diesel generator is minimized while maximizing the efficiency of the storage bank in chapter 4, is depicted in Figure 3-6. The AMPC controller provides control commands to the various components on the electric grid. The main objective is to make maximum use of the renewable power source, i.e., the solar system, while using the least amount of power from the diesel generator. The AMPC controller does not directly control the operation of the solar system but allows for the maximization of

solar power usage by tracking a reduced power profile. The state information fed back to the controller consists of information on the power delivery by the DG, storage system, and its current energy level along with power output by the solar system. The controller used a technique that solves the micro-grid system as a continuous system given a time horizon and selects piece-wise optimal mode sequences and control inputs. The controller then sends the power commands U to the respective systems on the power grid. The current state information is then returned from the systems back to the controller to reduce the accumulation of modeling errors, and the controller increments its prediction horizon. This process is repeated iteratively for each partition during the prediction horizon.

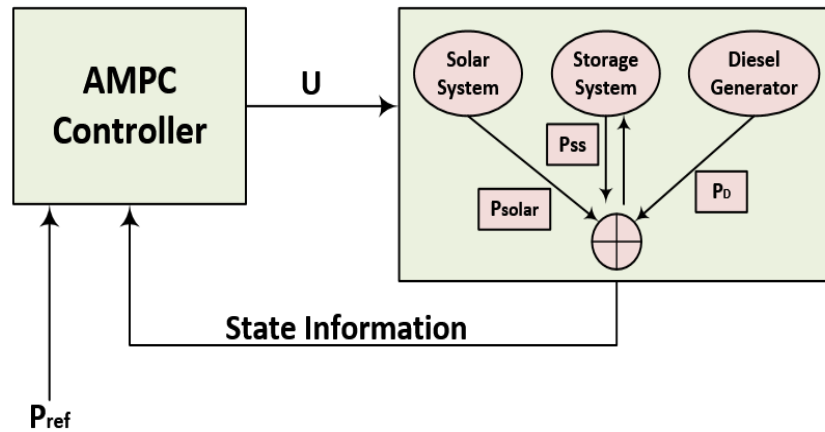


Figure 3-2: Implementation of the AMPC scheme

3.3.5 Formulations of the AMPC Optimization Problem

This section describes the formulation and implementation of the adaptive model predictive control on the stand-alone micro-grid system, where a convex analysis is enforced on the mode switching, to guarantee autonomy and best performance from the controller and the optimization algorithm. The assumptions, cost function, system dynamics, constraints are discussed below;

3.3.5.1 Assumptions

- Generator and storage system charge/discharge efficiencies are assumed constant.
- Power Transmission Line loss is assumed as part of the reference load profile

3.3.5.2 System Dynamics

The state variables, x , and the control inputs admit expressions as:

$$x = \begin{bmatrix} E_{ss} \\ P_{ss} \\ P_d \end{bmatrix}, \quad u = \begin{bmatrix} U_{ss} \\ U_d \end{bmatrix} \quad (3-27)$$

Then, the control system is modeled as a continuous linear time-invariant system with three states variables and two control inputs as follows:

$$\dot{x} = A_{\sigma}x + Bu \quad \sigma = 0,1 \quad (3-28)$$

Where each hybrid mode is represented by a different dynamic stated in the matrix A:

$$A_{\sigma=0} = \begin{bmatrix} -\delta_{ss} & -1/(\eta_{dis}E_{ss}^{max}) & 0 \\ 0 & -1/\tau_{ss} & 0 \\ 0 & 0 & -1/\tau_d \end{bmatrix} \quad A_{\sigma=1} = \begin{bmatrix} -\delta_{ss} & -\eta_{chrg}/(E_{ss}^{max}) & 0 \\ 0 & -1/\tau_{ss} & 0 \\ 0 & 0 & -1/\tau_d \end{bmatrix} \quad (3-29)$$

The inputs are related to the states through B matrix, which remains the same regardless of the operation mode.

$$B = \begin{bmatrix} 0 & 0 \\ 1/\tau_{ss} & 0 \\ 0 & 1/\tau_d \end{bmatrix} \quad (3-30)$$

3.3.5.3 Cost Function

The optimization problem is formulated as follows:

$$\underset{u_{\sigma=0}, u_{\sigma=1}}{\text{minimize}} \quad v \int_{t_0}^{t_f} w_1 P_d^2 + w_2 (E_{ss} - E_{ss}^{nom})^2 + w_3 (P_d + P_{ss} - P_{Load}^{ref}(t))^2 + \Psi(x) \quad (3-31)$$

Subject to $\dot{x} = \hat{A}x + B\hat{u}$

$$\underline{x} \leq x \leq \bar{x}$$

Where, $\hat{A} = vA_{\sigma=0} + (1-v)A_{\sigma=1} \quad v \in [0,1]$

$$\hat{u} = vu_{\sigma=0} + (1-v)u_{\sigma=1}$$

$$\Psi(x) = (x < \underline{x})(x - \underline{x})^2 + (x > \bar{x})(x - \bar{x})^2$$

Where w_x are tracking weights, $w_1 = 5, w_2 = 2$ and $w_3 = 40$. The optimizer solves this problem as an embedded problem where $v \in [0,1]$.

3.3.5.4 State Constraints

In an attempt to model the system to be able to deliver a realistic power load, it is imperative that the storage bank be protected from deep discharge and overcharge. This implies that the net energy in the storage bank should be constrained for efficient usage of the battery. Furthermore, the power input/output from the battery needs to accommodate the maximum and minimum capacities. The constraints on the diesel generator are strictly determined by the model used. Equations (3-28) to (3-32) are used to enforce power and energy constraints.

$$\begin{bmatrix} E_{ss}^{min} \\ P_{ss}^{min} \\ P_d^{min} \end{bmatrix} \leq \begin{bmatrix} E_{ss} \\ P_{ss} \\ P_d \end{bmatrix} \leq \begin{bmatrix} E_{ss}^{max} \\ P_{ss}^{max} \\ P_d^{max} \end{bmatrix} \quad (3-32a)$$

Furthermore, the initial state, initial time, and final time are fixed, while the final state is free. So that:

$$E_{ss,t_0} = E_{ss,nom}$$

The power balance equation admits expression as:

$$P_{solar} + P_{ss} + P_d = P_{load} \quad (3-32b)$$

The control outputs from the MPC depend on the current mode of operation of the system, v . These outputs are determined by using two different approaches using the embedded value of v provided by the optimization algorithm:

- Logic Projection

The hybrid mode v is computed as a continuous state ranging from $[0, 1]$. Once a value has been assigned, this is projected to either mode 0 or mode 1, satisfying the following logic:

$$\begin{aligned} & \text{if } v > 0.5 \text{ then } v = 1 \\ & \text{else } v = 0 \end{aligned}$$

- Projection Based on U_{ss}

In this case, the sign of the control input U_{ss} determines whether the system goes to charging or discharging mode. i.e.,

$$\begin{aligned} & \text{if } U_{ss} > 0 \text{ then } v = 0 \\ & \text{else } v = 1 \end{aligned}$$

From either logic, an optimal sequence of control inputs is obtained for the entire time horizon, which minimizes the power delivered from the diesel generator while maximizing the efficiency of the storage bank. The whole process is repeated for each time window until the total simulation time has been spanned. Each iteration produces an optimal control output and optimal hybrid mode, which can then be compiled into the optimal sequences, as shown in the simulation results in chapter 4.

3.4 Dynamic Modeling of the Renewable-based Micro-grid Components

This section describes the modeling of the dynamic behavior of a renewable energy-based micro-grid used in chapters 5-7 of this thesis, which is a significant concept in control engineering and, most notably, in the AMPC control scheme. More so, the mathematical models of the renewable generation technologies (Photovoltaic or Wind turbine system), and energy storage system (Batteries and hydrogen-based systems) with high penetration in micro-grids are discussed elaborately in this section. Note that, since the main idea of these models is to build the simplest models that measure up with the objectives, then the model design

must be precise and simple enough to prevent computational burden when it is numerically solved. In general, the essence of modeling in control engineering is for control design and simulation to analyze the system behavior. Furthermore, accurate modeling is a significant step forward for energy management and helps the optimization algorithm adapts to exact dispatch decisions [5], [68]. In the AMPC control scheme, model design plays a significant role; meanwhile, these models are incorporated into an optimization problem, which needs simple formulations. In the following subsections, we modeled each of the micro-grid components in the proposed network of micro-grids used in chapters 5-7 separately.

3.4.1 Modeling of the Distributed Energy Resources

The mathematical models of the DERs (renewable energy-based resources) utilized in the micro-grids of chapters 5-7 are described as follows:

3.4.1.1 Photovoltaic System Modeling

Photovoltaic (PV) cells are electronic devices that generate electrical energy from solar radiation. Therefore, the energy the cells transform depends on the temperature, material properties, and solar radiation. This study utilized a two-diode equivalent-circuit model for excellent PV cell performance [14]. The mathematical equations, which models the current-voltage behavior of the ideal PV cell, therefore admits expressions as [14]:

$$I = I_{ph} - I_{D1} - I_{D2} - I_{sh} \quad (3-33)$$

$$I_{D1} = I_{O1} \left[\exp\left(\frac{qV}{A_1 kT}\right) - 1 \right] \quad (3-34)$$

$$I_{D2} = I_{O2} \left[\exp\left(\frac{qV}{A_2 kT}\right) - 1 \right] \quad (3-35)$$

$$I = I_{ph} - I_{O1} \left[\exp\left(\frac{qV}{A_1 kT}\right) - 1 \right] - I_{O2} \left[\exp\left(\frac{qV}{A_2 kT}\right) - 1 \right] - I_{sh} \quad (3-36)$$

Equation (3-36) is the fundamental equation of the PV cell model, which does not reflect the functional I-V characteristics of PV cells. Practical PV module consists of various elements, such as R_s , and R_p , that need to be introduced into the above Equation (3-36). The functional output current of the PV cell admits expression as [216]:

$$I = I_{ph} - I_{O1} \left[\exp\left(\frac{V+IR_s}{A_1 V_t}\right) - 1 \right] - I_{O2} \left[\exp\left(\frac{V+IR_s}{A_2 V_t}\right) - 1 \right] - \frac{V+IR_s}{R_p} \quad (3-37)$$

Where,

$$V_t = \frac{N_s kT}{q} \quad (3-38)$$

Where, I_{ph} is the photo-generated current by a PV cell, I_{D1}, I_{D2} are the diode currents, I_{O1}, I_{O2} are the reverse saturation current of diodes D_1, D_2 , in Ampere. V_t is the thermal voltage, V is the cell output voltage, N_s, N_p is the number of PV cells connected in series and parallel, k is the Boltzmann constant ($1.38 * 10^{-23}$ J/K), q is the charge on the electron ($1.602 * 10^{-19}$). A_1, A_2 are the ideality factors of diodes D_1, D_2 , T is the Reference cell-operating temperature, 20°C. The PV cell output current, as defined by equation (3-37), is the single PV unit. Hence, in order to achieve the desired voltage and current output level, the PV cells are connected in series and parallel. Where the PV modules are composed of parallel-connected N_p cells, the output current of the PV module admits expression as [14]:

$$I_{module} = I_{cell} * N_p \quad (3-39)$$

The equation for the PV current as a function of temperature and irradiance admits expression as:

$$I_{ph} = (I_{sc} + K_i \Delta T) \frac{G}{G_{STC}} \quad (3-40)$$

Where I_{sc} is the short circuit current under standard test conditions (STC), $\Delta T = T - T_{STC}$ (In Kelvin, $T_{STC} = 25^\circ\text{C}$) are the actual and nominal temperature, G is the surface irradiance of the cell, G_{STC} is the nominal Irradiance under STC ($1000\text{W}/\text{m}^2$, K_i is the short circuit current coefficient, usually provided by the manufacturer. The diode saturation current I_{O1} is dependent on temperature and therefore admits expression as [14]:

$$I_{O1} = I_o, n \left(\frac{T_n}{T} \right)^3 \exp \left[\frac{qE_g}{A_1 k} \left(\frac{1}{T_n} - \frac{1}{T} \right) \right] \quad (3-41)$$

Where E_g is the band-gap energy of the semi-conductor ($E_g = 1.12\text{eV}$ for the polycrystalline silicon at 25°C , I_o, n is the standard test condition (STC) nominal saturation current, which admits expression as:

$$I_o, n = \frac{I_{sc, n}}{\left[\exp \left(\frac{V_{oc, n}}{V_{t, n} A} \right) - 1 \right]} \quad (3-42)$$

Considering temperature variations, an improved equation to describe the saturation current is obtained from Equations (3-41) and (3-42), which admits expression as [217]:

$$I_o = \frac{(I_{sc, n} + K_i \Delta T)}{\exp \left[(V_{oc, n} + K_v \Delta T) / A_1 V_{t, n} \right] - 1} \quad (3-43)$$

Where K_v is the open-circuit voltage coefficient (value is available on datasheets). More so, a power inverter or a DC/DC converter is used to interface the photovoltaic panel with the micro-grid. Maximum Power Point Tracking (MPPT) algorithm is used to track the optimal generation point, which works efficiently with the power electronics associated with the photovoltaic panel.

3.4.1.2 Wind Turbine System Modeling

Wind energy, which is a sustainable power source, uses the rotor blades to convert the kinetic energy in the wind velocity into electrical energy utilizing a technique known as aerodynamic techniques. Wind power has many points of interest over the different forms of energy, such as excellent return on investment and high-power density. Wind turbines are used to transform wind energy into electric energy. Note that the wind energy system converts kinetic energy from the wind into electrical energy. Hence, the kinetic energy generated by the dynamic system admits expression as [216]:

$$E_k = \frac{1}{2}mV^2 \quad (3-44)$$

Where m is the air mass, V is the velocity of the wind. Similarly, the mass (m) is given as:

$$m = \rho(Ad) \quad (3-45)$$

Where ρ is the air density in Kg/m^3 , A is the rotor blade swept area in m^2 and d is the distance covered by the wind in m . Moreover, according to Betz theory, the wind turbine kinetic energy for time (t), i.e., mechanical power (P_w), which is captured by the corresponding mechanical torque and wind turbine admit expressions as [218]:

$$P_w = \frac{E_k}{t} = \frac{\frac{1}{2}\rho Adv^2}{t} = \frac{1}{2}\rho AdV^3 = \frac{1}{2}\pi\rho R^2V^3C_p \quad (3-46)$$

$$T_m = \frac{P_w}{\omega_w} = \frac{1}{2}\pi\rho R^2V^3C_p \frac{1}{\omega_w} \quad (3-47)$$

Wind turbine active power depends on the turbine power coefficient or otherwise known as turbine efficiency, which represents the turbine conversion efficiency, and it is given by $C_p(\lambda, \beta)$. The power or wind energy utilization coefficient of the turbine is a function of tip speed ratio, λ and pitch angle, β .

Thus, the tip speed ratio, λ , is given as the turbine speed to the wind speed ratio, which is given as:

$$\lambda = \frac{\omega R}{V} \quad (3-48)$$

Where ω is the turbine angular speed, R is the turbine radius. Similarly, the wind turbine stored real power and the wind turbine torque expressed by Equations (3-49) and (3-50), respectively, can comprehensively be written as utilized in this research work as:

$$P_w = \frac{1}{2}C_p(\lambda, \beta)\rho Adv^3 \quad (3-49)$$

$$T_m = \frac{1}{2}C_t(\lambda, \beta)\rho ARV^2 \quad (3-50)$$

Where the wind turbine torque coefficient is defined as:

$$C_t(\lambda, \beta) = C_p(\lambda, \beta)/\lambda \quad (3-51)$$

Hence, the most extreme power can be extricated from the turbine just when $C_p(\lambda, \beta)$ is 0.48, λ is 8.1, and β is 0. Therefore, the turbine power coefficient $C_p(\lambda, \beta)$, which is a non-linear function, admits expression using the generic function [219]:

$$C_p(\lambda, \beta) = 0.0068\lambda + 0.5176 \left(\frac{116}{\lambda_i} - 0.4\beta - 5 \right) e^{\frac{-21}{\lambda_i}} \quad (3-52)$$

Where,

$$\frac{1}{\lambda_i} = \frac{1}{\lambda + 0.08\beta} - \frac{0.035}{\beta^3 + 1} \quad (3-53)$$

Note that if the pitch angle $\beta=0$, then C_p is a function of the turbine tip speed ratio, λ . Equation (3-52) is reduced to:

$$C_p(\lambda, \beta) = 0.0068\lambda + 0.5176 \left(\frac{116}{\lambda_i} - 5 \right) e^{\frac{-21}{\lambda_i}} \quad (3-54)$$

It is worth mentioning that the wind turbine used in the simulation utilized Equation (3-54) to calculate the turbine power coefficient. Similarly, the transmission of energy via the gearbox to the generator is given as:

$$\frac{d\omega_{gen}}{dt} = \frac{T - T_w}{J_{eq}} - \frac{B_m}{J_{eq}} \omega_{gen} \quad (3-55)$$

Where ω_{gen} is the generator angular speed, T is the mechanical torque, B_m is the damping coefficient, T_w is the aerodynamic torque and J_{eq} is the equivalent rotational inertia of the generator, where [220], [221]:

$$J_{eq} = J_{gen} + \frac{J_w}{n_g^2} \quad (3-56)$$

Where J_w and J_{gen} are the rotational inertia corresponding to generator and rotor and n_g is the gear ratio. Similar to the photovoltaic case, wind turbines also utilize the MPPT control algorithm for optimal power output.

3.4.2 Modeling of the Distributed Energy Storage System

ESSs installation in an electrical power network gives the prospect for better economic dispatch management of renewable energies. In the meantime, the control scheme must be able to determine which ESS to use in real-time, depending on the operating conditions. Similarly, the mathematical models of the distributed energy storage systems utilized in the micro-grid architecture of chapters 5-7 are described as follows:

3.4.2.1 Battery Storage System Modeling

The Battery Energy Storage System (BESS) is an electrical energy storage device. The two battery types utilized in this study are lead-acid and lithium-ion batteries. Therefore, to improve the stability and reliability of the micro-grid network, it is appropriate to introduce the Energy Storage Systems, ESS, into the micro-grid network. Hence, the ESS discharges its power and supplies the loads in order to meet any local shortage in supplying the loads to the customer [68]. It is worth noting that the operation of the micro-grid EMS is simple if only one ESS is used, such as a battery, i.e., the imbalance between generation and demand is absorbed by the battery, given its SOC is between the upper and lower limits. Meanwhile, it is expected that power generation will be halted or that excess energy will be sold to the grid (for grid-connected micro-grids) if the upper limit is reached. Hence, more loads must be disconnected, or the lack of energy must be purchased from the grid, should it reach its lower limit. More so, the criterion is mainly to utilize the control technique to schedule the appropriate storage system with higher efficiency to balance the mismatch between the generation and demand, in the presence of several energy storage systems (such as batteries, hydrogen, ultra-capacitors, or flywheels) [222], [223]. The switching rules among various ESSs are often-times based on the stored energy. The fuel cell and electrolyser switching during micro-grid operation that utilizes batteries and hydrogen as energy buffer are usually based on the SOC level of the battery. i.e., the fuel cell is activated as soon as the level of SOC is deficient. Similarly, the electrolyser is switched ON, should the battery SOC level be high as per given limits. Therefore, it is expedient to protect the battery bank from undercharging (low SOC level) or overcharging (high SOC level). In this case, in order to prolong the life span (integrity) of the battery, energy is transferred from the grid by the control system. The mathematical model of the battery storage is based on a basic voltage source model and an internal resistor. The battery voltage is expressed as a function of the battery power and battery current, which is given as [220]:

$$V_{bt} = V_{bt,int} - R_i I_{bt} \quad (3-57)$$

Moreover, charging and discharging of batteries are modeled differently. Thus, when the battery is charging:

$$V_{bt,int} = V_{bt,0} - K_{bt} \frac{C_{max,bt}}{C_{max,bt} - C_{bt,t}} I_{bt,ch} - K_{bt} \frac{C_{max,bt}(\delta_{bt,ch})}{C_{max,bt} - C_{bt,t}} C_{bt,t} + A_{bt} e^{-B_{bt} C_{bt,t}} \quad (3-58)$$

Similarly, during the discharging period of the battery, the expression is as follows:

$$V_{bt,int} = V_{bt,0} - K_{bt} \frac{C_{max,bt}}{C_{max,bt} - C_{bt,t}} I_{bt,dis} - K_{bt} \frac{C_{max,bt}(\delta_{bt,dis})}{C_{bt,t} + 0.1 C_{max,bt}} C_{bt,t} + A_{bt} e^{-B_{bt} C_{bt,t}} \quad (3-59)$$

Where $V_{bt,0}$ is the open circuit battery voltage, V, K_{bt} is the polarization constant (internal parameter of the battery, V), $C_{max,bt}$ is the maximum capacity (Ah) of the battery, $C_{bt,t}$ is the battery current capacity (Ah),

$I_{bt,ch}$ and $I_{bt,dis}$ are the charge and discharge currents, respectively. Note that this study assumed the $C_{max,bt} \neq C_{bt,t}$, which might result due to aging degradation of the battery. This assumption was necessary in order for the value of $V_{bt,int}$ not to approach ∞ during charging and discharging. Thus, $\delta_{bt,ch}$ and $\delta_{bt,dis}$ are the binary variables of the charge and discharge state of the battery respectively, A_{bt} is the amplitude of the exponential zone, V, B_{bt} is the inverse of the time constant in the exponential zone (Ah_{-1}), R_i is the internal ohmic battery resistor. The battery capacity (Ah) admits expression as [224]:

$$C_{bt,t} = \int_0^t I_{bt,t} dt \quad (3-60)$$

Lastly, the battery state of charge (SOC) is related to the battery capacity as follows:

$$SOC_{bt,t} = \frac{C_{bt,t}}{C_{max,bt}} \quad (3-61)$$

Therefore, in order to model the dynamic behavior of the battery storage, the battery State of Charge, SOC_{BS} , is taken into account as the state variable. The charging and discharging power are segregated, consequent to the disparity in power flow efficiencies between charging and discharging (i.e., $\eta = P_{out}/P_{in}$). Hence, the battery storage discrete-time model admits expression as [18]:

$$SOC_{BS}(t_{k+1}) = SOC_{BS}(t_k) + \frac{\eta_{ch} P_{ch}(t_k) T_s}{C_{BS,r}} - \frac{P_{dis}(t_k) T_s}{\eta_{dis} C_{BS,r}} \quad (3-62)$$

Where the battery charging and discharging powers are P_{ch} and P_{dis} , respectively, kW, the storage battery charging and discharging efficiencies are η_{ch} and η_{dis} , respectively, 90% and the battery storage rated capacity is $C_{BS,r}$, kWh.

3.4.2.2 Ultracapacitor Dynamical Modeling

An ultracapacitor is an electrical component used to store electrical energy. It consists of two metal plates separated by a nonconducting dielectric layer. The energy stored in a capacitor admits expression as:

$$E = \frac{1}{2} C U^2 \quad (3-63)$$

where C is the capacitance (in Farads), and U is the voltage between terminals. The stored charge Q in the capacitor is obtained by the product of the capacitance and the voltage. Reference [225] describes the comparison between the dynamical models of ultracapacitors. Therefore, only the simplified model of the ultracapacitor is developed in this section. Hence, the total capacitance of an ultracapacitor $C_{uc}(t)$ depends on voltage, and it is expressed as [226], [227]:

$$C_{uc}(t) = C_{uc,0} + k_{uc} U_{uc}(t) \quad (3-64)$$

where $C_{uc,0}$ is the initial capacitance (electrostatic capacitance) of the capacitor, and k_{uc} is a constant that models the linear dependence with the voltage.

$$I_{uc}(t) = \frac{dQ_{uc}}{dt} = \frac{d(C_{uc}(t)U_{uc}(t))}{dt} \quad (3-65)$$

$$I_{uc}(t) = \left(C_{uc,0} + 2k_{uc}U_{uc}(t) \right) \frac{dU_{uc}(t)}{dt} \quad (3-66)$$

The following expression is used to model the energy stored in the ultracapacitor:

$$E_{uc}(t) = \frac{1}{2} \left(C_{uc,0} + \frac{4}{3}k_{uc}U_{uc}(t) \right) U_{uc}^2(t) \quad (3-67)$$

The SOC is expressed as the ratio between the current stored energy and its maximum value, which is given as:

$$SOC_{uc}(t) = \frac{\left(C_{uc,0} + \frac{4}{3}k_{uc}U_{uc}(t) \right) U_{uc}^2(t)}{\left(C_{uc,0} + \frac{4}{3}k_{uc}U_{uc}^{max}(t) \right) \left(U_{uc}^{max}(t) \right)^2} \quad (3-68)$$

This mathematical model is used in the MATLAB/Simulink of chapters 5-7, considering constant capacitance and the model of the conventional capacitor.

3.4.3 Modeling of the Hydrogen Storage System

Hydrogen is often seen as a potential option to be used as an energy storage device, particularly when hydrogen is generated with sustainable sources of energy. A complete hydrogen-energy storage system consists of a system for hydrogen production, a hydrogen storage system, and another system for converting hydrogen into electricity, such as a fuel cell or a hydrogen engine. Nonetheless, the most intriguing choice to use in micro-grids is hydrogen production by coupling electrolyser to renewable sources. In this study, a metal hydride is used to store hydrogen, in which the fuel cell can easily double the conversion capacity for the normal operating temperature to convert into electricity [220].

3.4.3.1 Mathematical Modeling of Electrolyser

The electrolysers are electrochemical devices, which, when the direct current is applied, can separate hydrogen and oxygen from the water molecules. Thus, the mathematical model of the electrolyser is a simplification of the Equation presented in refs [220], [158]. The electrolyser stack voltage $V_{elz}(t)$, V, is expressed as the product of the number of electrolysis cells N_{elz}^{cell} and the single cell voltage V_{elz}^{cell} .

$$V_{elz}(t) = N_{elz}^{cell} V_{elz}^{cell}(t) \quad (3-69)$$

Similarly, the single-cell voltage is expressed by the following Equation [5]:

$$V_{elz}^{cell}(t) = V_{elz,0}^{cell}(t) + V_{elz,act}^{cell}(t) + V_{elz,ohm}^{cell}(t) + V_{elz,conc}^{cell}(t) \quad (3-70)$$

Where, $V_{elz,0}^{cell}$ is the Nernst voltage or reversible potential, $V_{elz,act}^{cell}$ is the activation overpotential, $V_{elz,ohm}^{cell}$ is the ohmic overvoltage and $V_{elz,conc}^{cell}$ provides the losses due to concentration mass. Therefore, the voltage drop is the sum of the following terms:

$$V_{elz,0}^{cell}(t) = E_{elz}^0 + \frac{\Delta S_{elz}^0}{2F} (T_{elz}(t) - T_{elz}^0) + \frac{2.3RT_{elz}(t)}{2F} \ln \left(\frac{PH_2(t)PO_2^{1/2}(t)}{PH_2O(t)} \right) \quad (3-71)$$

$$V_{elz,act}^{cell}(t) = \frac{RT_{elz}(t)}{F} \left[\sinh^{-1} \left(\frac{I_{elz}(t)}{2A_{elz}i_{a0,elz}} \right) + \sinh^{-1} \left(\frac{I_{elz}(t)}{2A_{elz}i_{c0,elz}} \right) \right] \quad (3-72)$$

$$V_{elz,ohm}^{cell}(t) = I_{elz}(t)R_{ohm} \quad (3-73)$$

$$V_{elz,conc}^{cell}(t) = K_{1,elz}^{conc} e^{(K_{2,elz}^{conc} I_{elz}(t))} \quad (3-74)$$

Where $T_{elz}(t)$ is the electrolyser temperature, T_{elz}^0 is the temperature in standard conditions, ΔS_{elz}^0 is the entropy change, R and F are ideal gas and Faraday constant respectively, PO_2 is the oxygen partial pressure, PH_2 is the hydrogen partial pressure, I_{elz} is the electrolyser current, $i_{a0,elz}$ and $i_{c0,elz}$ are the anode and cathode current densities respectively, and $K_{1,elz}^{conc}$ and $K_{2,elz}^{conc}$ are the concentration-losses factors of the electrolyser. Therefore, taking into account the reaction in the electrolysis stack, the mass flow of hydrogen is modeled as follows:

$$W_{elz}^{H_2,pro}(t) = N_{elz}^{cell} \frac{I_{elz}(t)}{F} \quad (3-75)$$

3.4.3.2 Mathematical Modeling of Metal Hydride

Metal hydride is a hydrogen storage technology utilized in micro-grid system to store hydrogen at a moderate pressure. Concerning metal hydrides, certain metal (M), such as iron, nickel, aluminum, titanium, etc. produce a metal hydride compound via an easily controllable reversible reaction as they react with hydrogen. Hence, hydrogen is stored at moderate pressures with this technology, typically around 2 bar. The general expression is as follows [6]:



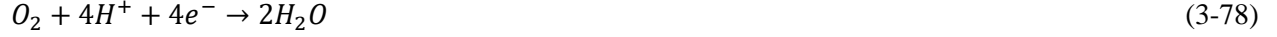
Meanwhile, this study utilized ref [228] for the mathematical model of metal hydride in the simulation.

3.4.3.3 Mathematical Modeling of Fuel Cell

Fuel cells are electrochemical devices that are used for producing energy from hydrogen and oxygen flows. The anode, which is one of the electrodes, is utilized to separate the molecules of hydrogen gas into proton and electron, using a catalyst for the reaction [229]:



Similarly, the protons move toward the cathode through the electrolyte.



Therefore, the fuel cell overall reaction is expressed as:



Moreover, the fuel cell dynamic, defined by the balances of mass and heat, results in a slow transient response contrasted with ultra-capacitor or batteries. This study utilized Proton-Exchange-Membrane Fuel Cell (PEMFC) since it operates at relatively low temperatures and has a faster response time. Moreover, they utilize a solid polymer membrane as the electrolyte and platinum as the catalyst. Hence the mathematical model used in this study is based on a simplified model of the study in refs [220, 230]. A fuel stack comprises of several cells N_{fc}^{cell} which are series-connected. The stack voltage admits expression as [220]:

$$V_{fc}(t) = N_{fc}^{cell} V_{fc}^{cell}(t) \quad (3-80)$$

Similarly, the single-cell voltage is expressed by the following Equation:

$$V_{fc}^{cell}(t) = V_{fc,0}^{cell}(t) - V_{fc,act}^{cell}(t) - V_{fc,ohm}^{cell}(t) - V_{fc,conc}^{cell}(t) \quad (3-81)$$

Descriptions of the parameters are similar to the electrolyser.

Thus, the voltage drop is a sum of four terms, which can be expressed with the following expression:

$$V_{fc,0}^{cell}(t) = E_{fc}^0 + \frac{\Delta S_{fc}^0}{2F} (T_{fc}(t) - T_{fc}^0) + \frac{RT_{fc}(t)}{2F} \ln \left(\frac{PH_2(t)PO_2^{1/2}(t)}{PH_2O(t)} \right) \quad (3-82)$$

More so, the activation losses in the fuel cell can be modeled as a function of two constant coefficients $K_{1,act}$ and $K_{2,act}$ and the stack current, I_{fc} .

$$V_{fc,act}^{cell}(t) = -K_{1,act} (1 - e^{(-I_{fc}/K_{2,act})}) \quad (3-83)$$

Similarly, the ohmic losses can be modeled as a function of the equivalent ohmic resistor of the cell R_{ohm} and the stack current I_{fc} .

$$V_{fc,ohm}^{cell}(t) = I_{fc}(t) R_{ohm} \quad (3-84)$$

The concentration losses can be modeled as a function of two constant coefficients $K_{1,fc}^{conc}$ and $K_{2,fc}^{conc}$ and the stack current.

$$V_{fc,conc}^{cell}(t) = K_{1,fc}^{conc} e^{(K_{2,fc}^{conc} I_{fc}(t))} \quad (3-85)$$

3.4.4 Dynamic Modeling of the Load

The loads in this study are classified as essential loads and curtailable loads based on a demand management perspective. The power generations should regularly meet the demand for power of the critical loads. Thus,

each EMU's load forecasting strategies can assist the adaptive controller in making important decisions for the network under study, such as charging and discharging the ESS and buying or selling it to the host grid. The load is predicted by the EMU at-time step, which uses the preceding duration data for a future predefined horizon N_p [68]. Moreover, as the AMPC procedure continues, estimates are subsequently revised and delivered to the EMU responsible for updating the parameters of the prediction model to introduce corrections and minimize errors. Consequently, the total micro-grid load demand is expressed as [68, 231]:

$$P_{load}(t_k) = P_{load-curt}(t_k)(1 - \theta(t_k)) + P_{load-crit}(t_k) \quad (3-86)$$

Where the curtailable load demand and essential load demand are $P_{load-curt}(t_k)$ and $P_{load-crit}(t_k)$, respectively, and the curtailment ratio of the curtailable loads is $\theta(t_k)$.

3.4.5 Main Grid

The energy exchange between the main grid and micro-grid is implemented as an economic transaction, where energy is sold to or purchased from the host grid. Hence, economic transactions are based on the energy price in the energy markets. Forecast algorithms are the best optimization approach to know the value of the energy prices at every instant of time. The necessary models are usually based on causal models, artificial intelligence-based models, and stochastic time series. Reference [232] reviews some of the most famous electricity price forecasting methods.

3.5 Formulations of EMS-Based AMPC Optimization Problem

The primary goal of EMS in a micro-grid network is to reduce the costs of purchased electricity while at the same time maintaining the power balance, generation limits, ESS limits, and power exchange limits. Moreover, AMPC problem formulation requires a micro-grid model for predictions; It also requires minimizing the concept of cost function and imposing operational constraints. Hence, this section describes the formulation of the EMS optimization problem used in chapter 5 of this thesis. Consequently, the problem formulation is implemented by specifying the objective function, as well as the functional and operational constraints associated with each source of energy [68].

3.5.1 Cost Function Formulations

The main objective of the EMS is to ensure a reliable supply of electrical power to its local customers. Meanwhile, the EMS fulfills the following objectives: lowering running costs by decreasing the energy exchanged with the grid, increasing the battery life by preventing deep overcharging and discharging, protecting electrolysers and fuel cells from regular usage by limiting their power rates, and ensuring energy efficiency at the plant by using the most effective storage. The fulfillment of these objectives is attributable

to their weights in the cost function [158, 233]. The cost function can incorporate terms that consider the values of the different powers involved (identified with the cost of utilizing each DER) and the power rates (identified with their lifetimes). It may also penalize the stored energy deviation from a desired point of operation. Therefore, the quadratic cost function associated with each energy source is given to minimize the total system cost, which is solved by the proposed control algorithm (AMPC).

Notice that two objective functions are obtained for the various scenarios investigated in chapter 5, and the AMPC algorithm solver tries to minimize it. The first multi-objective function (Equation (3-87a)) is used in the scenario when disturbance prediction is not incorporated in the AMPC algorithm. In contrast, the second multi-objective function (Equation (3-87b)) considers the integration of disturbance prediction. The aim is to investigate the impact of integrating disturbance prediction on the performance of the EMS in micro-grid in terms of cost minimization. Therefore, in order to track the reference outputs, the controller is designed to set $P_{net} = 0$, which consequently adds a perturbation on P_{net} of which the responsibility of the controller is to balance the rest of the control variables ($P_{fc}, P_{elz}, P_{grid}$). Moreover, the highest weight value is often assigned to the P_{net} variable in order to drive the system to attain the system's power balance ($P_{net} = P_{gen} - P_L = 0$).

$$\min J = \sum_{k=1}^{N_c} \alpha_1 P_{grid}^2(t+k) + \alpha_2 P_{fc}^2(t+k) + \alpha_3 P_{elz}^2(t+k) + \alpha_4 P_{bat}^2(t+k) + \beta_1 \Delta P_{grid}^2(t+k) + \beta_2 \Delta P_{fc}^2(t+k) + \beta_3 \Delta P_{elz}^2(t+k) + \beta_4 \Delta P_{bat}^2(t+k) + \sum_{k=1}^{N_p} \gamma_1 (SOC(t+k) - SOC_{ref})^2 + \gamma_2 (LOH(t+k) - LOH_{ref})^2 \quad (3-87a)$$

$$\min J = \sum_{k=1}^{N_c} \alpha_1 P_{grid}^2(t+k) + \alpha_2 P_{fc}^2(t+k) + \alpha_3 P_{elz}^2(t+k) + \alpha_4 P_{net}^2(t+k) + \beta_1 \Delta P_{grid}^2(t+k) + \beta_2 \Delta P_{fc}^2(t+k) + \beta_3 \Delta P_{elz}^2(t+k) + \beta_4 \Delta P_{net}^2(t+k) + \sum_{k=1}^{N_p} \gamma_1 (SOC(t+k) - SOC_{ref})^2 + \gamma_2 (LOH(t+k) - LOH_{ref})^2 \quad (3-87b)$$

Where N_c is the time horizon and α_i, β_i , and γ_i are the weights for each variable. The first four terms in this cost function weigh the usage of the manipulated variable, the subsequent four terms penalize the rate, and the last two terms help to keep the stored energy around an operating point. More so, weighting values (in the cost function and operational constraints) are often associated with the priority of using a particular unit, either for operating costs (reference tracking) or for efficiency purposes. For example, it is appropriate to use batteries first, if possible, in a micro-grid with hydrogen storage, when there is a significant mismatch between generation and demand because hydrogen has a lower path efficiency. As a consequence, the weight of the battery will be smaller than that of the fuel cell. This study has selected a quadratic cost function as the system costs to be minimized. Meanwhile, the battery bank utilized in this micro-grid is directly connected to the DC bus, therefore, P_{bat} is not taken as the manipulated variables [220]. The

minimization also includes constraints, accurately measured, as shown in Table 1. Notice that some of them are physical limits (e.g., the power generated by the generator or the fuel cell), and others are limits that are imposed to prevent system failure (e.g., power rate required by the fuel cell).

3.5.2 Dynamic System Constraints Formulations

In the optimization problem, which is to minimize the cost function of Equation (3-87), and solved by the proposed advanced control algorithm, the physical and operational constraints must be put into consideration. The physical constraints include the limited power that can be supplied by the units (external grid, DERs, batteries, fuel cells, electrolysers, etc.). They are physical limits that cannot be trespassed for productive reasons. Notice that there is an upper threshold for all units, but it is often normal for a lower threshold to occur, meaning that once the unit is attached, a minimum power must be supplied. Such constraints relate in this way to the power (variable $u(t)$) and also to the capacity of the storage units (maximum energy which can be stored in a battery or an ultra-capacitor). In addition, equipment constraints in terms of capacity limits and power rates are implemented to maximize performance, lifespan, and operating & maintenance costs. The battery bank will, therefore, operate in a range of SOC values to prevent overcharging and undercharging, which significantly decreases the number of possible cycles [220, 234]. The following constraints are considered in this study:

3.5.2.1 Inequality Constraints

The constraints imposed in the problem of optimal control include the generation limits of the units, which admit expressions such as [220]:

$$P_{gen}^{min} \leq P_{gen}(t) \leq P_{gen}^{max} \quad (3-88)$$

$$P_{grid}^{min} \leq P_{grid}(t) \leq P_{grid}^{max} \quad (3-89)$$

$$P_{fc}^{min} \leq P_{fc}(t) \leq P_{fc}^{max} \quad (3-90)$$

$$P_{elz}^{min} \leq P_{elz}(t) \leq P_{elz}^{max} \quad (3-91)$$

The storage limits admit expressions as:

$$SOC^{min} \leq SOC(t) \leq SOC^{max} \quad (3-92)$$

$$LOH^{min} \leq LOH(t) \leq LOH^{max} \quad (3-93)$$

Notice that the maximum and minimum values can be the same physical limits, and a protective band can be considered as well, preventing working close to hazardous regions [1, 68].

$$\Delta P_{gen}^{min} \leq \Delta P_{gen}(t) \leq \Delta P_{gen}^{max} \quad (3-94)$$

$$\Delta P_{grid}^{min} \leq \Delta P_{grid}(t) \leq \Delta P_{grid}^{max} \quad (3-95)$$

$$\Delta P_{fc}^{min} \leq \Delta P_{fc}(t) \leq \Delta P_{fc}^{max} \quad (3-96)$$

$$\Delta P_{elz}^{min} \leq \Delta P_{elz}(t) \leq \Delta P_{elz}^{max} \quad (3-97)$$

$$\Delta SOC^{min} \leq \Delta SOC(t) \leq \Delta SOC^{max} \quad (3-98)$$

In the same way, the other kind of constraints is imposed in order to prevent sudden shifts in the power supplied by the units. These are limits that influence the degradation of the units and will be significant in costly equipment such as fuel cells. It is worthy of note that some of these constraints can be shifted to the soft constraints category if the inequalities are replaced by a weighted term in the cost function. That is the case with the energy-storage capacity constraints [5].

3.5.2.2 Energy Balance Constraints

Including the constraints of the energy balance at each time instant is essential mainly for the purposes of the power system's stability. More so, to keep the network running effectively and reliably, the micro-grids must meet the power balance constraint [68].

$$\sum_{i=1}^{n_g} P_{gen,i}(t) + \sum_{i=1}^{n_e} P_{ext,i}(t) + \sum_{i=1}^{n_s} P_{sto,i}(t) - \sum_{i=1}^{n_l} P_{load,i}(t) = 0 \quad (3-99)$$

Where $P_{gen,i}$ is the power generated by the generation unit i , $P_{sto,i}$ is the power exchange with the storage units, $P_{ext,i}$ is the power exchanged with the external connections such as the main utility grid or other micro-grids, $P_{load,i}$ is the power consumed by the loads. During micro-grid operations, the balance between energy production and demand must always be met; thus, Equation (3-99) must be applied as a constraint for equality to the formulation.

3.6 Formulations of DR-Based AMPC Optimization Problem

In this section, the general AMPC formulations for the DR technique in micro-grid used in chapter 6 of this thesis are formulated, which is similar to the previous AMPC optimization formulations. The method discussed in the previous section is further extended to include load curtailment and shifting. AMPC problem formulation requires a micro-grid model; It also requires minimizing the concept of cost function and imposing operational constraints. Hence, this section describes the formulation of the DR technique for the EMS optimization problem of the micro-grid used in chapter 6. Consequently, the problem formulation is carried out by specifying the objective function, as well as the functional and operational constraints associated with each source of energy [68].

3.6.1 DR-Based Cost Function Formulations

The cost function can incorporate terms that consider the values of the different powers involved (identified with the cost of utilizing each DER) and also the power rates (identified with their lifetimes). It may also

penalize the stored energy deviation from a desired point of operation. Therefore, the quadratic cost function associated with each energy source is given to minimize the total system cost, which is solved by the proposed control algorithm (Adaptive MPC):

$$\begin{aligned} \min J = & \sum_{k=1}^{N_c} \alpha_1 P_{gen}^2(t+k) + \alpha_2 P_{fc}^2(t+k) + \alpha_3 P_{elz}^2(t+k) + \alpha_4 P_{bat}^2(t+k) + \beta_1 \Delta P_{gen}^2(t+k) + \\ & \beta_2 \Delta P_{fc}^2(t+k) + \beta_3 \Delta P_{elz}^2(t+k) + \beta_4 \Delta P_{bat}^2(t+k) + \sum_{k=1}^{N_p} \gamma_1 (SOC(t+k) - SOC_{ref})^2 + \gamma_2 (LOH(t+k) - \\ & LOH_{ref})^2 + \varphi_1 P_{Curt-load}^2(t+k) \end{aligned} \quad (3-100)$$

3.6.2 DR-Based System constraints Formulations

Similarly, in order to consider the load curtailment technique of some adjustable loads in the micro-grid system in chapter 6 of this thesis, the model-based design shown in Figures 6-1 and 6-2 are utilized. The basic EMS presented in the previous section is modified by adding curtailable loads to the micro-grid design. Moreover, since some of the loads are curtailable loads, i.e., loads that can be adjusted during specific periods in order to enhance the operation of the micro-grid or during contingencies, therefore, its associated power (P_{load}) can be manipulated by the EMS. Meanwhile, it is worth mentioning that P_{load} is part of the vector of manipulated variables instead of a disturbance.

Hence, some additional constraints need to be applied to the optimization problem, as the load can only be adjusted to a certain level, so its limits need to be set.

$$P_{Curt-loads}^{min}(t) \leq P_{Curt-load}(t) \leq P_{Curt-loads}^{max}(t) \quad \forall t \quad (3-101a)$$

$$C_{Curt-load} = m \cdot [\sum_{t=1}^{24} P_{Curt-load}(t)] \quad (3-101b)$$

Where m and $C_{Curt-load}$ are shedding prices and shedding costs, respectively.

Therefore, the minimum and maximum values may change at each instant (and can be set to avoid any curtailment if needed). The other physical and operational constraints required to solve the optimization problem, such as energy balance and amplitude and rate constraints, are described in the previous section. More so, since load adjustment can result in discomfort to the user, a set point $P_{Curt-loadref}$ can be utilized to avoid large deviations from the desired value and its associated weight $\varphi(t)$ can be set to a high value to prevent curtailment at a specific time instant or interval. Therefore, the Quadratic Programming (QP) is used to solve the optimization problem, as all the variables are continuous (continuous-valued variables).

3.7 Formulations of EMS-Based AMPC Optimization Problem with EV Integration

The AMPC algorithm is used to minimize the cost function, which is formulated as a sum of the different cost functions of the micro-grid components:

$$\min J(t) = \sum_{k=1}^{24} [J_{grid}(t+k|t) + J_{bat,uc}(t+k|t) + J_{H_2}(t+k|t)] \quad (3-102)$$

The cost function of the energy exchange with the host grid is given as J_{grid} . Similarly, the battery/ultra-capacitor and the hydrogen are $J_{bat,uc}$ and J_{H_2} , respectively. Moreover, the grid cost function is simply the economic revenue of selling energy to the grid or the economical cost of buying energy from the grid, which admits expression as follows:

$$J_{grid}(t+k|t) = \left(-\mathcal{F}_{sale}^{DM}(t+k|t) * P_{sale}(t+k|t) + \mathcal{F}_{purc}^{DM}(t+k|t) * P_{purc}(t+k|t) \right) * T_s \quad (3-103)$$

Where $\mathcal{F}_{sale}^{DM}(t+k|t)$ and $\mathcal{F}_{purc}^{DM}(t+k|t)$ correspond to the forecast values for the energy prices, while $P_{sale}(t+k|t)$ and $P_{purc}(t+k|t)$ are the energy sale and purchase with the host grid, respectively.

Where both the energy sale and purchase with the host grid admit expressions as the following equations:

$$P_{sale}(t_k) = \begin{cases} P_{host\ grid}(t_k), & P_{host\ grid}(t_k) \geq 0 \\ 0, & P_{host\ grid}(t_k) < 0 \end{cases} \quad (3-104)$$

$$P_{purc}(t_k) = \begin{cases} P_{host\ grid}(t_k), & P_{host\ grid}(t_k) > 0 \\ 0, & P_{host\ grid}(t_k) \leq 0 \end{cases} \quad (3-105)$$

The above piece-wise functions are implemented in the AMPC algorithm utilizing the transformation technique illustrated in ref [235], which results in the MLD constraints in ref [18].

Equation (3-106) gives the expression for the cost function of the batteries. The proposed algorithm minimizes the economic cost related to the use of the batteries. The battery manufacturers measure the life of the ESS based on the number of cycles of charging and discharge. The main mechanism to be avoided relates to the exposure of batteries to a high-stress current ratio in the charging and discharging process. Therefore, in order to penalize the high values of P_{bat}^2 , a second term in the cost function of the batteries is incorporated in the expression of Equation (3-106).

$$J_{bat,UC}(t+k|t) = \frac{CC_{bat,UC}}{2 * Cycles_{bat,UC}} (P_{bat,UC-ch}(t+k|t) + P_{bat,UC-dis}(t+k|t)) * T_s + Cost_{degr,ch} * P_{bat,UC-ch}^2(t+k|t) + Cost_{degr,dis} * P_{bat,UC-dis}^2(t+k|t) \quad (3-106)$$

Where $CC_{bat,UC}$ corresponds to the cost function of the battery and ultra-capacitor, $Cycles_{bat,UC}$ are the number of the battery and ultra-capacitor life cycles. The parameters $Cost_{degr,ch}$ and $Cost_{degr,dis}$ are the cost associated with the degradation mechanisms of the batteries and capacitor. Since hydrogen storage is implemented with the following components, fuel cell, electrolyser, and hydrogen tank, the cost function of hydrogen storage is simply the sum of the cost functions of these components. Therefore, the compression cost of hydrogen storage is not put into consideration in order to simplify the cost. In a similar vein with batteries, the fuel cells and electrolysers have a limited lifetime. Meanwhile, this lifetime is often expressed as several life hours. Hence, the lifetime can be mitigated should the degradation aspects associated with the technology are not minimized. For this reason, not only are working hours for

electrolysers and fuel cells reduced, but also start-up/shutdown cycles and fluctuations in operating conditions are also included. Batteries (Lithium-ion batteries) have virtually low or no cost of operation and maintenance (O&M) [236]. Details of the characteristics of each battery used in this research work are given in Table D-7. However, electrolysers and fuel cells require maintenance aspects included in the cost function on an hourly basis. The cost function of hydrogen storage is expressed as Equation (3-107a).

$$J_{H_2}(t + k|t) = J_{elz}(t + k|t) + J_{fc}(t + k|t) \quad (3-107a)$$

Where,

$$J_{elz}(t + k|t) = \left(\frac{CC_{elz}}{Hours_{elz}} + Cost_{O\&M,elz} \right) \delta_{elz}(t + k|t) + Cost_{Start,elz} * \sigma_{elz}^{on}(t + k|t) + Cost_{degrd,elz} * \vartheta_{elz}^2(t + k|t) \quad (3-107b)$$

$$J_{fc}(t + k|t) = \left(\frac{CC_{fc}}{Hours_{fc}} + Cost_{O\&M,fc} \right) \delta_{fc}(t + k|t) + Cost_{Start,fc} * \sigma_{fc}^{on}(t + k|t) + Cost_{degrd,fc} * \vartheta_{fc}^2(t + k|t) \quad (3-107c)$$

Therefore, the capital cost of the fuel cell and the electrolyser are denoted as CC_{fc} and CC_{elz} respectively. $Hours_{elz}$ and $Hours_{fc}$ are the lifetime hours of the electrolyzer and the fuel cell from the manufactures, $Cost_{O\&M,fc}$ and $Cost_{O\&M,elz}$ are the two terms associated with the operation and maintenance cost of the fuel cell and the electrolyzer, $Cost_{Start,elz}$ and $Cost_{Start,fc}$ are the costs associated with the degradation processes linked to the start-up and shutdown of the components. Lastly, the costs related to the degradation processes linked to the power fluctuations in the fuel cell and the electrolyser are denoted by $Cost_{degrd,fc}$ and $Cost_{degrd,elz}$, respectively. Therefore, the third terms in the cost function of Equations (3-107b) and (3-107c) are incorporated in order to minimize the power fluctuations of fuel cells and electrolysers. The logical power variation ϑ_{fc} and ϑ_{elz} , of the fuel cell and electrolyzer is described as the power variation in all the instants except those where the component moves from the start-up state to the energized state or from the energized state toward switch off. Hence, in order to solve the optimization problem with the cost functions of Equations (3-102) to (3-107c), some physical limits must be strictly adhered to and should not be violated. The physical constraints are imposed by the ESS 'upper and lower limits, which can consume or supply the maximum and minimum energy storage levels that have been stored in each ESS (the main grid power exchange is also considered). Therefore, the minimization of the cost function is subject to the following constraints along the schedule horizon ($k = 1, \dots, SK$):

$$P_{WT}(t + k|t) + P_{PV}(t + k|t) - P_{load}(t + k|t) + P_{grid}(t + k|t) + P_{bat,uc}(t + k|t) - Z_{elz}(t + k|t) + Z_{fc}(t + k|t) = 0 \quad (3-108)$$

$$0 \leq \delta_i(t + k|t) \leq 1|_{i=elz,fc} \quad (3-109)$$

$$P_i^{min} \leq P_i(t + k|t) \leq P_i^{max}|_{i=grid,bat,elz,fc} \quad (3-110)$$

$$SOC_i^{min} \leq SOC_i(t + k|t) \leq LOH_i^{max}|_{i=bat,UC} \quad (3-111)$$

$$LOH_i^{min} \leq LOH_i(t + k|t) \leq LOH_i^{max}|_{i=elz,fc} \quad (3-112)$$

Equation (3-108) corresponds to the energy balance in the micro-grid, while Equations (3-109) - (3-112) are the physical inequality constraints of the micro-grid components.

Similarly, the conversions implemented in ref [235] makes it feasible to incorporate the binary and auxiliary variables embedded in a discrete-time dynamic system to explain the evolution of the system's continuous and logical signals in a unified model. Therefore, in order to accomplish the charging process, the following additional constraints are imposed:

- Fulfill the necessary energy E_{ev} for the desired charge at a constant power P_{ev-ch} :

$$\sum_{k=1}^{N_p} P_{ev-ch} T_s \delta_{ev}(t) = E_{ev} \quad (3-113)$$

- Charge during a total number of instants:

$$0 \leq \sum_{k=1}^{N_p} \delta_{on}(k) \leq N_{ev} \quad (3-114)$$

- Charging without any form of interruption (only one transition):

$$0 \leq \sum_{k=1}^{N_p} \sigma_{ev}(k) \leq 1 \quad (3-115)$$

- Energy balance at each instant t:

$$\sum_{i=1}^{n_g} P_{gen-i}(t) + \sum_{i=1}^{n_e} P_{ext-i}(t) + \sum_{i=1}^{n_s} P_{stor-i}(t) - P_{ev-ch} \delta_{ev}(t) = 0 \quad (3-116)$$

Where N_p is the schedule horizon (usually 24 hours).

For the sake of simplicity, we consider just a few numbers of electric vehicles. Meanwhile, the formulation can be extended to any number of electric vehicles. This can be done by simply adding as many δ (for the connection state) and σ (for transitions) as the number of EVs and the associated constraints. The solver finds an optimal solution for the micro-grid, providing a set of the control variables, which are logic and continuous, and the AMPC controller is formulated as a mixed-integer quadratic programming (MIQP) problem. The different operation modes in the micro-grid are modeled with the mixed logic dynamical (MLD) framework. The output signals which are generated by the solver are the values of exchange power with the main grid (P_{grid}), the power of electrolyser, fuel cell, and battery (P_{elz} , P_{fc} , and P_{bat}), the activation signals for the electrolyzer and fuel cell (δ_{elz} and δ_{fc}) and the activation and transition of the electric vehicle (δ_{ev} and σ_{ev}). Note that the sampling time is 1 hour, and the schedule horizon is 24 hours.

3.8 Control Oriented Linear Model

The control-oriented model of the micro-grid incorporated into the AMPC optimization procedure is a simplified model. It is worth mentioning that at the EMS level, the generators and loads dynamics are very fast compared to the characteristic sampling time; therefore, it can be neglected. Hence, the main dynamics of interest in this study are the storage units, which, together with the balance equation of powers in the bus, will constitute the model to be used by the AMPC control algorithms. The proposed control algorithm (AMPC) utilized a control-oriented linear model for its control design. Hence, a state-space model can be derived utilizing Equations (3-92) - (3-93) for the battery and the hydrogen storage. Thus, the state vector is expressed as [220]:

$$v(t) = [SOC(t) \ LOH(t)]^T \quad (3-117)$$

Similarly, the vector of the manipulated variable is given as:

$$v(t) = [P_{H_2}(t) \ P_{grid}(t)]^T \quad (3-118)$$

Where $SOC(t)$ is the state of charge of the battery and $LOH(t)$ is the hydrogen level in the hydride tank. Meanwhile, the battery's fixed efficiency value was used to prevent the use of binary variables.

$$SOC(t + 1) = SOC(t) - \frac{\eta_{bat} T_s}{C_{max}} P_{bat}(t) \quad (3-119)$$

$$LOH(t + 1) = LOH(t) + \frac{\eta_{elz} T_s}{V_{max}} P_{elz}(t) - \frac{T_s}{\eta_{fc} V_{max}} P_{fc}(t) \quad (3-120)$$

Where P_{bat} is the power supplied by the battery and V_{max} is the maximum volume of H_2 (normal cubic meters) that can be stored in the tanks. The manipulated variables are the power that can be exchanged with the grid (P_{grid}), fuel cell (P_{fc}) and electrolyser (P_{elz}). As it is evident in Figures 5-1 and 5-2, the battery is attached to the DC bus and absorbs the unbalance, so P_{bat} must compensate for the remainder of the power in the DC bus [220, 237].

$$P_{bat}(t) = P_{load}(t) + P_{elz}(t) - P_{fc}(t) - P_{grid}(t) - P_{gen}(t) \quad (3-121)$$

Note that the imbalances generated by the difference between power generated by the renewables (non-dispatch-able units, i.e., Solar and Wind), and the demand is considered as the disturbances, $d(t)$. Since the demand and generation have a similar impact on the energy balance (one positive and the other negative), it is expedient to group such disturbances into one variable only: Therefore, the generation and demand net effect admits expression as:

$$d(t) = P_{gen}(t) - P_{load}(t) \quad (3-122)$$

It is worth mentioning that the generation and demand are measurable quantities; therefore, they are measurable disturbances. Hence, the storage expressions, defining Equation (3-122) as the measurable disturbance are:

$$SOC(t + 1) = SOC(t) - \frac{\eta_{bat}T_s}{C_{max}} (P_{elz}(t) - P_{fc}(t) - P_{grid}(t) - d(t)) \quad (3-123)$$

$$LOH(t + 1) = LOH(t) + \frac{\eta_{elz}T_s}{V_{max}} P_{elz}(t) - \frac{T_s}{\eta_{fc}V_{max}} P_{fc}(t) \quad (3-124)$$

However, the conversion values for SOC and LOH vary from charging power to electrical and hydrogen storage between 10 and 90%, and the charging and discharge capacity vary from 600 to 1800 W. The mean value obtained for the battery's conversion coefficient admits expression as:

$$K_{bat} = \frac{\eta_{bat}}{C_{max}} \quad (3-125)$$

Similarly, in the case of hydrogen, the mean values are expressed as [238]:

$$K_{elz} = \frac{\eta_{elz}}{V_{max}} \quad [\text{For charging, electrolyser}] \quad (3-126)$$

$$K_{fc} = \frac{1}{\eta_{fc}V_{max}} \quad [\text{For discharging, fuel cell}] \quad (3-127)$$

The mathematical descriptions of the matrix's forms of the SOC and LOH used in chapters 5-7 are given in Appendix A. Hence, the state considered in the optimization process is the level of the storage devices (batteries (SOC) and hydrogen (LOH)), and the control actions are the power exchanged with the grid and the power of the hydrogen storage network (including an electrolyser, a fuel cell, and hydrogen tanks).

Consequently, a multi-objective function is used to accomplish the entirety of the previous objectives, and the solver aims to minimize it. In summary, the overall objective function of the energy management problem, which is solved by the AMPC algorithm, can be formulated as:

$$\text{Minimize } J(3 - 87a), (3 - 87b), (3 - 100) \text{ \& } (3 - 102) \quad (3-128)$$

Subject to:

Dynamic constraint - (3-62) & (3-68)

Equality constraints - (3-99) & (3-108)

Inequality constraints - (3-88) – (3-98), (3-101a) – (3-101b) and (3-109) - (3-116).

3.9 System Modeling of the Two-Area Power System with a Stand-Alone Micro-grid

This section describes the system modeling of the two-area power system with a stand-alone micro-grid used in chapter 8 of this thesis. In the system model, as shown in Figures 8-1 and 8-2, the following equations are formulated from the dynamic characteristics of the power and frequency changes in the two-area power system with a stand-alone micro-grid:

$$\Delta \dot{F}_1(t) = \frac{1}{2H} [\Delta P_{f_filt1}(t) + \Delta P_{PV1}(t) + \Delta P_{W1}(t) - \Delta P_{bat1}(t) - \Delta P_{L1}(t) - D\Delta F_1(t) - \Delta P_4(t)] \quad (3-129)$$

$$\Delta \dot{F}_2(t) = \frac{K_{P1}}{T_{P1}} \Delta P_{tie}(t) - \frac{1}{T_{P2}} \Delta F_2(t) + \frac{K_{P2}}{T_{P2}} \Delta P_4(t) - \frac{K_{P2}}{T_{P2}} \Delta P_{L2}(t) \quad (3-130)$$

$$\Delta \dot{P}_1(t) = -a_1 \Delta P_1(t) + K_1 \Delta P_{C1}(t) \quad (3-131)$$

$$\Delta \dot{P}_{fC1}(t) = \frac{1}{T_{fC1}} [\Delta P_{Cf1}(t) - \Delta P_{fC1}(t)] \quad (3-132)$$

$$\Delta \dot{P}_{f_inv1}(t) = \frac{1}{T_{inv1}} [\Delta P_{fC1}(t) - \Delta P_{f_inv1}(t)] \quad (3-133)$$

$$\Delta \dot{P}_{f_filt1}(t) = \frac{1}{T_{filt1}} [\Delta P_{f_inv1}(t) - \Delta P_{f_filt1}(t)] \quad (3-134)$$

$$\Delta \dot{P}_{bat1}(t) = \frac{1}{T_b} [\Delta F_1(t) - \Delta P_{bat1}(t)] \quad (3-135)$$

$$\Delta \dot{P}_{PV1}(t) = (b_1 - a_1) \Delta P_1(t) - C_1 \Delta P_{PV1}(t) + K_1 \Delta P_{C1}(t) \quad (3-136)$$

$$\Delta \dot{P}_2(t) = -\frac{R}{T_g} \Delta F_2(t) - \frac{1}{T_g} \Delta P_2(t) + \frac{1}{T_g} \Delta P_{C2}(t) + \frac{1}{T_g} \Delta P_{L3}(t) \quad (3-137)$$

$$\Delta \dot{P}_3(t) = \frac{1}{T_t} \Delta P_2(t) - \frac{1}{T_t} \Delta P_3(t) \quad (3-138)$$

$$\Delta \dot{P}_4(t) = \frac{K_r T_r}{T_t T_r} \Delta P_2(t) + \left(\frac{1}{T_r} - \frac{K_r T_r}{T_t T_r} \right) \Delta P_3(t) - \frac{1}{T_r} \Delta P_4(t) \quad (3-139)$$

$$ACE_1(t) = \Delta P_{tie}(t) = \frac{2\pi T_{12} (\Delta F_1(s) - \Delta F_2(s))}{s} \quad (3-140)$$

$$ACE_2(t) = -\Delta P_{tie}(t) + B \Delta F_2(t) \quad (3-141)$$

$$\Delta \dot{P}_{tie}(t) = \frac{1}{T_{UPFC1}} \left[2\pi T_{12} (\Delta P_{PV1}(t) + \Delta P_{filt1}(t) + \Delta P_{W1}(t) - \Delta P_{bat1}(t)) - \Delta P_{tie}(t) - \Delta F_2(t) - \Delta P_{L1}(t) \right] \quad (3-142)$$

Where $\Delta P_{PV1}(t)$ is the power change of PV, $\Delta P_1(t)$ is the intermediate power change of PV, $\Delta P_{tie}(t)$ is the total tie-line power change in this system, $\Delta P_2(t)$, $\Delta P_3(t)$, and $\Delta P_4(t)$ are the power change of governor, steam turbine, and re-heater, respectively. $\Delta F_1(t)$, and $\Delta F_2(t)$ are the frequency deviations of area 1 and area 2, respectively, $\Delta P_{C1}(t)$ and $\Delta P_{C2}(t)$ are the control action of area 1 and area 2, respectively, $\Delta P_{L1}(t)$, $\Delta P_{L2}(t)$, and $\Delta P_{L3}(t)$ are the load changes, B is the frequency bias factor, and R is the regulation parameter (Hz/p.u.MW). The definitions of other parameters are listed in the nomenclature section. The state-space models of the stand-alone micro-grid system used in chapter 8 are described in Appendix C. More so, the modeling of UPFC used in the proposed system model is described in ref [26].

3.10 Adaptive MPC-Based Power Scheduling of Renewable Energy-Based Micro-grid

AMPC is a control strategy used in micro-grids and has vast potential for addressing numerous complex problems in the area of micro-grids. While other proven methods can be used to control micro-grids, AMPC

offers a generalized structure for handling most of the concerns in an organized way using some common ideas. The approach taken into consideration in this study is primarily to adaptively control the EMS in micro-grid (power management) to ensure a reliable supply of electrical power to local load consumers. The primary responsibility of the adaptive controller is to coordinate and, at the same time, manage the power in the micro-grid network by suitably allowing the optimal operation of each generation unit. The problem of AMPC-based optimization offers a solution that indicates an input trajectory and states in the future that meets operational constraints while optimizing those parameters. For each sampling instant, an optimal plan is formulated based on generation and demand forecast and similarly on the knowledge of the level of energy storage. More so, the first element in the control sequence is introduced, and the horizon is moved [26]. Therefore, using the newly available information, a new optimization problem will be solved at the next sampling time. The new optimal design will theoretically compensate for the disturbance that acts on the micro-grid by using the feedback mechanism. AMPC is responsible for the efficient operation of the micro-grid under consideration [68, 220]. The principal sources of uncertainty in this energy management problem are due to incident irradiation, wind speed, and load power forecast. Therefore, the conventional MPC is not successful in managing the varying dynamics of renewable sources, as its control efficiency is deteriorating due to variations in their production capacity. Hence, it is appropriate to use the AMPC controller, which updates the plant's internal model for any changes in operating conditions. Figures 3-3 and 3-4 show the block diagram and the flowchart of the AMPC-based EMS control scheme [68, 157]. The state-space model of Equations (3-143a) and (3-143b) are often utilized to model an AMPC, which admit expressions as:

$$x(t + 1) = Ax(t) + Bu(t) \tag{3-143a}$$

$$y(t) = Cx(t) \tag{3-143b}$$

Where the system state composed of the charging state of the Energy Storage Systems (ESSs) is given as, $x(t)$, similarly, the manipulated vector variables, consisting of the dispatchable generation and the power exchanged by the ESSs, are given as, $u(t)$ and the output vector, which in this case corresponds with the state as $y(t)$. Hence, the AMPC's state-space model can be implemented and can be solved at the same time using Quadratic Programming (QP). As with any network, micro-grids are susceptible to disturbance during normal operation. There are two simple sources of disturbance in micro-grids: the power generated by the RESs (which is usually non-dispatchable) and the power demanded. These are external inputs to the system, which the controller cannot manipulate. As renewable sources are used for the generation, this makes them a problem to be solved by the control system because of their time-varying existence, the complexity of prediction, and lack of manipulative capability. The initial formulation of AMPC does not contain disturbances, but in this context, several AMPC strategies have been introduced to ensure stability

and adherence to constraints [239]. Note that the feedback mechanism allows AMPC to reject disturbances, like any other controller. If disturbances can be measured (or estimated), however, their impact on the output can be included in the dynamic model. Thus, the controller can predict their influence on system performance. In this way, AMPC will have a feedforward effect inherently. The impact of these disturbances, $d(t)$, can be applied to the AMPC state-space formulation. Hence, the system's dynamic model can be written as [5]:

$$x(t + 1) = Ax(t) + Bu(t) + B_d d(t) \quad (3-144a)$$

$$y(t) = Cx(t) \quad (3-144b)$$

Where B_d is the matrix quantifying the effect of disturbances on the states. Now, the forecast includes disturbance values along the horizon that can be calculated (in the case of RESs, weather forecasts may provide them) or that may be considered constant and equal to the current $d(t)$ value. The discrete-time space models of Equation (3-145a) and (3-145b) are obtained mainly by discretization with sample time T_s , which are given by the following Equations [240]:

$$x(k + 1) = A_d x(k) + BU(k) + B_d d(k) \quad (3-145a)$$

$$y(k) = Cx(k) \quad (3-145b)$$

Where $x(k + 1)$, $x(k)$, $d(k)$, $U(k)$, and $y(k)$ are the discrete-time forms of $dx(t)/dt$, $x(t)$, $d(t)$, $U(t)$, and $y(t)$, respectively, $A_d = e^{AT_s}$, $B_{1d} = \int_0^{T_s} e^{At} B dt$, $B_{2d} = \int_0^{T_s} e^{At} B_1 dt$. The incremental form of Equations (3-146a) and (3-146b) are expressed as follows [8], [241]:

$$\Delta x(k + 1) = A_d \Delta x(k) + B \Delta U(k) + B_d \Delta d(k) \quad (3-146a)$$

$$\Delta y(k) = C \Delta x(k) \quad (3-146b)$$

Where $\Delta x(k + 1)$, $\Delta x(k)$, $\Delta d(k)$, $\Delta U(k)$ and $\Delta y(k)$ are the incremental forms of $x(k + 1)$, $x(k)$, $d(k)$, $U(k)$, and $y(k)$, respectively.

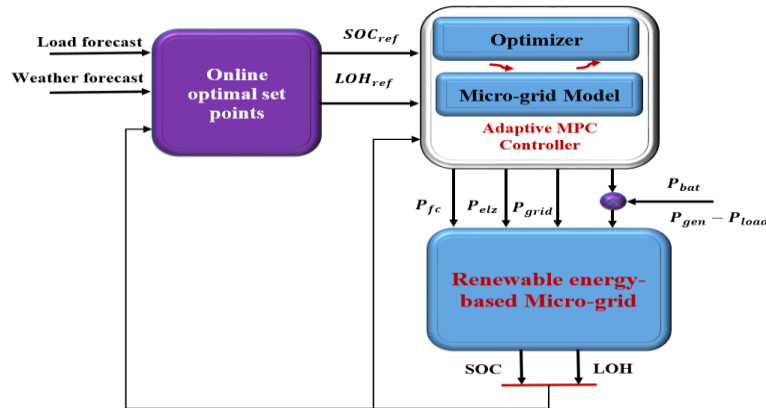


Figure 3-3: Block representation of Adaptive MPC Control Unit [68]

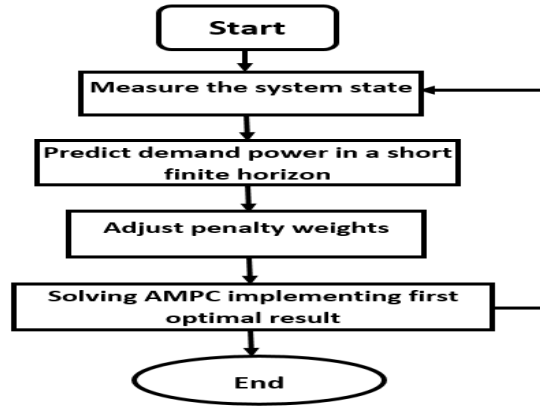


Figure 3-4: Flowchart of ems-based AMPC algorithm[68]

The MPC is widely divided into two parts: a model identifier for obtaining plant predictions provided by the optimizer, and an optimizer for deriving control action [242]. Therefore, in order to solve the cost function, the MPC optimizer adopts the receding horizon concept. It is also worth noting that only the first component corresponding to the first instant prediction of the optimal solution is retained, and this optimization process is repeated until an optimal control output is obtained that satisfies all the constraints involved. However, determining the controller stability in indirect adaptive control techniques is unwieldy for time-varying non-linear systems. AMPC is also divided into two parts, the identifier for the plant model and the synthesizer for the controller [243]. The following objectives were explicitly taken into account in the development of AMPC: track the SOC and LOH references in predicted conditions, limit the fuel cell and electrolyser power rate to protect this costly equipment from extensive usage, protect the battery bank against deep overcharging and discharging. Therefore, it is easier to use the battery in a micro-grid with hydrogen storage as the first form of energy storage wherever possible. Since the efficiency of the hydrogen is much lower than the efficiency of the batteries, this approach is only used when there is a huge imbalance between supply and demand. Hence, the AMPC actualizes these goals by formulating a deterministic optimization model with an appropriate objective function and many constraints [220, 242].

3.11 Adaptive MPC Controller Design of Two-Area Power System with a Stand-Alone Micro-grid

In this section, in order to implement Model Predictive Control (MPC) based on adaptive mode, a conventional model predictive controller for the nominal operating conditions of the control system is designed. Then the plant models and the nominal conditions used by the MPC controller are updated over time and remain constant over the prediction horizon [244]. Moreover, an AMPC algorithm is used to fine-tune the weights of different targets spontaneously, as per the state of the systems. The main idea of the proposed technique is to use a discrete-time space model to formulate a system dynamic characteristic of the LFC problem, and then to obtain a predictive dynamic model by simply introducing an expanded state

vector. Therefore, based on the cost function, a rolling optimization of the control signal is implemented by minimizing the weighted sum of squared predicted errors and square future control values [242], [245]. The expanded discrete-time state-space model formulations from the controller design are discussed in ref [26]. The detailed structure of the proposed control scheme (AMPC) for the LFC problem of a multi-area interconnected power system with renewable energy sources is depicted in Figure 3-5 based on the above analysis. Moreover, the flow chart of the proposed control scheme adopted in this study is shown in Figure 3-6.

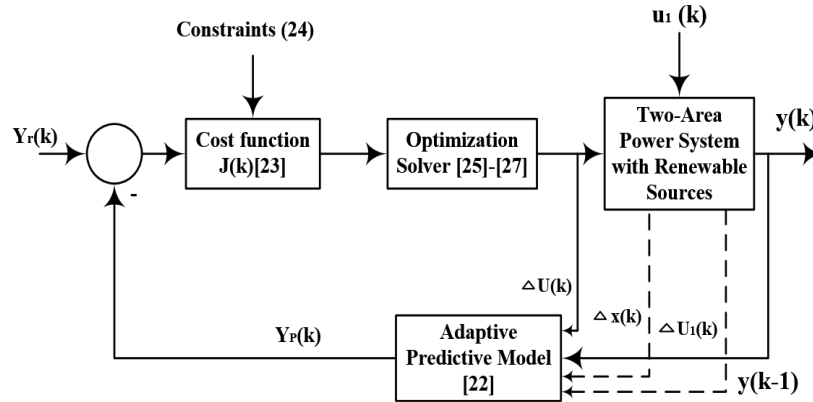


Figure 3-5: Block diagram of an AMPC scheme for the optimal LFC problem under study

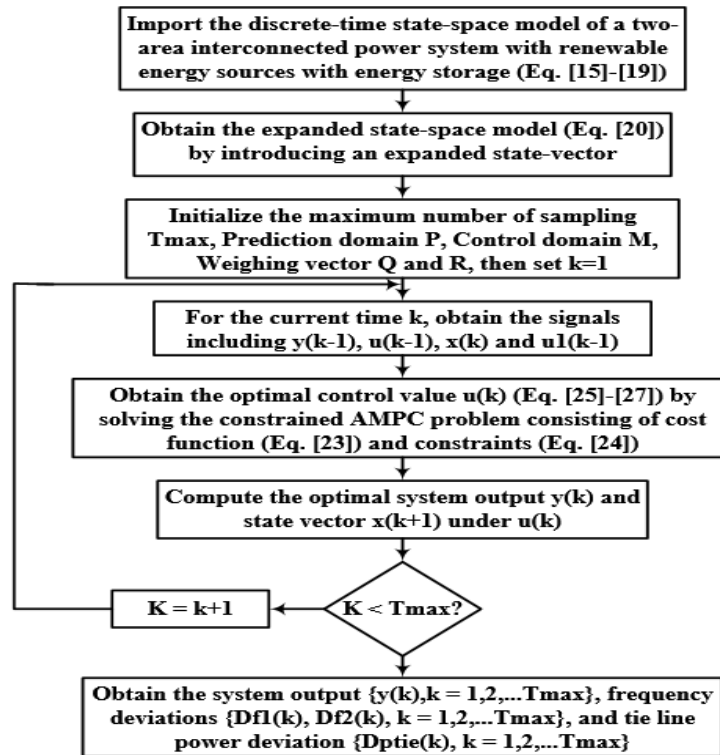


Figure 3- 6: The flowchart of AMPC for the LFC problem in a multi-area interconnected power system

3.12 Chapter Summary

This chapter presented the mathematical modeling of the dynamic behavior of the various micro-grid systems used in this thesis (grid-connected and stand-alone micro-grid). A detailed derivation of the mathematical thermo-electrical model was described, considering the wavelength-specific effects to enhance the predictions of temperature and module performance. More so, the system modeling of the stand-alone micro-grid system that is used in the subsequent chapter have been discussed. The system model is used to investigate the optimal control strategy to efficiently manage the stand-alone micro-grid used in the next chapter. Furthermore, the research methodologies used to solve different control and energy management issues in the micro-grid systems of the subsequent chapters have been discussed. This chapter also discussed the formulations of the EMS-based AMPC optimization problem, cost functions, dynamic system constraints, and the control-oriented linear model, which are to be solved by the proposed algorithm (AMPC). More so, the fundamentals, ideas, and formulations of the AMPC control technique have been discussed. The mathematical modeling and the research methodologies described in this chapter are used in the subsequent chapters to investigate the various cases and to address issues related to the control and energy management system in micro-grid operation. The simulation results obtained due to the implementation of the methodologies discussed in this chapter are outlined and discussed in subsequent chapters.

CHAPTER FOUR

OPTIMAL CONTROL STRATEGY FOR ENERGY MANAGEMENT IN A STAND-ALONE MICRO-GRID

4.1 Introduction

This chapter investigates an optimal control strategy that efficiently manages a stand-alone residential micro-grid comprising of renewable and non-renewable energy sources. An adaptive model predictive control (AMPC) algorithm is implemented for choosing an optimal mode and set of inputs for the system to track both a constant and load-varying power demand profile. However, in order to implement MPC based on adaptive mode, a traditional MPC controller is designed for the nominal operating conditions of the control system, and then the plant models and nominal conditions used by the MPC controller are updated at run time and then remain constant over the prediction horizon. This suggests there is a need to self-learn the theory, design technique, and implementation of MPC in a simulation-oriented fashion. Most of the challenges faced in the implementation of traditional MPC are the system identification of the plant, design technique of MPC in MATLAB and Simulink, the tuning art of MPC as well as the simulating of the MPC with non-linear plant in Simulink. Therefore, in the bid to fully understand how MPC is designed and implemented in an electrical network, the MPC controller is used in a wavelength-based thermo-electrical model of a photovoltaic (PV) module. The essence of this model is mainly to predict the impact of each module wavelength on both the temperature and the output power of the PV module. More so, since the output power is affected by the module temperature, it is expedient to design a controller that locates the optimal cut-off spectral wavelength to lessen the module temperature, therefore, getting the most out of the output power over a period of time. In this vein, a Model Predictive Controller whose objective is to maximize the output power by simply controlling the input power through filtering the spectrum wavelength is designed for a Photovoltaic (PV) system. The main objective of this case study is to improve the PV module efficiency by using an optimal control scheme to design an active filtering process that enhances the output power through controlling the input power. The detailed derivation of the mathematical thermo-electrical model considering the wavelength-specific effects, which permits improving the predictions of temperature and module performance, are discussed in the previous chapter. The design and simulation of the plant model, as well as the MPC controller, are carried out on the MATLAB/Simulink environment. Subsequent to the above investigation, the PV system is used as a renewable source in a micro-grid that consists of a fossil fuel energy plant and grid-level energy storage. The residential customer is modeled using an expected demand. The objective of the optimal control scheme is for the generation to meet the demand, minimize the use of fossil fuels and ensure the energy storage is always maintained

around a nominal point such that it is not over-depleted. Hence, the formulation of the cost function, system constraints, system dynamics, and the control scheme are discussed in the previous chapter. This chapter presents the results and analysis obtained in the two case studies conducted.

4.2 Description of the System Models

In this section, the MATLAB/Simulink environment is used to model the system dynamics of the two cases investigated in this chapter. The first model is the wavelength-based thermo-electrical model of a PV module. The purpose of the model is to accurately predict the impact of each module wavelength on both the temperature and the output power of the PV module. The various thermal and thermo-electrical models in literature [9], [207] that predict the PV module temperature, output power, and the interaction between them have some shortcomings. Firstly, the estimated input power in these models depends on the supposition that the generated current is proportional to the total power density of the incident solar irradiance ignoring the wave-specific effects. Notably, the PV cell reacts to a specific wavelength range of the sun-oriented irradiance to create power. This range relies upon the photovoltaic material. In this manner, just this segment of the solar irradiance ought to be taken into account to compute the input power to the PV material. Secondly, these models, therefore, utilized a constant absorption coefficient for all wavelengths neglecting the various optical properties of the distinctive module layers and the internal light reflections between these layers. This possibly influences the predictions of the model input and output power. Moreover, the temperature of the PV module is a function of the thermal properties of the material composing the module, the incident radiant power density, the heat transfer exchange with the surroundings and the output electrical power [246], [247].

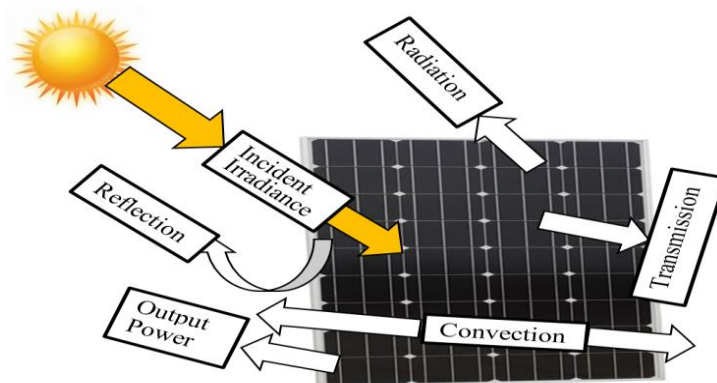


Figure 4-1: Heat transfer and exchange of energy in the PV module

Similarly, the PV system used previously is integrated into the stand-alone micro-grid system in case study 2. The MATLAB/Simulink environment is used to model the system dynamics of the renewable energy-based micro-grid depicted in Figure 4-2. The micro-grid system consists of three energy sources, such as a PV system, a storage system (SS), and a diesel generator (DG). The 50kW PV solar system is the

representative of renewable energy sources used. The storage system has been approximated for a maximum storage capacity of $800kWh$ using an energy/power flow model with self-discharge depicting the losses incurred with the storage bank, which allows for bi-directional power flows to/from the micro-grid. The DG considered is a commercially available $150kW$ diesel-powered generator whose usage is to be maintained at a minimum.

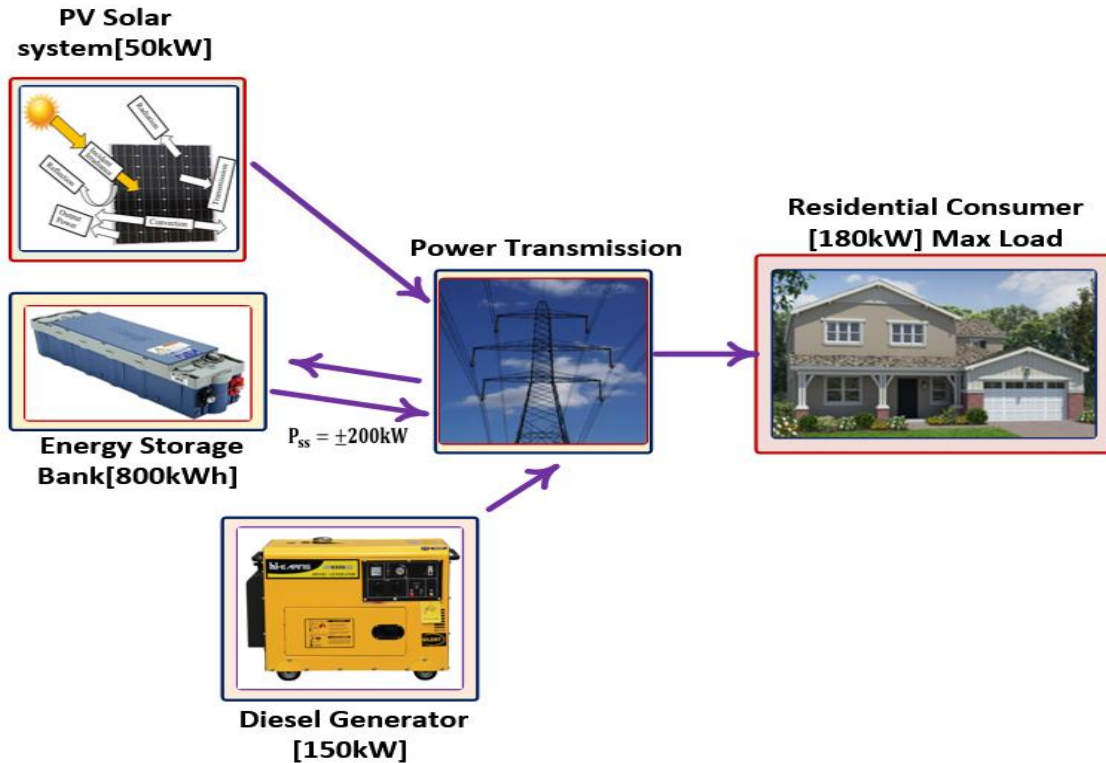


Figure 4-2: The model-based design description of the micro-grid under study

4.3 Simulation Results and Discussions

This section presents the results of the MATLAB/Simulink simulation of the two case studies. The first case study is to locate the optimal output power of the PV module at each ambient temperature and also to investigate the tracking response performance of the MPC controller between the module temperature and the reference temperature of the PV module.

4.3.1 Scenario 1: Location of the Optimal Power at Each Ambient Temperature

In this section, a Simulink model was utilized for the Design of Experiment (DOE), so as to find the optimal output power at each ambient temperature, T_{amb} . The DOE has two essential input factors, the ultraviolet (UV) cut-off wavelength λ_{UV} and ambient temperature T_{amb} . Thus, these input factors of DOE presume that the UV cut-off wavelength range is $300 \leq \lambda_{UV} \leq 430$ divided into 14 levels, and the ambient

temperature range is $280 \leq T_{amb} \leq 340$ divided into 10 levels. Meanwhile, at each simulation, both the PV output power and the temperature are measured and recorded. Notice that the duration of the simulation must be based on the time constant of the system.

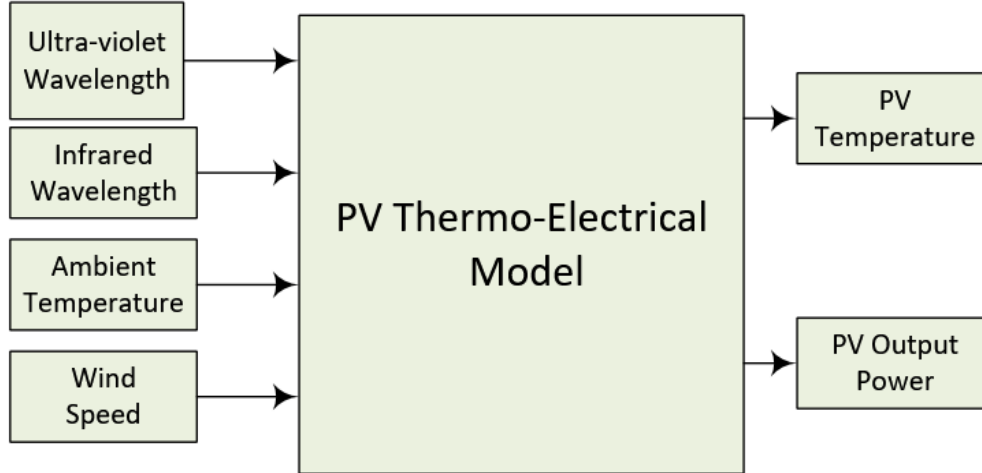


Figure 4-3: System model for the design of experiment (DOE)

The heat capacity of the module is calculated using the parameters given in Table D-1. The inputs to this model are ultraviolet wavelength λ_{UV} , the infrared wavelength λ_{IR} (it is constant and has a value of 11,100nm), the ambient temperature, T_{amb} , and the wind speed, WS. T_{amb} and W_{spd} are the measured inputs and λ_{UV} is the manipulated variable. The PV model computes the heat transfer and the input power using Equations (3-10) and (3-21), respectively. The PV plant outputs are the module temperature and output power, of which both are measurable quantities. Figure 4-4 depicts the plot of the representation of the PV module output power against the ambient temperature and, likewise, the PV temperature against the ambient temperature. Hence, it can be seen that the relationship between the PV output power and ambient temperature is inversely proportional, as said earlier, the higher the ambient temperature, the lesser the output power of the PV module. The PV temperature has an increasing relationship with ambient temperature. Moreover, at each ambient temperature, the maximum output power is selected. Therefore, a linear fit expression is generated for the ambient and PV module temperature that maximizes the PV module output power. The expression for the linear fit between the PV temperature and the ambient temperature is given as:

$$T_m = 0.916T_{amb} + 79.79 \quad (4-1)$$

More so, the reference PV module temperature for MPC is generated by using Equation (4-1), and then, the controller will attempt to maintain this reference temperature by manipulating the cut-off wavelength λ_{UV} , so that at any given ambient temperature, the maximum output power can be generated.

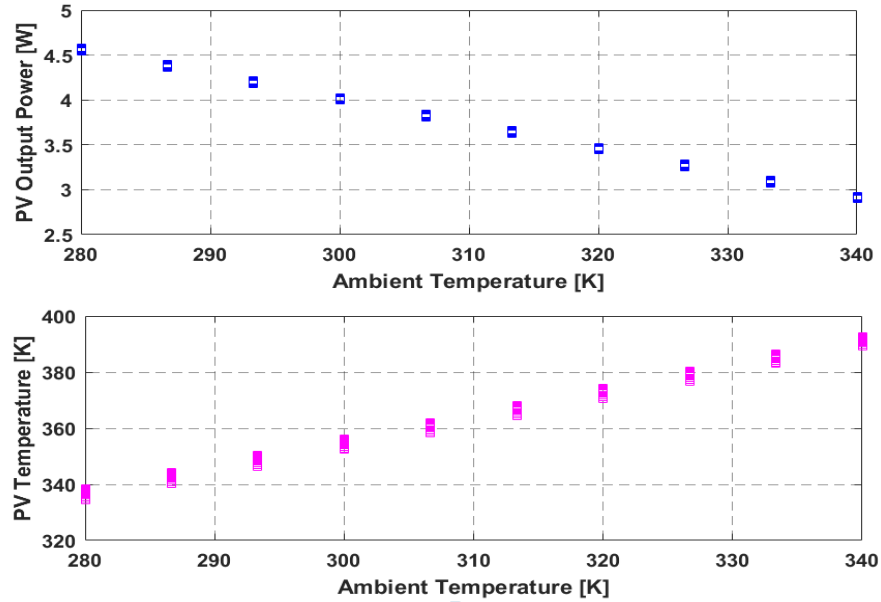


Figure 4-4: The output power and temperature of a PV module against the ambient temperature

4.3.2 Scenario 2: Generation of data required for system linearization from the PV module

The generation of an approximate linearized plant model is essential for designing an MPC controller. In this section, the input-output data that is required for the system identification are extracted. As earlier said, the thermo-electrical model given in Equation (3-1) is used as the plant that data are derived from it. Therefore, in order to generate the necessary data for linearization, two-step changes in λ_{UV} is connected with the plant model. The ultraviolet wavelength, λ_{UV} has a value that changes from minimum (300 nm) to maximum (430 nm) and thenceforth back to the minimum (300 nm). Figure 4-5 depicts the System model utilized to generate the data required for the system linearization from the PV module. From Figure 4-5, it is seen that the wind speed and the ambient temperature are provided as a lookup table as these inputs change dynamically with time. The manipulated input λ_{IR} is maintained at a value of 1100 nm. The module temperature and output power would dynamically be affected due to the reduction in the module input power when the value of λ_{UV} is changed to a value higher than 300 nm. Therefore, stepping the value of λ_{UV} from 430 to 300 nm increases the input power, which, therefore, increases the module temperature.

Figure 4-5 is used to extract the matrix components A, B, C, and D that are augmented state-space models used in predictive control design. These components are extracted from the system model and are represented in a state-space format. The results of the system linearization are as follows:

System identification of the PV_Linear_Model

$$\text{Stp_size} = 10 \tag{4-2}$$

System = Discrete-time identified state-space model:

$$x(t + T_s) = Ax(t) + Bu(t) + Ke(t) \quad (4-3)$$

$$y(t) = Cx(t) + Du(t) + e(t) \quad (4-4)$$

$$A = \begin{bmatrix} 0 & 1 & 0 \\ 0 & 0 & 1 \\ 0.9681 & -2.936 & 2.9677 \end{bmatrix}, B = \begin{bmatrix} -0.0007632 \\ -0.0007444 \\ -0.0007262 \end{bmatrix}, C = [1 \ 0 \ 0], K = \begin{bmatrix} 0 \\ 0 \\ 0 \end{bmatrix}, D = [0] \quad (4-5)$$

Sample time: 10 seconds, Discrete-time state-state model.

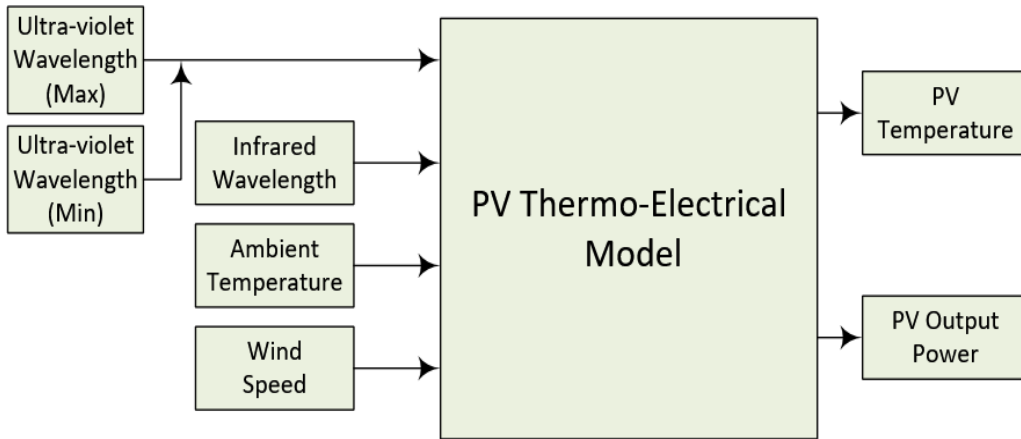


Figure 4-5: System linearization from the PV module

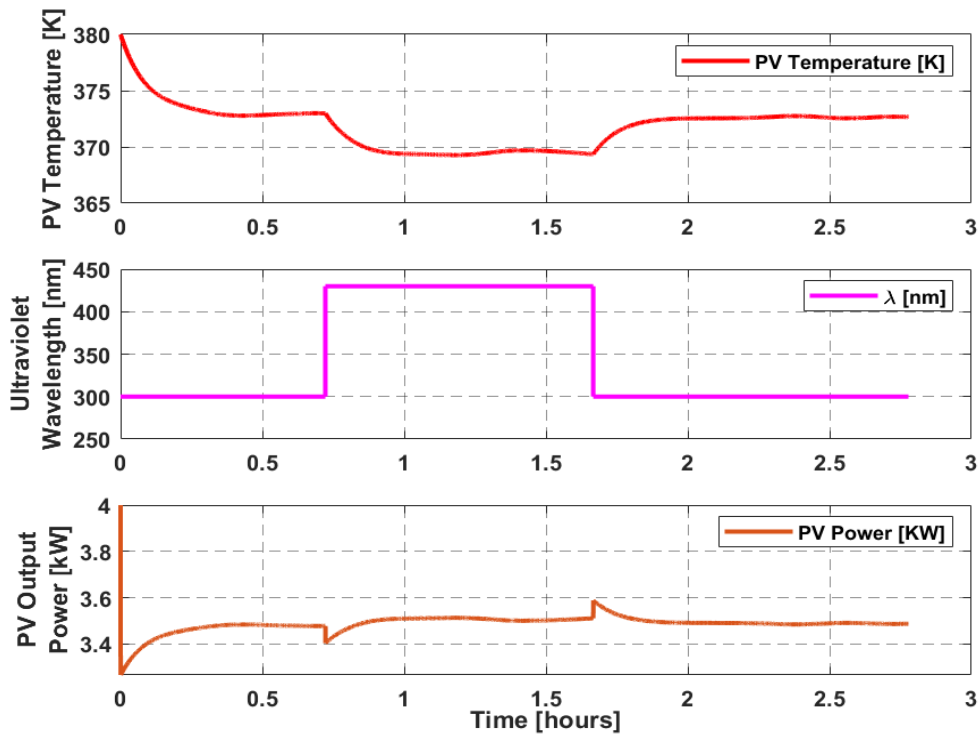


Figure 4-6: System identification of the input and output parameters of the PV module

Figure 4-6 shows the system identification of the input (ultraviolet wavelength λ_{UV}) and output (PV module temperature T_{module} and output power P_{out}) parameters of the PV module. It is evident in Figure 4-6 that at a wavelength of 300 nm, there is a reduction in the temperature of the PV module. Whereas the PV output power increases at that value of the ultraviolet wavelength, and this takes place for 2520 seconds. At 2520 seconds, the value of the ultraviolet wavelength increased to 430 nm. It maintained the value until 6120 seconds; during this period, the PV module temperature decreases drastically, which consequently increases the output power of the PV module. Subsequently, the value λ_{UV} further reduced to 300 nm, which at the same time affects both the PV module temperature and output power, as shown in Figure 4-6. Subsequent to the system linearization of the PV module, it is essential to determine the accuracy of the data generated from the linearized model by comparing it with the actual data before linearization. Figure 4-7 depicts the response of actual and linearized data for step changes. A function called compare was used to generate a comparison plot between the linearized model and the actual data of the PV module under study. The match percentage, as seen in Figure 4-7 is 92.36%, which signifies a good match between the linearized model and the actual plant.

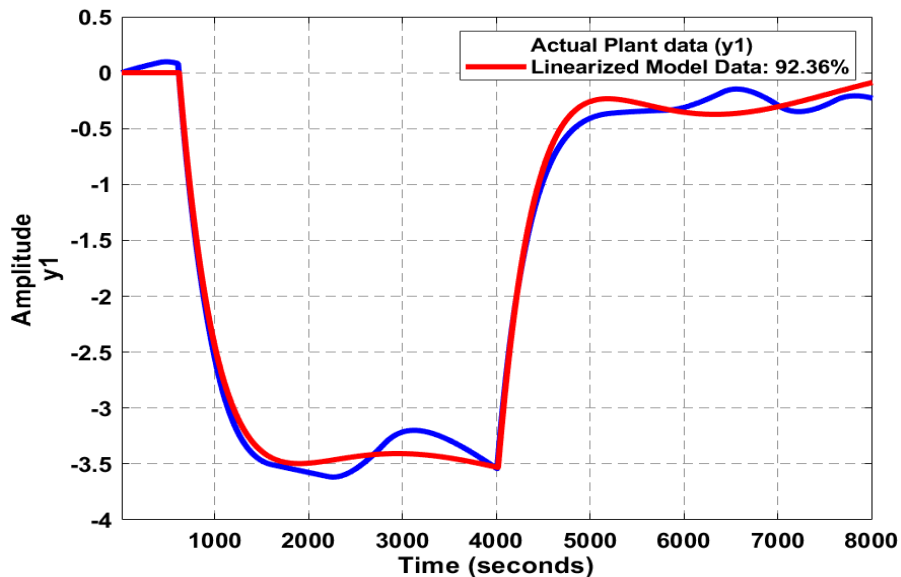


Figure 4-7: Simulated response comparison of the linearized and actual plant model data

4.3.3 MPC Controller Tracking Performance of the PV Module Temperature

MPC control is a robust control scheme used in the industries to control sophisticated appliances that have to do with the prediction of their future output. Therefore, providing MPC with the constraints for the actuators, their rates, together with the range for the outputs, permits the MPC quadratic solver to select physically obtainable values, also lessening the tuning time. The range of λ_{UV} is [300, 430] nm. The range for T_m is not completely known as it relies on the solar irradiance conditions, wind speed and ambient

temperature in addition to λ_{UV} . A broad range value of [62, 482] F was selected to investigate the impact of temperature on PV power efficiency. Meanwhile, the MPC controller is designed to provide a change in frequency $\Delta\lambda_{UV}$ rather than an absolute value of λ_{UV} . This practice in control design is prevalent. More so, the range of $\Delta\lambda_{UV}$ is [0, 130] nm whereas the nominal value for λ_{UV} is 300 nm. Similarly, the range of ΔT_m is [-100, 100] F while the nominal value for T_m is 372 °F. The system identification process obtained from Figure 4-5 was used to generate the nominal values of T_m and λ_{UV} . To design the MPC controller, the linear model obtained in Figure 4-5 was loaded and simulated on MATLAB/Simulink, and then the MPC Designer App GUI was opened to starting the MPC controller design process. The controller was configured using the MPC structure button. The plant model (Linearized) was imported to generate an MPC controller for the plant model. The MPC Designer APP requires that the inputs and outputs be scaled. Subsequent to the scaling, the controller is then tuned, then the prediction and control horizon for MPC were selected. Therefore, in order to select the control and prediction horizon, it is imperative to know the time constant as well as the sampling frequency of the sensors. The control and prediction horizons were set to 2 and 10 respectively for better performance of the controller.

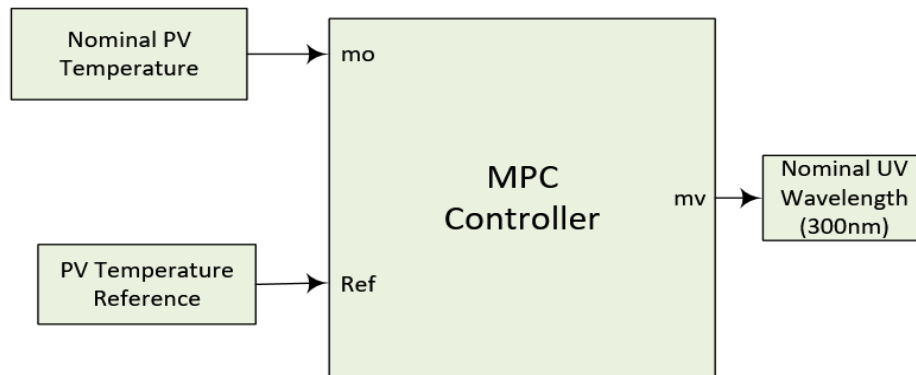


Figure 4-8: The simulation of the MPC controller

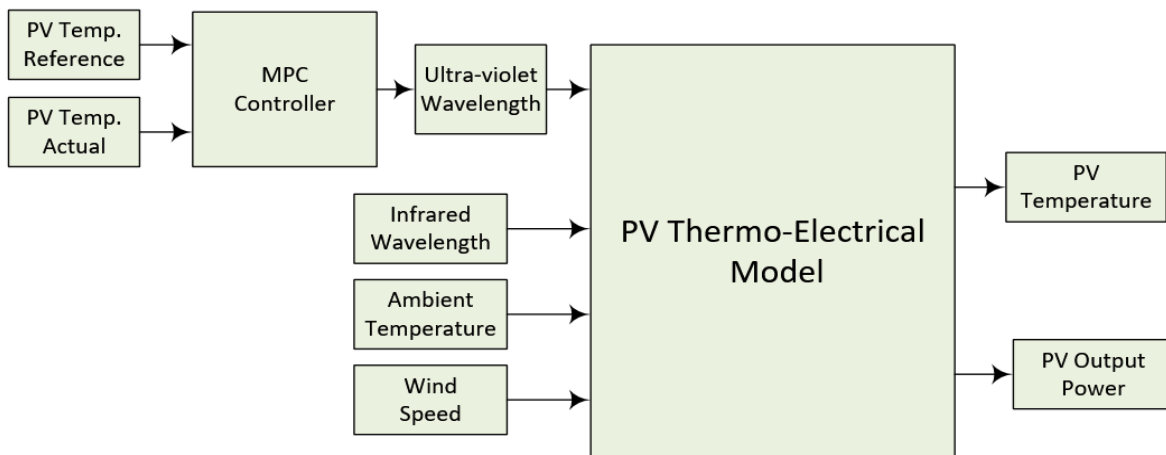


Figure 4-9: Overall simulation of MPC controller with the PV model

Furthermore, the constraints tab was used to define the range of the actuators, their rates, and the output. It is worth mentioning that the linear PV model, combined with the MPC controller, was utilized to simulate the design under study. The simulation of the MPC controller is depicted in Figure 4-8, which shows the block assembly of the components. Figure 4-9 shows the overall simulation of the MPC controller with the PV model. More so, it shows the integration of the designed MPC into the Simulink environment for evaluating the designed controller.

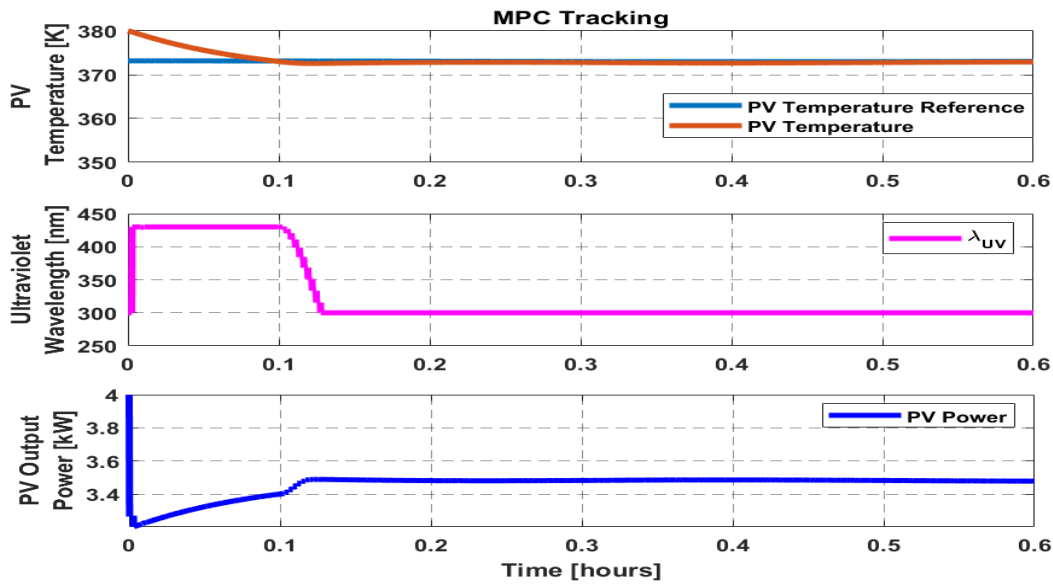


Figure 4-10: MPC controller performance for the first 2160 seconds of the simulation

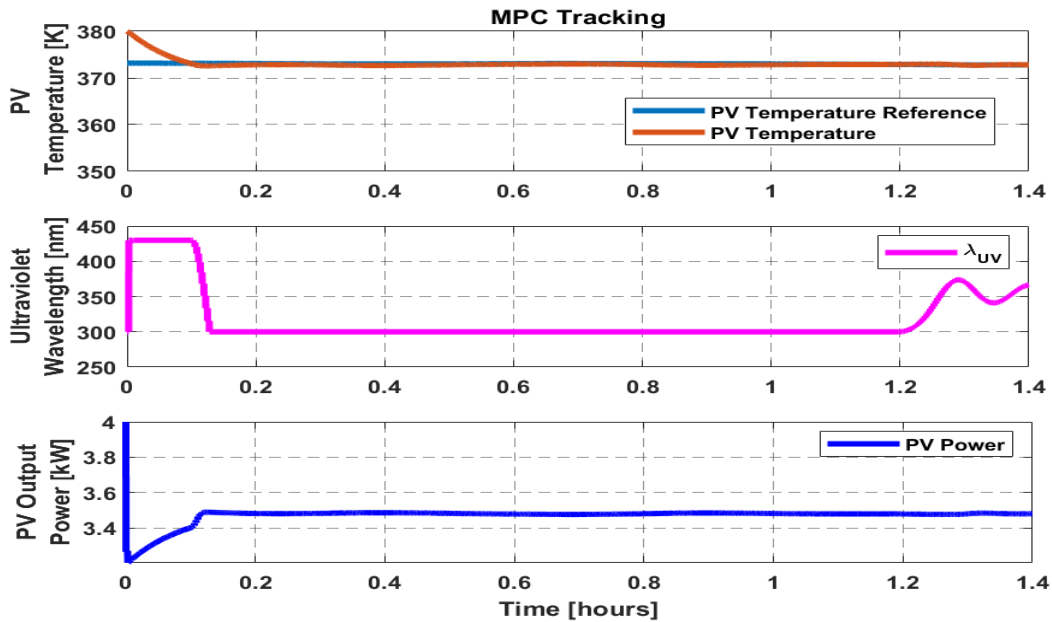


Figure 4-11: MPC controller performance for the first 1:40 hours of the simulation

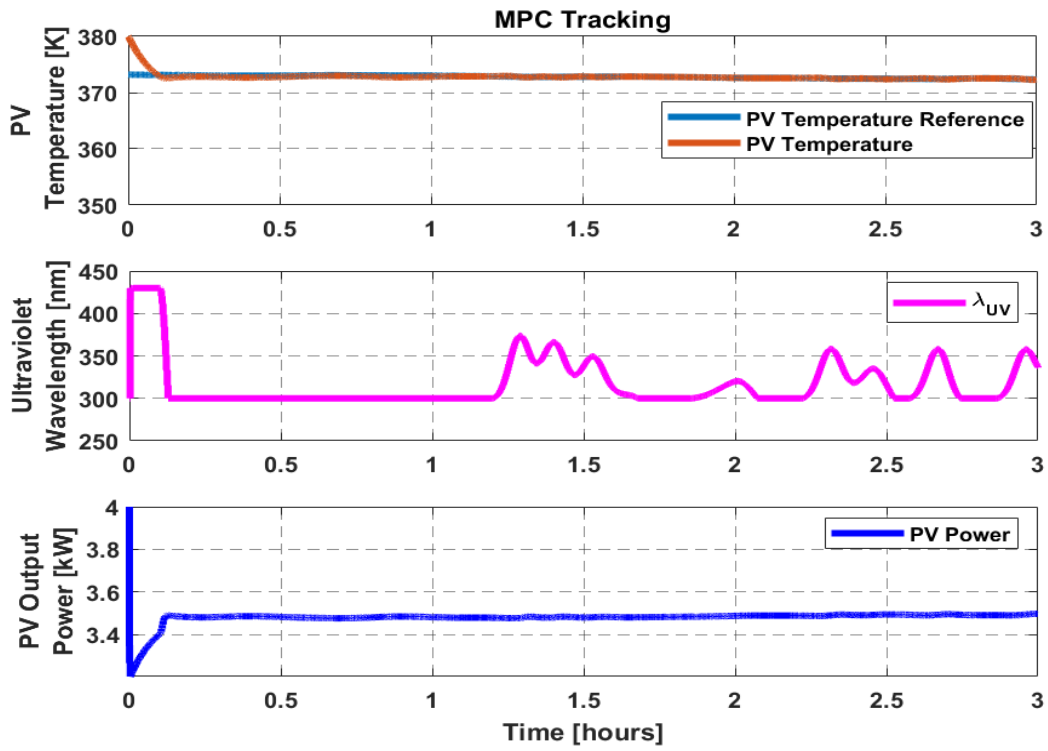


Figure 4-12: MPC controller performance for 3 hours of the simulation

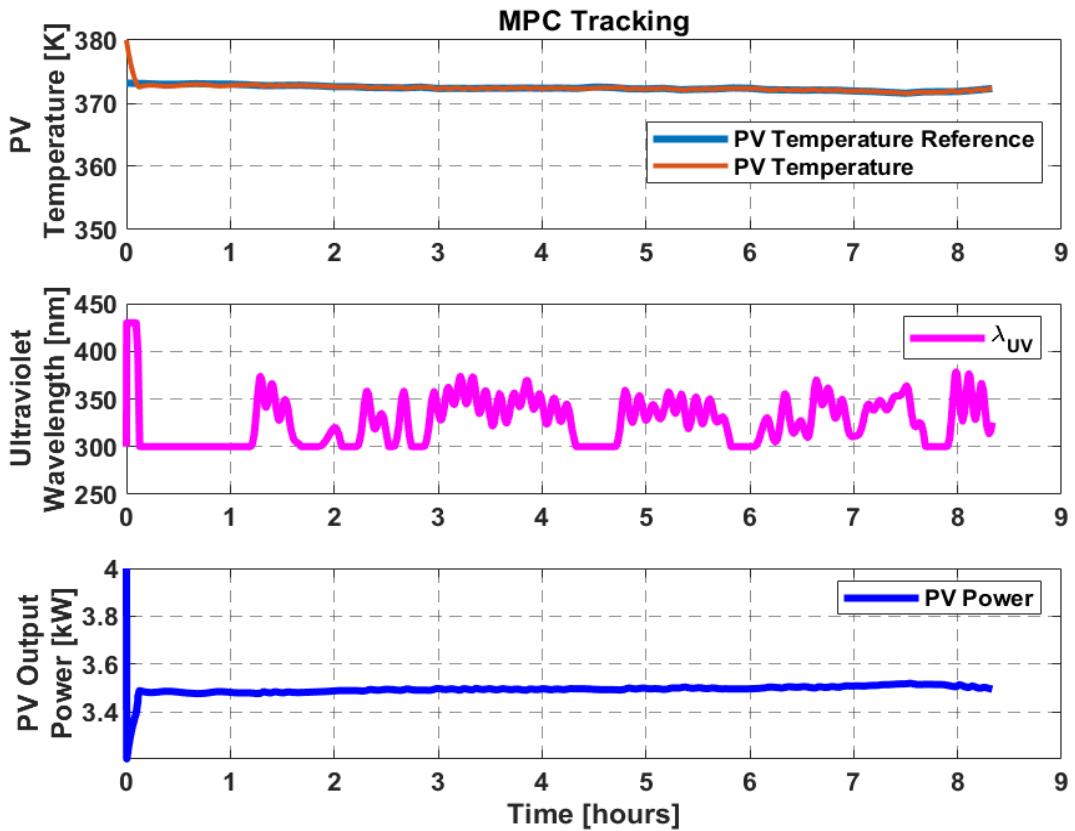


Figure 4-13: MPC controller performance for 9 hours of the simulation

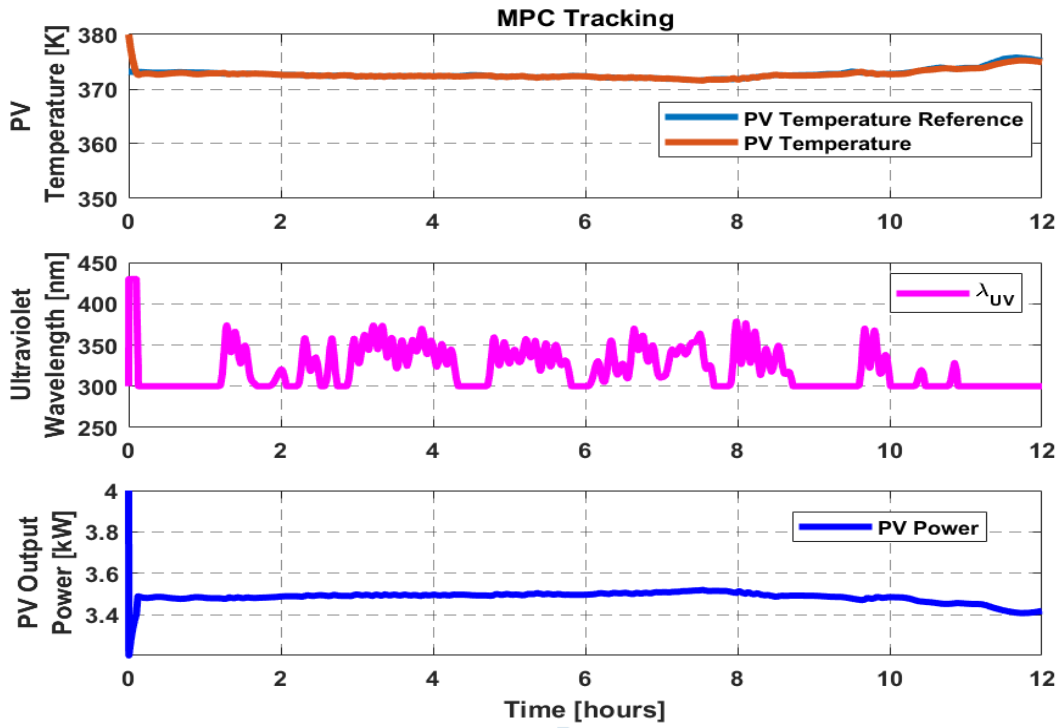


Figure 4-14: MPC controller performance for 12 hours of the simulation

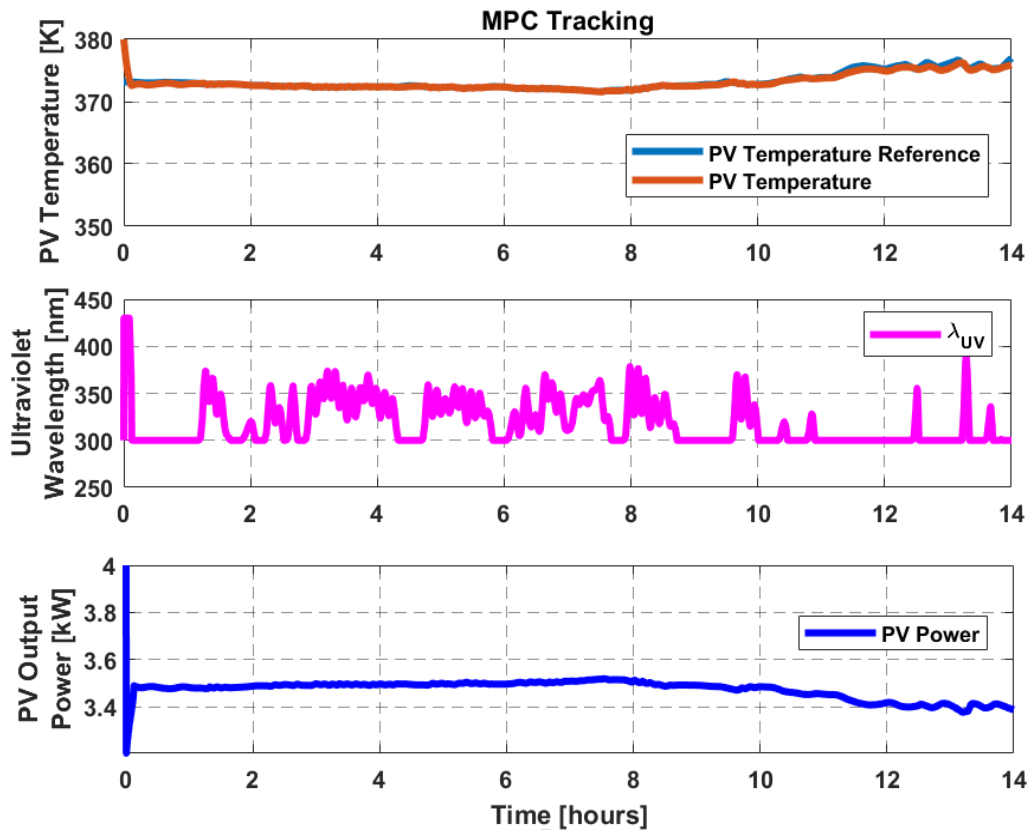


Figure 4-15: MPC controller performance for 14 hours of the simulation

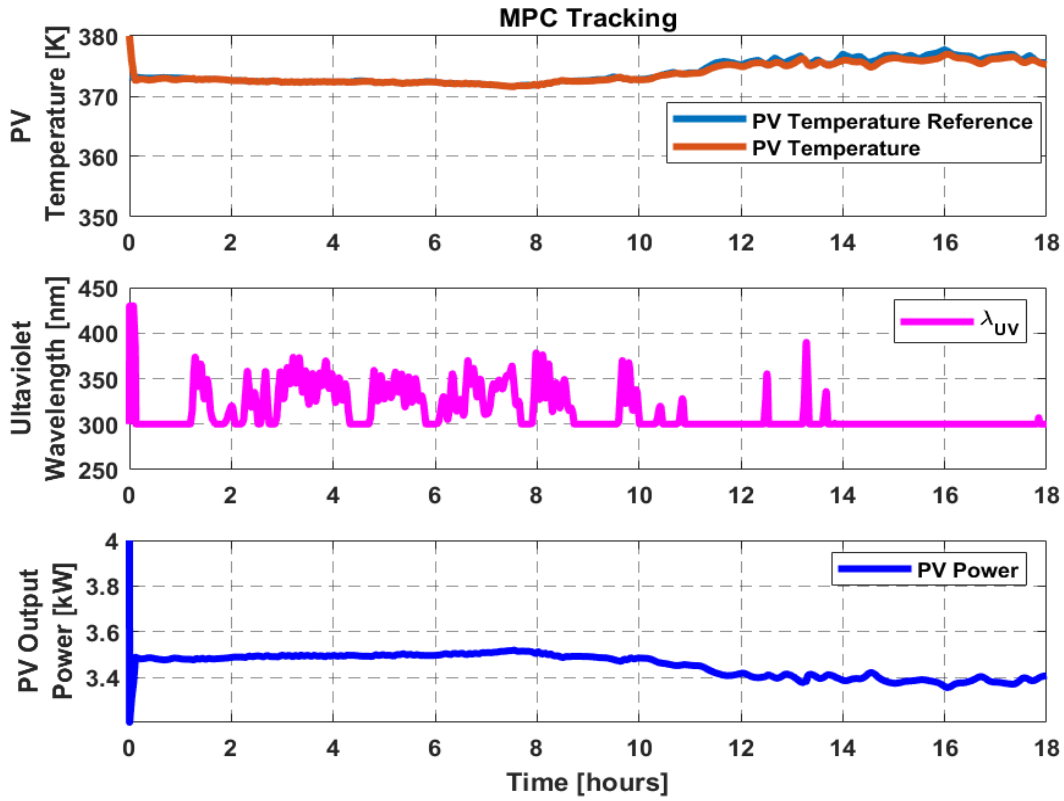


Figure 4-16: MPC controller performance for 18 hours of the simulation

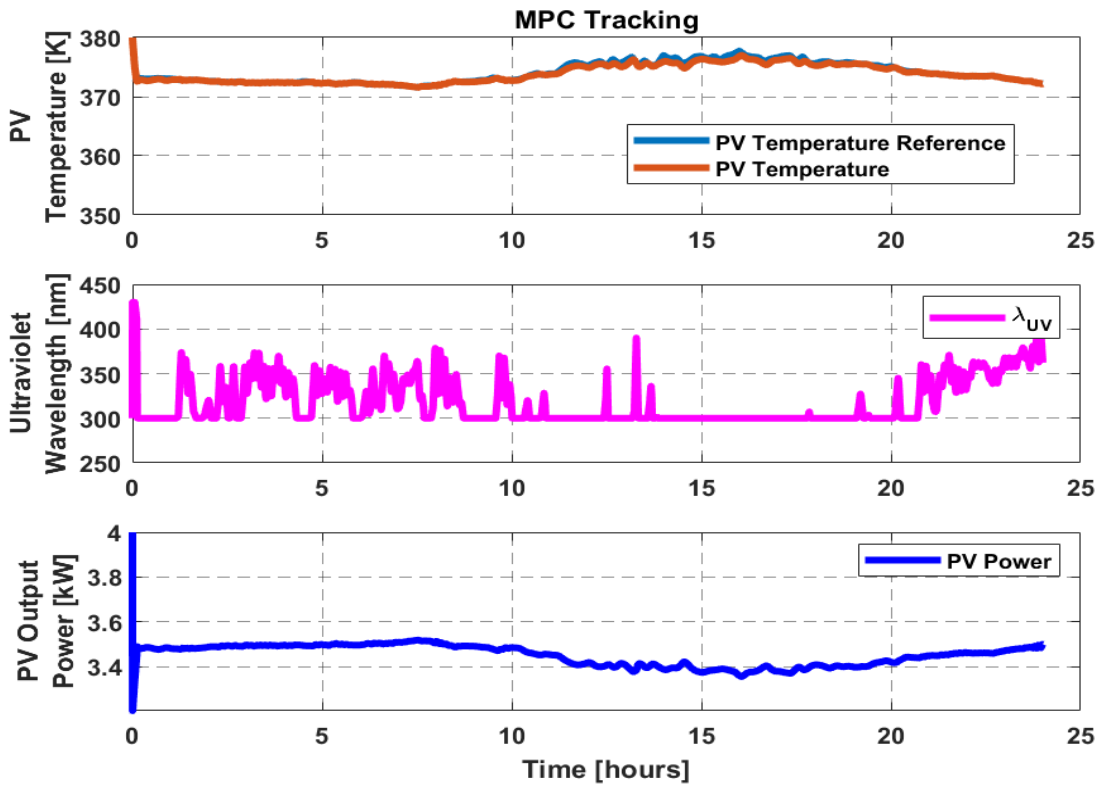


Figure 4-17: MPC controller performance for 24 hours of the simulation

Figures 4-10 to 4-17 show the study of MPC controller performance in terms of good tracking response at different hours of the simulation. The simulation was run for 24 hours, and the tracking performances of the MPC were investigated at various hours of the simulation. The tracking response of Figures 4-10 to 4-14 is fairly good, as it is evident, that the module temperature is lower than the reference temperature. Moreover, the MPC commands the lowest λ_{UV} value, which is 300 nm. This results in filtering, which in turn will generate the highest PV module temperature obtainable at the given ambient conditions. Figures 4-15 to 4-17 depict good tracking response of the MPC controller, as it is evident in these figures, the module and reference temperature are precisely on each other, which therefore shows excellent tracking performance. Hence, it is noticed from Figure 4-14 to 4-17 that, at about 2 hours, power is at the maximum value of this portion of the simulation.

Similarly, this section further presents the results of the MATLAB/Simulink simulation of Figure 4-2. The problem to be solved by the AMPC control algorithm is to perform an optimal power reference tracking problem, where the consumption of energy from the diesel generator is minimized while maximizing the efficiency of the storage bank. The AMPC control technique is implemented for choosing an optimal mode of inputs for the system for tracking both a constant and load-varying power demand profile. Therefore, the main goal is to maximize the use of renewable sources and minimizing the use of traditional sources.

4.3.4 Reference Power Profile

The load reference profile obtained from [215] for a 24hrs time horizon and is shown in Fig. 4-18. This power demand profile reflects real-world characteristics and has a peak power demand of 180kW. In this context, the reference to be tracked is modeled as in Equation 4-6, where the power from the solar plant is subtracted from the consumer load to provide the full reference power that the micro-grid needs to deliver. Therefore, other renewable energy sources can, at this point, be used further to reduce the power levels of the demand profile.

$$P_{ref} = P_{load} - P_{solar}(t) \quad (4-6)$$

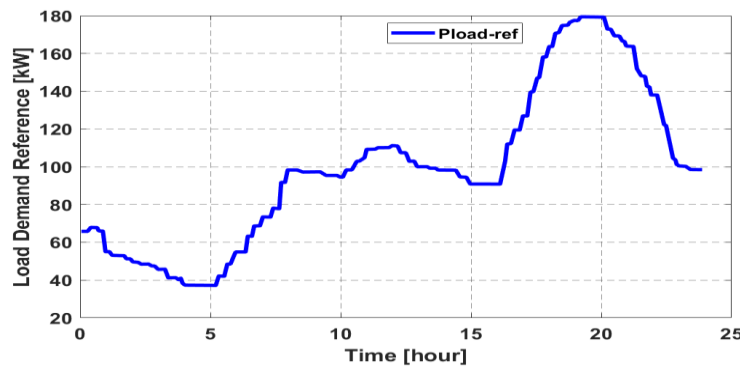


Figure 4-18: Consumer load power

Figure 4-18 is the reference power demand curve that would need to be met by the energy management unit. The power demand profile is known 24hrs in advance. Having a reference power profile to meet 24hrs in advance is a standard model that is currently in use by energy exchanges where 15min intervals that are bid reserved and sold 24hrs in advance. While this allows for an efficient overall strategy, near term load demands are mostly met by the surplus that is passed to the micro-grid as a factor of safety. The proposed model can efficiently manage power demands that are made known a few minutes to hours in advance. Meeting such immediate demands is limited to the response rate of the fastest energy producer, which in this case, is the energy storage.

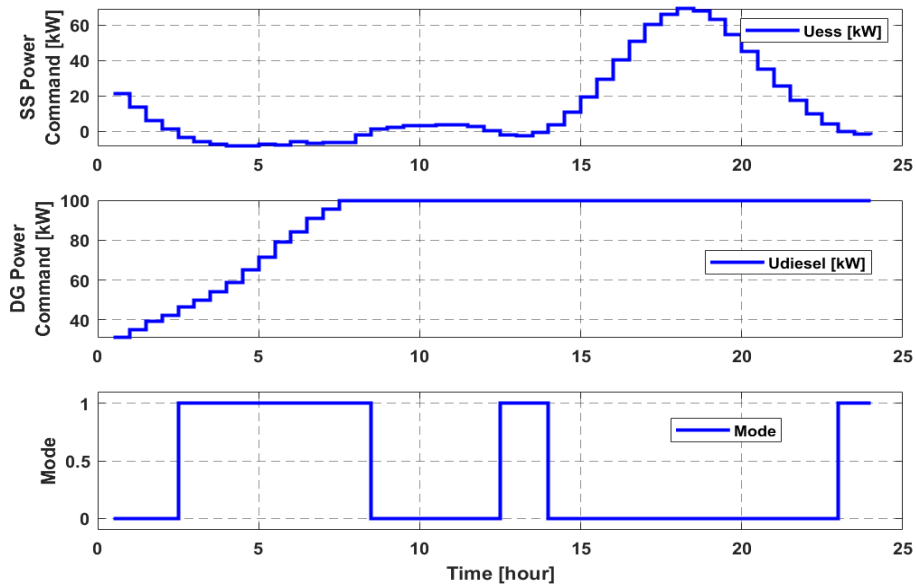


Figure 4-19: Optimal control inputs for tracking a 50-kW constant load

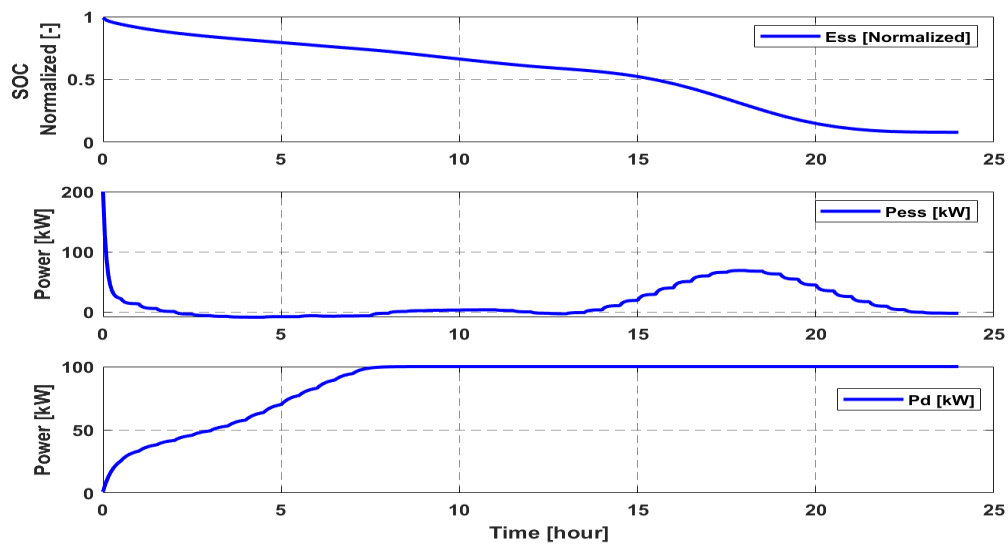


Figure 4-20: Trajectory followed by the state variables with a 50-kW constant load

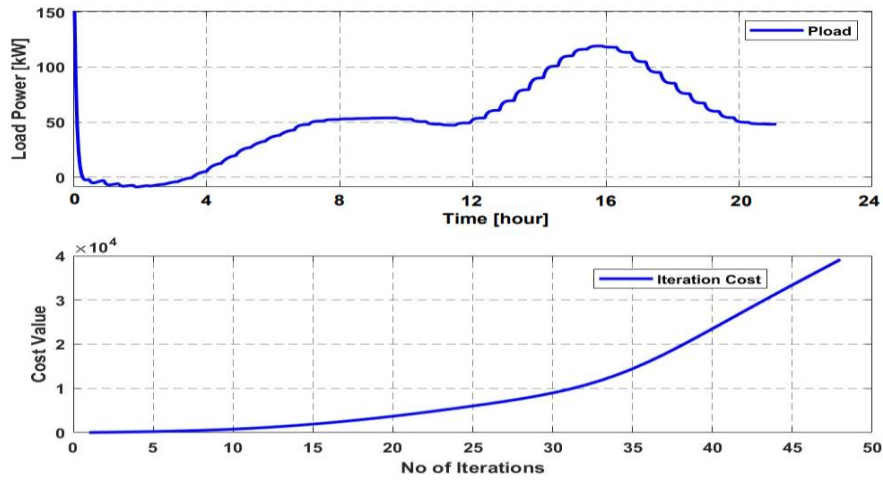


Figure 4-21: The load power and cost value with a 50-kW constant load

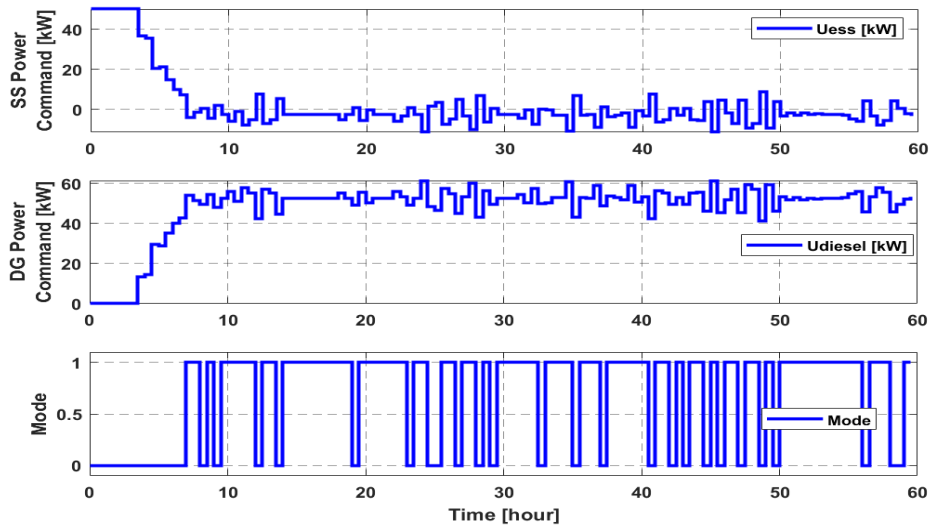


Figure 4-22: Optimal control inputs for tracking a 50-kW constant load

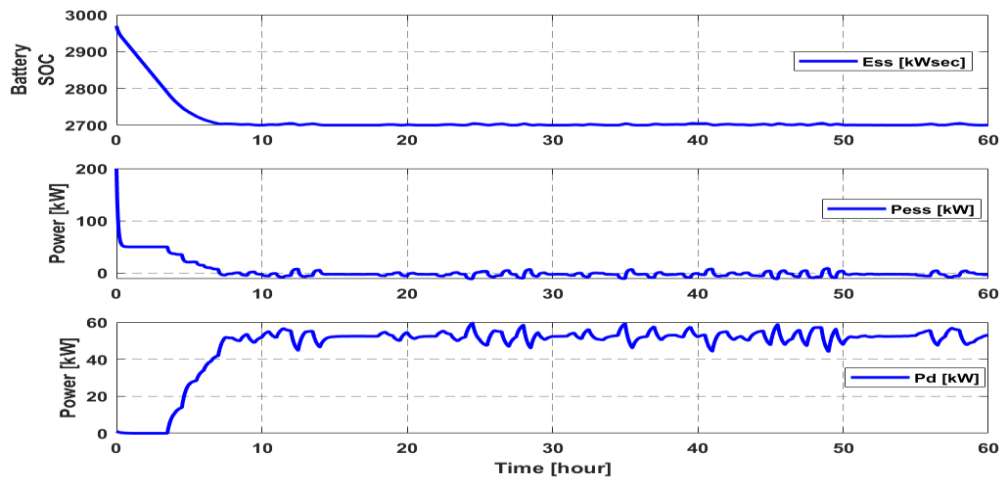


Figure 4-23: Trajectory followed by the state variables with a 50-kW constant load

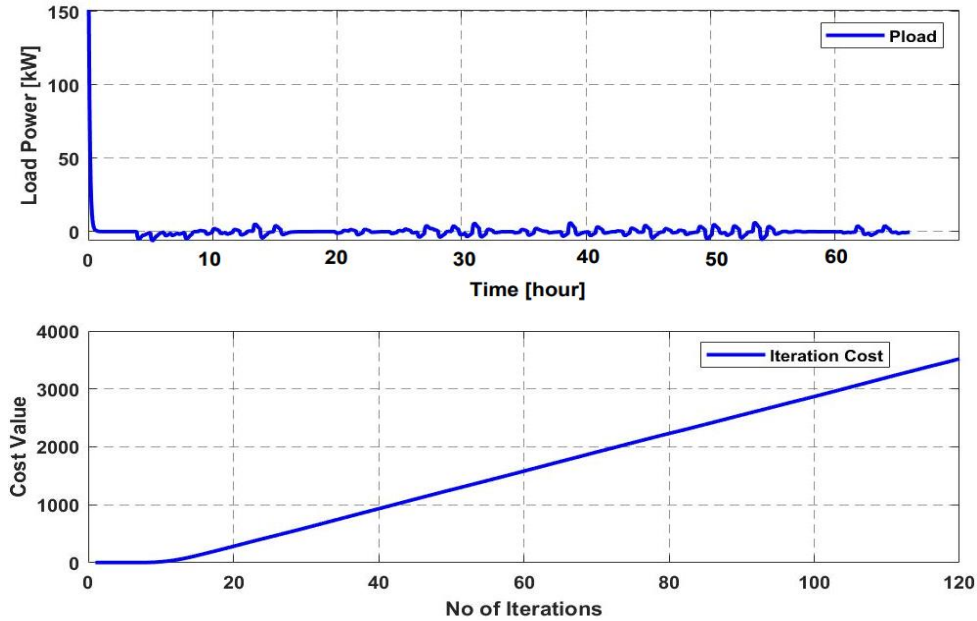


Figure 4-24: The load power and cost value with a 50-kW constant load

Figures 4-19 to 4-21 depict the three sets of control inputs commands, the trajectory followed by the state variables, the remaining load power (Generations-Consumptions), and the corresponding iteration cost obtained from tracking a 50-kW power reference load (constant). Notice that all simulations are run using the set of initial conditions. The reference to be tracked is modeled as Equation (4-6), where the power from the solar system is subtracted from the consumer load to provide the full reference power that the energy sources will need to deliver. This means that the solar system is the primary source of the small-scale micro-grid; the diesel plant only supplies the remaining load demand reference that the solar system could not meet. The objective is to use the AMPC control algorithm to optimally track this power reference, such that the consumption of energy from the diesel generator is minimized while maximizing the efficiency of the storage bank. Hence, the simulation here was performed in hours for a total of 24 hours spanned. It is evident from Figures 4-19 to 4-21 that the power produced by the diesel generator does oscillate about a constant value of 50-kW, as it is trying to follow the reference. Furthermore, it is seen that as the diesel generator tries to stabilize, the hybrid state continues to switch from one mode to another, as it is expected since the system is trying to find the correct balance between the two sources (diesel generation and storage system). Thus, it is clear that as the diesel generator is delivering the required power, the power produced by the energy storage system drops. The simulation was further run for 60 hours to investigate the tracking performance of the proposed algorithm with regards to the supply and the constant load demand reference. Figures 4-22 to 4-24 show the outcome of the simulation. It is evident from the result that, when the diesel plant reaches its generation limit, the battery starts supplying the load demand until its SOC value gets to its limit.

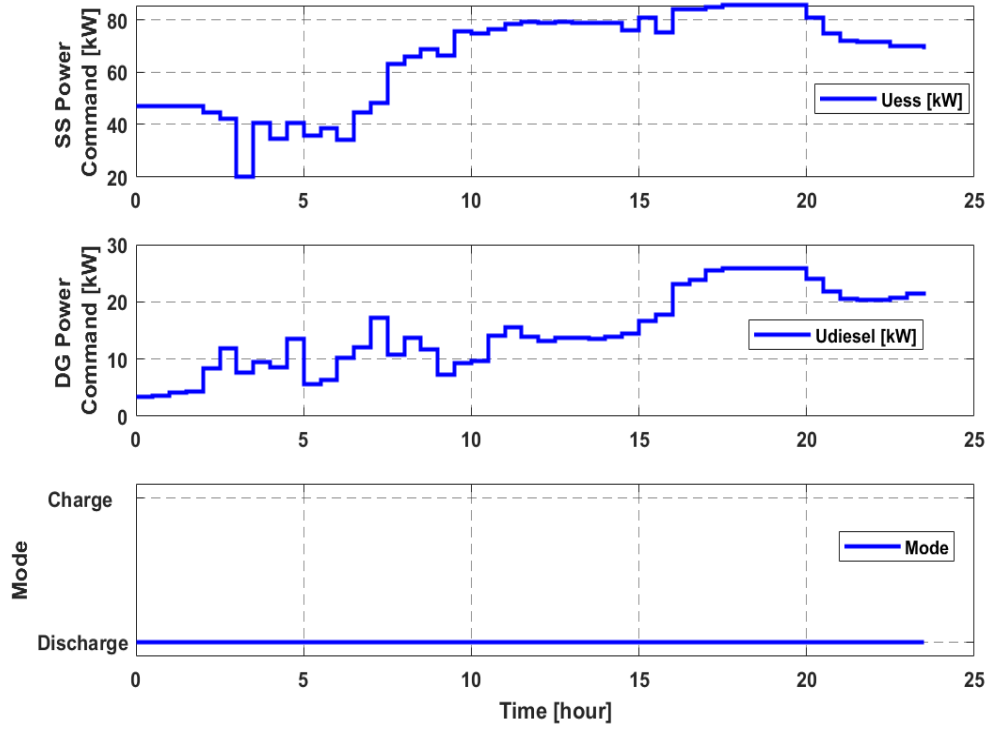


Figure 4-25: Optimal control inputs for tracking a load-varying profile reference ($W_x[2,5,10]$)

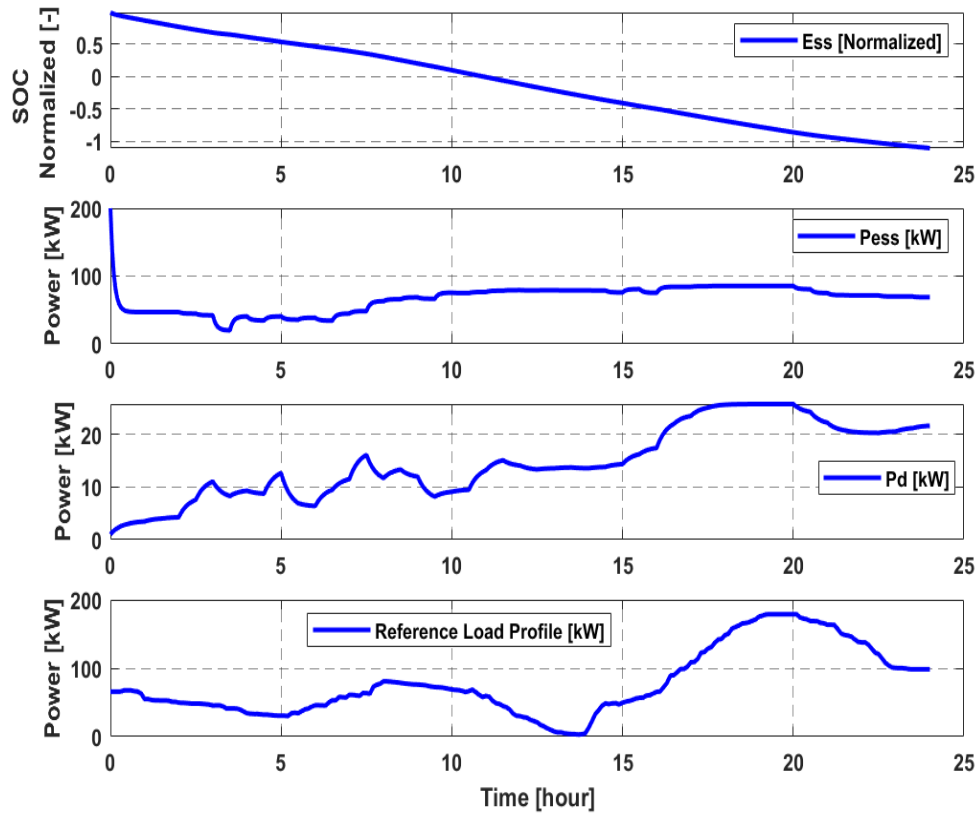


Figure 4-26: Trajectory followed by the state variables with a load-varying profile reference ($W_x[2,5,10]$)

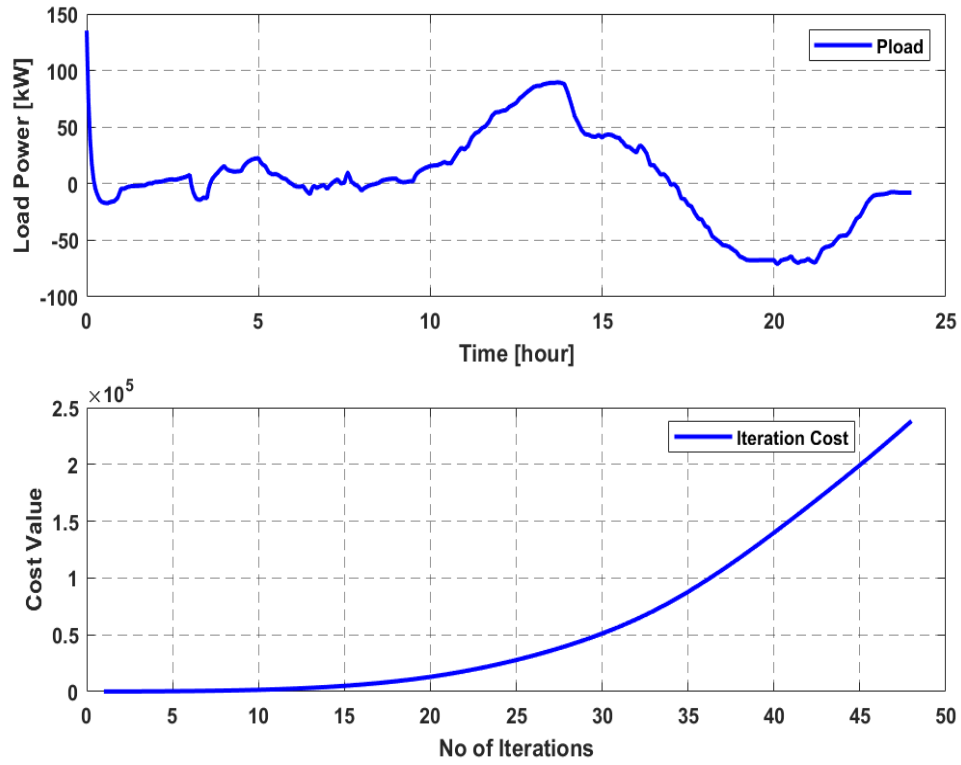


Figure 4-27: The load power and cost value with a load-varying profile reference ($W_x[2,5,10]$)

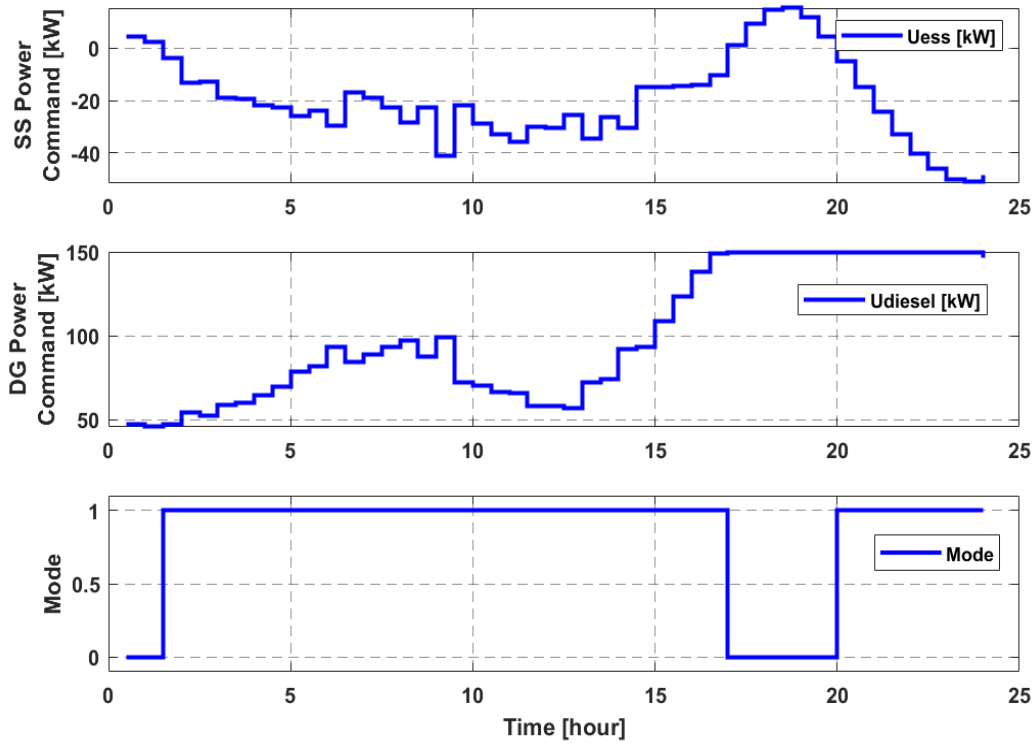


Figure 4-28: Optimal control inputs for tracking a load-varying profile reference ($W_x[5,2,20]$)

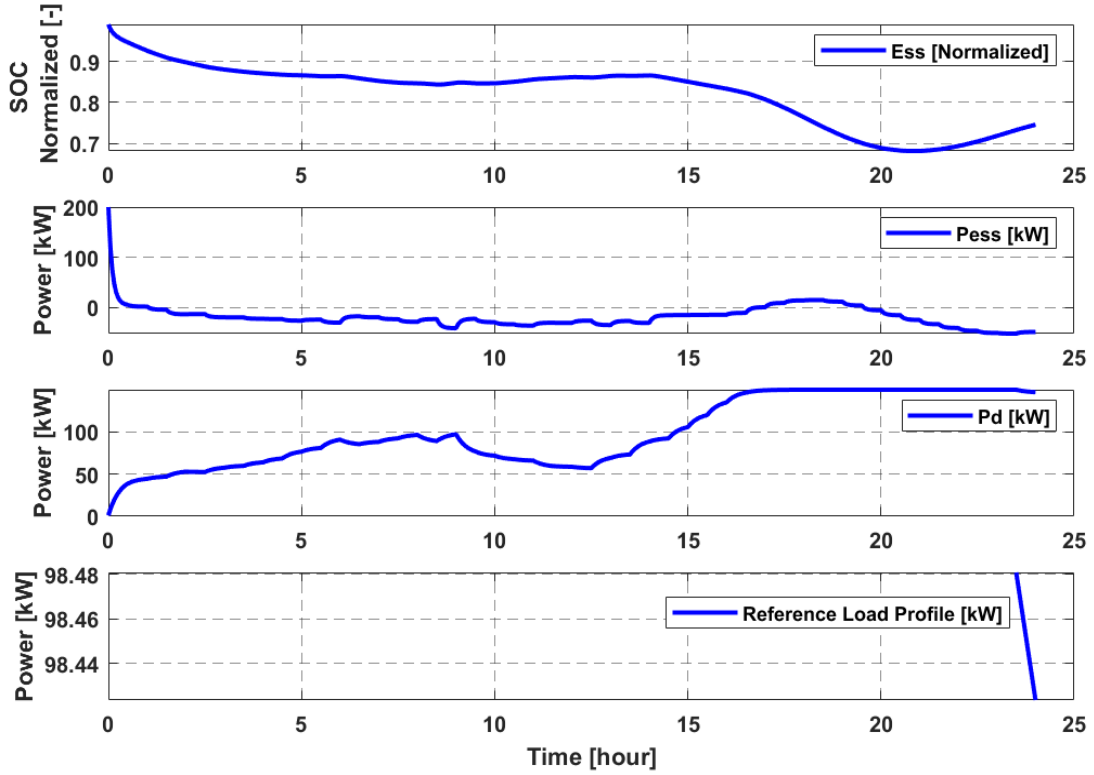


Figure 4-29: Trajectory followed by the state variables with a load-varying profile reference ($W_x[5,2,20]$)

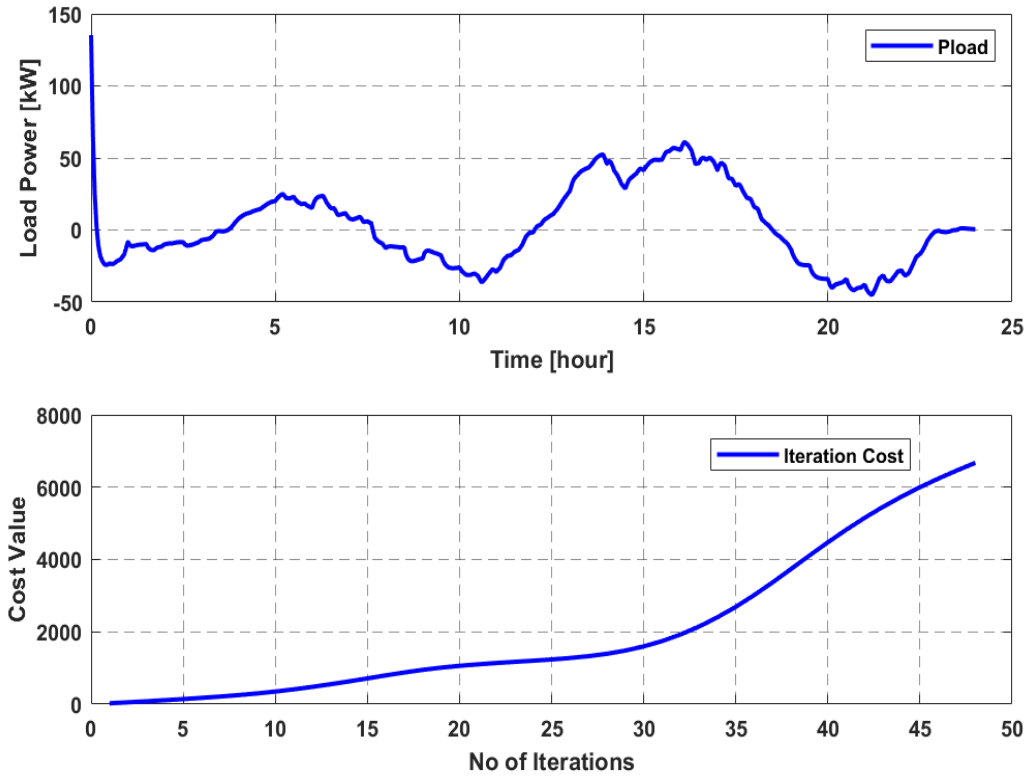


Figure 4-30: The load power and cost value with a load-varying profile reference ($W_x[5,2,20]$)

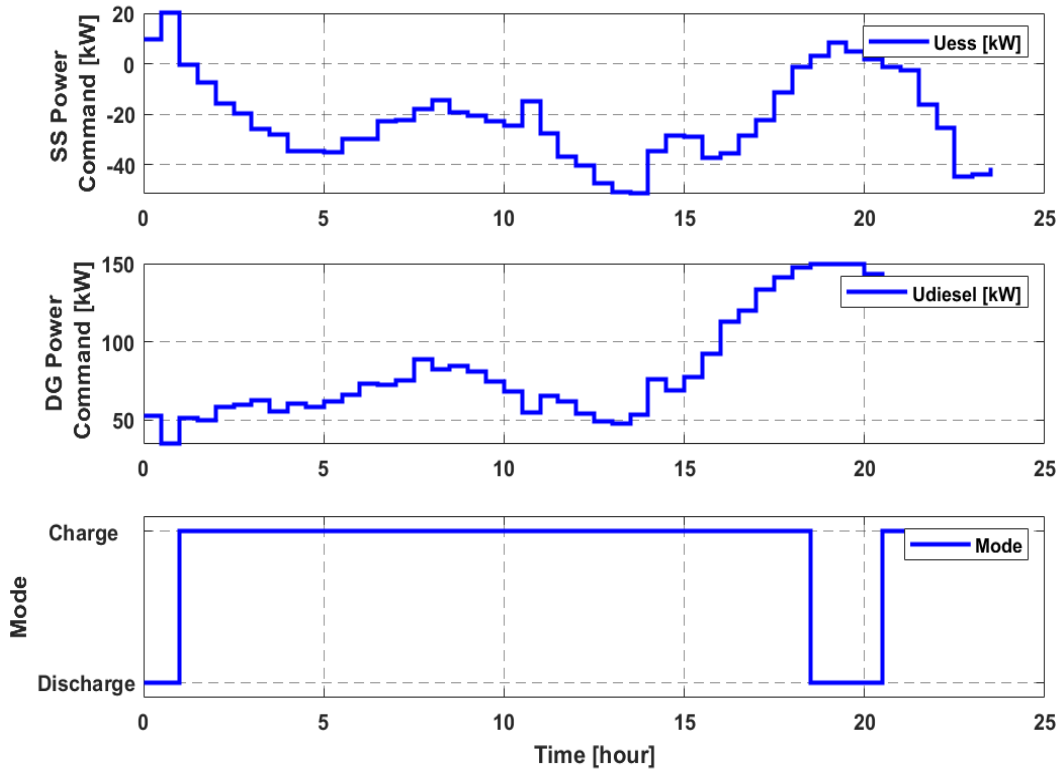


Figure 4-31: Optimal control inputs for tracking a load-varying profile reference ($W_x[5,2,40]$)

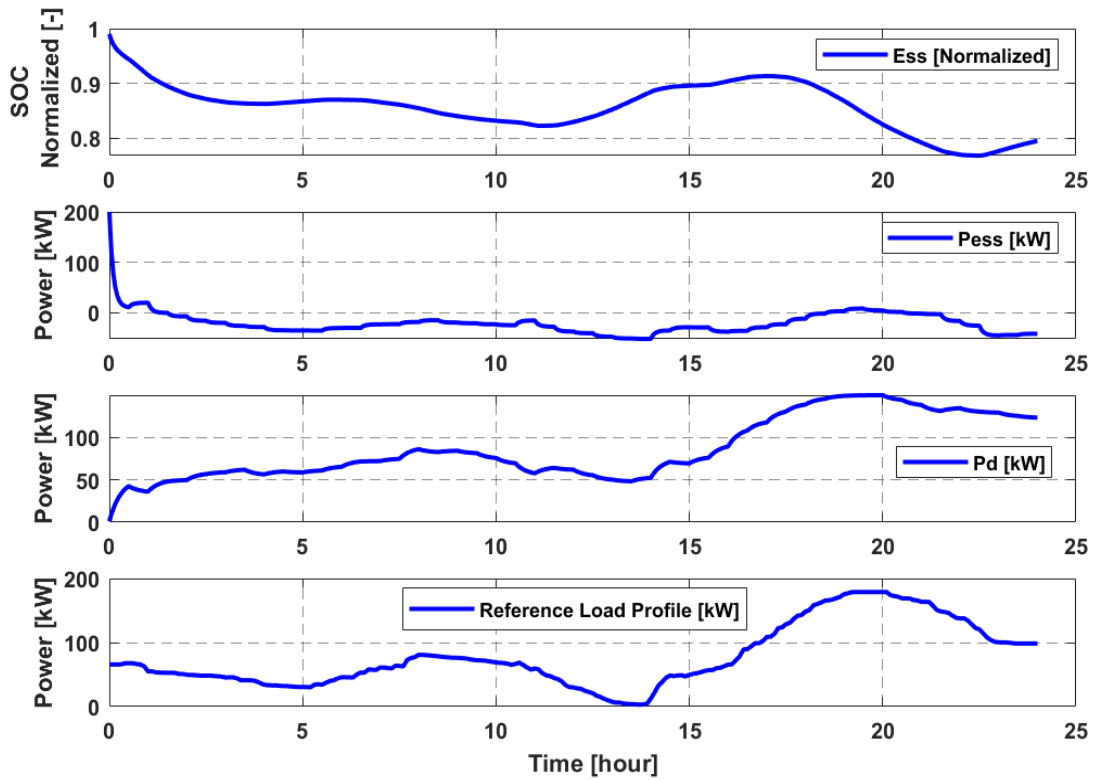


Figure 4-32: Trajectory followed by the state variables with a load-varying profile reference ($W_x[5,2,40]$)

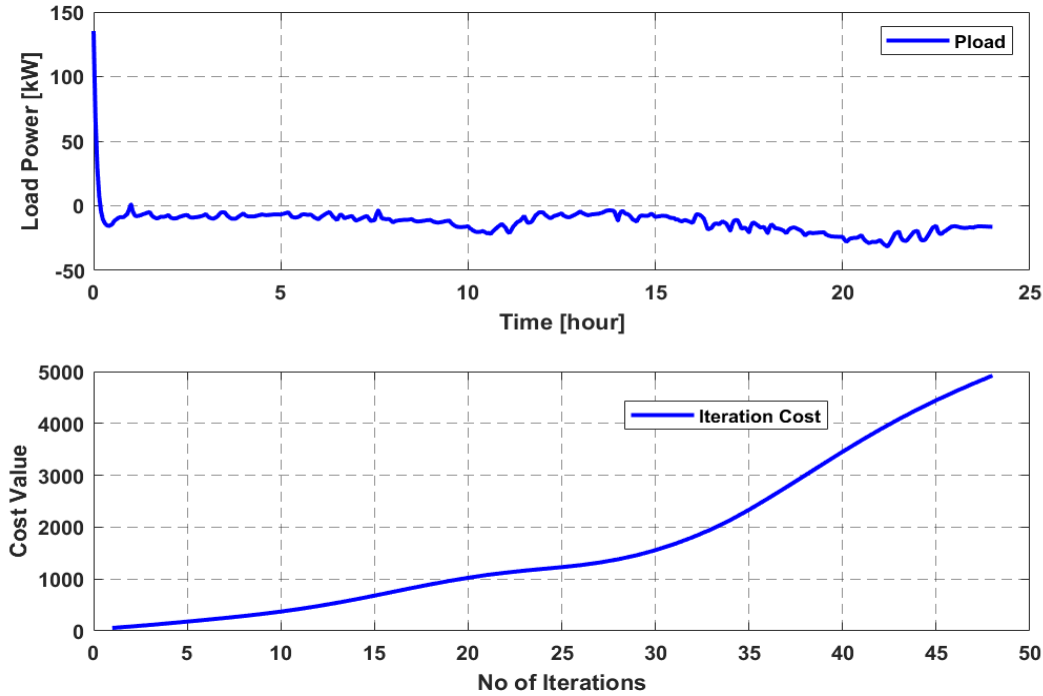


Figure 4-33: The load power and cost value with a load-varying profile reference ($W_x[5,2,40]$)

In a similar vein, to further assess the robustness of the proposed controller, a load-varying reference profile is used instead of the 50-kW constant load. Figures 4-25 to 4-33 show the performance of the system when subjected to these control inputs. Similar to the previous cases, the power required to deliver such a reference profile is a combination of both the diesel generator and the storage bank. The simulations were run at several tracking weights to investigate how the proposed algorithm is used to fine-tune the weights of different targets spontaneously, as per the states of the system. It is also evident from the results that the diesel generator provides most of the power after the solar generation has depleted its energy on the varying-load demand. The diesel generator reaches its maximum capacity after about 20 hours, the time at which a mode switch is required. Consequently, the rest of the power needs to be provided by the battery. However, the battery capacity is not enough to provide the 30kW left to deliver the required power load. This is one of the cases where the reference profile load is being well tracked, but due to the limitations on maximum power delivered by the energy sources, the full power demanded by the load cannot be met.

4.4 Chapter Summary

This chapter investigated an optimal control strategy that efficiently manages a stand-alone residential micro-grid comprising of renewable and non-renewable energy sources. An adaptive model predictive control algorithm is implemented for choosing an optimal mode and set of inputs for the system to track both a constant and load-varying power demand profile. Therefore, to understand how MPC is designed and implemented in an electrical network, the MPC controller is used in a wavelength-based thermo-

electrical model of a photovoltaic (PV) module. The MPC is used to predict the impact of each module wavelength on both the output power and the temperature of the PV module based on the individual energy contribution of wavelength. This designed model has been able to show its prediction accuracy of the interaction between the module output power and its temperature. A predictive model controller was designed to maximize the PV output power by controlling the input power by filtering the spectrum wavelength for a PV system. From the results, the MPC controller shows an excellent tracking response performance between the module temperature and the reference temperature of the PV module. Consequently, the PV system used in the previous case was used as the renewable source in a residential micro-grid. The AMPC algorithm was implemented to track the power transmitted to residential micro-grid. Hence, it follows a pre-specified reference power profile that is assumed to capture all variations seen in the real-world due to solar geometry and weather, among other factors. The main objective of delivering power to a consumer load from two different sources of energy was accomplished by a hybrid switching between charging and discharging modes of the storage system, as well as a convex logic implemented on the control inputs, that maximized the efficiency of the storage bank and minimized the consumption of energy from the diesel generator. Therefore, excellent results were obtained for tracking both a constant and a time-varying load reference power profile. The cost function was minimized, which guaranteed minimum usage of non-renewable energy sources as it maximizes the consumption of power delivered by a renewable energy source. The model used in this chapter is a small-scale residential micro-grid with few energy sources. The reference power profile was not completely met due to the limitations on the maximum power that can be delivered by the energy sources, as well as the restrictions on the storage capacity of the battery. More so, the only renewable source in the model is the solar system, which is unusual in a practical grid network. Hence, it is expedient to expand the micro-grid model to include the behavioral models of multiple energy producers and storage types. The next chapter presents the optimal management of grid-connected micro-grids with diverse renewable energy sources and various energy storage systems. It further demonstrates how the use of an AMPC-based EMS can enhance micro-grid operation, provided there is effective forecasting.

CHAPTER FIVE

ENERGY MANAGEMENT SYSTEMS IN A RENEWABLE ENERGY-BASED MICRO-GRID

5.1 Introduction

The previous chapter investigated an optimal control strategy that efficiently managed a stand-alone residential micro-grid comprising of renewable and non-renewable energy sources. An adaptive model predictive control (AMPC) algorithm was implemented for choosing an optimal mode and set of inputs for the system to track both a constant and load-varying power demand profile. Therefore, to understand how MPC is designed and implemented in an electrical network, the MPC controller was used in a wavelength-based thermo-electrical model of a photovoltaic (PV) module. The MPC was used to predict the impact of each module wavelength on both the output power and the temperature of the PV module based on the individual energy contribution of wavelength. The model used in the previous chapter is a small-scale residential micro-grid with fewer energy sources. The reference power profile was not completely met due to the limitations on the maximum power that can be delivered by the energy sources, as well as the restrictions on the storage capacity of the battery. Therefore, to solve this problem, the micro-grid model of the previous chapter is expanded to include the behavioral models of multiple energy producers and storage types. More so, in the quest to addressing the issues related to the energy management system (EMS) in micro-grid operations, this chapter adopts the adaptive model-based horizon control technique to solve the EMS-based optimization problem. Furthermore, the impact of integrating the disturbance prediction on the performance of the energy management system based on the adaptive model predictive control algorithm to improve the operating costs of the micro-grid with hybrid-energy storage systems was investigated. The AMPC solves the energy optimization problem in a renewable energy-based micro-grid with various types of energy storage systems that exchange energy with the host grid. More so, this optimization problem is resolved at each sampling period to determine the minimum running costs while satisfying demand and taking into account technical and physical constraints. The state-space model is, therefore, used to evaluate the impact of the introduction of disturbance predictions on the performance of the EMS-based micro-grid with hybrid energy storage systems. Additionally, this chapter studied the behavior of the proposed controller under various external conditions, such as weather and demand changes. The general methods which are to be adopted in this chapter to control the EMS-based micro-grid effectively and also to guarantee steady electrical power supply to the local load consumers have been discussed in chapter 3. The formulations of the cost function and the system constraints, which are to be solved (minimized) by the proposed algorithm (AMPC), have been presented in chapter 3. More so, the

dynamical mathematical modeling of the micro-grid components is also discussed in chapter 3 to understand how they are controlled and operated. Subsequently, two distinct kinds of renewable energy sources (RESs) are considered and studied independently (Photovoltaic and wind turbine generations). The MATLAB simulation results show how the AMPC can adapt to various generation scenarios, providing an optimal solution to power-sharing among the distributed energy resources (DERs) and taking into consideration both the physical and operational constraints and, similarly, the optimization of the imposed operational criteria.

5.2 Description of the System Model under Study

In this section, the MATLAB/Simulink environment was used to model the system dynamics of a renewable energy-based micro-grid network consisting of RESs (Photovoltaic, PV, Wind Turbine, WT) and Battery Storage system [237]. This micro-grid network was used to examine the impacts of integrating disturbance predictions on energy management system performance based on the proposed control technique used. We investigated two cases in this chapter; case 1 considers the micro-grid operation using the sustainable generation sources (PV and Wind sources), the fuel cell, the lead-acid battery, and the external grid. Hence, in order to compensate for the shortcomings in Lead-Acid battery as highlighted in Table D-7, a hybrid storage configuration with a lithium-ion battery was added in case 2. It is necessary to note that, during the micro-grid's normal operation, the energy generated does typically not meet demand. The battery bank is mainly utilized to store excess energy from renewable sources, but can also be used by the electrolysis process to produce hydrogen.

Moreover, when power from renewable sources is not accessible, the generation deficits can be compensated by a fuel cell using hydrogen. The hydrogen storage network consists of a proton exchange membrane (PEM) electrolyser for hydrogen production and a metal hydride tank for hydrogen storage. In addition, power electronics are used to connect the components to the current DC bus. More so, both the fuel cell and the PEM electrolyser units have their own local controllers, which execute the commands for power conversion. Moreover, two DC-DC converters associated with fuel cell and electrolyser enable the DC bus to transmit power.

Conversely, the lead-acid battery bank is directly plugged into the DC bus. Thus, the battery bank maintains the bus voltage, thereby simplifying the configuration. The DC micro-grid should, therefore, adopt this configuration option to minimize costs and improve reliability, as the batteries absorb any unbalance in the network [220]. Figures 5-1 and 5-2 demonstrate the design overview of the proposed micro-grid electric and control signal system for cases 1 and 2. Case 1 solved the EMS-based energy optimization problem using an AMPC algorithm in a renewable energy micro-grid consisting of generation sources (PV and Wind sources), lead-acid battery, fuel cell, and external grid with the inclusion of the three scenarios considered

in this chapter. Similarly, a renewable energy-based micro-grid, composed of the generation sources (PV and Wind sources), fuel cell, hybrid storage systems (lead-acid and lithium-ion battery), and the external grid is used to solve the EMS-based energy optimization problem with the inclusion of the three scenarios considered in this chapter in case 2. Therefore, a proper model of the dynamics relating to the uncertainty dimension of the micro-grid components should be considered in this design in order to design the micro-grid network in an optimal way.

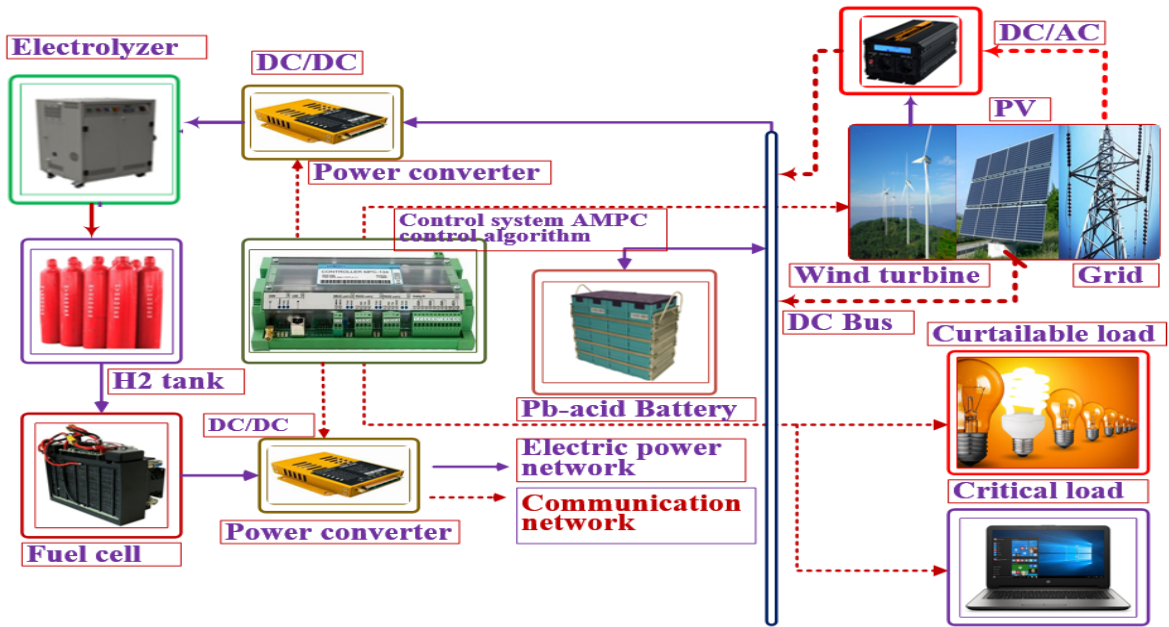


Figure 5-1: The model-based design description of the proposed micro-grid system for case 1

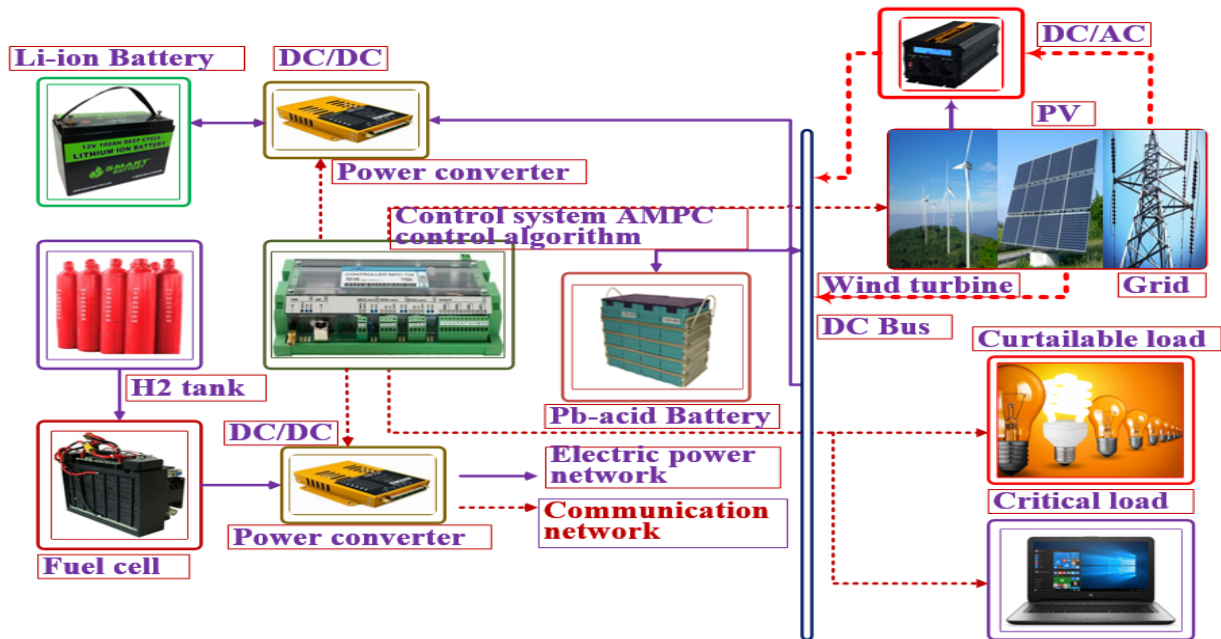


Figure 5-2: The model-based design description of the proposed micro-grid system for case 2

5.3 Simulation Results and Discussions

This section presents the MATLAB/Simulink simulation of a renewable energy-based micro-grid network composed of RESs (Photovoltaic, PV, Wind turbine, WT) and battery energy system. This micro-grid network was utilized to test the control technique applied to energy management to show the impact of integrating disturbance predictions on its performance. Therefore, two cases of separate generation scenarios were investigated in order to show the effectiveness of the proposed AMPC scheme. Case 1, therefore, considered micro-grid operation using generation sources (Photovoltaic, PV or Wind Turbine, WT), lead-acid battery, fuel cell, and external grid. In order to have a hybrid storage configuration, a lithium-ion battery was added in case 2.

The proposed micro-grid system shown in Figures 5-1 and 5-2 were simulated on the MATLAB/Simulink environment. The EMS-based energy optimization problem in a renewable energy micro-grid with different types of energy storage systems was solved using an AMPC control algorithm with or without the inclusion of disturbance predictions, which exchanges energy with the host grid. The problem of optimization is solved at each sampling time to determine minimum running costs when satisfying the demand and respecting the technical and physical constraints. The behavior of the proposed controller was studied under various external conditions such as weather and demand changes. Subsequently, we considered two distinct kinds of renewable energy sources (RESs), which were studied independently (Photovoltaic and wind turbine generations). The results of the MATLAB simulation demonstrate how the AMPC can adapt to different generation scenarios, providing an optimized solution for power-sharing among distributed energy resources (DERs) and considering both the physical and operational constraints, as well as optimizing the imposed operating criteria.

Furthermore, three scenarios were investigated as regards the incorporation of disturbance predictions in the proposed control algorithm of EMS to examine the impacts of the level of disturbance predictions on its performance and to show the effectiveness of the control algorithm on the cost function minimization. More so, these three scenarios were simulated on the MATLAB/Simulink environment to compare these conditions with similar inputs. The performance criteria utilized to show the degree of effectiveness is the cost functions, J , defined in Equations (3-87a) and (3-87b).

5.3.1 Micro-Grid Operation with Generation Sources and the Lead-Acid Battery Storage

This section utilized Figure 5-1 to analyze the three scenarios, which are discussed in the following subsections. The first scenario is when the model used by the AMPC algorithm does not include any disturbance prediction. The second scenario is when disturbance prediction is incorporated into the model, but the controller does not have any information on the future evolution of disturbances (constant

disturbance prediction). Lastly, when the disturbance prediction is perfect (this is an optimal case that offers the best results that can be compared).

5.3.1.1 Scenario 1: The AMPC formulation without integrating disturbances prediction

In this section, the EMS-based energy optimization problem was solved in a renewable energy micro-grid, which comprises of generation sources (Photovoltaic, PV, Wind turbine, WT), lead-acid battery, fuel cell, PEM electrolyser and external grid using AMPC control algorithm. Simulations were conducted to study the controller behavior under various external conditions (changes in weather and demand) to illustrate the theoretical context. Two renewable sources (Photovoltaic, PV, Wind turbine, WT) were, therefore, considered and examined separately. Hence, in order to evaluate the performance of the control system under consideration of the proposed micro-grid of Figure 5-1, three distinct generation scenarios (Sunny, windy, and cloudy) were implemented over 24 hours simulation period without including disturbances.

The first case is based on a sunny day, which has high solar radiation values and sunshine period. The power that the photovoltaic array generates is mainly concentrated during mid-day. This generation profile corresponds to a sunny day, with high irradiance during the central hours of the day, getting surplus energy and deficit at night. The EMS controls all of the storage units (batteries and hydrogen) to meet demand. Thus, the battery is used during the night to meet the demand until electricity is abundant. The battery then begins charging, and since there is still a surplus of energy, it is stored using the electrolyser in the form of hydrogen and then sells electricity to the grid. If PV generation is unable to satisfy the demand, the battery will be used again until depleted, and then the fuel cell will continue to produce electricity with a small contribution to the grid. Note that within their operating limits, SOC and LOH evolve almost freely, since the weights utilized in the cost function for the reference tracking are small. A state-space AMPC is obtained using the model from Equations (3-119) and (3-120) without the consideration of the disturbance term. Figure 5-3 depicts the MATLAB/Simulink representation of the micro-grid model without disturbance prediction.

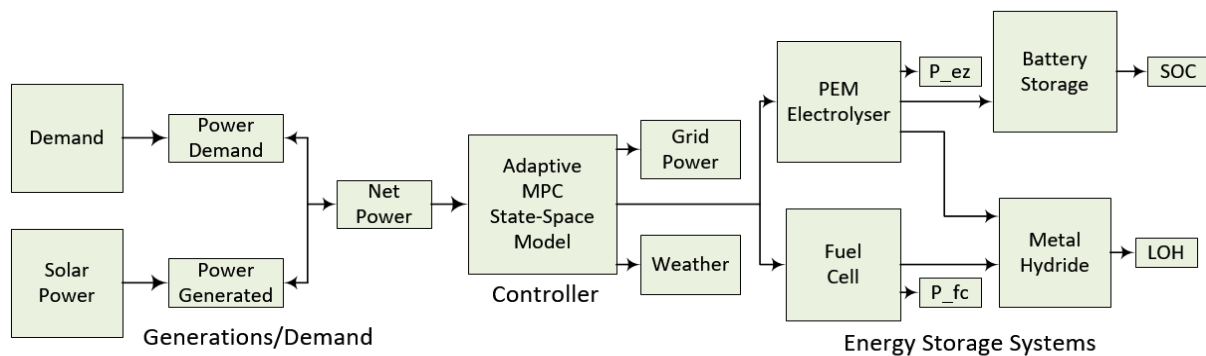


Figure 5-3: MATLAB/Simulink representation of scenario 1 without disturbance prediction (Sunny, windy, and cloudy).

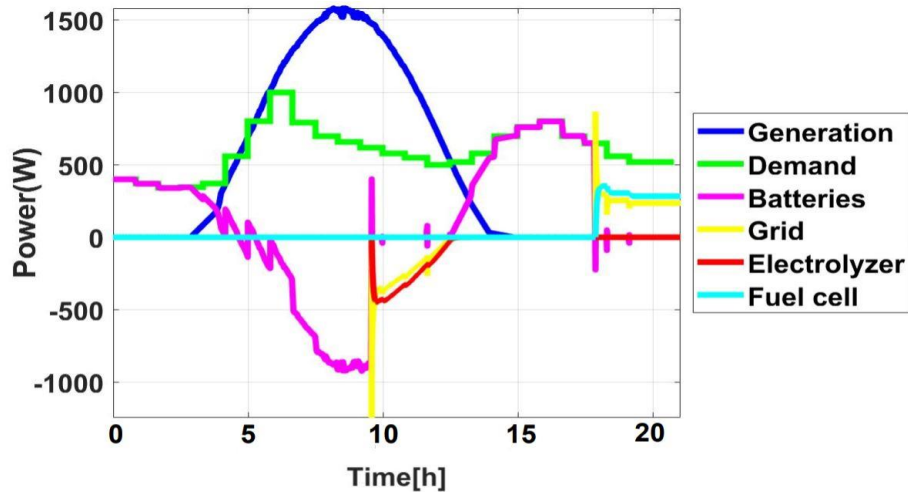


Figure 5-4: The power flow profile during the sunny day (scenario 1) without disturbances

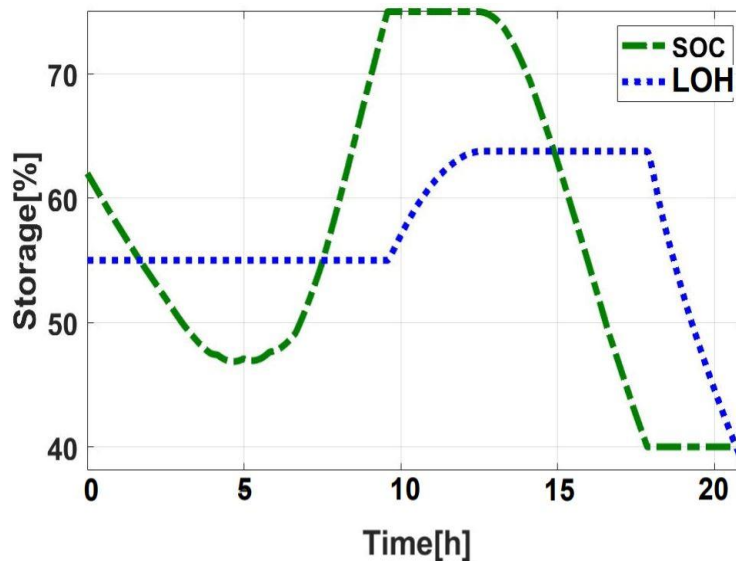


Figure 5-5: The level of storage during the sunny day (scenario 1) without disturbances

During the first hour of the day, as shown in Figures 5-4 and 5-5, there is a power deficit requiring the battery to compensate for the deficit in the micro-grid system. Hence, the control system realizes the impossibility of meeting the demand entirely only with the battery, at about 7:30, the generation exceeds the load, and then continue to supply the load. Meanwhile, the battery continues to charge until its SOC reached its upper limit (75%), at that point, the electrolyser was switched ON to control the SOC level due to excess energy because the irradiance was very high. Hence, the energy surplus had to be stored in the form of hydrogen. The electrolyser's power consumption grew gradually, as illustrated in Figure 5-4. Note that, during the first operation of the electrolyser, the controller simultaneously exports surplus energy to the grid to prevent intensive use of the electrolyser and slowly decreases as the electrolyser uses more electricity. Therefore, the battery begins discharging at 10:00 until the SOC value is close to the lower

threshold (40%). Then the controller decides to switch ON the fuel cell while simultaneously taking power from the grid to reach the reference point. The grid and fuel cell shared the demand for cost function based on their weights at the end of the day. The weights utilized in the Cost function are determined by power-sharing among battery, electrolyser, fuel cell, and external grid. In the middle of the day, a significant excess of power is generated. Once the batteries are fully charged, and the maximum electrolyser capacity is achieved, a small amount of surplus energy is sold to the host grid. Despite the extensive use of the electrolyser, as the batteries are used during the evening to cover the energy deficit, the final amount of hydrogen does not really meet its initial value [248].

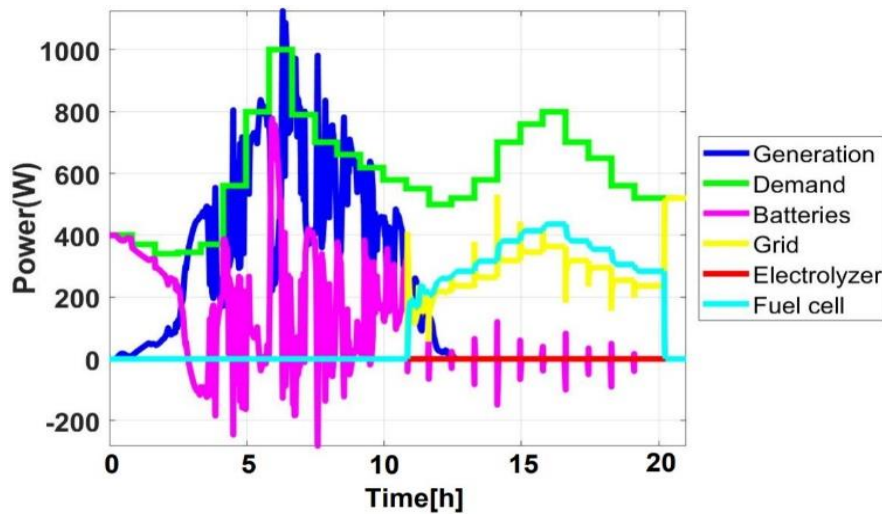


Figure 5-6: The power flow profile during the cloudy day (scenario 1) without disturbances

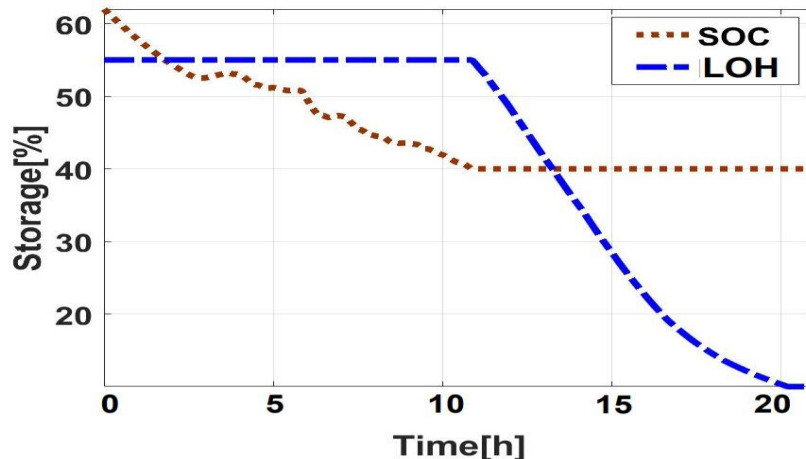


Figure 5-7: The level of storage during the cloudy day (scenario 1) without disturbances

In this scenario, due to the cloudy weather resulting in minimal or no availability of sunlight, the PV generation is unable to meet the demand for most of the day (most often, the net power is below zero). Figures 5-6 and 5-7 depict the power flow profile during periods of surplus or deficit energy and the storage level during cloudy days, respectively. The available resources such as the battery, fuel cell, and grid must,

therefore, supply any energy deficit within the micro-grid network. Hence, the EMS decides to utilize the battery to meet the load demand. Subsequently, the controller decides to switch ON the fuel cell even though the SOC is far from its minimum value (around $t = 12$ hour in a smooth way), which is also supported by the grid. It is worth mentioning that the controller does not activate the electrolyzer, as there is no extra energy in the form of hydrogen to store. Meanwhile, during the second half of the day, when the battery's minimum SOC has been reached, the fuel cell and the external grid feed the load. The fuel cell satisfies the load request for nearly 12 hours, and the batteries are only utilized to balance the power within the micro-grid. Following that, the batteries commit to supplying the power deficit. The batteries, however, reach their minimum SOC after 12.5 hours and again use the fuel cell. Therefore, the fuel cell is unable to satisfy the load demand on its own because of the thresholds in the power rate and the voltage limits, and it is required to purchase electricity from the grid.

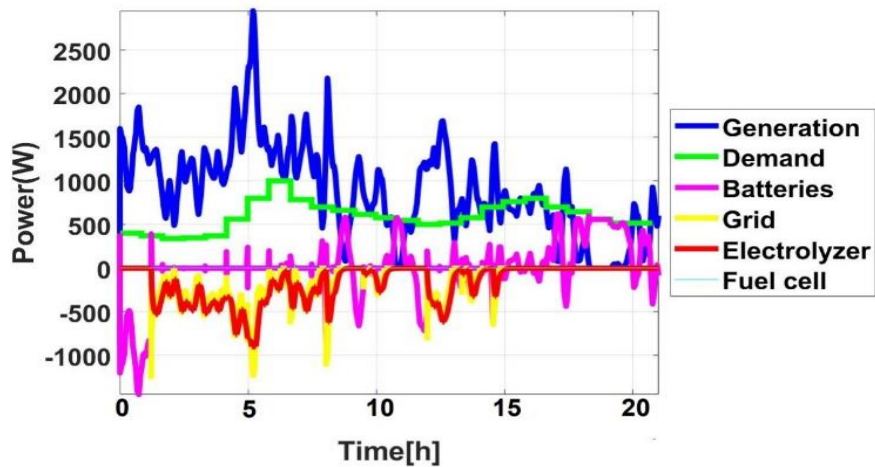


Figure 5-8: The power flow profile during the windy day (scenario 1) without disturbances

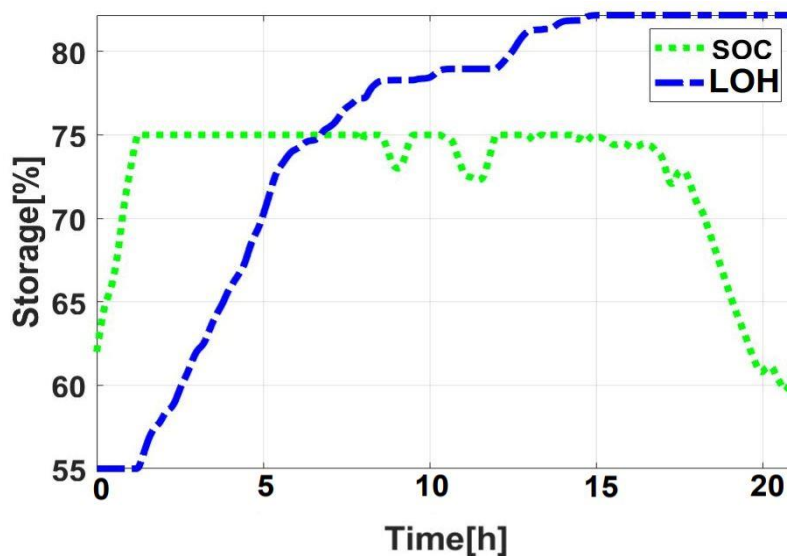


Figure 5-9: The level of storage during the windy day (case 1) without disturbances

In this scenario, a wind turbine is considered as a renewable energy source, which generates excess power in the micro-grid. As can be seen in Figures 5-8 and 5-9, the wind turbine produced a significant fluctuation in electricity. A predominantly stored energy, therefore, enabled the electrolyser to operate for most of the day, and some surplus energy is sold to the grid. It should be noted that the power rate constraints integrated into the controller design, irrespective of the high fluctuation in power produced by the wind turbine, instigated a smooth operation of the electrolyser, the behavior of which was thus quite satisfactory. Thus, the battery still stores energy, but it gets filled up early (from $t=2$ hours to 16 hours), only injecting power into the bus several times during that period. As there is an energy surplus for most of the day, there is no need to switch ON the fuel cell. This is also not subject to substantial consumption, which would drastically shorten its lifespan. The AMPC controller has adjusted the set points slowly according to the optimum estimated cost function. Moreover, by evaluating the cost function of the case of no disturbance prediction, we can, therefore, observe the impact on the micro-grid performance. The cost function, $J = 18.685$, for the case of no disturbance prediction.

5.3.1.2 Scenario 2: The AMPC formulation with the integration of both constant and perfect disturbances predictions

Similarly, in this section, the EMS-based energy optimization problem was solved in a renewable energy micro-grid, which comprises of generation sources (Photovoltaic, PV, Wind turbine, WT), lead-acid battery, fuel cell, PEM electrolyser, and an external grid using the AMPC control algorithm. Simulations were conducted to study the controller behavior under various external conditions (changes in weather and demand) to illustrate the theoretical context. Two renewable sources (Photovoltaic, PV, Wind turbine, WT) were, therefore, considered and examined altogether. More so, in order to evaluate the performance of the control system under consideration on the proposed micro-grid of Figure 5-1, three distinct generation scenarios (Sunny, windy, and cloudy) were implemented over 24 hours simulation period with the integration of both constant and perfect disturbances predictions. More so, we investigated the situation when the disturbances are incorporated into the model. Still, the controller does not have any information about the future evolution of disturbances (constant disturbance prediction). This approach is often utilized in AMPC control scheme, since there is no future information about the disturbance's prediction, the most appropriate assumption is that the disturbance will be the same across the horizon as in scenario 1. However, if the information of future disturbance evolution is available, it can be incorporated into the AMPC formulation, then, the disturbances prediction is perfect (this is an optimal case that offers the best results that can be compared). In this case study, the disturbance is given by the net power, i.e., the difference between generation and demand, $d(t) = P_{gen}(t) - P_{dem}(t)$, which can be estimated at the current

instant time, t . Evaluating the Matrix expression of Appendix A, for the case of the integration of disturbance prediction in the AMPC algorithm, it results in the matrix form in Appendix A.

Therefore, the effects of these disturbance predictions on the micro-grid performance are also investigated. Therefore, in order to compare both predictive disturbance situations, we performed some simulation with a constant disturbance based on the parameters given in Table D-3, with a shift in time horizon ($N_p = 50$) and control horizon ($N_c = 2$), note that these horizons are long enough to realize the impact of predictive disturbances. Figure 5-10 depicts the MATLAB/Simulink representation of the micro-grid model with constant and perfect disturbance predictions. Consequently, the results obtained utilizing constant disturbance predictions along the horizon are shown in Figures 5-11 and 5-12. Thus, the disturbance is estimated in the current instant during the minimization process and is kept constant.

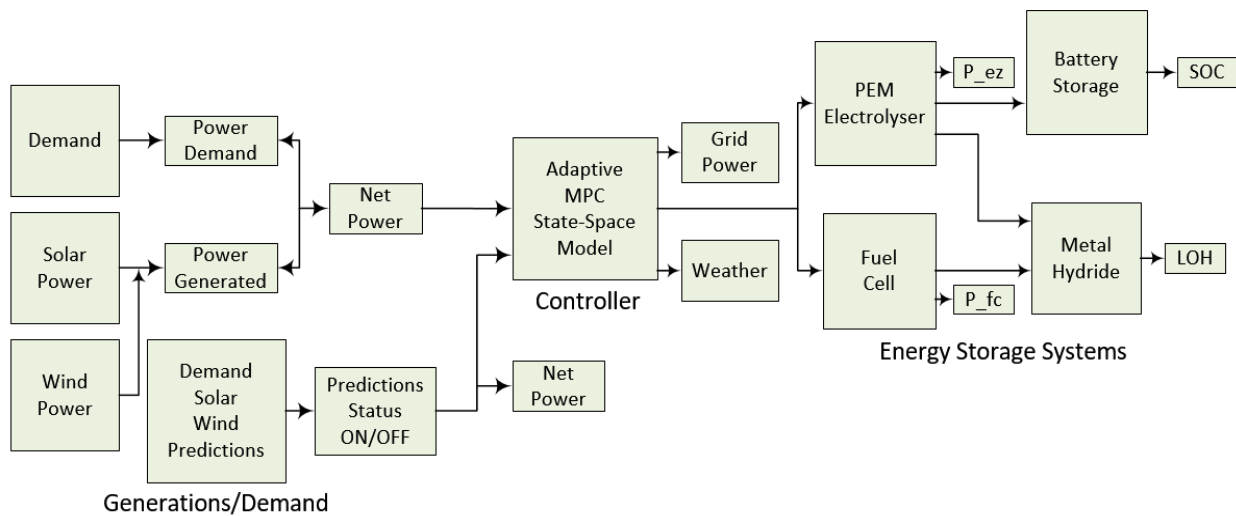


Figure 5-10: MATLAB/Simulink representation of scenario 2 with constant and perfect disturbance predictions

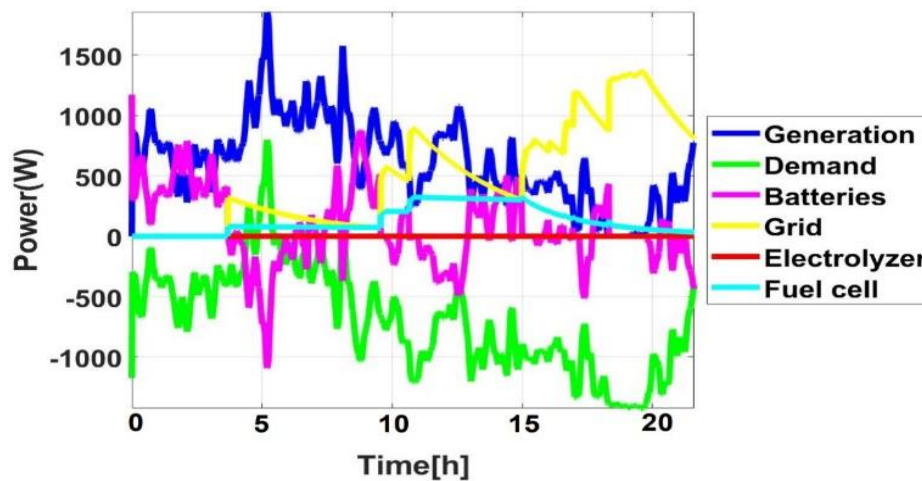


Figure 5-11: The power flow profile (scenario 2) for constant disturbances prediction

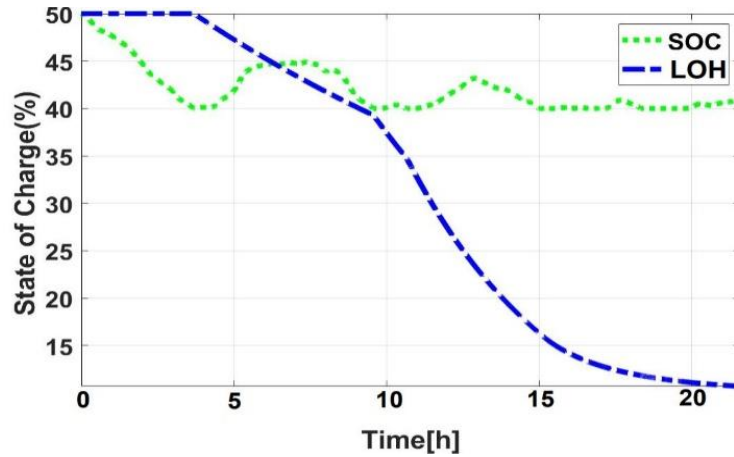


Figure 5-12: Storage levels (scenario 2) for constant disturbances prediction

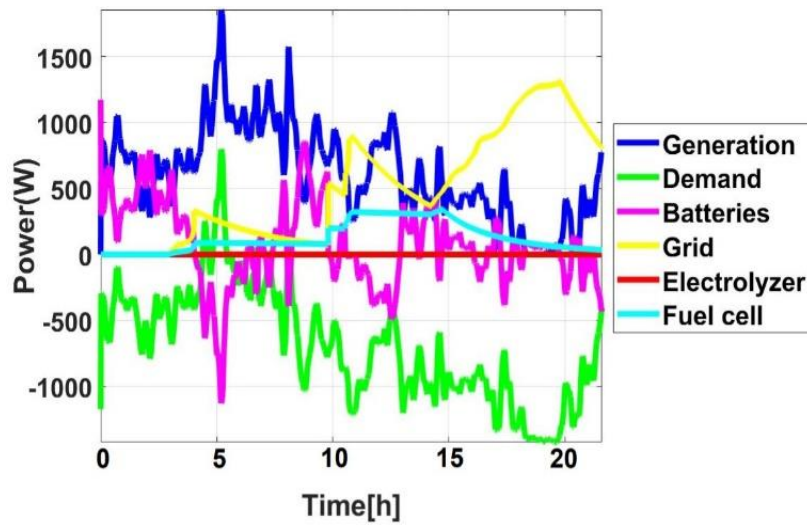


Figure 5-13: The power flow profile (scenario 2) for perfect disturbances prediction

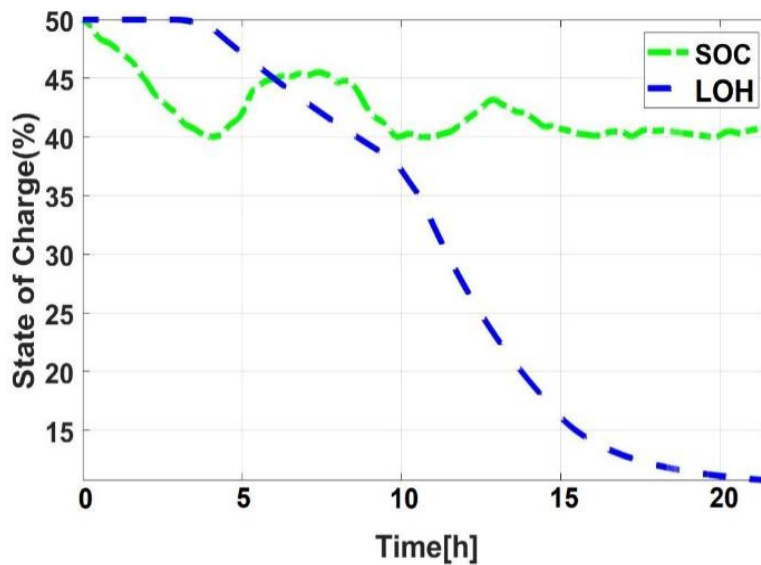


Figure 5-14: Storage levels (scenario 2) for perfect disturbances prediction

Figures 5-11 and 5-12 show the results of the power flows and storage level when the controller does not have enough information about the future evolution of disturbances (constant disturbance prediction). It is evident in the simulation results, most especially the power flows, which show more variations in the generation sources, which can result in the ill-performance of the micro-grid. The constant disturbance prediction is seldomly used in the control techniques. However, its incorporation does not effectively improve the performance of the micro-grid compared to the perfect disturbance predictions. Similarly, the power flows when future disturbances are identified and included in the free-response estimation, which is depicted in Figures 5-13 and 5-14. Since the micro-grid operation anticipates the progression of the disturbance, the power flows are steadier compared to when the disturbance is not predicted perfectly, which affects the micro-grid performance. Perfect disturbance prediction is useful when incorporated into the AMPC formulation, to prevent degradation and prolong micro-grid components' lifetime. Moreover, by evaluating the cost function of both disturbance prediction cases, therefore, it is evident that there is an improvement in the micro-grid performance. The cost function, $J = 14.968$, for the case of constant disturbance prediction and $J = 10.524$ for perfect knowledge of disturbance prediction of the AMPC controller, which signifies a 29.7% improvement. Therefore, with the following illustration, it is shown that the micro-grid operation can be improved by the AMPC prediction capabilities, provided there is a good forecast.

5.3.2 Micro-Grid Operation with Generation Sources and Hybrid Storage Systems (Lead Acid and Lithium-ion Batteries)

A new lithium-ion battery bank is added in this case to the micro-grid system of case 1. For this configuration, a new AMPC algorithm must be formulated. The fuel cell is used as a DG, with a cost associated with hydrogen usage (which is not generated in the micro-grid) to demonstrate an example of the generators capable of dispatching. The micro-grid is composed of a PV plant, two different types of batteries, and a fuel cell, as illustrated in Figure 5-2. The power exchanged with the DC bus can be balanced using this Li-ion battery using its DC/DC converter; so that a new manipulated, P_{bat2} , variable will appear [5]. The Lithium-ion battery absorbs any unbalance in the network, thus minimizing the costs and improves reliability. The reason for choosing lithium-ion batteries as the primary storage device is that lithium-ion batteries have some fantastic advantages such as (1) High energy efficiency (2) Longer cycle life (3) Relatively high energy density, and (4) Improved resiliency.

5.3.2.1 Scenario 1: The AMPC formulation without including disturbances prediction

The cost function has the form given by Equation (5-2). The value of α_4 has been chosen to be large, as shown in Table D-5, in order to impose that, the lead-acid battery is primarily utilized to sustain the DC but

at its operating voltage and does not contribute to the demand. The increments in power are weighted by the β values given in Table D-5. The chosen horizons are the time horizon ($N_p = 50$) and control horizon ($N_c = 2$). The results shown in Figures 5-16 and 5-17 indicate that the DERs operate in a coordinated manner during the day to meet demand. As the fuel cell consumes hydrogen, it is switched off for most of the day and only operates at midday ($t > 12$ hours) when the energy stored in the Li-ion batteries is not sufficient to fulfill the load (note that it reaches its 30% lower limit). Note that the lead-acid battery was not utilized for a few durations during the simulation. Meanwhile, this could easily be modified by changing the cost function weights α and β [1, 5]. Figure 5-15 depicts the MATLAB/Simulink representation of scenario 1 without disturbances prediction. The cost function was similarly evaluated for the case without any disturbance's prediction and $J = 15.625$. Consequently, it is evident in the cost evaluation, a reduction in the cost to 57.4% of the baseline value, taking into account the disturbances in the prediction model.

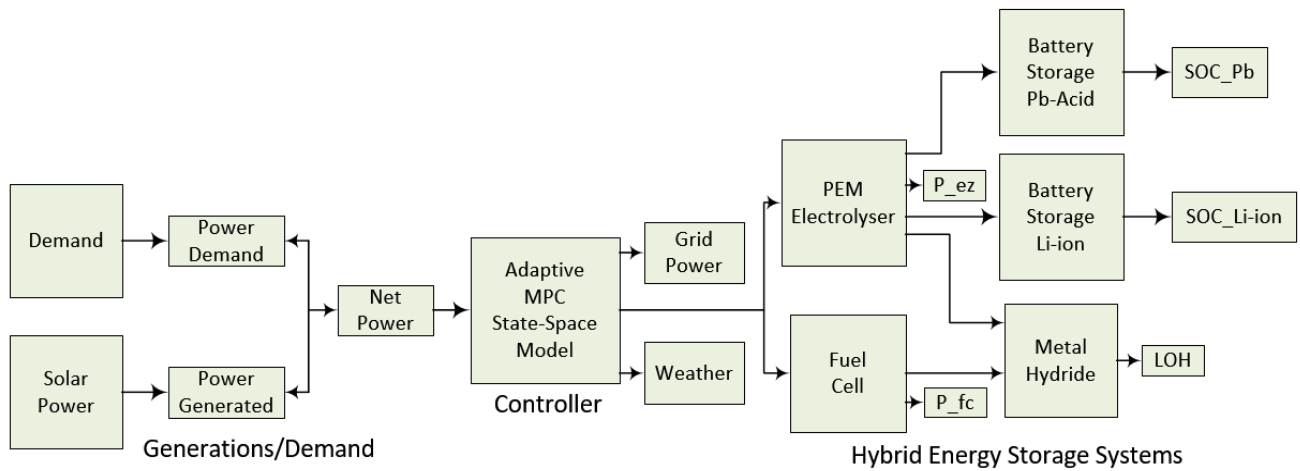


Figure 5-15: MATLAB/Simulink representation of scenario 1 without disturbance predictions

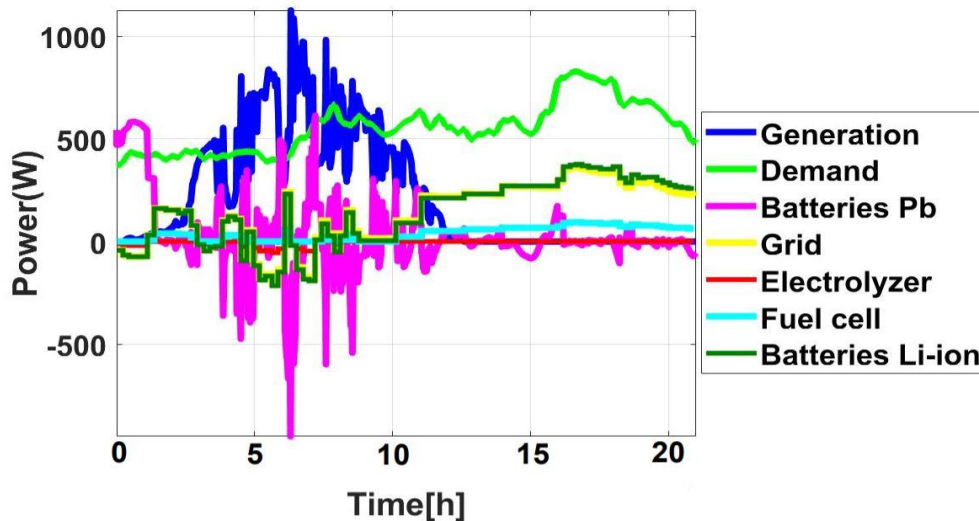


Figure 5-16: The power flow profile with hybrid storage system (scenario 1) without disturbances

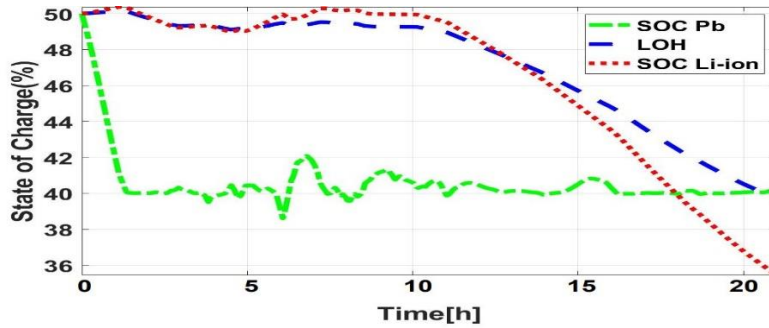


Figure 5-17: The level of storage with hybrid storage system (scenario 1) without disturbances

5.3.2.2 Scenario 2: The AMPC formulation with the integration of both constant and perfect disturbances predictions

Similarly, the AMPC formulation also integrates the disturbance predictions similar to case 1. The power flows and the storage level of both the batteries are more steady, which affects the performance of the micro-grid. As is evident in Figures 5-19 and 5-20, the micro-grid operation is improved due to the perfect disturbance prediction by the AMPC algorithm. The lead-acid battery was used for the first 4hrs to satisfy demand, and then the source of generation took over from 4hrs until 12 hrs of the simulation. The li-on battery maintained its State of Charge (SOC) of 50% until the 16 hours when the demand is quite high for only the lead battery to satisfy the demand. At this point, the li-ion battery continues to supply the demand until its SOC starts diminishing. Meanwhile, the grid tends to be ignored in meeting the available demand. Therefore, as the lead-acid battery charges up to SOC of 75%, it begins to meet the load demand. Hence, the li-ion battery starts to operate at 16hr until the SOC reaches its minimum limit of 40%. Figure 5-18 depicts the MATLAB/Simulink representation of the effects of perfect disturbance prediction on the micro-grid performance with hybrid storage systems. Moreover, by evaluating the cost function of both disturbance prediction cases, we can, therefore, quantify the improvement in the micro-grid performance. The cost function, $J = 9.426$, for the case of constant disturbance prediction and $J = 6.654$ for perfect knowledge of disturbance prediction of the AMPC controller, which signifies a 29.4% improvement.

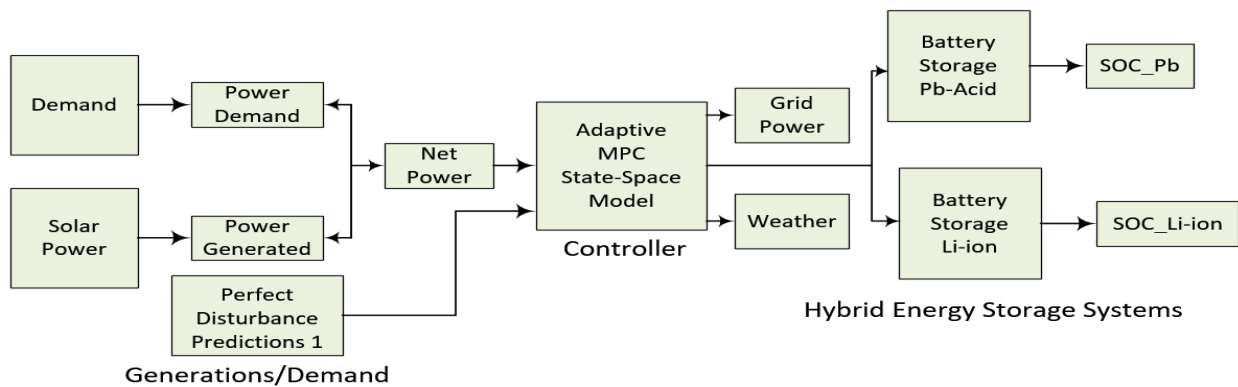


Figure 5-18: MATLAB/Simulink representation of scenario 2 with Perfect disturbances predictions

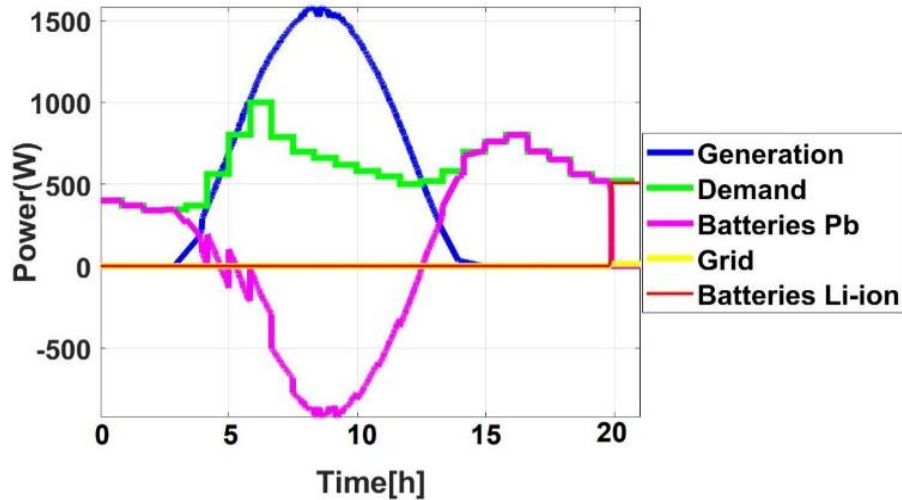


Figure 5-19: Power flows for perfect disturbance prediction with hybrid storage system (scenario 2)

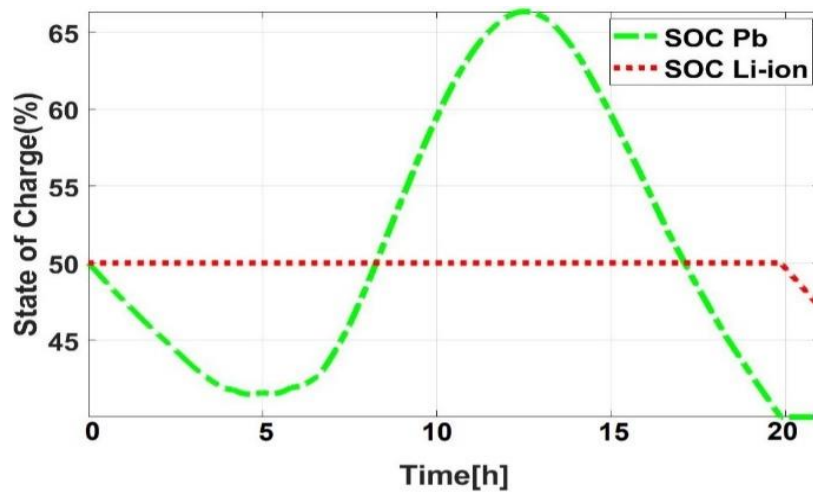


Figure 5-20: Storage levels for perfect disturbance prediction with hybrid storage system (scenario 2)

5.4 Chapter Summary

The availability of more reliable and effective energy management techniques is one of the main reasons for developing effective integrated systems based on distributed generations. In this context, the EMS-based AMPC algorithm was implemented for optimal management of micro-grids based on various energy storage systems. The AMPC solves an energy optimization problem with multiple types of energy storage systems in a renewable energy micro-grid, which exchanges electricity with the host grid. This problem of optimization is solved at each sampling time to determine minimum running costs while satisfying the demand and considering technical and physical constraints. The controller's proposed behavior has been observed under different external conditions, such as changes in weather and demand. Different scenarios and configurations were used to demonstrate the AMPC's versatility and applicability. The simulations, therefore, show how the AMPC was able to adjust to different scenarios, offering a reasonable solution for

power-sharing among the DERs and taking into account both the physical and operational constraints and the optimization of the operational criteria imposed on it. This chapter has further demonstrated how the use of an AMPC-based EMS can enhance micro-grid operation, provided there is effective forecasting. More so, it is evident in the cost function, J , obtained from the three scenarios conducted, the cost function was further minimized by introducing the lithium-ion battery storage into the micro-grid. Therefore, as it is evident from the results, the cost function obtained when the hybrid energy storage was used has a reduced cost compared to when just only one battery was used during the scenario of no disturbances. In addition, considering the case with and without the integration of the information of the disturbance prediction into the AMPC formulations, it is also evident from the cost function minimization that the perfect knowledge of the disturbance prediction is essential for effective micro-grid operations. In electrical networks, demand-side management (DSM) is a critical feature that enables consumers to make decisions about their energy usage and helps operators to reduce peak load demand and reshape the load profile/consumption pattern. Therefore, there are several benefits associated with the incorporation of the DSM concept in the EMS systems of the micro-grid. Such benefits are, but are not limited to, the following; environmental impacts and reduction in the overall running costs; enhancement in the system performance; effective decrease in the investment pressure on power generation, transmission, and distribution. Furthermore, the DSM makes it possible to develop demand-side response measures, which reduce the overload of the system during peak consumption periods. Hence, the next chapter extends the energy management systems in micro-grid developed in this chapter by adopting the concept of demand-side management, and the utilization of the demand response technique (DRT) in the framework of DSM to adjust controllable loads during the peak consumption periods, in order to further minimize the running cost.

CHAPTER SIX

DEMAND RESPONSE TECHNIQUES FOR ENERGY MANAGEMENT SYSTEM IN A STAND-ALONE MICRO-GRID

6.1 Introduction

In the previous chapter, the energy management system based adaptive model predictive control (AMPC) algorithm was implemented for optimal management of micro-grids based on various renewable energy sources and storage systems. The AMPC solved an energy optimization problem with multiple types of energy storage systems in a renewable energy micro-grid, which exchanged electricity with the host grid. This problem of optimization was solved at each sampling time to determine minimum running costs while satisfying the demand and considering technical and physical constraints. The proposed behavior of the controller has been observed under different external conditions, such as changes in weather and demand. Different scenarios and configurations were used to demonstrate the versatility and applicability of the adaptive model predictive controller. The simulations, therefore, showed how the AMPC was able to adjust to different scenarios, offering a reasonable solution for power-sharing among the distributed energy resources (DERs) and taking into account both the physical and operational constraints and the optimization of the operational criteria imposed on it. More so, the previous chapter has further demonstrated how the use of an AMPC controller is used to solve the energy management problems, can enhance the micro-grid operation, provided there is effective forecasting. Therefore, the application of demand response (DR) techniques to renewable energy-based micro-grid is discussed in this chapter. Thus, with DR techniques, specific loads can be modified (both in amplitude and in connection times) to help achieve the objectives of the micro-grid operation. For instance, in shiftable loads, their activation can be halted, restarted, or deferred to other time slots. Meanwhile, they can as well be deferred from peak to off-peak period considering the electricity tariffs or operational needs. Within the timespan, shiftable loads are adjustable, but their demands cannot be modified, so they cannot operate before the earliest start time and the latest finish time. More so, they cannot be interrupted before completion once their work is initiated. Conversely, in curtailable loads, the consumption behavior of loads can be adjusted to a lower level if necessary. Although these loads have a nominal level, their magnitude is flexible so that when required, the level of demand can be lowered (e.g., at peak hours or in islanded mode). Examples of adjustable loads are heating systems and, in general, thermal loads. Reducing the consumption pattern or deferring the load to some other point in time, however, will affect the satisfaction of the consumer, which can be assessed by the quality of experience (QoE). The adaptability incorporated by the demand response technique involves the implementation of new manipulated variables (both continuous and binary) in the problem formulation,

making the optimization problem more complicated [249], [216]. The aim of the demand response technique in the energy management system is to use the diversity of the load consumption patterns and the energy available from the distributed energy resources, the demand response, and the Energy Storage System (ESS) to reduce the peak load demand and minimize the operating/electricity costs of the micro-grid system. Meanwhile, these techniques can be used in a grid-connected mode as well as in island mode. These can be used in both cases to enhance the economic benefit, but in the case of islanded mode, these can be critical because the grid is not available to supply the loads while power deficit occurs. In this scenario, the number of curtailed loads required are selected based on the projected energy deficit. Although these can be used at various timescales and control levels, load shifting is generally more geared towards power-sharing scheduling and load curtailment. In this chapter, the energy management system discussed in the previous chapter is extended to the case in which the micro-grid comprises the controllable loads (curtailable loads). The micro-grid used in the previous chapter is grid-connected. Therefore, most of the power deficits are met by the main-grid. However, in this chapter, a stand-alone micro-grid is used, with both critical and curtailable loads connected, to investigate the benefits of adopting the concept of DR technique for energy management system in a stand-alone micro-grid. Hence, it is worth noting that the proper management of the consumption pattern of the load can significantly enhance the micro-grid operation. More so, the objective of the DR technique in this chapter is to use the available renewable energy resources optimally, maximizes the economic benefit, and reduces the peak load demand without affecting customer satisfaction. Hence, the formulations of the DR-Based AMPC Optimization Problem, cost function, dynamic system constraints, and the control-oriented linear model, which are to be solved (minimized) by the proposed algorithm (AMPC), have been presented in chapter 3. This chapter presents the results and the discussion obtained in the various cases conducted.

6.2 Description of the System Model under Study

In this section, the MATLAB/Simulink environment was used to model the system dynamics of a renewable energy-based micro-grid network consisting of renewable energy sources (Photovoltaic, PV, Wind Turbine, WT) and Battery Storage system. Moreover, two different kinds of load were considered, the critical and the curtailable loads [237]. Five loads are present in the micro-grid systems of Figs. 6-1 and 6-2 to mimic different loads in which three of the loads represent curtailable loads, and the other two represent critical loads. Similar to the previous chapter, two cases are investigated in this chapter; case 1 considers the micro-grid operation using the sustainable generation sources (PV and Wind sources), the fuel cell, and the lead-acid battery. Hence, in order to have a hybrid storage configuration, a lithium-ion battery was added in case 2 [250]. It is necessary to note that, during the normal operation of the micro-grid, the energy generated does typically not meet the load demand. The battery bank is mainly utilized to store excess energy from

renewable sources, but can also be used by the electrolysis process to produce hydrogen. Moreover, when power from renewable sources is not accessible, the generation deficits can be compensated by a fuel cell using hydrogen. The hydrogen storage network consists of a proton exchange membrane (PEM) electrolyser for hydrogen production and a metal hydride tank for hydrogen storage. In addition, power electronics are used to connect the components to the current DC bus. More so, both the fuel cell and the PEM electrolyser units have their own local controllers, which execute the commands for power conversion. Moreover, two DC-DC converters associated with fuel cell and electrolyser enable the DC bus to transmit power [68], [251].

Conversely, the lead-acid battery bank is directly plugged into the DC bus. Thus, the battery bank maintains the bus voltage, thereby simplifying the configuration. The DC micro-grid should, therefore, adopt this configuration option in order to minimize costs and improve reliability, as the batteries absorb any unbalance in the network [220]. Figures 6-1 and 6-2 demonstrate the design overview of the proposed micro-grid electrical system and control signal system for cases 1 and 2. Case 1 and 2 solved the DR-based energy optimization problem using an AMPC algorithm in a renewable energy micro-grid of Figures 6-1 and 6-2. The DR program is used to control the mismatch between the generations and loads. Therefore, since the micro-grid model used in this chapter is a stand-alone micro-grid, i.e., $P_{grid}(t) = 0$, the renewable energy sources should be optimally utilized to meet the operational objective of the micro-grid. Curtailment strategies are employed when the load demand is more than the generations in an AC/DC micro-grid system with critical and curtailable loads. The essence is to match the energy generations with the load profiles of the consumers [223], [14]. Therefore, if the renewable energy sources available can be optimally used and at the same time avoid drawing maximum power from the system, then we can reduce the peak expectations from the utility. More so, since the aim of conducting the DR activity is to facilitate the penetration of renewable energy sources to make the distribution system environmentally friendly and further reduces the dependency on the main-grid for power supply. It is evident from Figures 6-1 and 6-2 that the primary generation sources are solar and wind, which are intermittent in nature. Hence, these may not be enough to meet the peak demand of the customer. Therefore, it is expedient to store those energies with the storage devices during off-peak hours and discharge during the peak hours, so that the load characteristics can be flattened. More so, for reliable micro-grid operation, the consumers are expected to follow a given consumption pattern, as well as the time of the consumption pattern. Thus, this is implemented in such a way that the consumption patterns do match with the renewable generations available to avoid straining the storage devices and perhaps reduces the dependency on the main-grid for energy supply. Otherwise, it could result in loads curtailment to save the operation of the micro-grid [252].

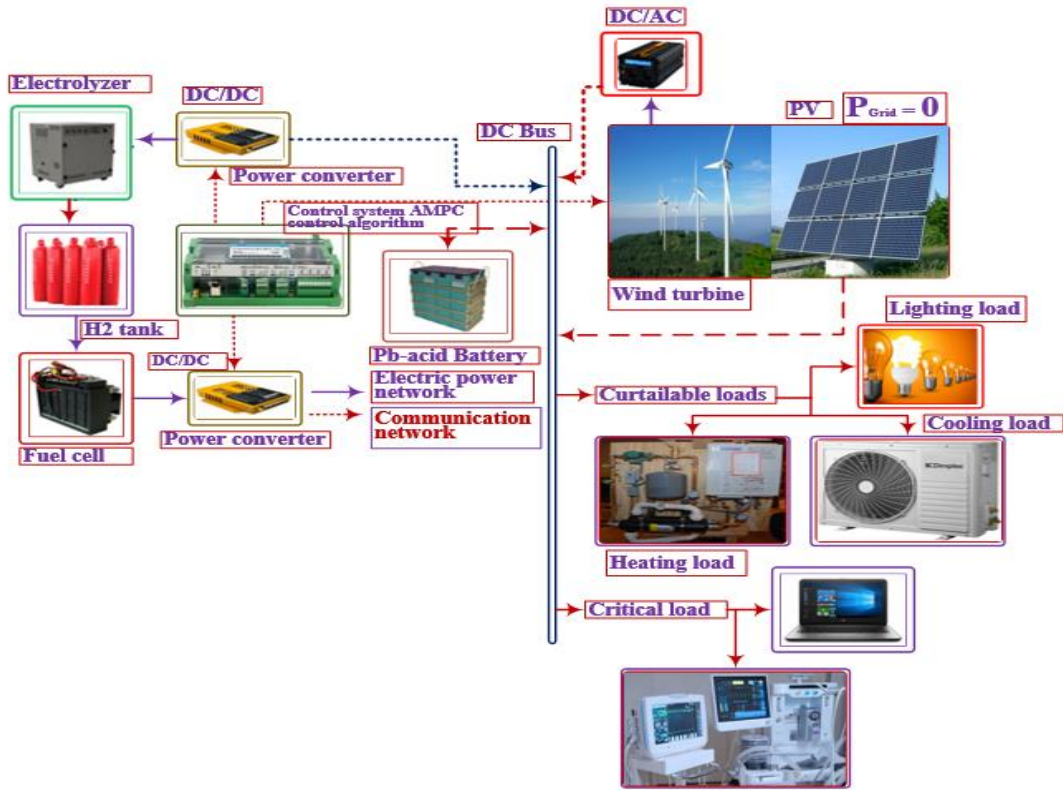


Figure 6-1: The model-based design description of the DR technique in the micro-grid system for case 1

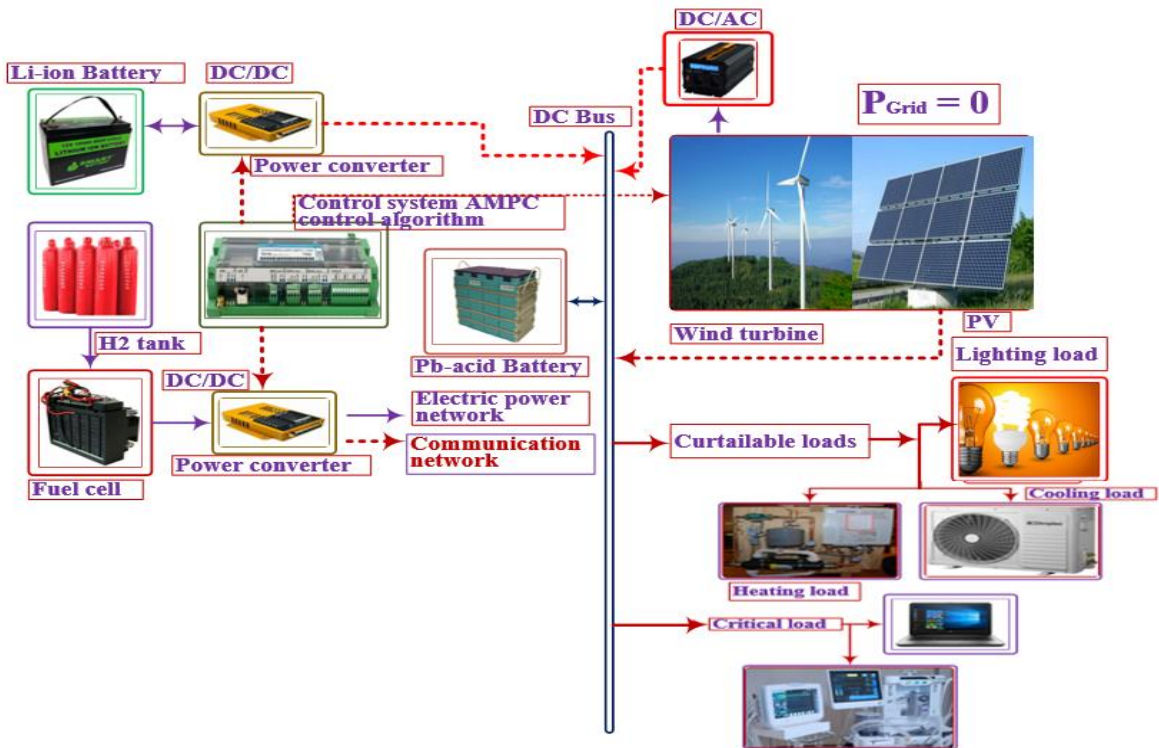


Figure 6-2: The model-based design description of the DR technique in the micro-grid system for case 2

6.3 Simulation Results and Discussions

This section presents the MATLAB/Simulink simulation of a renewable energy-based micro-grid network composed of RESs (Photovoltaic, PV, Wind turbine, WT), battery energy system, and two different kinds of loads. This micro-grid network was utilized to test the control technique applied to its energy management system to show the benefits of incorporating the DR program in a micro-grid with renewable sources as the main generations. Therefore, two cases of separate generation scenarios were investigated in order to show the effectiveness of the proposed AMPC scheme. Case 1, therefore, considered micro-grid operation using generation sources (Photovoltaic, PV or Wind Turbine, WT), lead-acid battery, and fuel cell. In order to have a hybrid storage configuration, a lithium-ion battery was added in case 2. The proposed micro-grid system shown in Figures 6-1 and 6-2 were simulated on the MATLAB/Simulink environment [253].

The EMS-based energy optimization problem in a renewable energy micro-grid with different types of energy storage systems was solved using AMPC control algorithms. Therefore, the DR-based optimization problem is solved at each sampling time to determine minimum running costs when satisfying the demand and respecting the technical and physical constraints. The behavior of the proposed controller was studied under various external conditions such as weather and demand changes. Subsequently, we considered two distinct kinds of renewable energy sources, which were studied independently (Photovoltaic and wind turbine generations). The results of the MATLAB simulation demonstrate how the AMPC can adapt to different generation scenarios, providing an optimized solution such as the reduction in the operation cost, peak demand, while considering both the physical and operational constraints, as well as optimizing the imposed operating criteria. DR techniques can help manage the micro-grid most, especially when the external grid cannot supply energy. i.e., the micro-grid is operating in the isolated mode. If the loads are Heating, Ventilating, and Air Conditioning (HVAC) or home appliances, this curtailment can easily be assumed. The model-based design description of the DR technique in the micro-grid system in Figures 6-1 and 6-2 are used, considering the possibility of operating in isolated mode. Under certain conditions, the load may be curtailed in order to maintain the micro-grid in operation even if the load demand is not fully met.

The micro-grid operates in the islanded mode during the simulations, so, therefore, $P_{grid}(t) = 0$, and this variable could be eliminated in the model. Therefore, in order to evaluate the performance of the control system under consideration on the micro-grid, three distinct generation scenarios (Sunny, windy, and cloudy) were implemented over 24 hours simulation period. The first case is based on a sunny day, which has high solar radiation values and sunshine period. The power that the photovoltaic array generates is mainly concentrated during mid-day. This generation profile corresponds to a sunny day, with high

irradiance during the central hours of the day, getting surplus energy and deficit at night. The EMS controls all of the storage units (batteries and hydrogen) to meet demand. Thus, the battery is used during the early hours of the day and in the night to meet the demand until electricity is abundant. Note that within their operating limits, SOC and LOH evolve almost freely, since the weights utilized in the cost function for tracking the reference are small. Hence, the state considered in the optimization process is the level of the storage devices (batteries (SOC) and hydrogen (LOH)), and the control actions are the power exchanged with the generation sources and the power of the hydrogen storage network (including an electrolyser, a fuel cell, and hydrogen tanks). Consequently, a multi-objective function is used to accomplish the entirety of the DR-based micro-grid objectives, and the solver aims to minimize it.

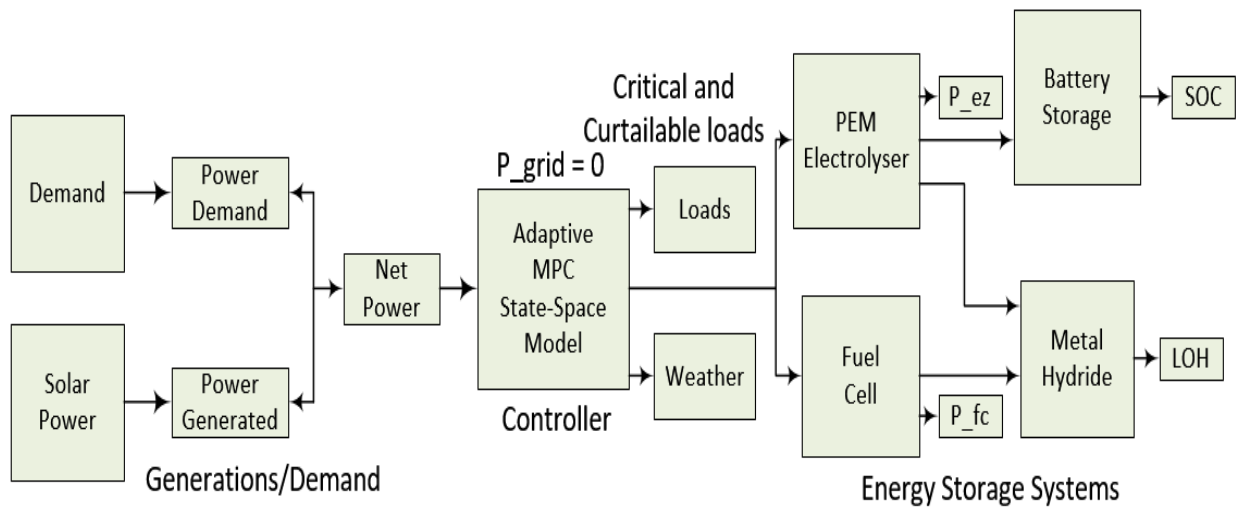


Figure 6-3: MATLAB/Simulink representation of scenario 1 with load curtailment (Sunny, windy, and cloudy).

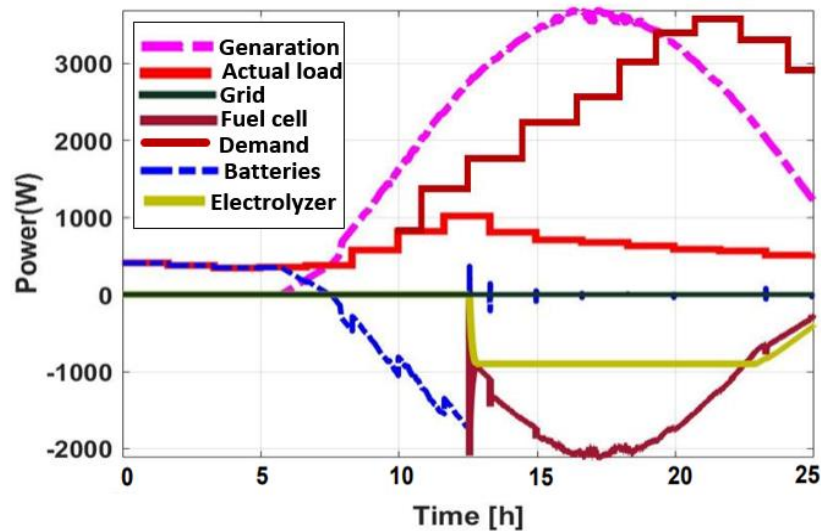


Figure 6-4: The power flow profile during the sunny day with load curtailment (scenario 1)

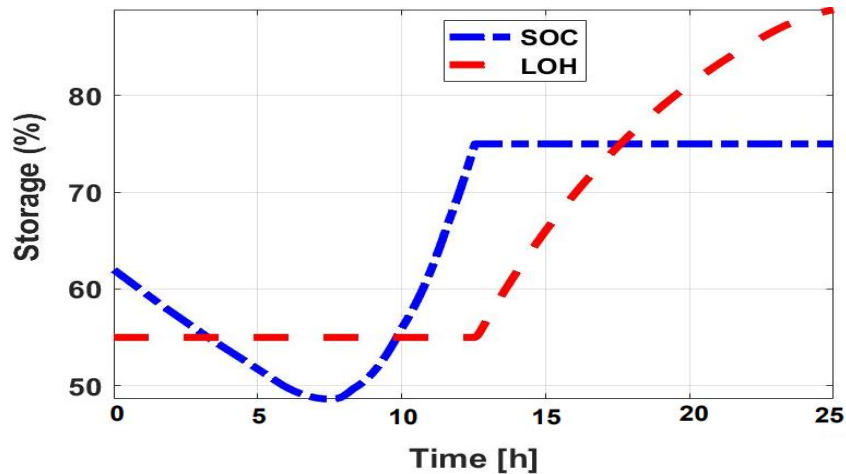


Figure 6-5: The level of storage during the sunny day with load curtailment (scenario 1)

Simulation has been carried out for a sunny day. From the two Figures 6-1 and 6-2, the micro-grid is islanded; therefore, in order to keep it operating in the absence of grid generation, the load can be adjusted. The load profile can then be modified accordingly. A maximum curtailment of 50% is allowed. In islanded mode, load shedding is mainly used to balance the local supply. More so, the micro-grid can utilize only the DERs to serve the loads in the islanded operating mode of the micro-grid. Since the non-dispatchable renewable generations (i.e., PV and WT) in the micro-grid only serve for a small proportion of the loads. We can also observe the charging/discharging cycles of the battery from Figures 6-4 and 6-5. The battery is charged when the renewable generation is high and discharged when it is low, serving as the storage for the renewable energy sources in the micro-grid. It is evident from Figures 6-4 and 6-5 that, during the first hour of the day, a power deficit occurs, which requires the battery to compensate for the power deficit in the micro-grid system. Hence, the control system realizes the impossibility of meeting the demand completely only with the battery, at about 7:30 hours, the generation exceeds the load, and then continue to supply the load. Meanwhile, the battery continues to charge until its SOC reached its upper limit (75%), at that point, the electrolyser was switched ON to control the SOC level due to excess energy because the irradiance was very high. Hence, the energy surplus had to be stored in the form of hydrogen. Therefore, the battery begins discharging at 9:00 hours until the SOC value is close to the lower threshold, and then the controller decides to switch ON the fuel cell. In the middle of the day, a large excess of power is generated. Despite the extensive use of the electrolyser, as the batteries are used during the evening to cover the energy deficit, the final amount of hydrogen does not meet its initial value. As was previously mentioned, the load demand is often supplied by the battery with some contributions from the fuel cell. However, the principle of load curtailment is implemented in order to meet the objectives set for the micro-grid operation when the storage units are about to reach their lower limits. It is worth noting that the extent of the load curtailment when the load demand eventually becomes higher than the supply will depend on

the weights of the cost function and the constraints. Nonetheless, if curtailment action is not carried out due to some reason that cannot be compromised, the simulation studies can as well be used to check the resiliency and reliability in the operation of the micro-grid. Although the load is supplied at 100% during the first hours of the day due to the presence of the sunlight. Therefore, since the micro-grid is operating in the islanded mode, later in the day, when the sun is no longer available, the stored energy by the battery is used to supply the load until the storage devices are depleted, and the load cannot be fed at all. Consequently, the micro-grid must be shut down in such a situation.

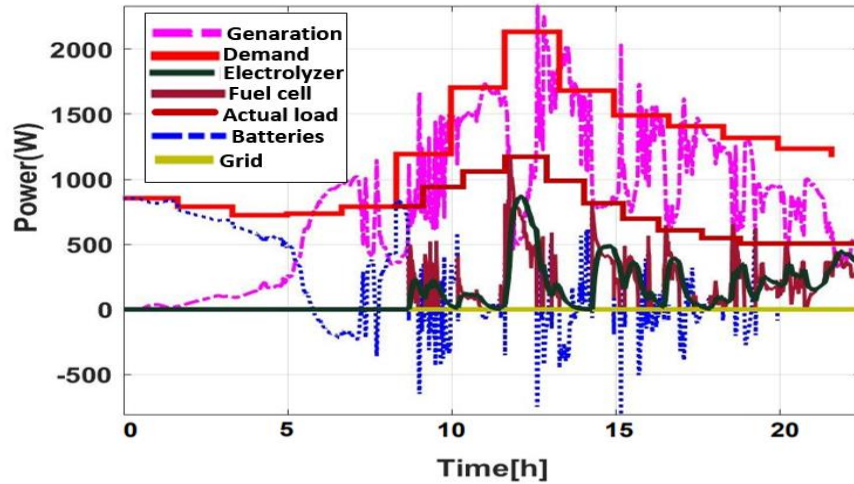


Figure 6-6: The power flow profile during the cloudy day with load curtailment (scenario 1)

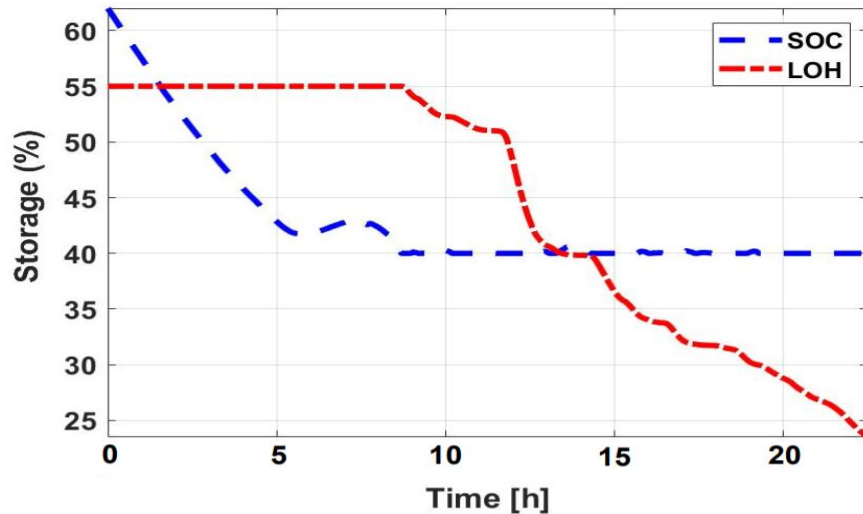


Figure 6-7: The level of storage during the cloudy day with load curtailment (scenario 1)

Similarly, simulation has been carried out for a cloudy (rainy) day. Therefore, due to the cloudy weather, which results in minimal or no availability of sunlight, the PV generation is unable to meet the demand for most of the day (most often, the net power is below zero). Hence, the available resources such as the wind generation, battery, and fuel cell must, therefore, supply any energy deficit within the micro-

grid network. Thus, the battery is charged when the renewable energy generation (wind generation) is high and discharged when it is low. Therefore, the batteries serve as the storage for renewable energy sources in the micro-grid. In the same manner, the EMS decides to utilize the battery to meet the load demand during the early hour of the day, when a power deficit occurs, which requires the battery to compensate for the power deficit in the micro-grid system. Subsequently, the controller decides to switch ON the fuel cell despite the fact that the SOC is far from its minimum value (around $t = 10$ hours in a smooth way), which is also supported by the wind generation. The controller does not activate the electrolyser during the first hour of the day, as there is no extra energy to store due to the non-availability of sunlight. Meanwhile, during the second half of the day, when the battery's minimum SOC has been reached, the fuel cell and the wind generation supply the load. Moreover, the fuel cell is unable to satisfy the load demand on its own because of the thresholds in the power rate and the voltage limits, and it requires the support of the wind generation. Furthermore, at around 17 hours of the day when the electricity demand continues to rise above the generation, there is a need to curtail some loads such as cooling and heating loads since the SOC of the batteries is minimum at that hour of the day in order to satisfy the demand and enhance the operation of the micro-grid. Therefore, at around 20 hours of the day, the fuel cell continues to meet the load demand for another 4 hours. Meanwhile, the batteries are only utilized to balance the power within the micro-grid. Following that, the batteries commit to supplying the power deficit. The batteries, however, reach their minimum SOC after 22 hours and again use the fuel cell. The simulation results of Figs. 6-6 and 6-7 show that the proposed DR technique has managed to bring the final consumption/demand close to the objective load curve. The proposed control algorithm (AMPC) has effectively regulated the consumption pattern of the controllable loads connected to the micro-grid system.

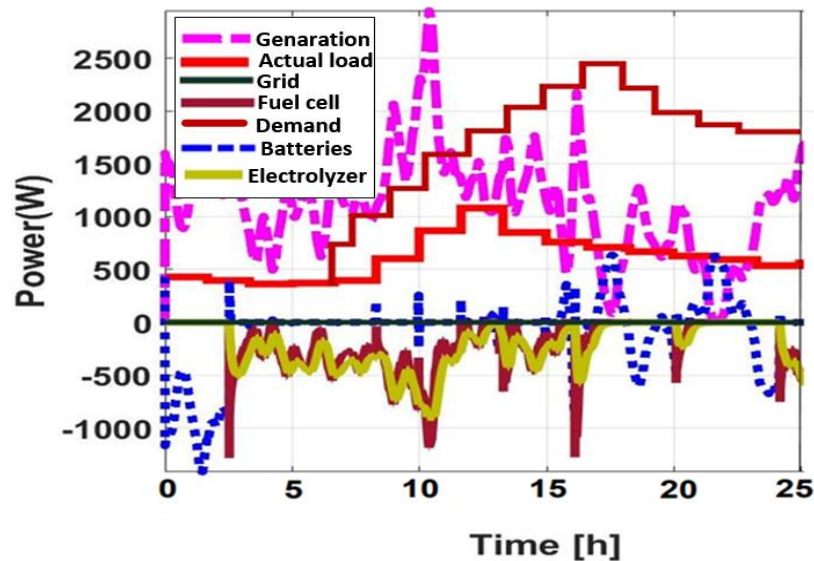


Figure 6-8: The power flow profile during the windy day with load curtailment (scenario 1)

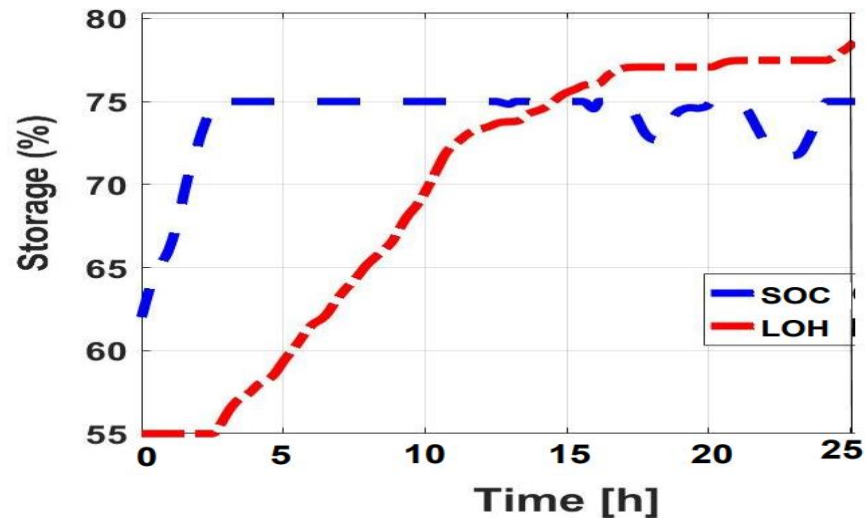


Figure 6-9: The level of storage during the windy day with load curtailment (scenario 1)

A wind turbine is, therefore, considered as the renewable energy source, which generates excess power in the micro-grid. It is worth noting that the wind turbine produces a significant fluctuation in power, as is evident in Figures 6-8 and 6-9. Therefore, enormous stored energy enables the electrolyser to operate for most of the day, which makes the generation surplus during some hours of the day. More so, it should be noted that the power rate constraints integrated into the controller design, irrespective of the high fluctuation in power produced by the wind turbine, instigated a smooth operation of the electrolyser, the behavior of which was thus quite satisfactory. Thus, the battery still stores energy, but it gets filled up early (from $t=3$ hours to 16 hours), only injecting power into the bus several times during that period. It is worth mentioning that the objective of the demand response technique (DRT) in the energy management system (EMS) is to use the diversity of the load consumption patterns and the energy available from the distributed energy resources (DERs) and the energy storage system (ESS) to reduce the peak load demand and minimize the operating/electricity costs of the micro-grid system. As there is energy surplus during the day, there is no need to switch ON the fuel cell during these hours of the day. Furthermore, at around 15 hours of the day when the demand for electricity rises slightly above the generation, there is a need to curtail some loads such as cooling and heating loads. During the windy weather condition, a maximum curtailment of 40% is allowed, since generation is surplus during the day and has charged up the batteries up to 75% SOC. Similarly, the level of hydrogen also keeps increasing by up to 78%. Therefore, in order to alleviate the system fluctuation caused by increasing demand for electricity, a reasonable goal of demand-side management activities could be to adjust the pattern of the load demand curve by minimizing the overall load demand for the distribution system during peak hours in order to reduce the overall planning and operating costs of the network. The AMPC controller has adjusted the set points slowly according to the optimum estimated cost function. Furthermore, reduction in the peak load demand improves system

sustainability by simply reducing the overall cost as well as the carbon emission level. The renewable energy-based micro-grid system benefitted from this DR technique, as the reduction in the peak load demand results in substantial cost savings. More so, since the costly loads such as heating and cooling loads that are typically turned ON during the peak load demand are being curtailed, which yielded less overall cost as compared to the micro-grid system in the previous chapter. Moreover, by evaluating the cost function, the cost function, $J = 12.542$ with load curtailment, as compared to the cost function obtained in the previous chapter without load curtailment, the cost function was $J = 18.685$.

In the second scenario, a new lithium-ion battery bank is added in this case to the micro-grid system of case 1. Therefore, for this configuration, a new AMPC algorithm must be devised. The micro-grid is composed of a PV plant, two different types of batteries, and a fuel cell, as illustrated in Figure 6-2. The power exchanged with the DC bus can be balanced using this Li-ion battery using its DC/DC converter; so that a new manipulated P_{bat2} , variable will appear [5].

Similarly, in this scenario, the micro-grid operates in the islanded mode during the simulations, so, therefore, $P_{grid}(t) = 0$, and this variable could be eliminated in the model. Therefore, in order to evaluate the performance of the control system under consideration on the micro-grid, three distinct generation scenarios (Sunny, windy, and cloudy) are implemented over 24 hours simulation period. Figure 6-10 is the MATLAB/Simulink of case 2 using Figure 6-2 as the micro-grid model-based design. The main generations in the micro-grid are solar and wind, which requires optimal utilization adopting the concept of DR technique to minimize the peak load demand and, at the same time, the electricity costs. The addition of Lithium-ion batteries further assists the micro-grid by storing energy during off-peak hours and discharge the energy during the peak hours of its operation.

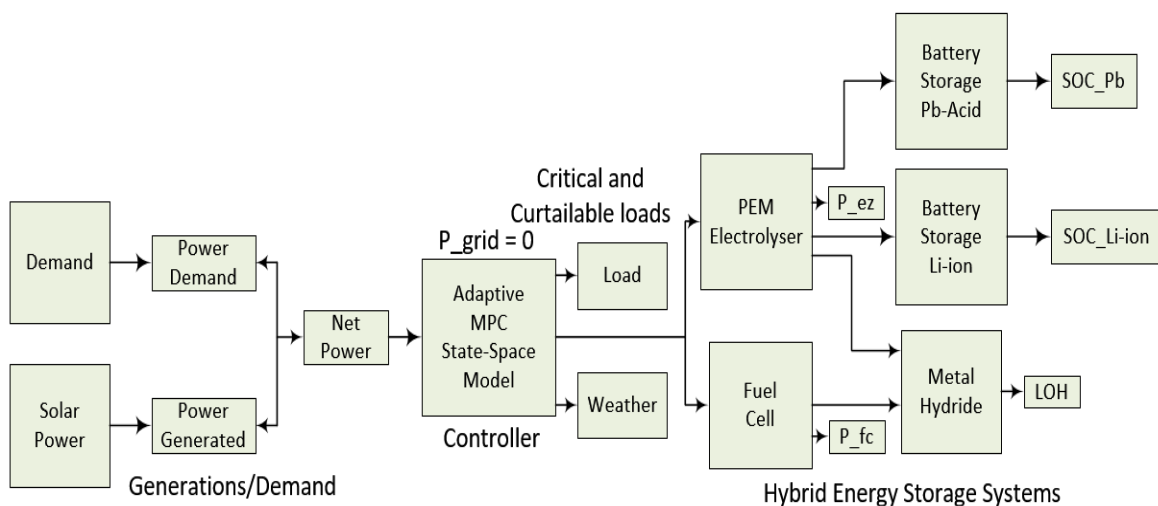


Figure 6-10: MATLAB/Simulink representation of scenario 2 with load curtailment (sunny, windy, and cloudy).

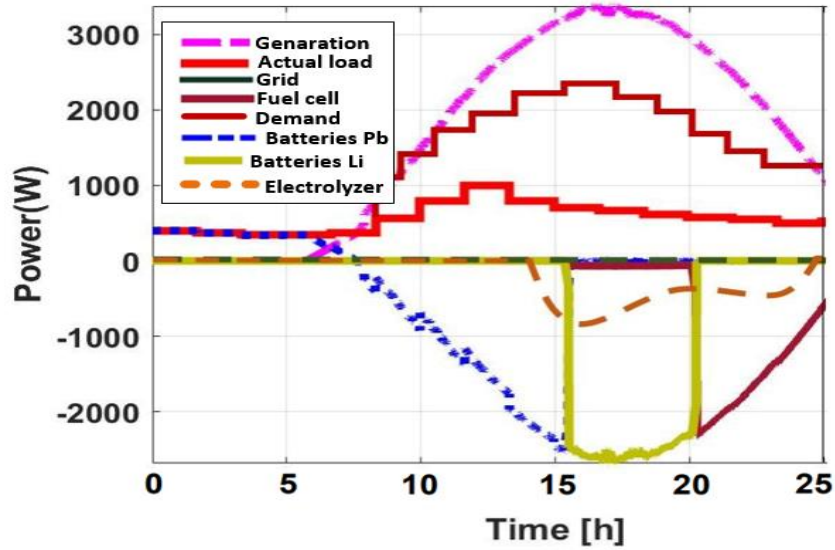


Figure 6-11: The power flow profile during the sunny day with load curtailment (scenario 2)

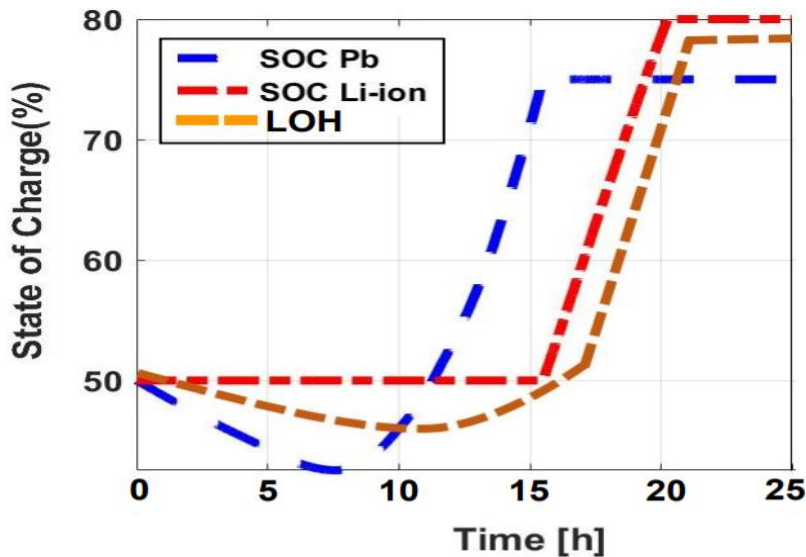


Figure 6-12: The level of storage during the sunny day with load curtailment (scenario 2)

Similarly, simulation has been carried out for a sunny day in scenario 2. Now, that $P_{grid}(t) = 0$, the micro-grid is operating in the islanded mode. Therefore, in order to keep it operating in the absence of generation, the load can be adjusted. The lead-acid battery is used for the first 7 hours to satisfy demand in the early hour of the day, as shown in Figures 6-11 and 6-12. Consequently, the generation sources start to supply at that hour of the day since the SOC of the battery has reached its lowest value. More so, the lithium-ion battery maintained its State of Charge (SOC) of 50% until the 16 hours when the demand is quite high for only the lead battery to satisfy the demand. At this point, the SOC of the lithium-ion battery starts diminishing. Since the micro-grid is operating in the islanded mode, the DERs are used in meeting the available demand. Therefore, as soon as the lead-acid battery has charged up to SOC of 75%, then it starts

to meet the load demand, the lithium-ion battery starts its operation at the 16 hours until SOC remains constant at 50%. At this hour of the day, the electricity demand continues to rise, and in order to preserve the lifespan of the batteries and other storage devices, there is a need to curtail some loads during the peak load demand. At around 16 hours of the day, some loads are adjusted to enhance the reliability and performance of the micro-grid. In this case, due to the introduction of the lithium-ion battery, the maximum load curtailment is reduced to 30%.

The Lithium-ion battery absorbs any unbalance in the network, thus minimizing the costs and improves reliability. The reason for choosing lithium-ion batteries as the primary storage device is that lithium-ion batteries have some fantastic advantages such as (1) High energy efficiency (2) Longer cycle life (3) Relatively high energy density, and (4) Improved resiliency.

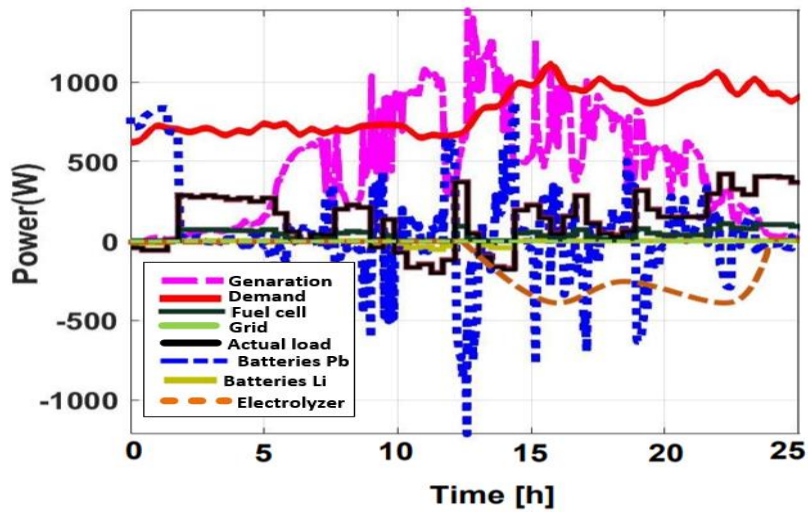


Figure 6-13: The power flow profile during the cloudy day with load curtailment (scenario 2)

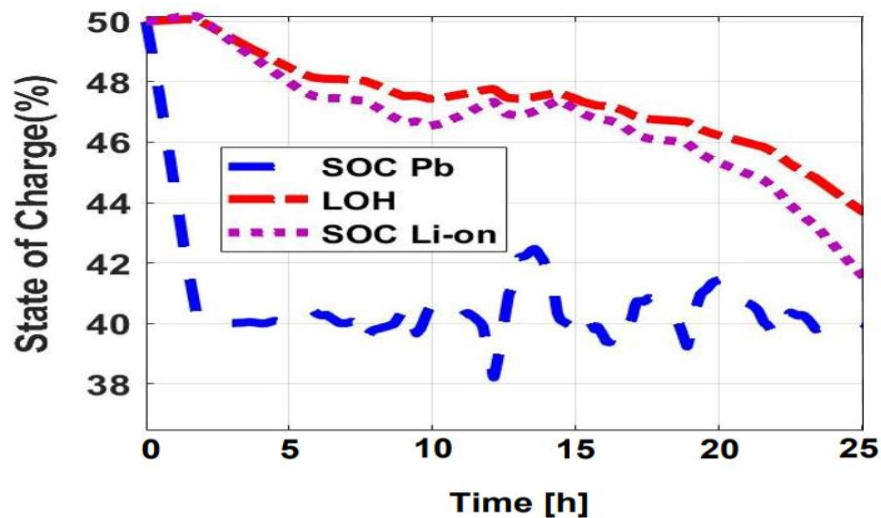


Figure 6-14: The level of storage during the cloudy day with load curtailment (scenario 2)

Similar to scenario 1, due to the cloudy weather, which results in minimal or no availability of sunlight, the PV generation is unable to meet the demand for most of the day (most often, the net power is below zero). Hence, the available resources such as the wind generation, batteries, and fuel cell must, therefore, supply any energy deficit within the micro-grid network. As it is evident in Figures 6-13 and 6-14, the lead-acid battery is used for the first 3 hours to satisfy demand in the early hour of the day, and then the generation source (wind generation) start to supply at that hour of the day since the SOC of the battery has reached its lowest value of 40%. The li-on battery continues to meet the demand to supplement the supply from the lead-acid battery. Subsequently, the controller decides to switch ON the fuel cell despite the fact that the SOC is far from its minimum value (around $t = 3$ hours in a smooth way), which is also supported by the wind generation. The controller does not activate the electrolyser during the first hour of the day, as there is no extra energy to store. Meanwhile, during the second half of the day, when the battery's minimum SOC has been reached, the fuel cell and the wind generation supply the load. Although, the fuel cell is unable to satisfy the load demand on its own accord because of the thresholds in the power rate and the voltage limits, and it requires the support of the wind generation. Furthermore, at around 17 hours of the day when the electricity demand continues to rise above the generation, there is a need to curtail some loads such as cooling and heating loads since the SOC of the batteries is minimum at that hour of the day in order to satisfy the demand and enhance the operation of the micro-grid. Note that due to the introduction of lithium-ion, which supplement the other storage devices, the maximum load curtailment is reduced to 30%. Therefore, from the simulation results of Figures 6-13 and 6-14, it is evident that the DR technique has successfully managed to bring the load consumption pattern to the objective load curve.

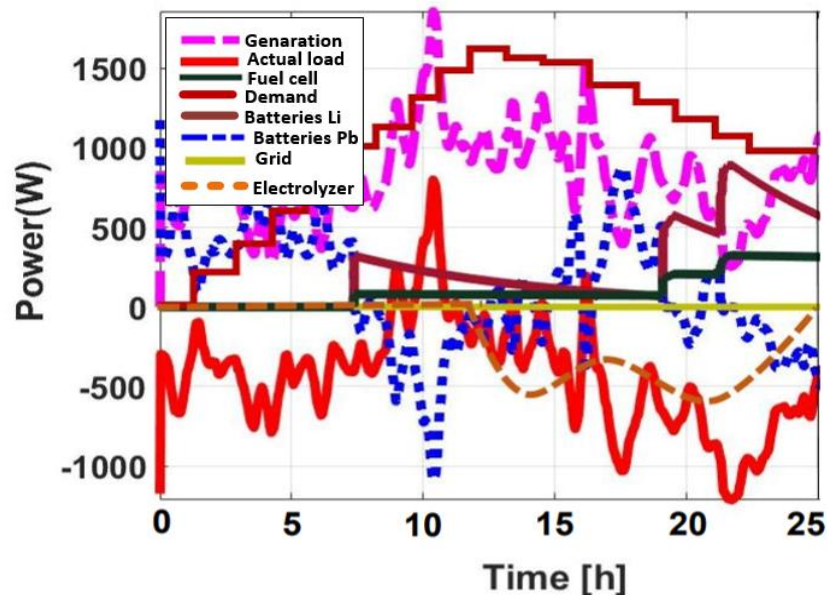


Figure 6-15: The power flow profile during the windy day with load curtailment (scenario 2)

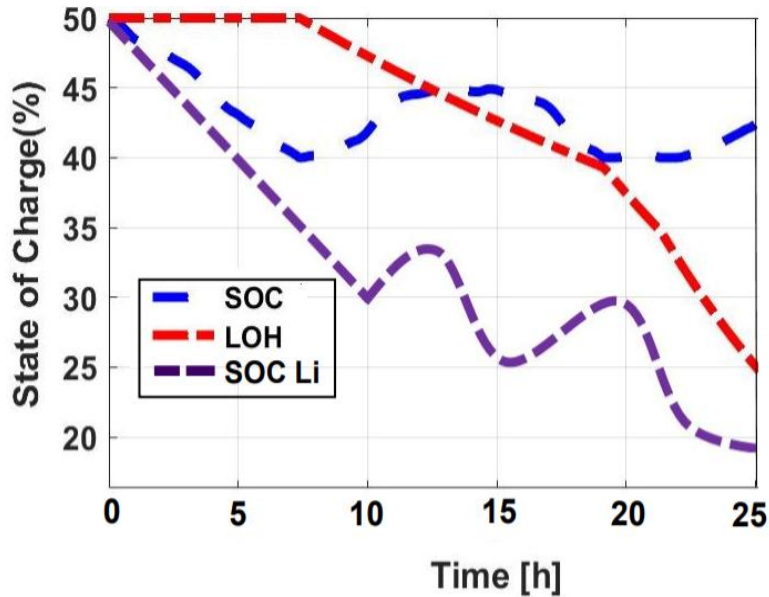


Figure 6- 16: The level of storage during the windy day with load curtailment (scenario 2)

During the windy period, the primary source of generation is the wind generation, fuel cell, as the PV system contributes little or no power to the load demand. Since the wind turbine is considered as the renewable energy source, which generates excess power in the micro-grid, it, therefore, produces a significant fluctuation in power, as can be seen in Figures 6-15 and 6-16. Therefore, due to the power supply from the wind turbine, the lead-acid battery stored some energy, which is used to supply the load at the early hour of the day up until 7:00 hours, then its SOC gets reduced to 40%. At this point, the lithium-ion battery continues to meet the load demand. The stored energy enables the electrolyser to operate for most of the day, which makes the generation surplus during some hours of the day. As there is energy surplus during the day, there is no need to switch ON the fuel cell during these hours of the day. Therefore, at around 10 hours of the day when the electricity demand rises slightly above the generation, there is a need to curtail some loads, such as cooling and heating loads. During the windy weather condition, a maximum curtailment of 30% is allowed, due to the introduction of the lithium-ion, which supplements the other storage devices. The AMPC controller has adjusted the set points slowly according to the optimum estimated cost function. Furthermore, reduction in the peak load demand improves system sustainability by merely reducing the overall cost as well as the carbon emission level. The renewable energy-based micro-grid system benefitted from this DR technique, as the reduction in the peak load demand results in substantial cost savings. Since the costly loads, such as heating and cooling loads that are typically turned ON during the peak load demand, are being curtailed, which yielded less overall cost as compared to the micro-grid system in the previous chapter. The cost function was similarly evaluated for scenario 2 with the DR technique. We can, therefore, quantify the improvement in the micro-grid performance. The cost function, $J = 8.335$ with load curtailment and hybrid energy storage, as compared to the cost function

obtained in the previous chapter without load curtailment (DR techniques), the cost function was $J = 15.625$. Consequently, it is evident in the cost evaluation, a reduction in the cost to 57.4% of the baseline value, taking into account the benefit of using the DR technique for EMS in micro-grid. More so, it is evident in the cost function, J , obtained from the three scenarios conducted, the cost function was further minimized by introducing the lithium-ion battery storage into the micro-grid. Therefore, as it is seen from the results, the cost function obtained when we utilized hybrid energy storage was reduced compared to when we used just only one battery [254].

6.4 Chapter Summary

Demand response techniques in the framework of demand-side management has the potential to provide many benefits to the entire renewable energy-based micro-grid system, particularly for micro-grid in islanded mode. This chapter investigated the demand response technique for the energy management system in micro-grid based on Adaptive Model Predictive Control. The proposed method is a generalized scheme based on load curtailment, which has been mathematically formulated as an optimization problem. The minimization problem obtained by using the DR technique for the Energy management system in a renewable energy-based micro-grid is solved using the AMPC algorithm. Simulations were carried out on the micro-grid, which contains renewable energy sources (PV and Wind), fuel cell, electrolyser, storage device, and different kinds of loads. (critical and curtailable loads). The AMPC solves an energy optimization problem with multiple types of energy storage systems in a renewable energy micro-grid. This problem of optimization is solved at each sampling time to determine minimum running costs while satisfying the demand and considering technical and physical constraints. The controller's proposed behavior has been observed under different external conditions, such as changes in weather and demand. The AMPC algorithm is proposed to optimally utilize the maximum power from the renewables by using hybrid storage systems. The simulation results have shown that the implementation of the DR technique for energy management in micro-grid reduces the peak load demand and, consequently, minimized the operation costs of the system. It is evident in the cost function obtained when the micro-grid adopts the DR technique during single battery storage, the cost function, $J = 12.542$ with load curtailment, as compared to the cost function obtained in the previous chapter without load curtailment, the cost function was, $J = 18.685$. More so, comparing the cost function when a hybrid storage system is used with the DR technique. The cost function, $J = 8.335$ with load curtailment and hybrid energy storage, as compared to the cost function obtained in the previous chapter without load curtailment (DR techniques), the cost function was $J = 15.625$. The results of the simulation show that the proposed algorithm can regulate a vast number of the controllable devices of various types, and achieves substantial savings while reducing the peak load demand of the renewable energy-based micro-grid. The simulation results are extremely satisfactory and

can be generalized for implementation in real-time. The Electric Vehicles can act as loads when connected to the micro-grid. However, they can as well supply energy to the micro-grid during energy deficit due to their storage capability. Therefore, due to these functions, they can be considered as prosumers. Hence, proper management of the loads and EV charging can significantly enhance the micro-grid operation. The AMPC technique could be adapted to this framework, and the concept of Vehicle-to-Grid (V2G) is taken into considerations in the next chapter. Therefore, in order to demonstrate the V2G capabilities, the next chapter presents some simulations to illustrate the concept of load shifting, in a renewable energy-based micro-grid with EVs integration. The charging of EVs can be included in the DSM strategy (because EVs are loads for the micro-grid). Potentially, a significant number of idle EVs can theoretically be used to build a distributed energy storage network to support renewable generation. With the ever-increasing price of fossil fuel, continuous deterioration of the environment, and rapid growth of battery technology, EVs have become a significant field of micro-grid research and have attracted considerable interest.

CHAPTER SEVEN

ENERGY MANAGEMENT SYSTEM OF A MICRO-GRID WITH THE INTEGRATION OF ELECTRIC VEHICLES

7.1 Introduction

The previous chapter investigated the benefits of adopting the concept of the demand response (DR) technique for the energy management system in a stand-alone micro-grid with both critical and curtailable loads. The proposed method was a generalized scheme based on load curtailment, which was mathematically formulated as an optimization problem. The minimization problem obtained by using the DR technique for the energy management system (EMS) in a renewable energy-based micro-grid was solved using the AMPC algorithm. Hence, the objective of the DR technique in the previous chapter was to use the available renewable energy resources optimally, maximizes the economic benefit, and reduces the peak load demand. Therefore, it is evident in the simulation results that the implementation of the DR technique for energy management in micro-grid reduced the peak load demand and, consequently, minimized the operation costs of the system. More so, it is evident from the results that the proper management of the consumption pattern of the loads significantly enhanced the micro-grid operation. Specifically, the combination of hydrogen storage with electrical batteries and supercapacitors appears to be an effective solution for erratic and volatile fluctuations in the generation of renewable energy. The use of energy storage compensates for the variability in the production of renewable energy and the random behavior of the consumer. In addition, the micro-grid may use EVs as a large amount of energy storage to provide local demand, compensate for the intermittent generation of RESs, or exchange power with the grid. Similarly, Electric Vehicles can act as loads when connected to the micro-grid. However, they can as well supply energy to the micro-grid during energy deficit due to their storage capability. Therefore, due to these functions, they can be considered as prosumers. Hence, proper management of the loads and EV charging can significantly enhance the micro-grid operation. This chapter extends the model-design of the energy management system in the micro-grid developed in the previous chapter to the case when electric vehicles (EVs) are integrated [254], [5]. This chapter addresses the problems of control and energy management in micro-grid with the incorporation of renewable energy generation, hybrid storage technologies, and the integration of the EVs with V2G technology. The AMPC control technique is used to optimize the charge/discharge of the EVs in a receding horizon manner in order to reduce operational cost in a renewable energy-based micro-grid. V2G systems integration can be a crucial element in the assurance of network reliability against variability in loads. In this context, the purpose of this chapter is to present an AMPC algorithm for the optimization of a micro-grid coupled with a V2G system consisting of six electric

vehicle charging stations. More so, the proposed algorithm effectively manages the use of renewable energy sources, vehicles charge, energy storage units, and the purchase and sale of electric power to the external network. Two scenarios are investigated in this chapter to examine the performance of the proposed controller to manage the renewable energy sources in the micro-grid system. Hence, the first case uses a load shifting mechanism to solve the charge management problem during a known interval of parking time. The second case is the introduction of EVs with V2G capabilities when connected with the micro-grid. In this case, the vehicle battery collaborates with the ESS of the micro-grid to maximize costs benefits and mitigate the intermittency of renewable generation. More so, to demonstrate the V2G capabilities, this chapter further presents some simulations to illustrate the concept of load shifting in a renewable energy-based micro-grid with EVs integration [237]. Furthermore, other benefits of V2G concepts, such as voltage and frequency control for the micro-grid stability, are investigated. Therefore, it is evident from the obtained results that the proposed control algorithm was able to effectively manage the renewable energy sources, energy storage units, vehicles charge, and the purchase and sale of electric power with the grid. The formulations of the EMS-based adaptive MPC optimization problem, cost functions, dynamic system constraints, and the control-oriented linear model, which are to be solved (minimized) by the proposed algorithm (AMPC), have been presented in chapter 3. This chapter presents the results and the discussions obtained in the various cases conducted.

7.2 Description of the Dynamic Modeling of the micro-grid System

In this section, the MATLAB/Simulink environment was utilized to model the system dynamics of a renewable energy-based micro-grid network consisting of RESs (photovoltaic, wind turbine), battery storage system, ultra-capacitor, loads, and electric vehicle. It also includes a hydrogen storage system, comprising a PEM (proton exchange membrane) electrolyser to produce hydrogen, a metal hydride tank to store hydrogen, and a PEM fuel cell to produce energy [237], [253]. Figure 7-1 illustrates the model-based design description of micro-grid with the integration of electric vehicles.

The Simulink model is used to simulate the dynamics of electric vehicles. The EVs are interfaced with the micro-grid via the power supply and the loads. Two case studies are implemented in this chapter, and the first case is the management of EVs charging without V2G technologies, otherwise known as V1G (EV does not supply energy to the micro-grid). The second case is the management of EVs charging with V2G capabilities (EV can exchange energy with the micro-grid). The EV charging station can charge up to six cars simultaneously. It is worth mentioning that the energy produced during the normal operation of micro-grid does not match the demand. Therefore, it is expedient to store the excess energy from the renewable sources in the batteries or, better still, to use it to produce hydrogen through the electrolysis process. Thus, the metal hydride tank is used to store the hydrogen produced by the electrolyser. The fuel cell uses the

hydrogen to supplement the mismatch between the supply and demand, should the power from the renewable sources not be accessible. More so, the micro-grid has a link to the main network, which allows the purchase and sale of energy. Hybrid storage enables two-stage operating strategies: the battery can absorb/provide small amounts of energy on fast transients, while hydrogen storage supplements the largest oscillations. In this context, car batteries can be used by the micro-grid to increase the buffer capacity of fast transients when the cars are parked [220], [149].

The load shifting mechanism is used for the charge management of the EVs. Therefore, where cars are parked over a period of time, the charging process can be optimized with regard to energy price levels and operating costs for micro-grids. Given that charging is carried out at a constant capacity, optimization can be accomplished by estimating the best charging interval (within the parking period of the car). Case 1 describes the management of EVs charging without V2G technologies, i.e., EVs do not exchange energy with the micro-grid. The optimization gives the values of δ_{ev} , given a parking time interval, which indicates the best connection time. It is worth mentioning that the value of δ_{ev} is 0 if the vehicle is not connected at instant t and takes the value of 1 when it is connected at that instant. More so, the transition from disconnected to connected is indicated by $\sigma(t)_{ev}$.

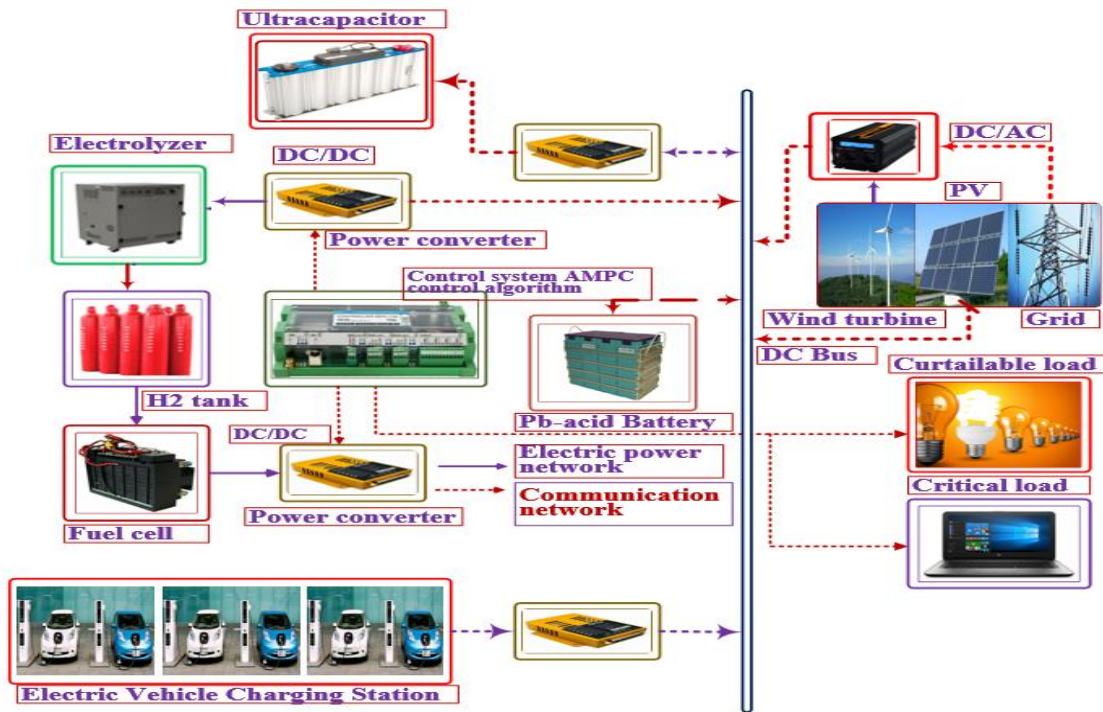


Figure 7-1: The model-based design description of the micro-grid with electric vehicles

On the other hand, the objective of case 2 is mainly to adapt the AMPC algorithm to optimize the micro-grid with V2G technology, which consists of six charging points for the electric vehicles. The proposed algorithm performs the management of renewable energy sources, energy storage units, vehicles charge,

and the purchase and sale of electric power with the grid. This application is an extension of the case 1, which discusses the charging management of micro-grid without V2G technology. In this context, the micro-grid power exchange with the EV batteries is bidirectional. More so, provided the car is fully charged at the scheduled pickup time, the charging process can be interrupted when necessary. Similar to the micro-grid used in the previous chapters, in this case, a charging station for six EVs is included, as shown in Figure 7-1. Therefore, the main objective of the EMS is to evaluate the various powers such as P_{grid} , P_{bat} (the grid and battery bank power), P_{H_2} (the power of the hydrogen storage), and P_{ev-i} (the powers of the six-vehicle batteries) such that the overall system performance is optimized. Two control layers are considered in the proposed solution, first is the upper layer, which comprises a scheduler that aims at the economic benefit of the charging station [252]. The second is the charging station management unit (CSMU), which manages the EV charging based on the type of charge (fast or slow) or the parking time. More so, the lower level is a fast power-sharing technique, which runs every second. Similarly, the upper layer considers load shifting and the electricity tariffs, and MIQP solves the formulation. Conversely, the fast QP algorithm is used to solve the formulation of the lower layer, which is responsible for tracking the power targets evaluated by the upper layer.

7.3 Simulation Results and Discussions

This section presents the MATLAB/Simulink simulation of a renewable energy-based micro-grid network consisting of RESs (photovoltaic, PV, wind turbine, WT), Battery Storage system, ultra-capacitor, loads, and electric vehicle. It also includes a hydrogen storage system, comprising a PEM (proton exchange membrane) electrolyser to produce hydrogen, a metal hydride tank to store hydrogen, and a PEM fuel cell to produce energy. The Simulink model is used to simulate the dynamics of the EVs and is therefore interfaced with the micro-grid through the power supply and the loads. Two case studies are investigated in this chapter, and the first case is the management of EVs charging without V2G technologies, otherwise known as V1G (EV does not supply energy to the micro-grid). The second case is the management of EVs charging with V2G capabilities (EV can exchange energy with the micro-grid). The EV charging station can charge up to six cars simultaneously. The AMPC algorithm is used to optimize the micro-grid for the two cases (with and without the V2G technology), which consists of six charging points for the electric vehicles. The proposed algorithm performs the management of renewable energy sources, energy storage units, vehicles charge, and the purchase and sale of electric power with the grid. More so, the EVs can act simultaneously as loads and as generators. Hence, due to these capabilities, they can be considered as prosumers. Therefore, the charging station can charge up to six vehicles due to the V2G technology and can also exchange energy with the micro-grid. Hence, depending on the electricity tariffs, the EVs can buy

or sell energy from/to the grid. Thus, during fast transients, the EVs batteries are used by the micro-grid to increase the buffer capacity when the cars are packed [18], [255].

For the sake of simplicity, this study considers the incorporation of six electric vehicles into the micro-grid. More so, the formulation can be extended to any number of electric vehicles, based on the number of charging points available to charge the EVs in the charging hub. The number of EVs integrated into the micro-grid system in this study is limited to six, since only six charging points are available for the charging management scheme. The formulations of any number of EVs can be implemented by adding as many δ (for the connection state) and σ (for transitions) as the number of EVs and the associated constraints. The solver finds an optimal solution for the micro-grid, providing a set of the control variables, which are logic and continuous, and the AMPC controller is formulated as a mixed-integer quadratic programming (MIQP) problem. The different operation modes in the micro-grid are modeled with the mixed logic dynamical (MLD) framework. The output signals which are generated by the solver are the values of exchange power with the main grid (P_{grid}), the power of electrolyser, fuel cell, and battery (P_{elz} , P_{fc} , and P_{bat}), the activation signals for the electrolyser and fuel cell (δ_{elz} and δ_{fc}) and the activation and transition of the Electric Vehicle (δ_{ev} and σ_{ev}). Note that the sampling time is 1 hour, and the schedule horizon is 24 hours. In this section, three scenarios for a sunny day are investigated. The first scenario is the micro-grid operation without the integration of electric vehicles. The second scenario is when the electric vehicles are parked from mid-night to 8 a.m. (meanwhile, the EVs batteries have to be fully charged at 8 a.m.), and lastly, the EVs are parked all day and can be charged at any interval along the entire day. Hence, the net power is computed as the difference between solar generation and the loads connected to the micro-grid. Figure 7-2 depicts the MATLAB/Simulink representation of a micro-grid with the integration of Electric Vehicles.

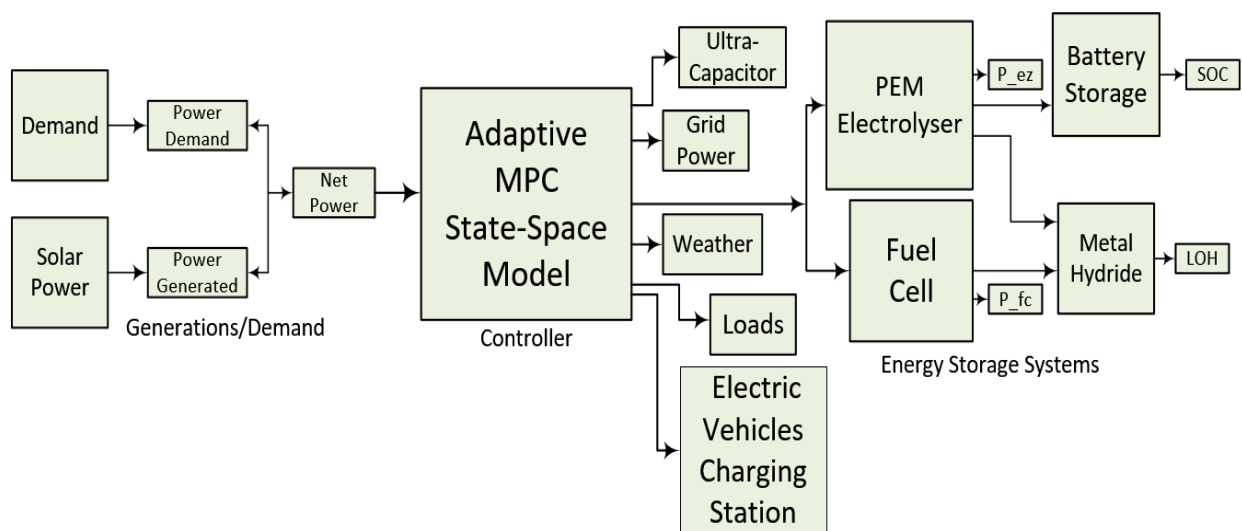


Figure 7-2: MATLAB/Simulink representation of a micro-grid with electric vehicle integration

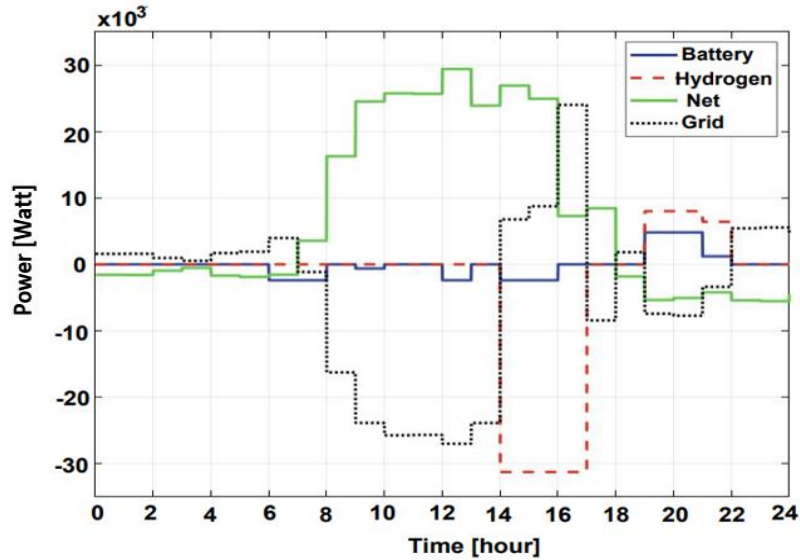


Figure 7-3: Power flows in the micro-grid without EV charge during a sunny day

Figure 7-3 depicts the first scenario in which the micro-grid operates without the incorporation of the electric vehicles (Energy management of the renewable micro-grid without considering the incorporation of electric vehicles, i.e., there is no parking lot). Since the micro-grid is not equipped with the EVs parking lots, it is expedient that the micro-grid optimally utilizes the available renewable energy sources with the storage systems and purchase energy from the grid at a low price during off-peak hours to reduce the operational costs. More so, the proposed control algorithm does the micro-grid scheduling by adjusting the value of generation and purchased energy during the day from the renewable generations and the grid, respectively, to minimize its costs. The results from the simulation-conducted show that the micro-grid operation is slightly different in the three scenarios, although the amount of power required to charge the electric vehicles is not too enormous compared to the other components of the micro-grid. The energy generated in the morning is surplus due to the abundance of the sun. It is evident from Figure 7-3 that the generated power by the PV system is very high in the morning and noontime owing to the availability of sunlight. Due to high irradiance from the sun, the power generated is surplus, and some of the power is stored in the battery to meet the load demand during the period of low irradiance, particularly at night. Therefore, the remaining of this surplus energy is sold to the grid since the electricity price is high. The power stored in the battery is used at 20 hours of the day to compensate for the power deficit. Moreover, the excess energy from the solar PV system (renewable source) is also used to produce hydrogen via the process known as electrolysis. This produced hydrogen is stored in the metal hydride tank, and it is used by the fuel cell to supplement the mismatch between the supply and demand when power from the renewable source is not available. Figure 7-3 illustrates the power flows in the micro-grid without implementing EVs charging mechanism during a sunny day.

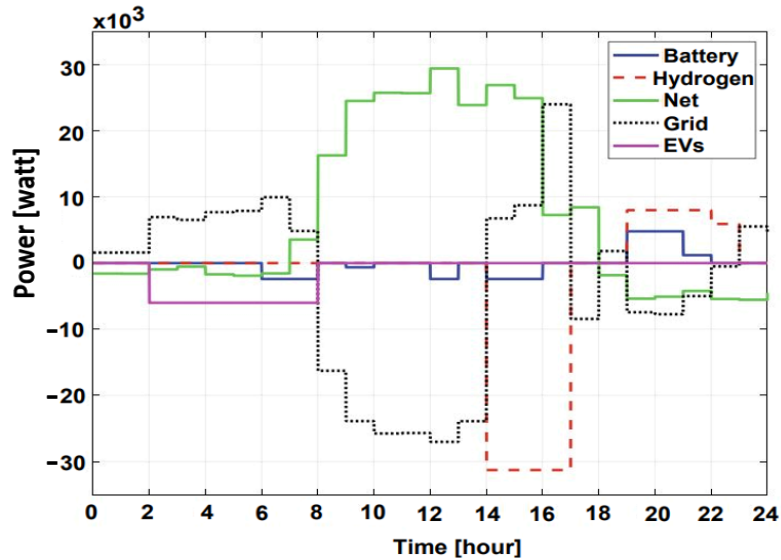


Figure 7-4: Power flows in the micro-grid with EVs mid-night charge during a sunny day

Figure 7-4 depicts the power flows in the micro-grid with EVs mid-night charge during a sunny day. In this scenario, the electric vehicles are parked at home parking lots from midnight to 8 a.m., and the EVs batteries have to be fully charged at 8 a.m. Hence, the micro-grid uses the capacity of the EVs batteries to store the low-cost power generation from renewable energy sources as well as the energy purchased from the grid.

Similar to the first scenario, the energy generated by the PV system in the morning is surplus owing to the abundance of sunlight. As it is evident in Figure 7-4, the solar irradiance is high between 8-15 hours of the day; therefore, the solar energy produced is in excess, and some of the power is stored in the battery to compensate for any power shortage at night. The irradiance level at night is low or completely zero; therefore, the battery supplies the loads and EVs until its SOC is minimum. Similarly, the fuel cell uses the hydrogen produced by the electrolyser to supplement the energy supplied by the storage devices to meet the load demand and to charge the EVs batteries parked at the parking lot until its LOH is minimum. Consequently, there is a need to patronize the grid for energy purchases when the energy from the renewable sources and the energy stored in the storage systems have been exhausted to ensure reliability in the micro-grid operation. Hence, this implies that most of the energy must be purchased from the grid in order to charge the EVs batteries during the night. The purpose of charging the EVs at midnight is because it is an off-peak period. During this period, most of the utility customers consume less energy, and the energy cost from the grid tends to be cheaper. Hence, load shifting activity in the charging management of EVs parked over a time-period optimizes the charging process with respect to the energy price level and the operating costs for micro-grids. The AMPC algorithm is applied to solve the optimization problem of the energy management system in micro-grid with EVs integration by estimating the best charging interval (within the parking period of the car).

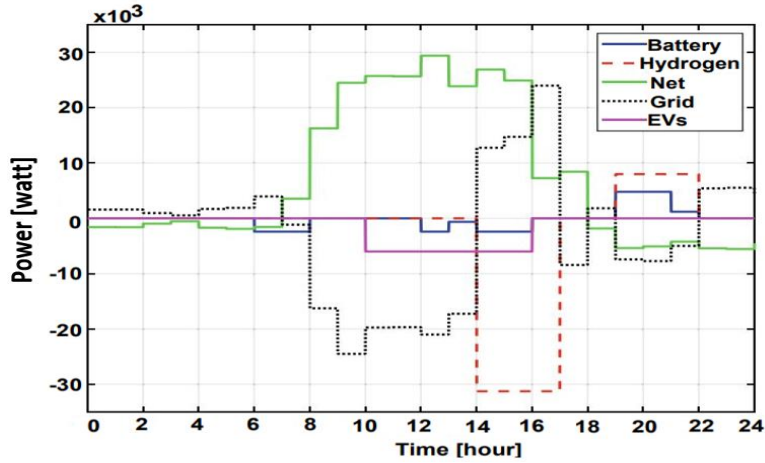


Figure 7-5: Power flows in the micro-grid with flexible EVs charge during a sunny day

Figure 7-5 illustrates the power flows in the micro-grid with flexible EVs charge during a sunny day. In the third scenario, EVs are parked all day and can be charged at any time of the day. Although the only weather condition considered in this section is a sunny day. Admittedly, sunlight is most of the time abundant in the morning till the noontime, as shown in Figure 7-5. Due to the high irradiance from the sun, the PV system generates enough energy to meet the load demand (EVs charging). Thus, it is expedient to shift most activities that require energy consumption to these hours of the day. Therefore, the optimizer around mid-day shifts the loads to where a surplus of energy exists. Since the case is conducted during a sunny day, there would be an energy surplus during the mid-day, which results in a lower cost of energy. Similar to the second scenario, the fuel cell also uses the hydrogen produced by the electrolyser to supplement the energy supplied by the storage devices to meet the load demand and to charge the EVs batteries parked at the parking lots. The essence of the flexibility in the EVs charging is to utilize the available renewable energy sources optimally to avoid continuous grid patronage for energy, which minimizes the micro-grid running costs. In conclusion, load shifting can be used to choose the best charging interval for EVs considering time constraints and optimizing operational costs. Therefore, the management of EVs charging without V2G technologies (EV does not supply energy to the micro-grid) has been addressed in this section.

Table 7-1: Characteristics and the simulation results of different case studies.

Case study	Energy exchange (micro-grid and main-grid)	Parking lots (EVs charging)	DR program	Operation Costs J
Scenario 1	✓			18.215
Scenario 2	✓	✓	✓	13.250
Scenario 3	✓	✓	✓	10.125

Table 7-1 shows the characteristics and the simulation results of the different case studies that are considered. It is evident in the cost function, J , obtained from the three scenarios conducted that incorporating the electric vehicle into the micro-grid system has minimized the operation cost of the micro-grid compared to when EVs are not integrated.

This section addresses the second case, which is the management of EVs charging with V2G capabilities (EV can exchange energy with the micro-grid). It is worth noting that the EV charging station can charge up to six cars simultaneously. Therefore, the objective of the AMPC control algorithm is to utilize the RES optimally during EVs charging, facilitates the purchase and sale management of electricity to the grid. More so, it also coordinates the use of the battery bank and the hydrogen storage to minimize the mismatch between the generation and demand, and lastly, performs the charging of EVs while fulfilling the micro-grid load demand at all times.

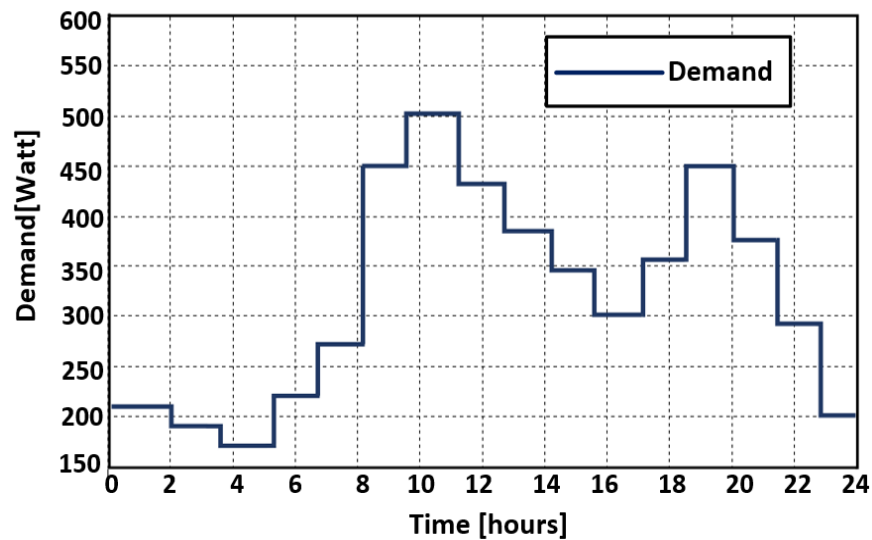


Figure 7-6: 24 hours demand vector

The 24 hours demand vector used in the simulation is depicted in Figure 7-6. It is evident that the demand rises in the morning to the highest level, that is, the consumption of energy is very high in the morning when everyone is still at home getting ready to leave for work. The energy consumption pattern levels out over the mid-day, since the majority of energy consumers are at their various workplaces, and then in the evening, it is seen that the energy consumption pattern rises to another level when everyone gets home from work. The simulations were carried out for a period of 24 hours to follow the energy consumption pattern of Figure 7-6. Three different simulations were performed in different scenarios to validate the controller performance. The first scenario considered was that of a sunny day. It is evident from the simulation results that three of the vehicles draw fast charges (1, 3, and 5), while the other three receives slow charge (2, 4, and 6).

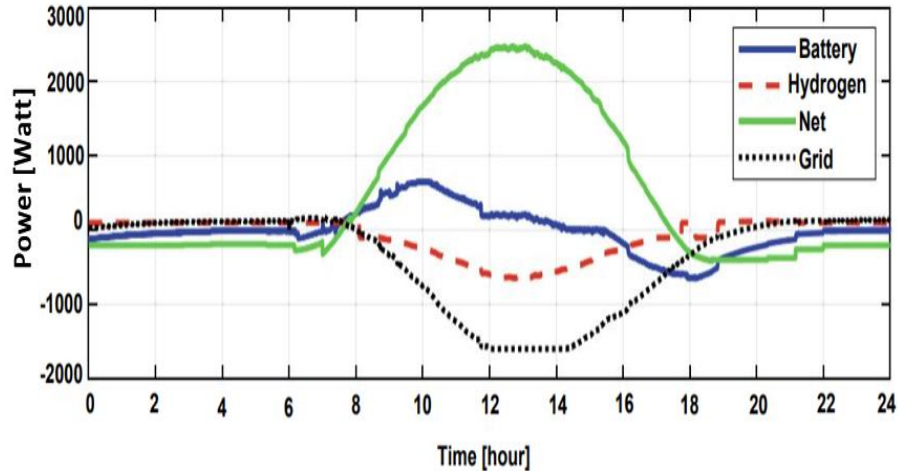


Figure 7-7: Power flow profile of the energy sources during a sunny day

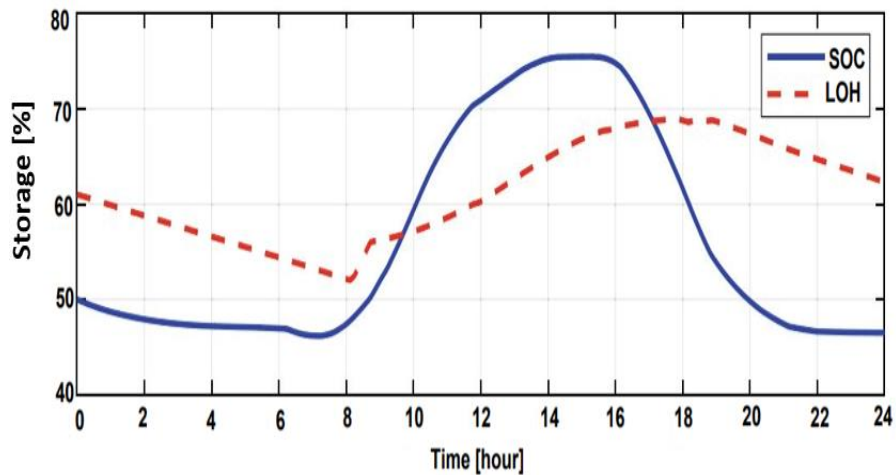


Figure 7-8: Level of storage during a sunny day

The behavior of the micro-grid ESSs, such as the battery and the hydrogen storage, changes throughout the day. It is clear from the Figures 7-7 and 7-8 that throughout the time of low sunlight irradiance (0-8 hours and 19-24 hours), storage systems operate during these hours to provide the energy required to satisfy demand and reduce the amount of electricity purchased from the external grid. On the other hand, during high sunlight irradiance (8-18 hours), there is an energy surplus from the PV system, part of the energy is sold to the grid, and the battery and hydrogen storage are charged with the rest of the energy through the electrolyser process. During the night hour of the day (18-19 hours), when there is less irradiance from the sun, the controller decides to switch between the fuel cell and electrolyser to supply the load, respecting the minimum operation time of each equipment for reliability in the micro-grid operation. It is seen that the AMPC algorithm provides an optimal power distribution between the battery, the electrolyser, and the energy sold to the grid. Furthermore, the EVs batteries are connected to the micro-grid to avoid any form

of fluctuation in the primary source of generation. Therefore, the energy stored in the EVs batteries during energy surplus is used by the micro-grid to meet the mismatch between generation and demand.

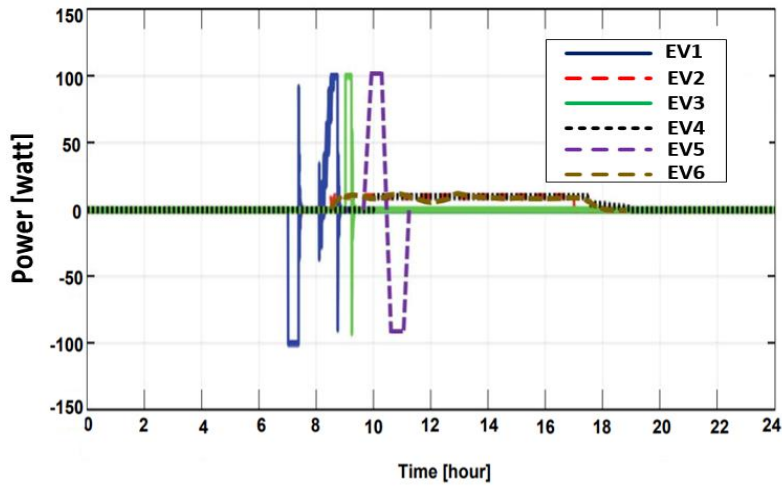


Figure 7-9: Power flow profile of the EVs charging management during a sunny day

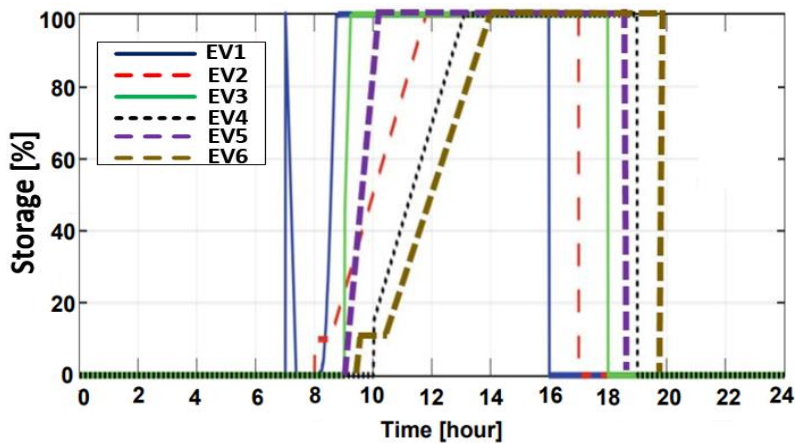


Figure 7-10: Level of storage of the EVs charging management during a sunny day

Figures 7-9 and 7-10 depict the power flow profile and the level of storage of the EVs charging management during a sunny day. The EV1 (that accepts fast charge) is parked at the parking lot to be charged at the 7 hours of the day, and the EV battery is used by the micro-grid as a storage system. Therefore, due to the abundance of sunlight, the PV system generates enough solar energy, which is used to charge the EVs connected to the charging points of the energy hub. In this scenario, six electric cars are connected to the station to be charged, and they are connected simultaneously. The charging process is shifted to the period of surplus energy generation, and it is evident in Figure 7-9 that EV1 is fully charged at 9 hours of the day. It is seen that there are some oscillations in the power of the three EVs (1, 3, and 5) during the charging process, and this is due to the aggressive tuning of the controller parameters. More so, in order for the other three EVs (2, 4, and 6) to be ready for pickup, they are charged in the slow charge mode in the most

convenient way. The sharp decrease in the SOC curves after 15 hours of the day is due to the disconnection of the EVs from the charging station.

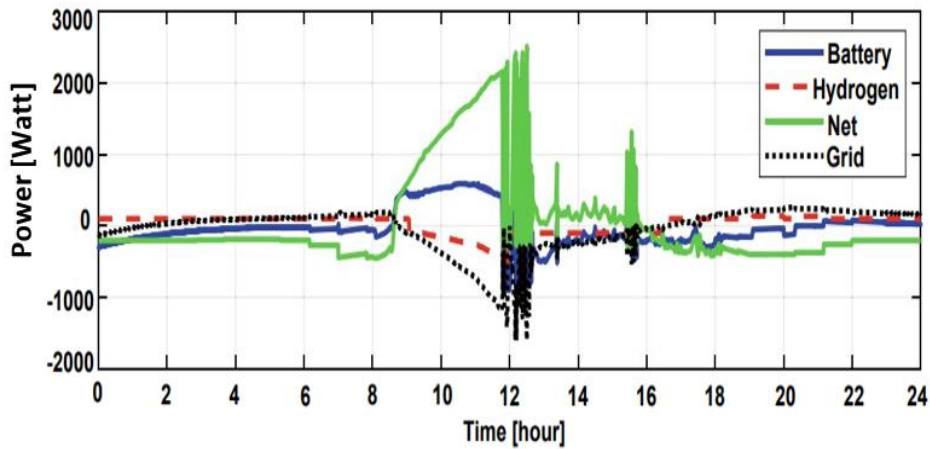


Figure 7-11: Power flow profile of the energy sources during a cloudy day

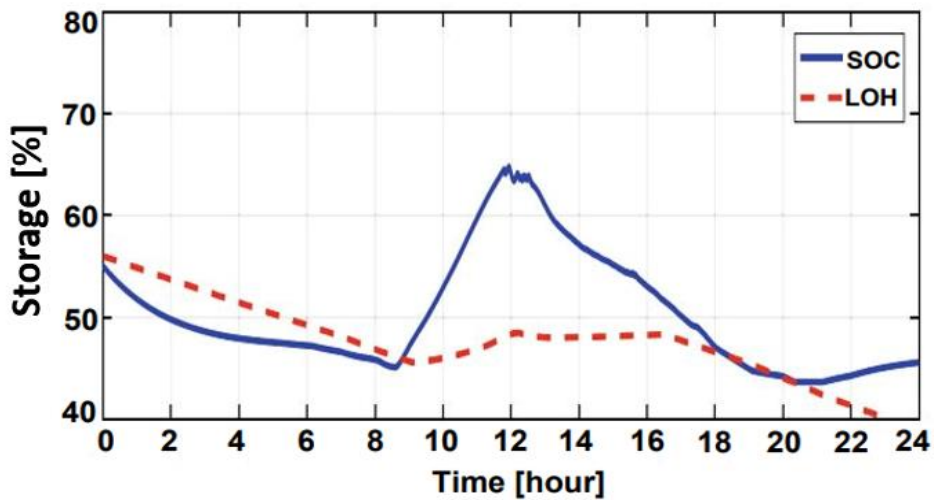


Figure 7-12: Level of storage during a cloudy day

Similarly, a simulation was performed for a cloudy day scenario, where the irradiance from the sun is too low or equals to zero. As it is evident from Figures 7-11 and 7-12, the behavior of the micro-grid during a cloudy day scenario is slightly different. Hence, since the control has to cope with the high-power fluctuation in the generation, the cloudy day connotes a big challenge for renewable micro-grids. In this weather situation, the irradiance from the sun is not sufficient to meet the demand. Therefore, it is expected that the battery bank absorbs high-frequency oscillations while the hydrogen provides energy for a long time, as the micro-grid comprises a hybrid storage system. More so, reducing switching in hydrogen storage is another problem that could be triggered by oscillation conditions. During cloudy weather, between the hours of 12 hours and 18 hours, as shown in Figure 7-12, the EVs batteries and the battery bank absorb most of the power fluctuations of the energy generation. Due to irradiance oscillation, a short switching

between the electrolyser and the fuel cell is observed around 12 hours to 13.30 hours. The energy stored by the hydrogen storage during the day is used to supply the load at night. Hence, compared to the scenario of the sunny day, the difference between the initial and final LOH is enormous. This occurrence is anticipated since the irradiance from the sun during the day is not adequate to supplement the energy expended at the nighttime. The energy profile sold to the external grid, and the lifespan of the battery is directly affected by the irradiance oscillation, which is caused by the cloudy weather. Consequently, due to the fluctuation conditions, the number of charge/discharge cycles increases.

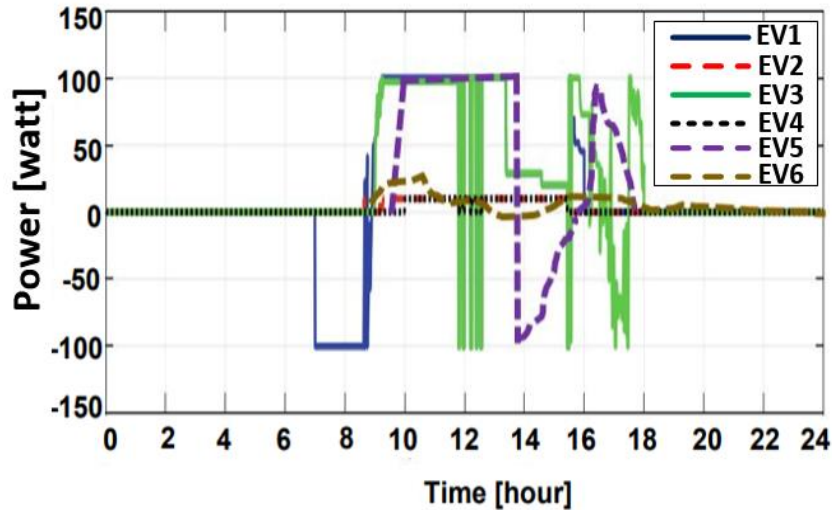


Figure 7-13: Power flow profile of the EVs charging management during a cloudy day

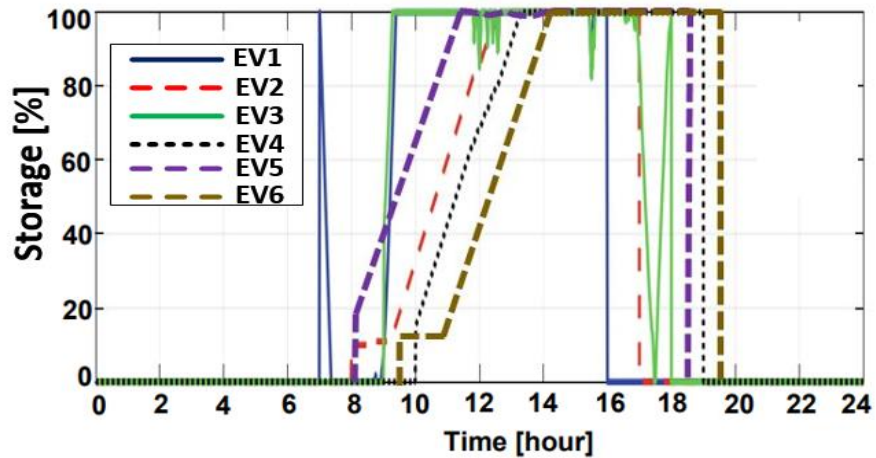


Figure 7-14: Level of storage of the EVs charging management during a cloudy day

Figures 7-13 and 7-14 depict the power flow profile and the level of storage of the EVs charging management during a cloudy day. Similar to the scenario of a sunny day, the EVs were parked at the parking lots to be charged. Since the EVs are not in motion (idle), their batteries are used as sources of energy to the loads connected to the micro-grid. The micro-grid uses the EVs as a storage system to compensate for

the stochastic nature of RES generation, perform primary frequency control, and thus contribute to improving the dynamic behavior of the systems. Due to the cloudy weather, the irradiance from the sunlight is not sufficient to effectively charge the EVs, the other sources of energy in the electrical network (wind generation, fuel cell, and the external grid) are used to meet the demand. Hence, as shown in Figure 6-17, the EV1 is already charged at around 9 hours of the day. The batteries of the EVs, which allow fast charge (EV1, EV3, and EV5), are used to reduce the power fluctuations during the cloudy period of the day. Thus, a slow charge is applied in EV2, EV4, and EV6, similar to the scenario of a sunny day.

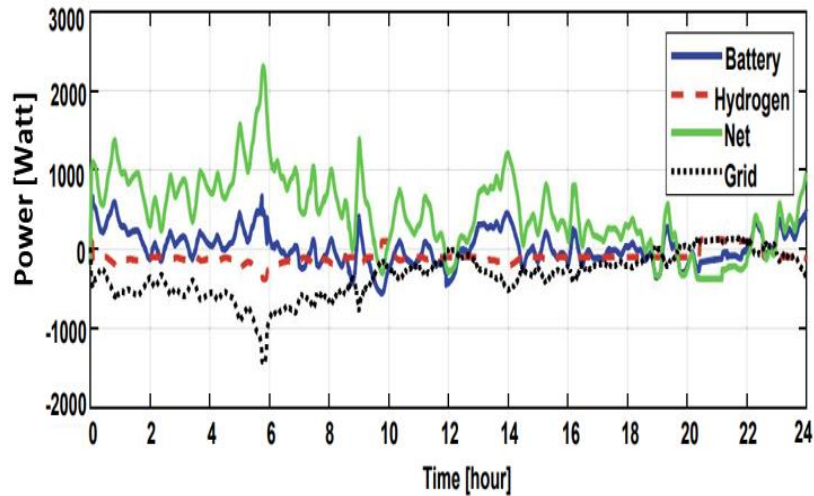


Figure 7-15: Power flow profile of the energy sources during a windy day

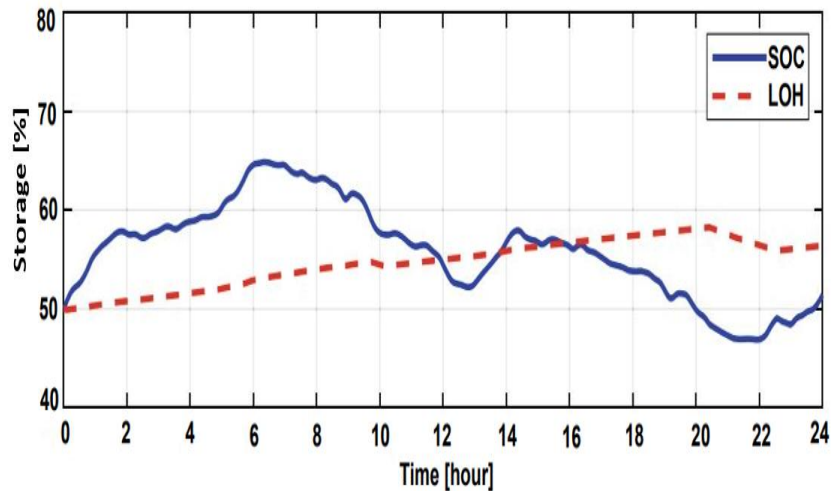


Figure 7-16: Level of storage during a windy day

Simulation is conducted similarly for the scenario of a windy day using a wind turbine as the renewable energy source. More so, it is evident in Figures 7-15 and 7-16 that compared to the cloudy day, the fluctuations are not so abrupt. Nonetheless, the wind turbine generation still presents a high stochastic behavior in its power profile. Therefore, there are some switching occurrences in hydrogen storage, for

instance, at 10 hours of the day when there is wind fluctuation and also when the load demand is expected to be met around the 20 hours of the day. The electrolyser operates for most hours of the day, and, as a result, the LOH value of the hydrogen storage is higher than it was at the beginning of the day.

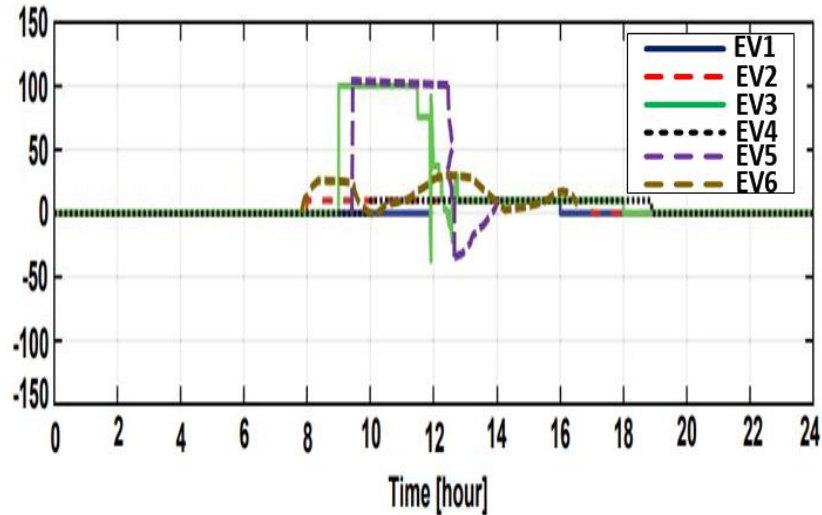


Figure 7-17: Power flow profile of the EVs charging management during a windy day

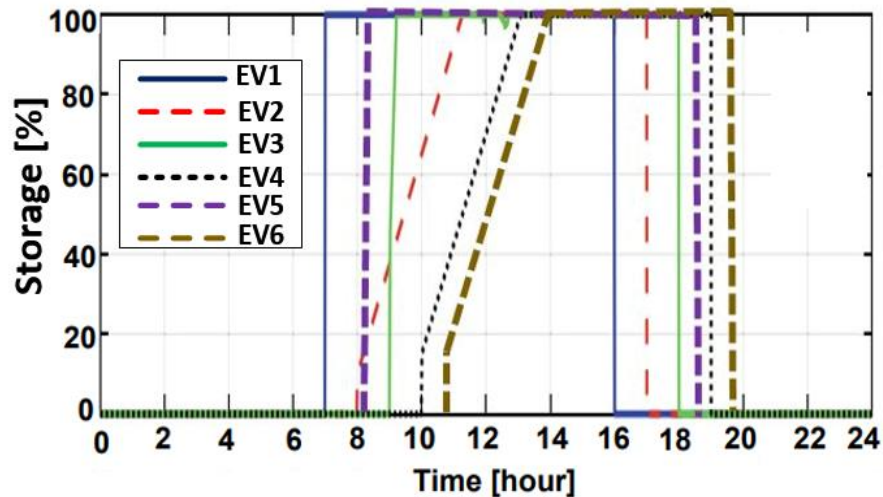


Figure 7-18: Level of storage of the EVs charging management during a windy day

As shown in Figures 7-17 and 7-18, the EVs batteries are scarcely used by the micro-grid, although they are accessible for energy balancing between the supply and demand. The simulation adopted four switching mechanisms between the fuel cell and the electrolyser. The switching mechanisms are essential due to the impact of the proposed constraints and the penalty function in order for the operating time of the individual equipment to be minimized. Since the weather condition is windy, the energy from the wind turbine is used to charge the EVs for some hours. Due to the abundance of wind, the energy from the wind generation is surplus, which energizes the electrolyser to operate for most hours of the day.

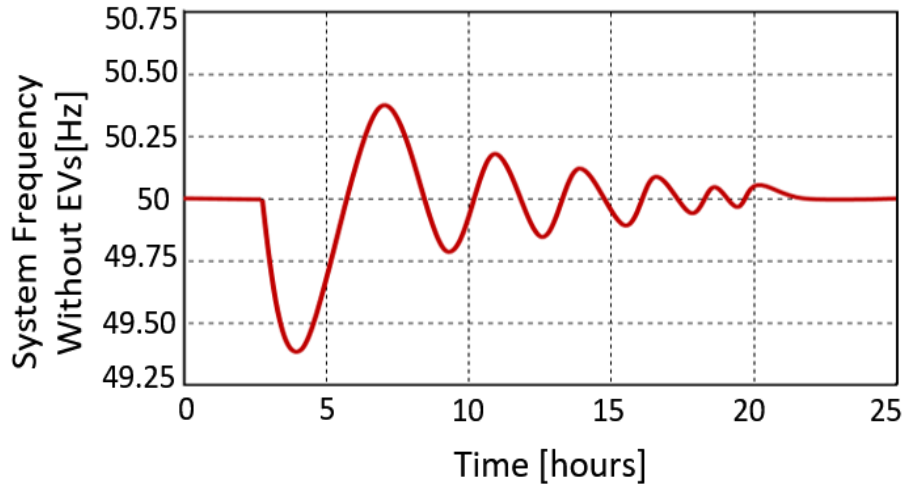


Figure 7-19: System frequency without EVs

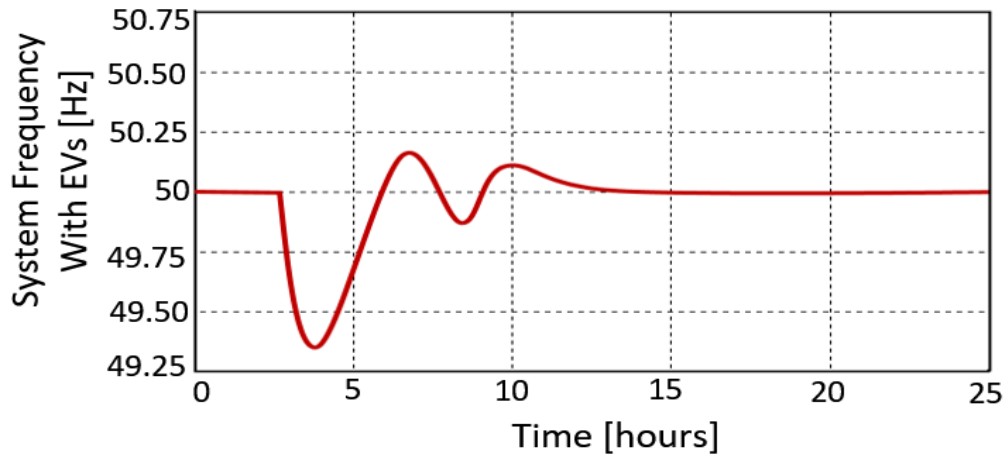


Figure 7-20: System frequency with EVs

Figures 7-19 and 7-20 illustrate the deviations in the system frequency without incorporating the electric vehicles and integrating EVs, respectively. The system frequency without EVs has more oscillations in the system response than when EVs are incorporated. The frequency when EVs are connected remains within the permissible limits. EVs are parked in the parking lots to store energy during the surplus energy from renewable energy sources, and the energy is used to compensate for any power imbalances between the generation and demand. It is seen from Figure 7-19 that the deviation of the frequency for the case without EVs is unable to restore to its nominal frequency until the renewable energy sources start generating at full power. The presence of the EVs was able to stabilize the grid frequency. It is evident in all the simulation results that the proposed controller has been able to manage the energy in the micro-grid, meet the load demand of the various loads connected to the micro-grid, and also efficiently charged the electric vehicles [26].

7.4 Chapter Summary

In this chapter, the problems of micro-grid control with the incorporation of renewable energy generation, hybrid storage technologies, and the integration of the EVs with V2G technology have been addressed. This chapter adopted the AMPC control technique to optimize the charge/discharge of the EVs in a receding horizon manner in order to reduce operational cost in a renewable energy-based micro-grid. Meanwhile, two scenarios were investigated; firstly, a load shifting mechanism was used to solve the charge management problem during a known interval of parking time. Secondly, the concept of EVs with V2G capabilities when connected with the micro-grid was introduced. In this case, the vehicle battery collaborated with the ESS of the micro-grid to maximize cost benefits and mitigate the intermittency of renewable generations. It is evident from the results when a load shifting mechanism was used to solve the charge management problem during a known interval of parking time that the cost function, J , obtained when the EVs were incorporated was drastically minimized compared to when EVs were not integrated as shown in Table 7-1. More so, the integration of the EVs was able to stabilize the grid frequency. The deviations in the system frequency when EVs were integrated quickly damped out. However, the system frequency response could not restore to its nominal value when EVs were not incorporated. It is evident from the obtained results that the proposed control algorithm was able to effectively manage the renewable energy sources, energy storage units, vehicles charge, and the purchase and sale of electric power with the grid. Frequency control is a central control concern in the design and operation of electrical power systems. It is becoming more and more important today due to the growing scale, the evolving structure, the advent of new distributed renewable energy sources and uncertainties, environmental and operational constraints, and the complexity of power systems. Therefore, to reduce the frequency deviation, the frequency control units can quickly compensate for the difference between the power supplies and power demand. The next chapter uses the adaptive model predictive control (AMPC) technique for load frequency control of a two-area interconnected power system with a stand-alone micro-grid. The purpose of this study in the next chapter is to solve the problems of frequency deviation against variations in system parameters and load disturbance of a typical stand-alone micro-grid.

CHAPTER EIGHT

LOAD FREQUENCY CONTROL OF A TWO-AREA POWER SYSTEM WITH A STAND-ALONE MICRO-GRID

8.1 Introduction

The previous chapter addressed the problems of control and energy management in micro-grid with the incorporation of renewable energy generation, hybrid storage technologies, and the EVs with V2G technology. The adaptive model predictive control (AMPC) technique was used to optimize the charge/discharge of six EVs in a receding horizon manner in order to reduce operational cost in a renewable energy-based micro-grid. Hence, the proposed algorithm effectively managed the renewable energy sources, vehicles charge, energy storage units, and the purchase and sale of electric power to the external network. More so, two scenarios were investigated in order to examine the performance of the proposed controller to manage the renewable energy sources in the micro-grid system. Furthermore, other benefits of V2G concepts, such as voltage and frequency control for the micro-grid stability, were investigated. Therefore, it is evident from the obtained results that the proposed control algorithm effectively managed the renewable energy sources, energy storage units, vehicles charge, and the purchase and sale of electric power with the grid. Frequency control is a central control concern in the design and operation of electrical power systems. It is becoming more important today due to the growing scale, the evolving structure, the advent of new distributed renewable energy sources and uncertainties, environmental and operational constraints, and the complexity of power systems. Therefore, to reduce the frequency deviation, the frequency control units can quickly compensate for the difference between the power supplies and power demand [256], [257]. It is worth noting that the traditional MPC controller is not reliable in the handling of changing dynamics, as the internal plant model used in the MPC for prediction is constant. The optimal result could not be obtained by an MPC controller with constant penalty weights while taking into account micro-grid complexities. This poses the need for an advanced control algorithm that takes the updated plant model at each time step for the current operating condition; thus, it makes accurate predictions for the new operating condition. Hence, in order to deal with changes in plant dynamics, the adaptive model predictive Control algorithm is utilized [26], [258]. The above analysis motivated the proposed advanced controller, adaptive model predictive load frequency control for a two-area power system with a stand-alone micro-grid. This chapter uses the adaptive model predictive control technique for load frequency control of a two-area interconnected power system with a stand-alone micro-grid. A generalized state-space model of a typical stand-alone micro-grid having controllable and uncontrollable generating power sources is derived. The same proposed control algorithm is used to predict the future output and control inputs for the micro-

grid frequency control. The purpose of this study is to solve the problems of frequency deviation against variations in system parameters and load disturbance of a typical stand-alone micro-grid. Therefore, in order to achieve better system performance, it is expedient to understand the effects of system parameters on the control performance of the proposed controller, which is essential for the controller design process. Hence, the effects of system parameters variation on the control performance of the AMPC control technique for frequency control in a stand-alone micro-grid are investigated. More so, based on the various cases considered in this chapter, it is evident that the closed-loop response obtained by the AMPC algorithm has proven to be faster and adaptable. The effectiveness and robustness of the AMPC control technique are demonstrated for different load, solar power, and wind power perturbations and similarly evaluated by the computation of quantitative performance indices under the variation of the system parameters. Furthermore, to be more realistic in our analysis of the proposed system model, certain physical constraints affecting the power system performance were included. Such physical constraints are the reheat turbine (RT), the time delay (TD), the generation rate constraint (GRC), and the dead band (DB) for the steam turbine. The impacts of these physical constraints on the system dynamic performance were also investigated [5], [223]. The simulation results of the proposed model demonstrated good dynamic response, robustness, optimum performance, and superiority of the proposed AMPC technique to the MPC control technique. The dynamic modeling, state-space representation, and the AMPC controller design for the stand-alone micro-grid are presented in chapter 3. This chapter presents the results and the discussions obtained in the various cases conducted [26], [259].

8.2 Description of the Dynamic Modeling of the Stand-Alone Micro-grid

A two-area interconnected power system, with control area 1 consisting of a multi-renewable energy-based micro-grid (PV generation system, fuel cell, wind turbine system, and battery) and control area 2 consisting of a thermal reheat turbine system, TD, DB, and GRC are shown in Figure 8-1. In addition, the simulation of the transfer function model carried out in this study used the governor's linearized models, thermal with reheat turbine, PV system, wind turbine system, fuel cell system, battery storage system, and UPFC connected along the AC-DC tie line as depicted in Figure 8-1. The deviation in frequency is caused by the mismatch between the power generated and the demand. Similarly, the micro-grid frequency is also deviated by the changes in solar irradiance and wind speed. The thermal generation (TG) with primary frequency control can generate power quickly to respond to changes in power demand or supply. The primary frequency control is based on the droop speed control technique, which results in a steady-state frequency error. Therefore, the secondary frequency control, which is based on the AMPC control technique, is applied to the ESS in order to restore the system frequency to its nominal value. Hence, the nominal power values of each micro-grid component (PV, WTG, TG, FC, ESS, and Load) are 100 kVA,

100 kVA, 160 kVA, 80 kVA, 90 kWh, and 200 kW, respectively [260]. The penetration of RESs, such as the generation of the Solar system and wind turbines in the microgrid, decreases overall device inertia and negatively affects the frequency and voltage stability of the microgrid. More so, it is highly anticipated that the LFC-based on the AMPC control technique to compensate for the active power imbalance in the stand-alone microgrid.

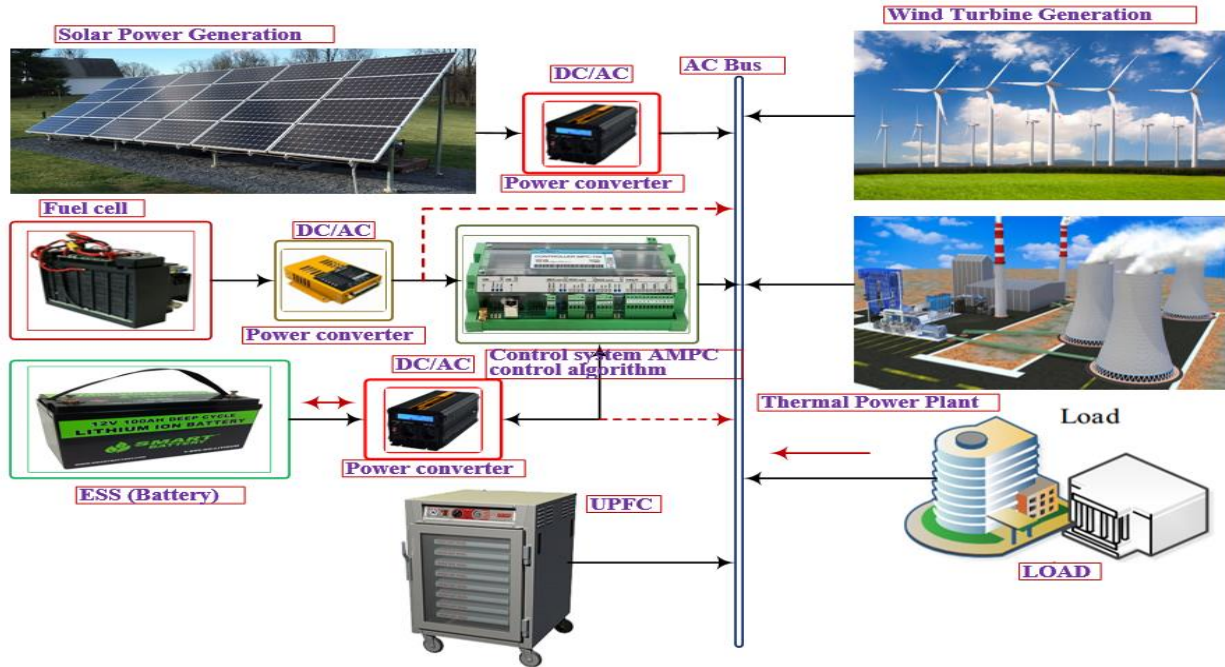


Figure 8-1: The model-based design description of the stand-alone micro-grid

Figure 8-2 illustrates the linearized model of the stand-alone micro-grid system, which is commonly studied for evaluating the frequency response of the stand-alone micro-grid system. Control area 2 units has its participation factor, K_t and regulation parameter, R , which determines their contributions to the nominal loading. In this study, two control techniques are being investigated in order to compare their control capacities in the minimization of area control error (ACE) of the control areas to nearly a zero value. Hence, to have a thorough insight into the AGC problem, it is imperative to integrate physical constraints in the dynamic model of the system to provide a more practical power system. Some of the generating units, therefore, have some essential physical constraints such as DB for the governor, TD, and GRC for the steam turbine. These non-linear characteristics have often been ignored in some literature [261], [262]. Thus, this chapter incorporates certain physical constraints to make up this defect in the proposed model. Also, the unified power flow controller (UPFC), a member of the flexible alternating currents transmission systems (FACTS) family, is used in series with a tie line further to improve the dynamic performance of the power system. Thus, frequency control in a two-area multi-renewable micro-grid source is achieved primarily by predicting control signals and future outputs, i.e., control actions and frequency deviations to the

controllable units. It is worthy of note that the renewable sources are presumed to operate at maximum power point [68]. The AMPC control design algorithm is used to accomplish the predictions where a state-space system model is used. In area 1, as shown in Figure 8-2, the PV system consists of the PV panel, maximum power point tracking (MPPT), inverter, and filter. K_{p1} is the gain of the PV system, a_1 and c_1 are the negative values of poles, and a_2 is the negative value of zero in the transfer function. Hence, it goes for all the generation sources in the system [14], [242]. The thermal system dynamic model comprises the speed control loop, steam turbine model, and the governor. Two types of wind turbine generators (fixed-speed WTG-based on an induction generator and variable speed WTG based on a doubly fed induction generator) are considered in this chapter to show the influence of various WTG models on the control performances.

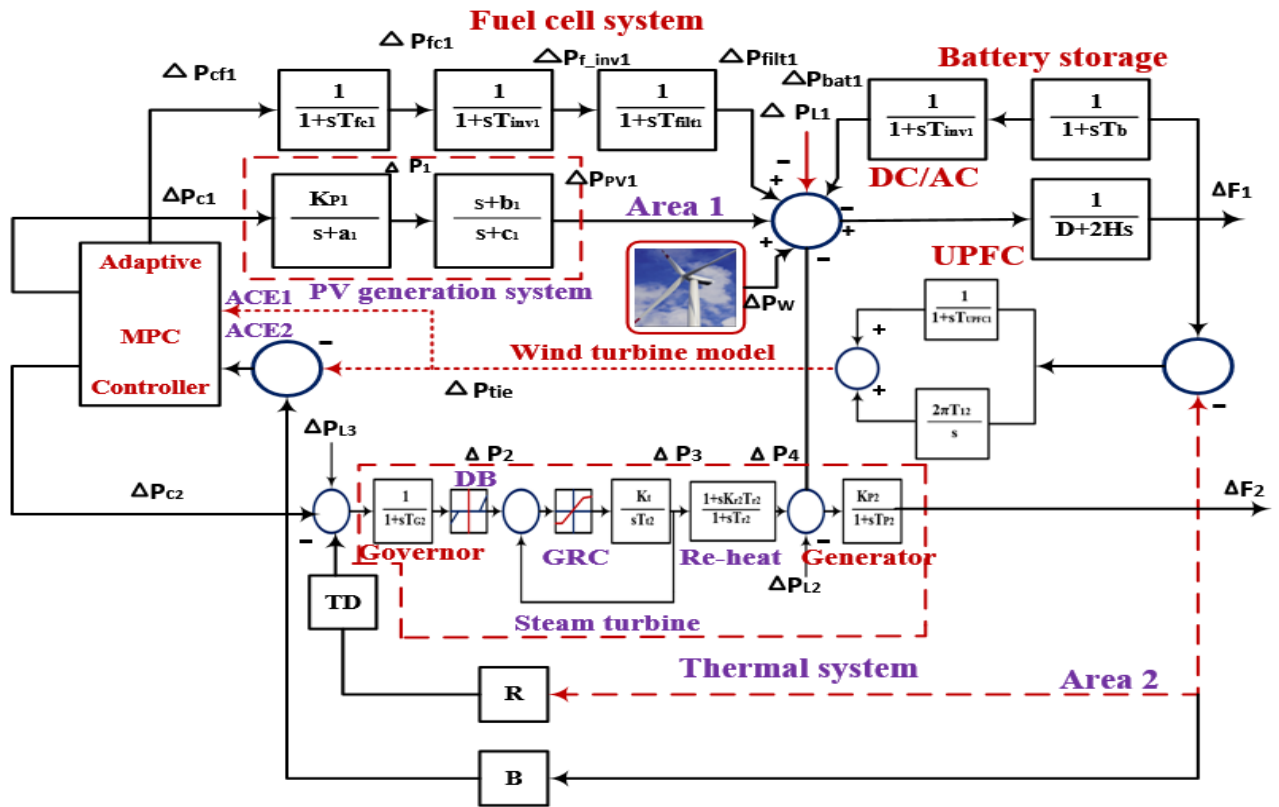


Figure 8-2: Transfer function model of a two-area multi-renewable energy sources-based autonomous micro-grid.

8.3 Simulation Results and Discussions

This section presents the simulation results and discussions of various cases of the LFC problem in two-area multi-renewable sources stand-alone micro-grid. Therefore, to demonstrate the effectiveness of the proposed AMPC scheme over the traditional MPC, we considered different cases, including variations in the system generation, load, and parameters. The two-area multi-source power network shown in Figure 8-

2, with renewable energy sources, is simulated in Simulink/MATLAB. More so, some physical constraints such as reheat turbine, GRC, TD, and DB that affect the performance of the power system are investigated for more practical study. It is worth mentioning that power generation can only be adjusted at a specified maximum rate in a power system with a steam turbine. Two types of wind turbine generators (WTGs) are considered in this section to depict the influence of various WTG models on the control performance of the two control algorithms under investigation. The dynamic responses of both controllers (AMPC and MPC) are evaluated considering the micro-grid system of Figure 8-2 under the condition of load perturbation, solar, and wind power fluctuations. Communication delays are, therefore, a significant challenge in the analysis of LFC problems due to the increasing complexity of power systems in a deregulated environment. Thus, to be more realistic in analyzing the proposed model, these physical constraints are included in the system model. The reheat unit has a generation rate of 10% puMW/min, the maximum value of DB for governor is set as 0.05 p.u, and the typical value of time delay is considered to be 2 sec for the present study. The system parameters used in the model simulation are shown in Table D-6.

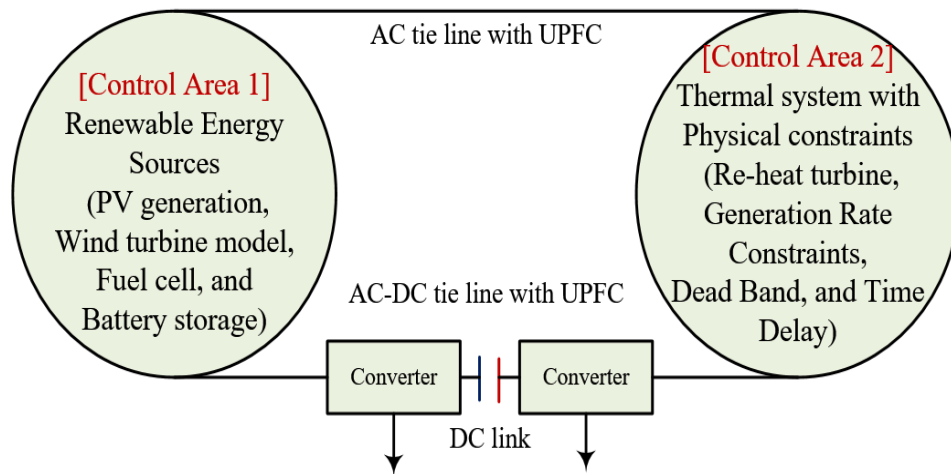


Figure 8-3: Two-area multi-renewable sources isolated micro-grid with UPFC

The simulations are implemented on MATLAB/Simulink 2018b software core i5 processor, 8th Gen, 2.5GHz, 8GB RAM. Fig. 8-3 shows the schematic representation of the system under study. Comparison based on good dynamic response, robustness, optimal performance and the superiority of the proposed AMPC technique to the MPC control technique is investigated. Several scenarios are conducted to assess the dynamic response and robustness of the secondary frequency control based on the AMPC by considering the system uncertainties. More so, under the conditions of load change and wind power fluctuations, the dynamic responses of both controllers are assessed by examining the MG system. Table 8-2 shows the various parameters setting of AMPC and MPC control techniques.

Table 8-1: The parameter settings of the AMPC and conventional MPC control schemes

Control Algorithms	Parameters Settings
AMPC	Prediction horizon, $P = 10$, control horizon, $M = 5$, weights on manipulated variables = 0.01, weights on manipulated variables rate = 0.02, weights on the output signals = 1.2, sampling interval = 0.0002 s, Max. control action = 0.2 pu, Min. control action = 0.2 pu, Max. Frequency deviation = 1 pu, Min. frequency deviation = 1 pu, weight vectors, $Q = E_{P \times P}$, $R = 0.01E_{M \times M}$.
Conventional MPC	Prediction horizon, $P = 10$, control horizon, $M = 5$, weight vectors, $Q = E_{P \times P}$, $R = 0.01E_{M \times M}$.

8.3.1 Case 1: Step load variation and dynamic system response

In this case, the dynamic system response of the micro-grid with series step changes in the load is evaluated. The load changes are implemented with an increase in the value of ΔP_L . The load connects to the stand-alone micro-grid system at 5 seconds with an amount of 0.02 p.u (2% step increase in load with AC tie line), as shown in Figure 8-4a, which results in the reduction of the frequency. The micro-grid frequency recovers to its nominal value due to the ESS with the secondary frequency control, which generates more active-power. It is evident in Figure 8-4b that the control performance of the micro-grid frequency with the AMPC control technique outperformed the MPC control technique. The frequency response using AMPC is better and faster, and the overshoot is quite lower than the MPC technique. The physical constraints (non-linear features) affect the optimum values of the controller parameters and the dynamic transient response of the thermal system, which results in more oscillations when the controller is not incorporated. The physical constraints significantly impact the control performance of the conventional MPC algorithm compared to the proposed AMPC controller in the thermal system. Moreover, the inclusion of the UPFC in series with the tie-line further improves the dynamic response of the system and the control parameter values. The performance indices (Criteria) utilized in this study include the integral of time multiplied square error (*ITSE*), the integral of time multiplied absolute value of the error (*ITAE*), the integral of the absolute value of the error (*IAE*), the integral of square error (*ISE*), the overshoot of ΔF_1 , ΔF_2 and ΔP_{tie} denoted as V_{p1} , V_{p2} and V_{p3} , respectively, the rise time of ΔF_1 , ΔF_2 and ΔP_{tie} is denoted as t_{r1} , t_{r2} , and

t_{r3} , respectively. More so, settling time of ΔF_1 , ΔF_2 and ΔP_{tie} is denoted as t_{s1} , t_{s2} , and t_{s3} , respectively, the steady-state error of ΔF_1 , ΔF_2 and ΔP_{tie} denoted as E_{ss1} , E_{ss2} , and E_{ss3} , respectively.

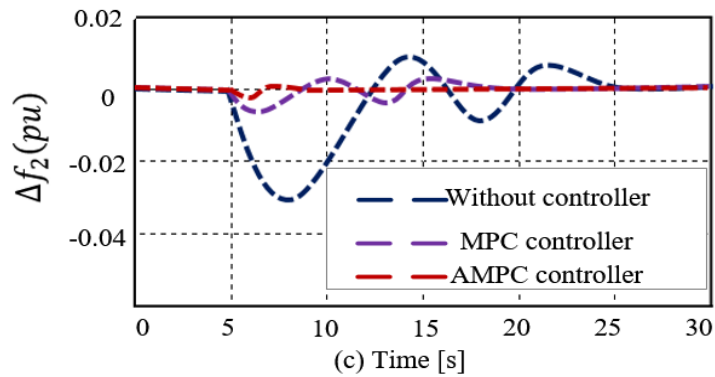
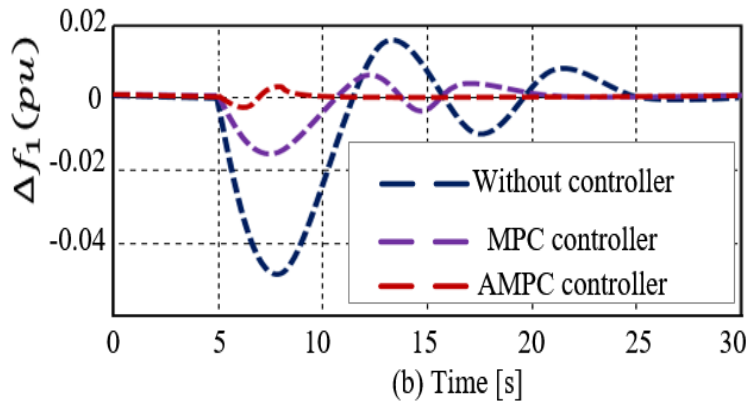
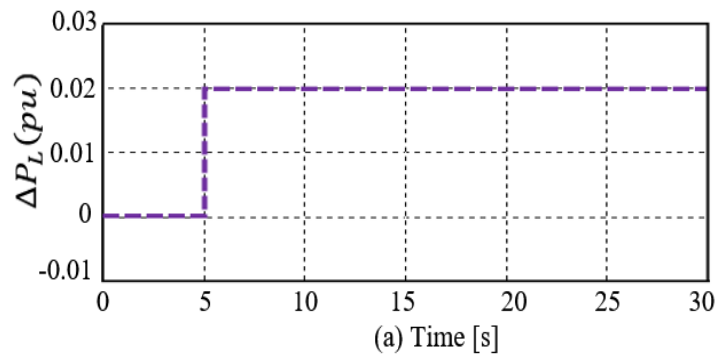
The performance indices utilized in this study are defined as follows [258], [263]:

$$ITSE = \int_0^{T_{max}} ((\Delta F_1)^2 + (\Delta F_2)^2 + (\Delta P_{tie})^2) dt \quad (8-1)$$

$$ISE = \int_0^{T_{max}} ((\Delta F_1)^2 + (\Delta F_2)^2 + (\Delta P_{tie})^2) dt \quad (8-2)$$

$$ITAE = \int_0^{T_{max}} t(|\Delta F_1| + |\Delta F_2| + |\Delta P_{tie}|) dt \quad (8-3)$$

$$IAE = \int_0^{T_{max}} (|\Delta F_1| + |\Delta F_2| + |\Delta P_{tie}|) dt \quad (8-4)$$



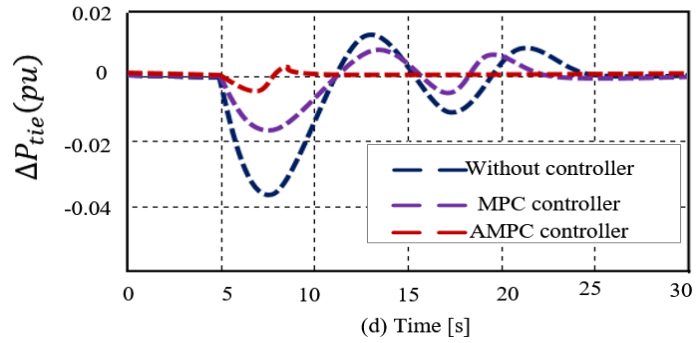
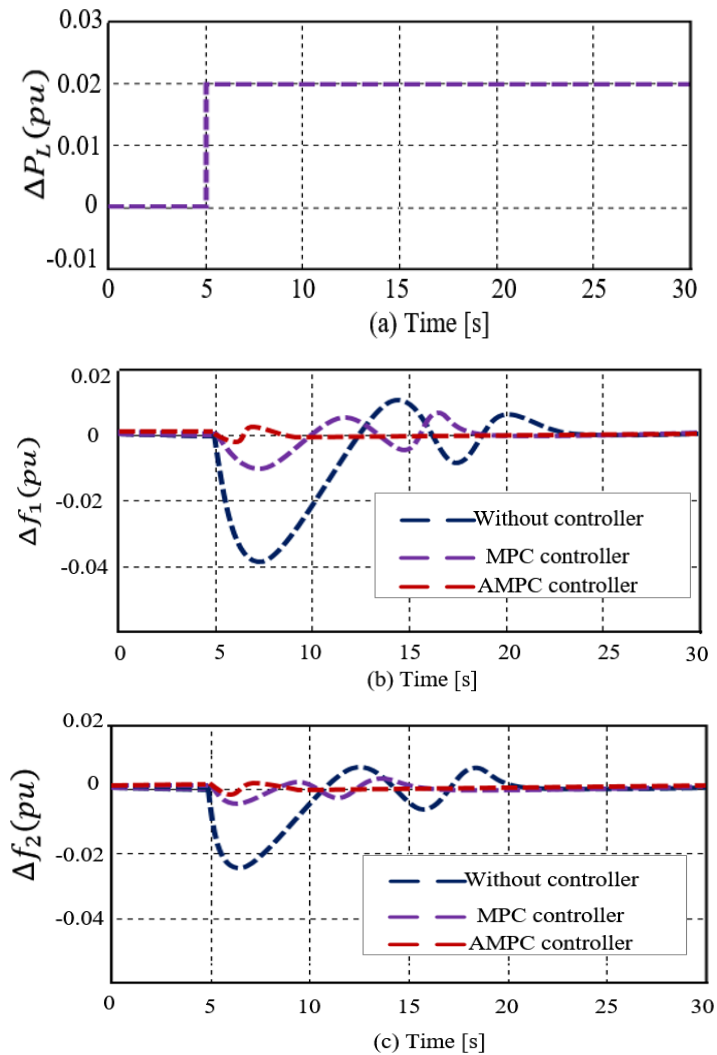


Figure 8-4: Dynamic response of the system for 2% step increase in load with AC tie-line: (a) Load disturbance (b) Area 1 frequency deviation (c) Area 2 frequency deviation (d) Tie-line power deviation

Figure 8-5 shows the dynamic response of the power system for 2% step increase in load with AC-DC tie-line. It is evident from Figure 8-5 that the dynamic responses of the system control parameters are better with the AC-DC tie compared to the results obtained with the AC tie-line, as shown in Figure 8-4.



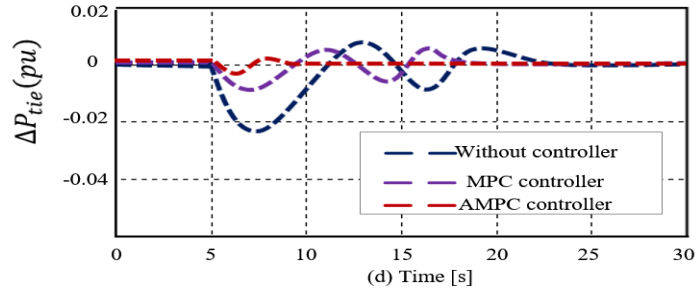
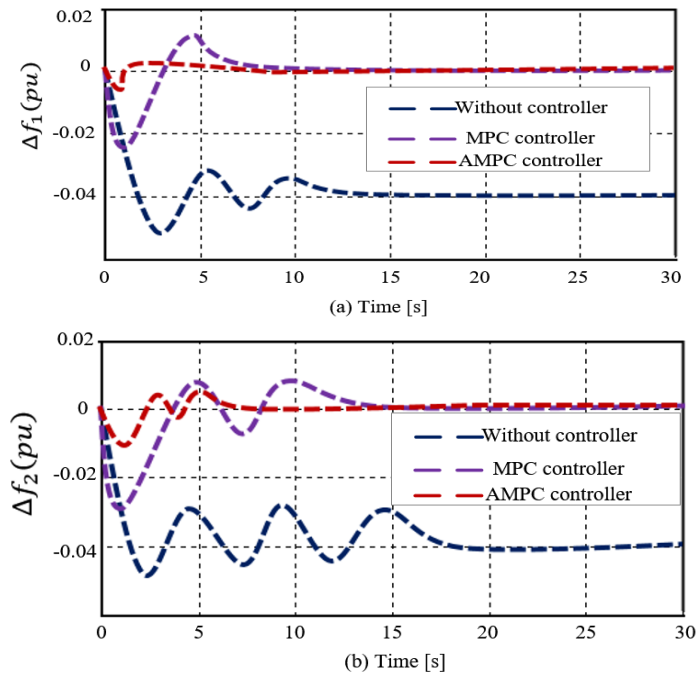


Figure 8-5: Dynamic response of the system for 2% step increase in load with AC-DC tie-line: (a) Load disturbance (b) Area 1 frequency deviation (c) Area 2 frequency deviation (d) Tie-line power deviation

8.3.2 Case 2: System dynamic response with dispatchable DERs

In this case, the frequency regulation in the power system is studied when there are just dispatchable units such as fuel cell, diesel units, and battery storage in the system. The load change of 0.02 p.u ($\Delta P_{L1} = \Delta P_{L2} = 0.2$) is utilized. Therefore, a negative frequency and tie-line power deviation responses are obtained for the load change, as there are only two dispatchable generation units in the system. The simulation period and sampling time are taken as 30 seconds and 0.02s, respectively. Due to the absence of renewable sources, there are few oscillations in the system response of area 1. Similarly, due to the non-linear features in area 2, more oscillations are seen in the dynamic response without a controller, and fewer oscillations with the conventional MPC control technique. The proposed AMPC control technique performs better than the conventional MPC based on the dynamic performance in case 2. The dynamic response of the tie-line is further improved due to the presence of UPFC, which is placed in series with the tie-line, as shown in Figure 8-6.



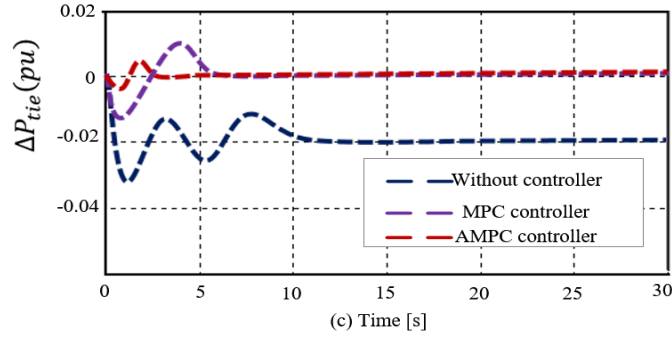
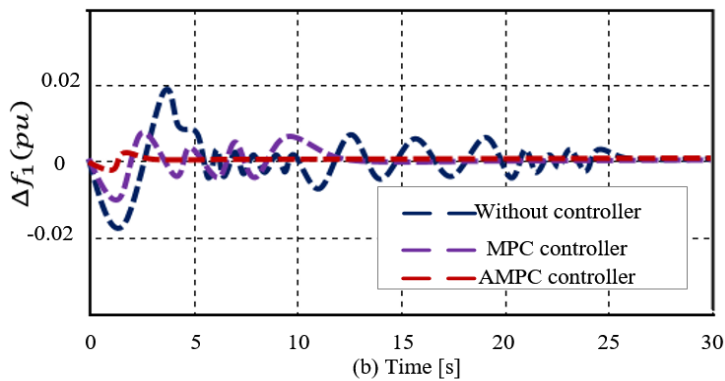
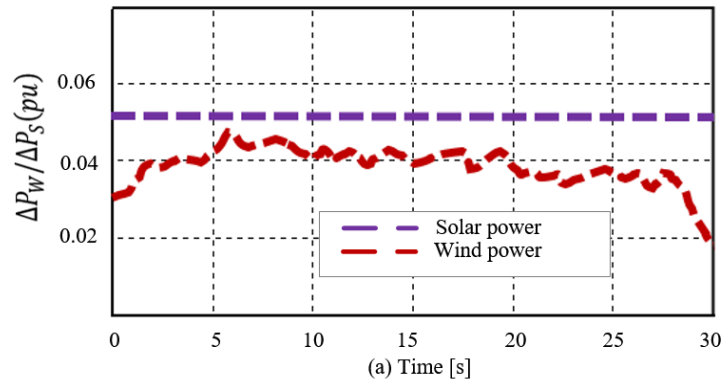


Figure 8-6: Dynamic response of the system with only dispatchable DERs (a) Area 1 frequency deviation (b) Area 2 frequency deviation (c) Tie-line power deviation

8.3.3 Case 3: System dynamic response with wind speed fluctuation of 2m/s

This case introduces the wind gust component of magnitude 3m/s for 5 seconds in the wind velocity, and the wind mean-velocity is taken as 7m/s. The load change of 0.02p.u is used, and the change in solar power is maintained constant at 0.05p.u. The wind power increases from 0 p.u to the average power of 0.02p.u. It is evident in the frequency response of the micro-grid system under the conditions of load change and wind perturbation of 2 m/s, which is shown in Figure 8-7. The performance of the proposed control technique is better and faster than the MPC control technique. The type of WTG model used in this section is the fixed-speed WTG-based on an induction generator.



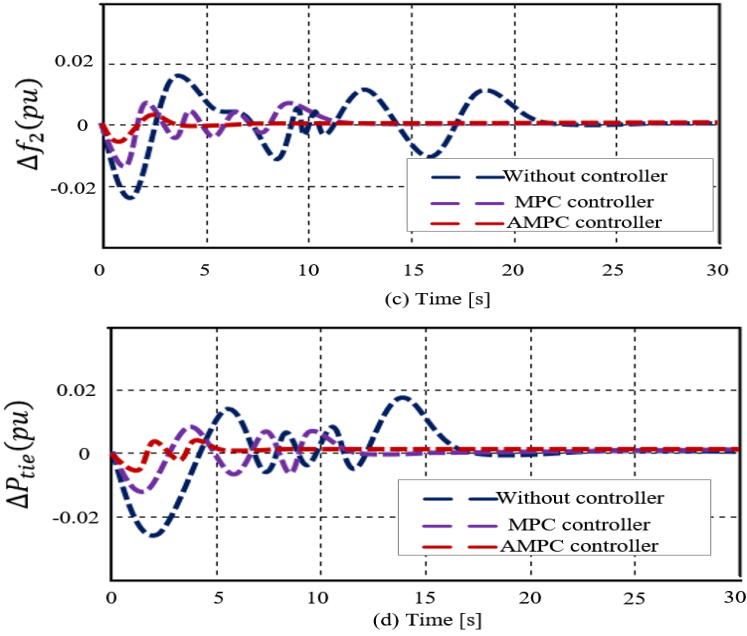
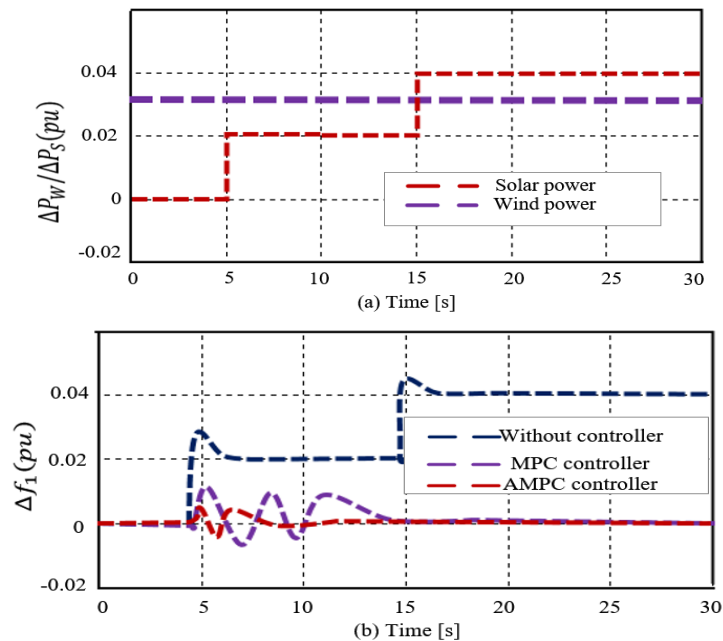


Figure 8-7: Dynamic response of the system with wind perturbation of 2 m/s (a) Wind perturbation (b) Area 1 frequency deviation (c) Area 2 frequency deviation (d) Tie-line power deviation

8.3.4 Case 4: System dynamic response with series step changes in solar power

In this case, a series step increase in solar power is considered. Meanwhile, the change in ΔP_W wind power is taken as 0.05 p.u throughout the simulation, and the load change of 0.02 p.u ($\Delta P_{L1} = \Delta P_{L2} = 0.2$) is used. It is evident in the frequency response of the micro-grid system under the conditions of load change and solar perturbation, which is shown in Figure 8-8. The performance of the proposed control technique is better and faster than the MPC control technique.



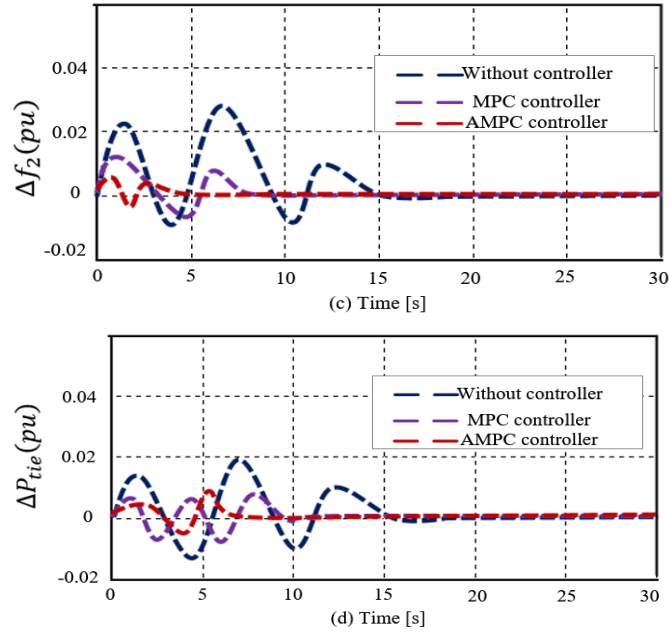
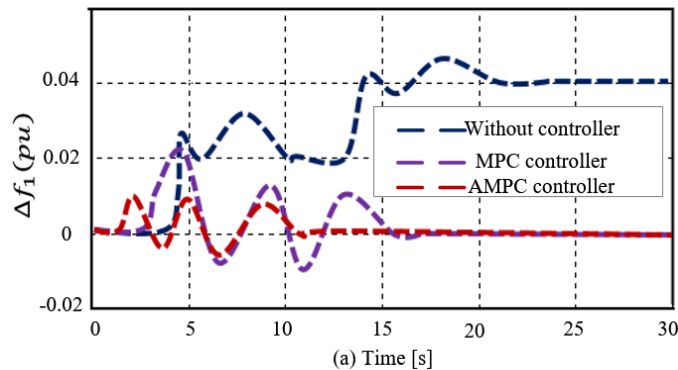


Figure 8-8: Dynamic response of the system with series of step changes in solar power (a) solar perturbation (b) Area 1 frequency deviation (c) Area 2 frequency deviation (d) Tie-line power deviation

8.3.5 Case 5: System dynamic response with all the disturbances in the system (ΔP_L , ΔP_W , and ΔP_S)

In this case, the dynamic response of the system is investigated, considering all the possible disturbances in the system. The disturbance studied in case-3, case-4, and case-5 are applied simultaneously. The performance comparison of the proposed AMPC control technique to the MPC control technique based on the performance indices ($ITSE$, $ITAE$, IAE , ISE , V_{p1} , V_{p2} , V_{p3} , t_{r1} , t_{r2} , and t_{r3}) are assessed and have been tabulated in Table 8-7. It is evident in the dynamic response of Fig. 8-9 and the performance indices in Table 8-7 that the proposed control technique performs better and more efficiently for load frequency control. Therefore, due to all the disturbances in the systems, more oscillations are seen in the dynamic response of area 1. However, the proposed AMPC control technique performs better than the conventional MPC based on the dynamic performance in case 1. The dynamic response of the tie-line is further improved due to the presence of UPFC, which is placed in series with the tie-line.



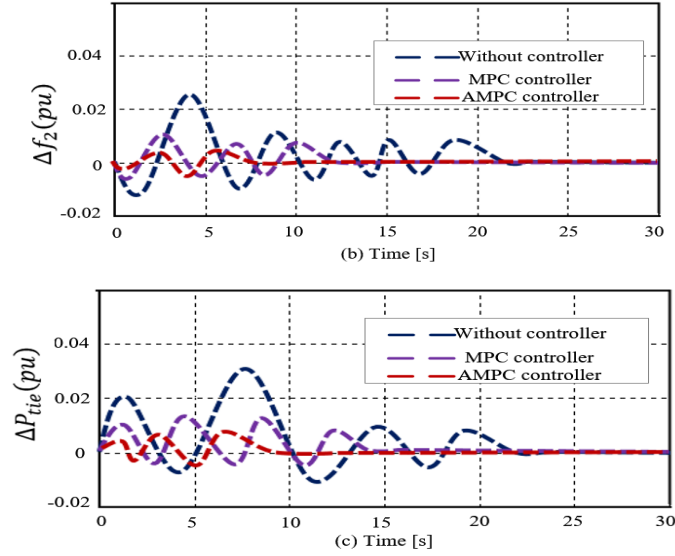


Figure 8-9: Dynamic response of the system with all the disturbances (a) Area 1 frequency deviation (b) Area 2 frequency deviation (c) Tie-line power deviation.

Table 8-2: Comparison of the system performance of the control techniques using the performance indices in CASE 1-A

Algorithms	AMPC	MPC	Without Controller	Algorithms	AMPC	MPC	Without Controller
Performance-indices				Performance-indices			
ITAE	7.35	19.28	134.39	V_{p2}	0.002	0.007	0.012
ITSE	0.44	0.96	9.87	t_{r2}	6.0	10.0	13.0
IAE	9.58	14.13	39.52	t_{s2}	6.0	17.0	23.0
ISE	0.32	0.98	8.65	$E_{ss2}(10^{-5})$	0.068	1.96	3.84
V_{p1}	0.005	0.008	0.018	V_{p3}	0.003	0.008	0.015
t_{r1}	7.0	12.0	15.0	t_{r3}	8.0	12.0	13.0
t_{s1}	8.0	18.0	25.0	t_{s3}	7.0	18.0	24.0
$E_{ss1}(10^{-5})$	0.41	1.80	3.68	$E_{ss3}(10^{-5})$	0.0052	0.083	0.091

Table 8-3: Comparison of the system performance of the control techniques using the performance indices in CASE 1-B

Algorithms	AMPC	MPC	Without Controller	Algorithms	AMPC	MPC	Without Controller
Performance-indices				Performance-indices			
ITAE	8.25	20.36	141.35	V_{p2}	0.001	0.003	0.008
ITSE	0.57	0.89	8.97	t_{r2}	6.0	9.0	13.0
IAE	10.51	16.83	42.52	t_{s2}	7.0	15.0	20.0
ISE	0.46	0.88	10.65	$E_{ss2}(10^{-5})$	0.048	1.86	3.75
V_{p1}	0.002	0.006	0.014	V_{p3}	0.003	0.009	0.01
t_{r1}	7.0	12.0	14.0	t_{r3}	8.0	13.0	14.0
t_{s1}	8.0	16.0	23.0	t_{s3}	9.0	18.0	27.0
$E_{ss1}(10^{-5})$	0.43	1.85	3.58	$E_{ss3}(10^{-5})$	0.0063	0.090	0.098

Table 8-4: Comparison of the system performance of the control techniques using the performance indices in CASE 2

Algorithms	AMPC	MPC	Without Controller	Algorithms	AMPC	MPC	Without Controller
Performance-indices				Performance-indices			
ITAE	6.27	18.75	214.18	V_{p2}	0.003	0.006	-0.035
ITSE	0.48	0.83	16.52	t_{r2}	4.0	5.0	4.0
IAE	8.54	12.15	48.95	t_{s2}	6.0	14.0	19.0
ISE	0.35	0.74	10.37	$E_{ss2}(10^{-5})$	0.065	1.92	3.86
V_{p1}	0.002	0.007	-0.03	V_{p3}	0.004	0.016	-0.017
t_{r1}	3.0	4.0	6.0	t_{r3}	3.0	4.0	4.0
t_{s1}	4.0	8.0	13.0	t_{s3}	3.0	7.0	12.0
$E_{ss1}(10^{-5})$	0.37	1.77	3.62	$E_{ss3}(10^{-5})$	0.0054	0.085	0.093

Table 8-5: Comparison of the system performance of the control techniques using the performance indices in CASE 3

Algorithms	AMPC	MPC	Without Controller	Algorithms	AMPC	MPC	Without Controller
Performance-indices				Performance-indices			
ITAE	6.32	18.26	245.42	V_{p2}	0.002	0.007	0.018
ITSE	0.36	0.83	16.75	t_{r2}	3.0	3.0	4.0
IAE	8.54	13.17	46.92	t_{s2}	4.0	12.0	23.0
ISE	0.27	0.85	11.58	$E_{ss2}(10^{-5})$	0.060	1.91	3.80
V_{p1}	0.001	0.005	0.02	V_{p3}	0.002	0.006	0.017
t_{r1}	2.0	3.0	4.0	t_{r3}	3.0	4.0	7.0
t_{s1}	3.0	13.0	26.0	t_{s3}	5.0	12.0	18.0
$E_{ss1}(10^{-5})$	0.40	1.66	3.85	$E_{ss3}(10^{-5})$	0.0042	0.075	0.081

Table 8-6: Comparison of the system performance of the control techniques using the performance indices in CASE 4

Algorithms	AMPC	MPC	Without Controller	Algorithms	AMPC	MPC	Without Controller
Performance-indices				Performance-indices			
ITAE	9.46	45.67	261.30	V_{p2}	0.002	0.013	0.022
ITSE	0.88	1.69	19.61	t_{r2}	2.0	3.0	3.0
IAE	13.54	18.43	57.38	t_{s2}	5.0	8.0	15.0
ISE	0.66	1.78	14.83	$E_{ss2}(10^{-5})$	0.055	1.79	3.70
V_{p1}	0.002	0.015	0.042	V_{p3}	0.004	0.006	0.017
t_{r1}	5.0	7.0	5.0	t_{r3}	3.0	3.0	4.0
t_{s1}	10.0	15.0	17.0	t_{s3}	6.0	10.0	16.0
$E_{ss1}(10^{-5})$	0.37	1.69	3.60	$E_{ss3}(10^{-5})$	0.0049	0.078	0.084

Table 8-7: Comparison of the system performance of the control techniques using the performance indices in CASE 5

Algorithms	AMPC	MPC	Without Controller	Algorithms	AMPC	MPC	Without Controller
Performance-indices				Performance-indices			
ITAE	7.25	18.97	217.16	V_{p2}	0.002	0.015	0.024
ITSE	0.52	0.88	16.92	t_{r2}	2.0	3.0	4.0
IAE	8.74	12.85	49.83	t_{s2}	7.0	13.0	23.0
ISE	0.39	0.77	7.87	$E_{ss2}(10^{-5})$	0.069	1.99	3.80
V_{p1}	0.004	0.022	0.045	V_{p3}	0.003	0.016	0.02
t_{r1}	3.0	5.0	5.0	t_{r3}	1.0	2.0	3.0
t_{s1}	10.0	17.0	22.0	t_{s3}	8.0	14.0	22.0
$E_{ss1}(10^{-5})$	0.42	1.85	3.66	$E_{ss3}(10^{-5})$	0.0054	0.085	0.095

Table 8-8: Comparison of the system performance of the control techniques using the performance indices in CASE 6

Algorithms	AMPC	MPC	Without Controller	Algorithms	AMPC	MPC	Without Controller
Performance-indices				Performance-indices			
ITAE	7.05	17.57	220.15	V_{p2}	0.014	0.02	0.041
ITSE	0.68	0.90	18.62	t_{r2}	2.0	3.0	4.0
IAE	9.62	14.74	53.45	t_{s2}	6.0	13.0	22.0
ISE	0.47	0.92	9.50	$E_{ss2}(10^{-5})$	0.078	1.98	3.89
V_{p1}	0.015	0.024	0.044	V_{p3}	0.012	0.018	0.028
t_{r1}	2.0	3.0	4.0	t_{r3}	2.0	3.0	3.0
t_{s1}	7.0	14.0	23.0	t_{s3}	7.0	12.0	21.0
$E_{ss1}(10^{-5})$	0.46	1.87	3.79	$E_{ss3}(10^{-5})$	0.0055	0.089	0.097

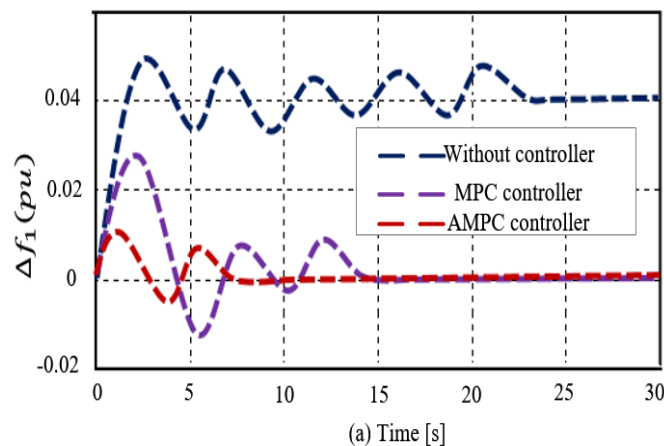
In this study, the objective function is defined based on the desired specifications and constraints. Generally, the designed objective function utilized to tune the controller is based on the performance index that considers the entire closed-loop response. Specific outputs in the specifications in the time domain are settling time, peak overshooting, rise time, and steady-state error. Therefore, the four types of performance indices often considered in the control design are the integral of squared error (ISE), integral of time multiplied absolute error (ITAE), integral of absolute error (IAE) and integral of time multiplied squared error (ITSE). Hence, it is evident from Tables 8-2 to 8-8, that in terms of the dynamic response performance and the performance indices used as the objective function in this study, the proposed AMPC control technique performs better than the MPC control technique. The dynamic response and the values of the performance criteria obtained are further improved due to the UPFC connected in series with the tie-line. The system performances could not have been these better should the UPFC is not included in the stand-alone micro-grid system. Hence, to justify the superiority of the proposed controller scheme (AMPC) to the

other controller (MPC), the standard objective functions such as IAE, ITAE, ISE, and ITSE (steady-state errors of both the area frequency and the tie-line power interchange between neighboring control areas) are utilized. Therefore, it is evident from Tables 8-2 to 8-8 that the estimated steady-state errors using ITSE and ISE are very close to zero, which is the ultimate goal of utilizing the various control techniques in this chapter.

8.3.6 Case 6: Robustness Analysis for Parametric Uncertainties

The AMPC operation is based on the prediction of the model utilized to estimate the future state variables. The mismatch between the designed model parameters and the actual model parameters often affects the control performance of the controllers. The effect of variation in the loading conditions and system parameters on the system dynamic performances of the AGC problem received less attention in the literature. Therefore, in order to demonstrate the robustness of the proposed control techniques against parameter uncertainties, this case introduces the parametric variation in the system model and studies the system response by the proposed AMPC control technique to the MPC control technique. The variation of multiple system parameters that have a significant influence on the control performance is investigated. The parametric variations/uncertainties are incorporated as follows: Inertia time constant, $H = +50\%$; Regulation constant, $R = +30\%$; Turbine time constant, $T_t = 50\%$; Governor time constant, $T_g = +50\%$; Load damping, $D = -40\%$; battery time constant, $T_b = -45\%$ and frequency bias factor, $B = +30\%$. The wind velocity is kept at 6.5m/s, the change in solar power is maintained at 0.05 p.u, and the load is 0.02 p.u.

It is evident in Figure 8-10 that AMPC performs the best in terms of the dynamic response and the performance indices stipulated in Table 8-8 under all of the conditions. More so, the dynamic responses of the AMPC control technique have fewer fluctuations, faster response, and better steady-state performance than the MPC control technique during parametric uncertainties. This validated the efficiency and robustness of the proposed AMPC algorithm against a wide range of parameter uncertainty.



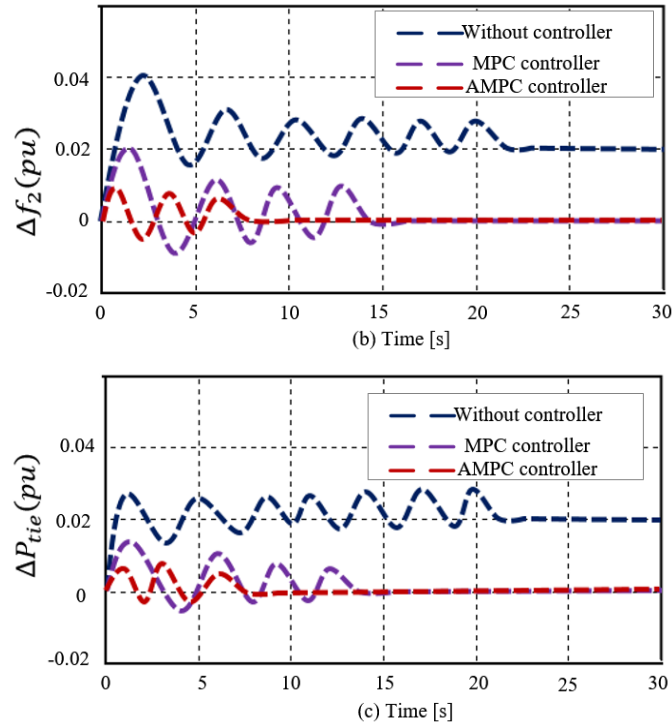


Figure 8-10: Dynamic response of the system with parametric variations (a) Area 1 frequency deviation (b) Area 2 frequency deviation (c) Tie-line power deviation

Table 8-9: Comparison of simulation results for different control techniques over 30 independent runs without physical constraints and UPFC

Algorithms	Maximum	Minimum	Standard deviation	Average
Adaptive MPC	0.7564	0.4582	0.2061	0.6517
MPC	0.8251	0.5563	0.3294	0.7063
Without controller	1.5564	0.9968	0.7842	1.2567

Table 8-10: Comparison of simulation results for different control techniques over 30 independent runs with physical constraints and UPFC

Algorithms	Maximum	Minimum	Standard deviation	Average
Adaptive MPC	0.7315	0.4132	0.2023	0.6311
MPC	0.8020	0.5333	0.3225	0.7001
Without controller	1.5254	0.9622	0.7540	1.2267

Tables 8-9 and 8-10 show the comparison of the simulation results for different control techniques over 30 independent runs with and without physical constraint and UPFC in the micro-grid system. The maximum, minimum, standard deviation, and the average of the objective function values are stipulated in Tables 8-9 and 8-10. Therefore, from the statistical analysis on Tables 8-9 and 8-10, it is seen that the minimum objective function values obtained with the proposed Adaptive MPC algorithm ($ITAE = 7.552, ITSE = 0.49, IAE = 8.462, ISE = 0.521$) compared to MPC control technique ($ITAE = 15.512, ITSE =$

1.69, $IAE = 12.872$, $ISE = 1.656$), and without controller ($ITAE = 137.512$, $ITSE = 16.26$, $IAE = 48.312$, $ISE = 12.753$). Therefore, going by the statistical analysis shown in Tables 8-9 and 8-10 and the performance indices evaluation, the proposed adaptive MPC outperformed the other considered control techniques.

Table 8-11: The system eigenvalues and minimum damping ratios with and without the proposed controller (AMPC) and UPFC

With Controller	With Controller without UPFC	With Controller in the presence of UPFC
-9.3251	-21.4051	-95.6351
-8.4327	-20.4751	-20.4821
-7.6320	-17.2108	-20.3581
-7.7211	-6.6217	-16.6521
-2.4351	-6.5808	-16.8157
-2.3842	-4.7185	-5.7581
-1.7358	-3.6172	-5.3885
-1.6654	-3.7251	-4.0531 ± 1.6706i
-1.2352	-2.6360	-3.5378
-1.0197	-2.3458	-3.5013
-0.2521 ± 0.8531i	-0.3351 ± 1.8457i	-2.8251
0.1427 ± 1.4530i	-0.8651 ± 0.7541i	-0.8241 ± 0.6845i
0.1672 ± 1.2538i	-0.8541	-0.9857
-0.4215	-0.3231	-0.5107
-0.2016	-0.0857	-0.2485
-0.05147	-0.0535	-0.0855
-0.04059	-0.0326	-0.0518
-0.03162	-6.0075	-0.0457
-6.6207	-6.3515	-5.6505
-6.2701	-	-6.5002
MDR = 0.0735	MDR = 0.0986	MDR = 0.1425

Table 8-11 shows the system eigenvalues and minimum damping ratio with physical constraints for all the cases. It can be seen that the system without controller (Adaptive MPC) is unstable, the reason being that not all the real parts of the eigenvalues are negative, and hence, some poles lie in the right half of the s-plane, making the system unstable. More so, the system becomes stable with the proposed controller (Adaptive MPC) as all the real parts of the eigenvalues are negative, and thus, all the poles lie in the left half of the s-plane, hence, making the system stable, this is evident from Table 8-11. Furthermore, in the presence of UPFC with the proposed controller, the system becomes more stable as the negative real parts of the eigenvalues are shifted toward the left half of the s-plane. Similarly, Table 8-11 depicts the minimum

damping ratios (MDR) for all cases. Therefore, it is worth mentioning that the MDR ought to be high, should we require reducing the system oscillations. The optimum value of MDR is obtained with the proposed controller compared to the case without the controller. More so, the value of the MDR is further improved in the presence of UPFC; hence, we can conclude that the proposed method reduces the oscillating state. The system becomes unstable without a controller when the physical constraints such as dead band (DB), time delay (TD), reheat turbine, and generation rate constraints (GRC) are considered. Therefore, for proper capabilities of the proposed controller, the TD value is selected such that the system becomes unstable without the controller for a better illustration. Nonetheless, the primary controller alone may be enough in the realistic system to stabilize the system with some steady-state error.

8.3.7 Impacts of the WTG Based on DFIG on the Performance of the Proposed Control Algorithms

Due to the economic gains, the use of variable speed WTG based on a doubly fed induction generator (DFIG) has gained more popularity recently. This section further investigated the impacts of Wind Turbine Generator based on DFIG on the performance of the proposed control algorithms. The block representation of the WTG that includes the generator and the windmill is depicted in Figure 8-11. The equations that describe the characteristics of the generator and the windmill admit expressions as follows [264]:

$$P_{\omega o} = 0.5C_p(\lambda, \beta)v_{\omega}^3\rho A_{\omega} \quad (8-5)$$

$$C_p(\lambda, \beta) = c_1(\beta)\lambda^2 + c_2(\beta)\lambda^3 + c_3(\beta)\lambda^4 \quad (8-6)$$

$$c_1(\beta) = c_{10} + c_{11}\beta + c_{12}\beta^2 + c_{13}\beta^3 + c_{14}\beta^4 \quad (8-7)$$

$$c_2(\beta) = c_{20} + c_{21}\beta + c_{22}\beta^2 + c_{23}\beta^3 + c_{24}\beta^4 \quad (8-8)$$

$$c_3(\beta) = c_{30} + c_{31}\beta + c_{32}\beta^2 + c_{33}\beta^3 + c_{34}\beta^4 \quad (8-9)$$

$$\lambda = \frac{R_{\omega}\omega}{v_{\omega}} \quad (8-10)$$

$$\omega = \int \frac{2}{J}(P_{\omega o} - P_{\omega})dt \quad (8-11)$$

$$s = \frac{\omega_o - \omega}{\omega_o} \quad (8-12)$$

$$P_{\omega} = \frac{-3V^2s(1+s)R_2}{(R_2 - sR_1)^2 + s^2(X_1 + X_2)^2} \quad (8-13)$$

Where, $c_{10} - c_{34}$ represent the windmill characteristics-constants. More explanations on the wind turbine generator can be found in ref [265].

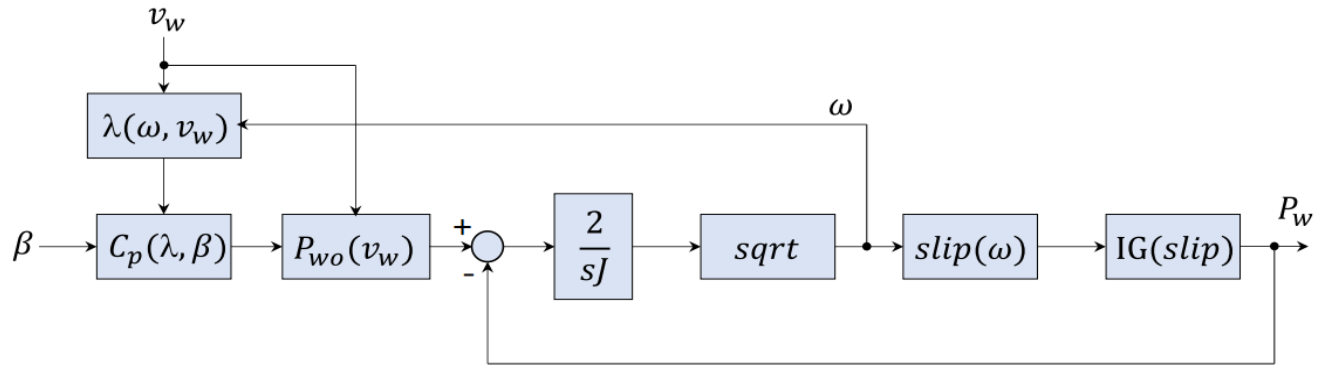


Figure 8-11: Block representation of the generator and windmill characteristics

The power output of the WTG can be regulated slightly by the change of the pitch angle, β . The change of the blade pitch angle for frequency control in a micro-grid has been considered in several studies. The study is focused primarily on the AMPC-based ESS controller; hence, it is assumed that the pitch angle β is equal to zero. The configuration parameters of the wind turbine generator are shown in Table 8-12.

Table 8-12: The configuration parameters of the wind turbine generator [265]

Windmill Parameters	Value	Generator	Value	Generator	Value
R_ω	14 m	Rated power WTG	160 kW	R_2	0.00443 Ω
J	62,993 kgm^2	V	380 V	X_1	0.0376 Ω
ρ	1.225 kg/m^3	R_1	0.00397 Ω	X_2	0.0534 Ω

It is worth mentioning that the controller design process, in this case, is similar to the previous design procedures. The ESS power output has a limited value of $\pm 0.5725 pu$. Therefore, to obtain the controller output, $u(k/k)$, the cost function is minimized, and it is subject to $-0.5725 \leq u(k) \leq 0.5725$. The frequency response of the stand-alone micro-grid with WTG based-DFIG is depicted in Figure 8-11. The deviation in the frequency response of the micro-grid with a variable-speed WTG is marginally reduced compared to the frequency deviation obtained in Figure 8-7. The reason for this drastic reduction in the frequency deviation of WTG based on DFIG is that the WTG can smoothen its power output. Hence, due to the WTG complex model, the control performance of the AMPC is slightly affected. Nonetheless, based on the results shown in Figure 8-12, the AMPC-based frequency control outperformed the MPC-based frequency control based on the dynamic response performance and the performance indices. It is worth mentioning that the computation time of the AMPC is considered in order to implement AMPC in a realistic micro-grid system due to the advancement in the complexity of an overall micro-grid system.

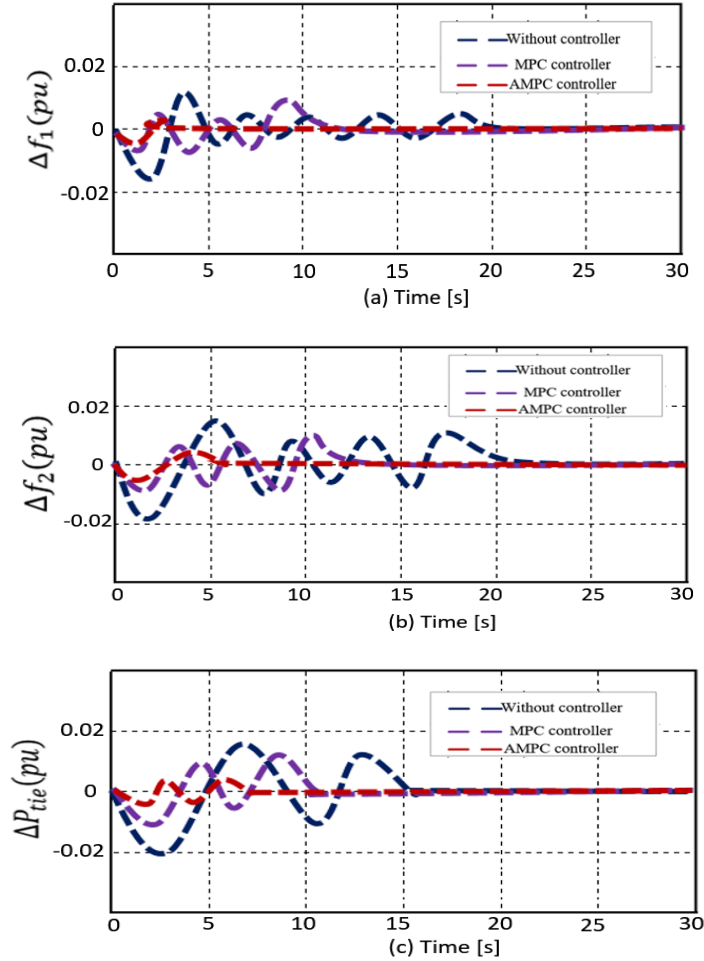


Figure 8-12: Dynamic response of the system with wind perturbation of 2 m/s (a) Area 1 frequency deviation (b) Area 2 frequency deviation (c) Tie-line power deviation

8.4 Chapter Summary

In this chapter, an adaptive model predictive control (AMPC) technique is proposed for load frequency control of a multi-area interconnected power system with renewable energy sources with the UPFC along both the AC tie line and AC-DC tie line for optimal system performance. The main goal of this study is to solve the problems of frequency deviation against variations in system parameters and load disturbance. The essence of using an AMPC control algorithm is to vary the plant model in the on-line MPC structure to overcome the uncertainty due to the variation of the governor and turbine parameters. The effects of parametric uncertainties on the performance of the control techniques have been investigated in this study. It is evident in the results obtained that the robustness of the AMPC control technique against the system uncertainties is stronger than that of conventional MPC control technique. The response time of AMPC-based micro-grid frequency regulation is faster than that of the MPC-based frequency control. Furthermore, due to the high penetration of renewable generations (wind power generation and Solar power generation),

the AMPC-based frequency control maintains the micro-grid frequency in the allowable frequency deviation range. From the six cases studied, it is observed that the proposed AMPC controller outperformed the conventional MPC in terms of the dynamic response performance and the performance indices. The proposed controller further demonstrated its superiority in the presence of physical constraints such as dead band (DB), time delay (TD), and generation rate constraint (GRC). The impact of the UPFC in series with the tie-line on the system dynamic performance was studied. Consequently, a significant improvement was observed in the dynamic response performance as well as in the performance indices. Furthermore, this chapter investigated further the impact of the WTG model on the dynamic performance of the proposed control algorithms in a stand-alone micro-grid using both fixed-speed and variable-speed WTGs. Thus, due to the WTG complex model of the variable-speed WTG, the control performance of the AMPC is slightly affected. Nonetheless, the AMPC-based frequency control outperformed the conventional MPC control algorithm based on dynamic response performance.

CHAPTER NINE

CONCLUSIONS AND FUTURE STUDIES

9.1 Closing Remarks

Micro-grids, and the integration of DER units in general, pose a range of operational problems that must be tackled in the design and implementation of the control systems to ensure that the present levels of reliability are not significantly affected and the potential benefits of the distributed generations are fully harnessed. This work proposes and presents new control algorithms for renewable energy microgrids with hybrid energy storage systems, which can operate in both grid-connected and islanded modes. Hence, this study aims to use adaptive model predictive control (AMPC) to provide solutions to the micro-grids control problems for effective and reliable operation of the renewable energy-based microgrids. The availability of more reliable and effective energy management techniques is one of the main reasons for developing effective integrated systems based on distributed generations. Firstly, an optimal control strategy that efficiently manages a stand-alone residential micro-grid comprising of renewable and non-renewable energy sources was investigated. An adaptive model predictive control algorithm is implemented for choosing an optimal mode and set of inputs for the system to track both a constant and load-varying power demand profile. The AMPC control algorithm was implemented to track the power transmitted to residential micro-grid. Excellent results were obtained for tracking both a constant and a time-varying load reference power profile. The cost function was minimized, which guaranteed minimum usage of non-renewable energy sources as it maximizes the consumption of power delivered by a renewable energy source. In the subsequent chapter, the EMS-based adaptive MPC algorithm was implemented for optimal micro-grids management based on various energy storage systems. The AMPC algorithm solves an energy optimization problem with multiple types of energy storage systems in a renewable energy microgrid, which exchanges electricity with the host grid. This optimization problem is solved at each sampling time to determine minimum running costs while satisfying the demand and considering technical and physical constraints. The controller's proposed behavior has been observed under different external conditions, such as changes in weather and demand. Different scenarios and configurations were used to demonstrate the AMPC's versatility and applicability. The demand response technique for the energy management system in micro-grid based on adaptive model predictive control was also investigated. The proposed method is a generalized scheme based on load curtailment, which has been mathematically formulated as an optimization problem. The minimization problem obtained by using the DR technique for the energy management system in a renewable energy-based micro-grid is solved using the AMPC algorithm. The AMPC algorithm is proposed to optimally utilize the maximum power from the renewables by using hybrid

storage systems. The simulation results have shown that implementing the DR technique for energy management in micro-grid reduces the peak load demand and, consequently, minimizes the system's operating costs. Therefore, to further investigate the significance and effectiveness of the proposed control algorithm, the AMPC control technique was used in the subsequent chapter to optimize the charge/discharge of the EVs in a receding horizon manner to reduce operational cost in a renewable energy-based micro-grid. It is evident from the results when a load shifting mechanism was used to solve the charge management problem during a known interval of parking time that the cost function, J , obtained when the EVs were incorporated was drastically minimized compared to when EVs were not integrated. Lastly, the proposed control technique (AMPC) was used for load frequency control of a two-area interconnected power system with renewable energy sources with the UPFC along both the AC tie line and AC-DC tie line for optimal system performance. The effects of parametric uncertainties on the performance of the control techniques were investigated in this study. Hence, it is evident from the results obtained that the robustness of the AMPC control technique against the system uncertainties is stronger than that of the conventional MPC control technique. The response time of AMPC-based micro-grid frequency regulation is faster than that of the MPC-based frequency control.

9.2 Recommendations for Future Studies

This thesis has investigated the application of adaptive model predictive control (AMPC) technique in a micro-grid with distributed energy resources (DERs), including distributed generators, energy storage and demand response to achieve higher penetration of renewable energy. However, there are further areas in this field of micro-grid control systems to cope with the intermittent, stochastic, and distributed nature of the generation and with the new consumption patterns that still need to be investigated. The following are some recommendations for further work:

- The proposed algorithm was mainly used as control system for microgrids integrated with PV systems, wind turbine, hydrogen storage systems and batteries. However, it can be applied to other system configurations based on the use of different renewable energy sources and different energy storage systems.
- One of the main goals in micro-grid operation is the optimization of the final energy price. It, therefore, makes it very important to have an accurate energy prediction algorithm from generation and consumption that requires a suitable energy price forecasting system. The complexity of the associated control problem of the integration of micro-grids into the electrical market requires advanced control algorithms such as Stochastic and Economic MPC. Thus, a performance comparison of these control methods also requires more investigation.

- Understanding how variations in parameters affect the output of the model is another critical area that needs attention as renewables uncertainties are major problems in microgrid operations. Sensitivity analysis of a renewable-based micro-grid with hybrid energy storage systems with different kinds of scenarios is essential to increase reliability and robustness, reduces costs, and improves the performance of the micro-grid.
- The energy management system (EMS) presented in this thesis could be extended to consider operational and degradation costs. It could further introduce a formulation to integrate the terms related to operational and degradation issues associated to hybrid storage systems in an MPC-based EMS.
- Other ESSs could be introduced in the AMPC algorithm such as flywheel, SMES, molten salts or graphene batteries to further improve the operation of the micro-grid.
- The single micro-grid EMS used in this thesis could be extended to the energy management problem of several interconnected micro-grids to determine the power flows inside each microgrid and with the main grid and also the energy interchange among them.
- The practical validation of the findings of this study may be considered by implementing a scaled-down laboratory research scheme. Prior to a full practical investigation, the hardware implementation of the micro-grid EMS can be initially considered in a hardware-in-loop test using the real time digital simulator (RTDS) to validate the results of this thesis. More so, the testing of AMPC using hardware in-loop simulation for the application of AMPC to a realistic micro-grid system could be considered.
- More specifically, another challenge which should be addressed in practice is the plant/model mismatch which requires additional solutions to maintaining the SoC of the energy storage system with the given limits.
- Finally, the load frequency control problem could be investigated using demand response and EV integration with micro-grid system.
- The obtained results in this thesis could be compared with existing state-of-the-art control methods available in the literature.
- Chapter 8 of this thesis could be further expanded by conducting a robustness analysis of the LFC system with more uncertainties in the model and, a detailed analysis can be carried out using a table.

REFERENCES

- [1] A. Parisio, E. Rikos, and L. Glielmo, "A model predictive control approach to microgrid operation optimization," *IEEE Transactions on Control Systems Technology*, vol. 22, pp. 1813-1827, 2014.
- [2] C. Wan, J. Lin, W. Guo, and Y. Song, "Maximum uncertainty boundary of volatile distributed generation in active distribution network," *IEEE Transactions on Smart Grid*, vol. 9, pp. 2930-2942, 2016.
- [3] S. Bahrami, M. H. Amini, M. Shafie-Khah, and J. P. Catalao, "A decentralized renewable generation management and demand response in power distribution networks," *IEEE Transactions on Sustainable Energy*, vol. 9, pp. 1783-1797, 2018.
- [4] C. Bordons, F. Garcia-Torres, and M. A. Ridao, *Model predictive control of microgrids* vol. 358: Springer, 2020.
- [5] C. Bordons, G. Teno, J. J. Marquez, and M. A. Ridao, "Effect of the Integration of Disturbances Prediction in Energy Management Systems for Microgrids," in *2019 International Conference on Smart Energy Systems and Technologies (SEST)*, 2019, pp. 1-6.
- [6] M. S. Taha and A.-R. M. Yasser, "Robust MPC-based energy management system of a hybrid energy source for remote communities," in *2016 IEEE Electrical Power and Energy Conference (EPEC)*, 2016, pp. 1-6.
- [7] S. Zhou, Y. Zhao, W. Gu, Z. Wu, Y. Li, Z. Qian, *et al.*, "Robust energy management in active distribution systems considering temporal and spatial correlation," *IEEE Access*, vol. 7, pp. 153635-153649, 2019.
- [8] N. Hatziargyriou, "Microgrids Control Issues," Wiley-IEEE Press, 2014, pp. 25-80.
- [9] E. Radziemska, "The effect of temperature on the power drop in crystalline silicon solar cells," *Renewable energy*, vol. 28, pp. 1-12, 2003.
- [10] P.A. Gbadega and A. K. Saha, "Effects and performance indicators evaluation of PV array topologies on PV systems operation under partial shading conditions," in *2019 Southern African Universities Power Engineering Conference/Robotics and Mechatronics/Pattern Recognition Association of South Africa (SAUPEC/RobMech/PRASA)*, 2019, pp. 322-327.
- [11] P. A. Gbadega, "Power losses in HVDC converter stations," M.sc thesis, UKZN, 2018, pp. 1-156.
- [12] P. A. Gbadega and A. K. Saha, "Loss Assessment of Key Equipment on Lcc-Based HVDC Converter Stations," in *2018 IEEE PES/IAS PowerAfrica*, 2018, pp. 44-52.
- [13] P. A. Gbadega and A. K. Saha, "Model predictive controller design of a wavelength-based thermo-electrical model of a photovoltaic (PV) module for optimal output power," in *International Journal of Engineering Research in Africa*, 2020, pp. 133-148.

- [14] P. A. Gbadega and A. K. Saha, "Electrical characteristics improvement of photovoltaic modules using two-diode model and its application under mismatch conditions," in *2019 Southern African Universities Power Engineering Conference/Robotics and Mechatronics/Pattern Recognition Association of South Africa (SAUPEC/RobMech/PRASA)*, 2019, pp. 328-333.
- [15] A. Baziar and A. Kavousi-Fard, "Considering uncertainty in the optimal energy management of renewable micro-grids including storage devices," *Renewable Energy*, vol. 59, pp. 158-166, 2013.
- [16] M. Mohiti, H. Monsef, A. Anvari-Moghaddam, and H. Lesani, "Two-stage robust optimization for resilient operation of microgrids considering hierarchical frequency control structure," *IEEE Transactions on Industrial Electronics*, vol. 67, pp. 9439-9449, 2019.
- [17] P. A. Gbadega and A. K. Saha, "Impact of Incorporating Disturbance Prediction on the Performance of Energy Management Systems in Micro-Grid," *IEEE Access*, vol. 8, pp. 162855-162879, 2020.
- [18] F. Garcia-Torres and C. Bordons, "Optimal economical schedule of hydrogen-based microgrids with hybrid storage using model predictive control," *IEEE Transactions on Industrial Electronics*, vol. 62, pp. 5195-5207, 2015.
- [19] P. Thounthong, V. Chunkag, P. Sethakul, S. Sikkabut, S. Pierfederici, and B. Davat, "Energy management of fuel cell/solar cell/supercapacitor hybrid power source," *Journal of power sources*, vol. 196, pp. 313-324, 2011.
- [20] T. Logenthiran, D. Srinivasan, and T. Z. Shun, "Demand side management in smart grid using heuristic optimization," *IEEE transactions on smart grid*, vol. 3, pp. 1244-1252, 2012.
- [21] H. K. Nunna and S. Doolla, "Energy management in microgrids using demand response and distributed storage—A multiagent approach," *IEEE Transactions on Power Delivery*, vol. 28, pp. 939-947, 2013.
- [22] D. Li, W.-Y. Chiu, and H. Sun, "Demand side management in microgrid control systems," in *Microgrid*, ed: Elsevier, 2017, pp. 203-230.
- [23] M. Gautschi, O. Scheuss, and C. Schluchter, "Simulation of an agent based vehicle-to-grid (v2g) implementation," *Electric Power Systems Research*, vol. 120, pp. 177-183, 2009.
- [24] P. C. Pradhan, R. K. Sahu, and S. Panda, "Firefly algorithm optimized fuzzy PID controller for AGC of multi-area multi-source power systems with UPFC and SMES," *Engineering Science and Technology, an International Journal*, vol. 19, pp. 338-354, 2016.
- [25] S. K. Pandey, S. R. Mohanty, and N. Kishor, "A literature survey on load–frequency control for conventional and distribution generation power systems," *Renewable and Sustainable Energy Reviews*, vol. 25, pp. 318-334, 2013.

- [26] P. A. Gbadega and A. K. Saha, "Load frequency control of a two-area power system with a stand-alone micro-grid based on adaptive model predictive control," *IEEE Journal of Emerging and Selected Topics in Power Electronics*, 2020.
- [27] D. E. Olivares, A. Mehrizi-Sani, A. H. Etemadi, C. A. Cañizares, R. Iravani, M. Kazerani, *et al.*, "Trends in microgrid control," *IEEE Transactions on smart grid*, vol. 5, pp. 1905-1919, 2014.
- [28] E. F. Camacho and C. Bordons, "Introduction to model predictive control," in *Model Predictive Control*, ed: Springer, 2007, pp. 1-11.
- [29] N. Bazmohammadi, A. Tahsiri, A. Anvari-Moghaddam, and J. M. Guerrero, "Stochastic predictive control of multi-microgrid systems," *IEEE Transactions on Industry Applications*, vol. 55, pp. 5311-5319, 2019.
- [30] A. Micallef, M. Apap, C. Spiteri-Staines, J. M. Guerrero, and J. C. Vasquez, "Reactive power sharing and voltage harmonic distortion compensation of droop controlled single phase islanded microgrids," *IEEE Transactions on Smart Grid*, vol. 5, pp. 1149-1158, 2014.
- [31] B. Zhu, H. Tazvinga, and X. Xia, "Switched model predictive control for energy dispatching of a photovoltaic-diesel-battery hybrid power system," *IEEE Transactions on Control Systems Technology*, vol. 23, pp. 1229-1236, 2014.
- [32] H. Shayeghi, E. Shahryari, M. Moradzadeh, and P. Siano, "A survey on microgrid energy management considering flexible energy sources," *Energies*, vol. 12, p. 2156, 2019.
- [33] A. C. Z. de Souza and M. Castilla, *Microgrids design and implementation*: Springer, 2019.
- [34] A. Elmouatamid, R. Ouladsine, M. Bakhouya, N. El Kamoun, M. Khaidar, and K. Zine-Dine, "Review of Control and Energy Management Approaches in Micro-Grid Systems," *Energies*, vol. 14, pp. 1-1, 2020.
- [35] P. A. Gbadega and A. K. Saha, "Loss assessment of MMC-based VSC-HVDC converters using IEC 62751-1-2 Std. and component datasheet parameters," in *2018 IEEE PES/IAS PowerAfrica*, 2018, pp. 1-9.
- [36] D. E. Olivares, C. A. Cañizares, and M. Kazerani, "A centralized optimal energy management system for microgrids," in *2011 IEEE Power and Energy Society General Meeting*, 2011, pp. 1-6.
- [37] F. Katiraei, R. Iravani, N. Hatzigiorgiou, and A. Dimeas, "Microgrids management," *IEEE power and energy magazine*, vol. 6, pp. 54-65, 2008.
- [38] N. M. Tabatabaei, E. Kabalci, and N. Bizon, *Microgrid architectures, control and protection methods*: Springer, 2019.
- [39] A. K. Basu, S. Chowdhury, S. Chowdhury, and S. Paul, "Microgrids: Energy management by strategic deployment of DERs—A comprehensive survey," *Renewable and Sustainable Energy Reviews*, vol. 15, pp. 4348-4356, 2011.

- [40] A. Molderink, V. Bakker, M. G. Bosman, J. L. Hurink, and G. J. Smit, "Management and control of domestic smart grid technology," *IEEE transactions on Smart Grid*, vol. 1, pp. 109-119, 2010.
- [41] M. Javidsharifi, T. Niknam, J. Aghaei, and G. Mokryani, "Multi-objective short-term scheduling of a renewable-based microgrid in the presence of tidal resources and storage devices," *Applied Energy*, vol. 216, pp. 367-381, 2018.
- [42] B. Bhandari, K.-T. Lee, C. S. Lee, C.-K. Song, R. K. Maskey, and S.-H. Ahn, "A novel off-grid hybrid power system comprised of solar photovoltaic, wind, and hydro energy sources," *Applied Energy*, vol. 133, pp. 236-242, 2014.
- [43] C. Wang, Y. Liu, X. Li, L. Guo, L. Qiao, and H. Lu, "Energy management system for stand-alone diesel-wind-biomass microgrid with energy storage system," *Energy*, vol. 97, pp. 90-104, 2016.
- [44] Y. Guo and C. Zhao, "Islanding-aware robust energy management for microgrids," *IEEE Transactions on Smart Grid*, vol. 9, pp. 1301-1309, 2016.
- [45] F.-F. Li and J. Qiu, "Multi-objective optimization for integrated hydro–photovoltaic power system," *Applied Energy*, vol. 167, pp. 377-384, 2016.
- [46] A. Askarzadeh, "A memory-based genetic algorithm for optimization of power generation in a microgrid," *IEEE transactions on sustainable energy*, vol. 9, pp. 1081-1089, 2017.
- [47] S. y. Obara, M. Kawai, O. Kawae, and Y. Morizane, "Operational planning of an independent microgrid containing tidal power generators, SOFCs, and photovoltaics," *Applied energy*, vol. 102, pp. 1343-1357, 2013.
- [48] J. P. Fossati, A. Galarza, A. Martín-Villate, J. M. Echeverría, and L. Fontán, "Optimal scheduling of a microgrid with a fuzzy logic controlled storage system," *International Journal of Electrical Power & Energy Systems*, vol. 68, pp. 61-70, 2015.
- [49] M. Motevasel, A. R. Seifi, and T. Niknam, "Multi-objective energy management of CHP (combined heat and power)-based micro-grid," *Energy*, vol. 51, pp. 123-136, 2013.
- [50] P. T. Baboli, M. Shahparasti, M. P. Moghaddam, M. R. Haghifam, and M. Mohamadian, "Energy management and operation modelling of hybrid AC–DC microgrid," *IET Generation, Transmission & Distribution*, vol. 8, pp. 1700-1711, 2014.
- [51] A. Chauhan and R. Saini, "A review on Integrated Renewable Energy System based power generation for stand-alone applications: Configurations, storage options, sizing methodologies and control," *Renewable and Sustainable Energy Reviews*, vol. 38, pp. 99-120, 2014.
- [52] K. S. Krishna and K. S. Kumar, "A review on hybrid renewable energy systems," *Renewable and Sustainable Energy Reviews*, vol. 52, pp. 907-916, 2015.

- [53] L. Olatomiwa, S. Mekhilef, M. S. Ismail, and M. Moghavvemi, "Energy management strategies in hybrid renewable energy systems: A review," *Renewable and Sustainable Energy Reviews*, vol. 62, pp. 821-835, 2016.
- [54] C. Gamarra and J. M. Guerrero, "Computational optimization techniques applied to microgrids planning: A review," *Renewable and Sustainable Energy Reviews*, vol. 48, pp. 413-424, 2015.
- [55] A. H. Fathima and K. Palanisamy, "Optimization in microgrids with hybrid energy systems—A review," *Renewable and Sustainable Energy Reviews*, vol. 45, pp. 431-446, 2015.
- [56] L. Meng, E. R. Sanseverino, A. Luna, T. Dragicevic, J. C. Vasquez, and J. M. Guerrero, "Microgrid supervisory controllers and energy management systems: A literature review," *Renewable and Sustainable Energy Reviews*, vol. 60, pp. 1263-1273, 2016.
- [57] A. A. Khan, M. Naeem, M. Iqbal, S. Qaisar, and A. Anpalagan, "A compendium of optimization objectives, constraints, tools and algorithms for energy management in microgrids," *Renewable and Sustainable Energy Reviews*, vol. 58, pp. 1664-1683, 2016.
- [58] A. Elmouatamid, R. Ouladsine, M. Bakhouya, N. El Kamoun, M. Khaidar, and K. Zine-Dine, "Review of Control and Energy Management Approaches in Micro-Grid Systems," *Energies*, vol. 14, p. 168, 2021.
- [59] M. Dali, J. Belhadj, and X. Roboam, "Hybrid solar–wind system with battery storage operating in grid-connected and standalone mode: control and energy management–experimental investigation," *Energy*, vol. 35, pp. 2587-2595, 2010.
- [60] M. R. Sandgani and S. Sirouspour, "Priority-based microgrid energy management in a network environment," *IEEE Transactions on Sustainable Energy*, vol. 9, pp. 980-990, 2017.
- [61] R. S. Chandan, T. S. Kiran, G. Swapna, and T. V. Muni, "Intelligent Control Strategy for Energy Management System with FC/Battery/SC," *JCR*, vol. 7, pp. 344-348, 2020.
- [62] Y. Zheng, B. M. Jenkins, K. Kornbluth, and C. Træholt, "Optimization under uncertainty of a biomass-integrated renewable energy microgrid with energy storage," *Renewable energy*, vol. 123, pp. 204-217, 2018.
- [63] B. Li, R. Roche, and A. Miraoui, "Microgrid sizing with combined evolutionary algorithm and MILP unit commitment," *Applied energy*, vol. 188, pp. 547-562, 2017.
- [64] A. Ghaffari and A. Askarzadeh, "Design optimization of a hybrid system subject to reliability level and renewable energy penetration," *Energy*, vol. 193, p. 116754, 2020.
- [65] N. Korolko and Z. Sahinoglu, "Robust optimization of EV charging schedules in unregulated electricity markets," *IEEE Transactions on Smart Grid*, vol. 8, pp. 149-157, 2015.

- [66] J. S. Vardakas, N. Zorba, and C. V. Verikoukis, "A survey on demand response programs in smart grids: Pricing methods and optimization algorithms," *IEEE Communications Surveys & Tutorials*, vol. 17, pp. 152-178, 2014.
- [67] O. Palizban, K. Kauhaniemi, and J. M. Guerrero, "Microgrids in active network management—Part I: Hierarchical control, energy storage, virtual power plants, and market participation," *Renewable and Sustainable Energy Reviews*, vol. 36, pp. 428-439, 2014.
- [68] P. A. Gbadega and A. K. Saha, "Adaptive model-based receding horizon control of interconnected renewable-based power micro-grids for effective control and optimal power exchanges," in *2020 International SAUPEC/RobMech/PRASA Conference*, 2020, pp. 1-6.
- [69] Z. Abdin, C. Webb, and E. Gray, "Solar hydrogen hybrid energy systems for off-grid electricity supply: A critical review," *Renewable and sustainable energy reviews*, vol. 52, pp. 1791-1808, 2015.
- [70] A. S. Al Busaidi, H. A. Kazem, A. H. Al-Badi, and M. F. Khan, "A review of optimum sizing of hybrid PV–Wind renewable energy systems in oman," *Renewable and Sustainable Energy Reviews*, vol. 53, pp. 185-193, 2016.
- [71] P. A. Gbadega and A. K. Saha, "Power losses assessments of LCC-based HVDC converter stations using datasheet parameters and IEC 61803 STD," in *2018 International Conference on the Domestic Use of Energy (DUE)*, 2018, pp. 1-10.
- [72] A. G. Tsikalakis and N. D. Hatziargyriou, "Centralized control for optimizing microgrids operation," in *2011 IEEE power and energy society general meeting*, 2011, pp. 1-8.
- [73] D. E. Olivares, C. A. Cañizares, and M. Kazerani, "A centralized energy management system for isolated microgrids," *IEEE Transactions on smart grid*, vol. 5, pp. 1864-1875, 2014.
- [74] M. Kermani, D. L. Carnì, S. Rotondo, A. Paolillo, F. Manzo, and L. Martirano, "A nearly zero-energy microgrid testbed laboratory: Centralized control strategy based on scada system," *Energies*, vol. 13, p. 2106, 2020.
- [75] D. Y. Yamashita, I. Vechiu, and J.-P. Gaubert, "A review of hierarchical control for building microgrids," *Renewable and Sustainable Energy Reviews*, vol. 118, p. 109523, 2020.
- [76] H. Pourbabak, T. Chen, and W. Su, "Centralized, decentralized, and distributed control for energy internet," in *The Energy Internet*, ed: Elsevier, 2019, pp. 3-19.
- [77] E. Kuznetsova, C. Ruiz, Y.-F. Li, and E. Zio, "Analysis of robust optimization for decentralized microgrid energy management under uncertainty," *International Journal of Electrical Power & Energy Systems*, vol. 64, pp. 815-832, 2015.
- [78] X. Li and S. Wang, "A review on energy management, operation control and application methods for grid battery energy storage systems," *CSEE Journal of Power and Energy Systems*, 2019.

- [79] D. K. Molzahn, F. Dörfler, H. Sandberg, S. H. Low, S. Chakrabarti, R. Baldick, *et al.*, "A survey of distributed optimization and control algorithms for electric power systems," *IEEE Transactions on Smart Grid*, vol. 8, pp. 2941-2962, 2017.
- [80] N. D. Van, M. Sualeh, D. Kim, and G.-W. Kim, "A Hierarchical Control System for Autonomous Driving towards Urban Challenges," *Applied Sciences*, vol. 10, p. 3543, 2020.
- [81] A. Bidram and A. Davoudi, "Hierarchical structure of microgrids control system," *IEEE Transactions on Smart Grid*, vol. 3, pp. 1963-1976, 2012.
- [82] O. Palizban and K. Kauhaniemi, "Hierarchical control structure in microgrids with distributed generation: Island and grid-connected mode," *Renewable and Sustainable Energy Reviews*, vol. 44, pp. 797-813, 2015.
- [83] A. Elmouatamid, Y. NaitMalek, R. Ouladsine, M. Bakhouya, N. Elkamoun, M. Khaidar, *et al.*, "A Micro-Grid System Infrastructure Implementing IoT/Big-Data Technologies for Efficient Energy Management in Buildings. Submitted to ATSPES'1 (Advanced Technologies for Solar Photovoltaics Energy Systems)," ed: Springer: Berlin/Heidelberg, Germany, 2020.
- [84] N. Prabakaran, A. R. A. Jerin, E. Najafi, and K. Palanisamy, "An overview of control techniques and technical challenge for inverters in micro grid," *Hybrid-Renewable Energy Systems in Microgrids*, pp. 97-107, 2018.
- [85] E. González-Romera, E. Romero-Cadaval, C. Roncero-Clemente, M. Ruiz-Cortés, F. Barrero-González, M.-I. Milanés Montero, *et al.*, "Secondary Control for Storage Power Converters in Isolated Nanogrids to Allow Peer-to-Peer Power Sharing," *Electronics*, vol. 9, p. 140, 2020.
- [86] J. M. Guerrero, M. Chandorkar, T.-L. Lee, and P. C. Loh, "Advanced control architectures for intelligent microgrids—Part I: Decentralized and hierarchical control," *IEEE Transactions on Industrial Electronics*, vol. 60, pp. 1254-1262, 2012.
- [87] J. M. Guerrero, P. C. Loh, T.-L. Lee, and M. Chandorkar, "Advanced control architectures for intelligent microgrids—Part II: Power quality, energy storage, and AC/DC microgrids," *IEEE Transactions on industrial electronics*, vol. 60, pp. 1263-1270, 2012.
- [88] M. Elkazaz, M. Sumner, and D. Thomas, "Energy management system for hybrid PV-wind-battery microgrid using convex programming, model predictive and rolling horizon predictive control with experimental validation," *International Journal of Electrical Power & Energy Systems*, vol. 115, p. 105483, 2020.
- [89] S. K. Sahoo, A. K. Sinha, and N. Kishore, "Control techniques in AC, DC, and hybrid AC–DC microgrid: a review," *IEEE Journal of Emerging and Selected Topics in Power Electronics*, vol. 6, pp. 738-759, 2017.

- [90] J. Kumar, A. Agarwal, and V. Agarwal, "A review on overall control of DC microgrids," *Journal of energy storage*, vol. 21, pp. 113-138, 2019.
- [91] N. Lidula and A. Rajapakse, "Microgrids research: A review of experimental microgrids and test systems," *Renewable and Sustainable Energy Reviews*, vol. 15, pp. 186-202, 2011.
- [92] M. Pandit, L. Srivastava, and M. Sharma, "Environmental economic dispatch in multi-area power system employing improved differential evolution with fuzzy selection," *Applied Soft Computing*, vol. 28, pp. 498-510, 2015.
- [93] J. Garcia-Gonzalez, R. M. R. de la Muela, L. M. Santos, and A. M. Gonzalez, "Stochastic joint optimization of wind generation and pumped-storage units in an electricity market," *IEEE Transactions on Power Systems*, vol. 23, pp. 460-468, 2008.
- [94] M. Petrollese, "Optimal generation scheduling for renewable microgrids using hydrogen storage systems," 2015.
- [95] P. A. Gbadega and A. K. Saha, "The Impacts of Harmonics Reduction on THD Analysis in HVDC Transmission System using Three-phase Multi-Pulse and higher Level Converters," in *2019 Southern African Universities Power Engineering Conference/Robotics and Mechatronics/Pattern Recognition Association of South Africa (SAUPEC/RobMech/PRASA)*, 2019, pp. 444-449.
- [96] P. A. Gbadega and A. K. Saha, "Comparative study of harmonics reduction and power factor enhancement of six and 12-pulses HVDC system using passive and shunt APFs harmonic filters," in *2018 International Conference on the Domestic Use of Energy (DUE)*, 2018, pp. 1-10.
- [97] W. Greenwell and A. Vahidi, "Predictive control of voltage and current in a fuel cell-ultracapacitor hybrid," *IEEE Transactions on Industrial Electronics*, vol. 57, pp. 1954-1963, 2009.
- [98] C. Dötsch, "Energy storage," in *Technology Guide*, ed: Springer, 2009, pp. 362-367.
- [99] J. P. Barton and D. G. Infield, "Energy storage and its use with intermittent renewable energy," *IEEE transactions on energy conversion*, vol. 19, pp. 441-448, 2004.
- [100] L. Guo, W. Liu, X. Li, Y. Liu, B. Jiao, W. Wang, *et al.*, "Energy management system for stand-alone wind-powered-desalination microgrid," *IEEE Transactions on Smart Grid*, vol. 7, pp. 1079-1087, 2014.
- [101] C.-S. Karavas, G. Kyriakarakos, K. G. Arvanitis, and G. Papadakis, "A multi-agent decentralized energy management system based on distributed intelligence for the design and control of autonomous polygeneration microgrids," *Energy Conversion and Management*, vol. 103, pp. 166-179, 2015.
- [102] S. A. Alavi, A. Ahmadian, and M. Aliakbar-Golkar, "Optimal probabilistic energy management in a typical micro-grid based-on robust optimization and point estimate method," *Energy Conversion and Management*, vol. 95, pp. 314-325, 2015.

- [103] A. Vahidi and W. Greenwell, "A decentralized model predictive control approach to power management of a fuel cell-ultracapacitor hybrid," in *2007 American Control Conference*, 2007, pp. 5431-5437.
- [104] A. Arce, J. Alejandro, and C. Bordons, "MPC for battery/fuel cell hybrid vehicles including fuel cell dynamics and battery performance improvement," *Journal of process control*, vol. 19, pp. 1289-1304, 2009.
- [105] C. Bordons, M. A. Ridao, A. Pérez, A. Arce, and D. Marcos, "Model predictive control for power management in hybrid fuel cell vehicles," in *2010 IEEE Vehicle Power and Propulsion Conference*, 2010, pp. 1-6.
- [106] M. N. Ambia and A. Al-Durra, "Adaptive power smoothing control in grid-connected and islanding modes of hybrid micro-grid energy management," *Journal of Renewable and Sustainable Energy*, vol. 7, p. 033104, 2015.
- [107] Y. Liu, S. Yu, Y. Zhu, D. Wang, and J. Liu, "Modeling, planning, application and management of energy systems for isolated areas: A review," *Renewable and Sustainable Energy Reviews*, vol. 82, pp. 460-470, 2018.
- [108] G. Aghajani, H. Shayanfar, and H. Shayeghi, "Presenting a multi-objective generation scheduling model for pricing demand response rate in micro-grid energy management," *Energy Conversion and Management*, vol. 106, pp. 308-321, 2015.
- [109] H. Falsafi, A. Zakariazadeh, and S. Jadid, "The role of demand response in single and multi-objective wind-thermal generation scheduling: A stochastic programming," *Energy*, vol. 64, pp. 853-867, 2014.
- [110] M. Hemmati, N. Amjady, and M. Ehsan, "System modeling and optimization for islanded micro-grid using multi-cross learning-based chaotic differential evolution algorithm," *International Journal of Electrical Power & Energy Systems*, vol. 56, pp. 349-360, 2014.
- [111] E. D. Mehleri, H. Sarimveis, N. C. Markatos, and L. G. Papageorgiou, "A mathematical programming approach for optimal design of distributed energy systems at the neighbourhood level," *Energy*, vol. 44, pp. 96-104, 2012.
- [112] C. Chen and S. Duan, "Optimal allocation of distributed generation and energy storage system in microgrids," *IET Renewable Power Generation*, vol. 8, pp. 581-589, 2014.
- [113] S. M. Nosratabadi, R.-A. Hooshmand, and E. Gholipour, "A comprehensive review on microgrid and virtual power plant concepts employed for distributed energy resources scheduling in power systems," *Renewable and Sustainable Energy Reviews*, vol. 67, pp. 341-363, 2017.
- [114] M. F. Zia, E. Elbouchikhi, and M. Benbouzid, "Microgrids energy management systems: A critical review on methods, solutions, and prospects," *Applied energy*, vol. 222, pp. 1033-1055, 2018.

- [115] C. Chen, S. Duan, T. Cai, B. Liu, and G. Hu, "Smart energy management system for optimal microgrid economic operation," *IET renewable power generation*, vol. 5, pp. 258-267, 2011.
- [116] B. Zhao, Y. Shi, X. Dong, W. Luan, and J. Bornemann, "Short-term operation scheduling in renewable-powered microgrids: A duality-based approach," *IEEE Transactions on sustainable energy*, vol. 5, pp. 209-217, 2013.
- [117] S. Mazzola, M. Astolfi, and E. Macchi, "A detailed model for the optimal management of a multigood microgrid," *Applied Energy*, vol. 154, pp. 862-873, 2015.
- [118] Q. Jiang, M. Xue, and G. Geng, "Energy management of microgrid in grid-connected and stand-alone modes," *IEEE transactions on power systems*, vol. 28, pp. 3380-3389, 2013.
- [119] A. Rabiee, M. Sadeghi, J. Aghaei, and A. Heidari, "Optimal operation of microgrids through simultaneous scheduling of electrical vehicles and responsive loads considering wind and PV units uncertainties," *Renewable and Sustainable Energy Reviews*, vol. 57, pp. 721-739, 2016.
- [120] S. Talari, M. Yazdaninejad, and M.-R. Haghifam, "Stochastic-based scheduling of the microgrid operation including wind turbines, photovoltaic cells, energy storages and responsive loads," *IET Generation, Transmission & Distribution*, vol. 9, pp. 1498-1509, 2015.
- [121] W. L. Theo, J. S. Lim, W. S. Ho, H. Hashim, and C. T. Lee, "Review of distributed generation (DG) system planning and optimisation techniques: Comparison of numerical and mathematical modelling methods," *Renewable and Sustainable Energy Reviews*, vol. 67, pp. 531-573, 2017.
- [122] J. Ahmad, M. Imran, A. Khalid, W. Iqbal, S. R. Ashraf, M. Adnan, *et al.*, "Techno economic analysis of a wind-photovoltaic-biomass hybrid renewable energy system for rural electrification: A case study of Kallar Kahar," *Energy*, vol. 148, pp. 208-234, 2018.
- [123] T. Wakui, T. Kinoshita, and R. Yokoyama, "A mixed-integer linear programming approach for cogeneration-based residential energy supply networks with power and heat interchanges," *Energy*, vol. 68, pp. 29-46, 2014.
- [124] Y. S. Manjili, A. Rajaei, M. Jamshidi, and B. T. Kelley, "Intelligent decision making for energy management in microgrids with air pollution reduction policy," in *2012 7th International Conference on System of Systems Engineering (SoSE)*, 2012, pp. 13-18.
- [125] G. Comodi, A. Giantomassi, M. Severini, S. Squartini, F. Ferracuti, A. Fonti, *et al.*, "Multi-apartment residential microgrid with electrical and thermal storage devices: Experimental analysis and simulation of energy management strategies," *Applied Energy*, vol. 137, pp. 854-866, 2015.
- [126] A. Hooshmand, B. Asghari, and R. Sharma, "A novel cost-aware multi-objective energy management method for microgrids," in *2013 IEEE PES Innovative Smart Grid Technologies Conference (ISGT)*, 2013, pp. 1-6.

- [127] W. Zhuo, "Microgrid energy management strategy with battery energy storage system and approximate dynamic programming," in *2018 37th Chinese Control Conference (CCC)*, 2018, pp. 7581-7587.
- [128] N. Wu and H. Wang, "Deep learning adaptive dynamic programming for real time energy management and control strategy of micro-grid," *Journal of cleaner production*, vol. 204, pp. 1169-1177, 2018.
- [129] N. A. Luu, Q.-T. Tran, and S. Bacha, "Optimal energy management for an island microgrid by using dynamic programming method," in *2015 IEEE Eindhoven PowerTech*, 2015, pp. 1-6.
- [130] H. Zhang, D. Yue, and X. Xie, "Robust optimization for dynamic economic dispatch under wind power uncertainty with different levels of uncertainty budget," *IEEE Access*, vol. 4, pp. 7633-7644, 2016.
- [131] P. Samadi, H. Mohsenian-Rad, V. W. Wong, and R. Schober, "Tackling the load uncertainty challenges for energy consumption scheduling in smart grid," *IEEE Transactions on Smart Grid*, vol. 4, pp. 1007-1016, 2013.
- [132] H. Farzin, M. Fotuhi-Firuzabad, and M. Moeini-Aghtaie, "Stochastic energy management of microgrids during unscheduled islanding period," *IEEE Transactions on Industrial Informatics*, vol. 13, pp. 1079-1087, 2016.
- [133] Y. Jiang, C. Wan, J. Wang, Y. Song, and Z. Y. Dong, "Stochastic receding horizon control of active distribution networks with distributed renewables," *IEEE Transactions on Power Systems*, vol. 34, pp. 1325-1341, 2018.
- [134] M. Zachar and P. Daoutidis, "Energy management and load shaping for commercial microgrids coupled with flexible building environment control," *Journal of Energy Storage*, vol. 16, pp. 61-75, 2018.
- [135] B. Khorramdel and M. Raoufat, "Optimal stochastic reactive power scheduling in a microgrid considering voltage droop scheme of DGs and uncertainty of wind farms," *Energy*, vol. 45, pp. 994-1006, 2012.
- [136] G.-C. Liao, "Solve environmental economic dispatch of Smart MicroGrid containing distributed generation system—Using chaotic quantum genetic algorithm," *International Journal of Electrical Power & Energy Systems*, vol. 43, pp. 779-787, 2012.
- [137] A. Takeuchi, T. Hayashi, Y. Nozaki, and T. Shimakage, "Optimal scheduling using metaheuristics for energy networks," *IEEE Transactions on Smart Grid*, vol. 3, pp. 968-974, 2012.
- [138] W. Gu, Z. Wu, and X. Yuan, "Microgrid economic optimal operation of the combined heat and power system with renewable energy," in *Ieee pes General Meeting*, 2010, pp. 1-6.

- [139] D. Ipsakis, S. Voutetakis, P. Seferlis, F. Stergiopoulos, S. Papadopoulou, and C. Elmasides, "The effect of the hysteresis band on power management strategies in a stand-alone power system," *Energy*, vol. 33, pp. 1537-1550, 2008.
- [140] K. Rouzbehi, A. Miranian, J. I. Candela, A. Luna, and P. Rodriguez, "Intelligent voltage control in a DC micro-grid containing PV generation and energy storage," in *2014 IEEE PES T&D Conference and Exposition*, 2014, pp. 1-5.
- [141] R. Dufo-Lopez, J. L. Bernal-Agustín, and J. Contreras, "Optimization of control strategies for stand-alone renewable energy systems with hydrogen storage," *Renewable energy*, vol. 32, pp. 1102-1126, 2007.
- [142] Y. E. García Vera, R. Dufo-López, and J. L. Bernal-Agustín, "Energy management in microgrids with renewable energy sources: A literature review," *Applied Sciences*, vol. 9, p. 3854, 2019.
- [143] B. Zhao, M. Xue, X. Zhang, C. Wang, and J. Zhao, "An MAS based energy management system for a stand-alone microgrid at high altitude," *Applied Energy*, vol. 143, pp. 251-261, 2015.
- [144] T. D. Huynh, N. R. Jennings, and N. R. Shadbolt, "An integrated trust and reputation model for open multi-agent systems," *Autonomous Agents and Multi-Agent Systems*, vol. 13, pp. 119-154, 2006.
- [145] T. Logenthiran, D. Srinivasan, and A. M. Khambadkone, "Multi-agent system for energy resource scheduling of integrated microgrids in a distributed system," *Electric Power Systems Research*, vol. 81, pp. 138-148, 2011.
- [146] M. Motevasel and A. R. Seifi, "Expert energy management of a micro-grid considering wind energy uncertainty," *Energy Conversion and Management*, vol. 83, pp. 58-72, 2014.
- [147] Y. J. Reddy, Y. P. Kumar, V. S. Kumar, and K. P. Raju, "Distributed ANNs in a layered architecture for energy management and maintenance scheduling of renewable energy HPS microgrids," in *2012 International Conference on Advances in Power Conversion and Energy Technologies (APCET)*, 2012, pp. 1-6.
- [148] G. K. Venayagamoorthy, R. K. Sharma, P. K. Gautam, and A. Ahmadi, "Dynamic energy management system for a smart microgrid," *IEEE transactions on neural networks and learning systems*, vol. 27, pp. 1643-1656, 2016.
- [149] H. Bevrani, B. François, and T. Ise, *Microgrid dynamics and control*: John Wiley & Sons, 2017.
- [150] G. Kyriakarakos, A. I. Dounis, K. G. Arvanitis, and G. Papadakis, "A fuzzy logic energy management system for polygeneration microgrids," *Renewable Energy*, vol. 41, pp. 315-327, 2012.
- [151] P. A. Gbadega and A. K. Saha, "Model-Based Receding Horizon Control of Wind Turbine System for Optimal Power Generation," in *Advanced Engineering Forum*, 2021, pp. 83-98.

- [152] M. Hosseinzadeh and F. R. Salmasi, "Robust optimal power management system for a hybrid AC/DC micro-grid," *IEEE Transactions on Sustainable Energy*, vol. 6, pp. 675-687, 2015.
- [153] X. Jin, K. Baker, S. Isley, and D. Christensen, "User-preference-driven model predictive control of residential building loads and battery storage for demand response," in *2017 American Control Conference (ACC)*, 2017, pp. 4147-4152.
- [154] I. Prodan and E. Zio, "A model predictive control framework for reliable microgrid energy management," *International Journal of Electrical Power & Energy Systems*, vol. 61, pp. 399-409, 2014.
- [155] A. Parisio, E. Rikos, and L. Glielmo, "Stochastic model predictive control for economic/environmental operation management of microgrids: An experimental case study," *Journal of Process Control*, vol. 43, pp. 24-37, 2016.
- [156] A. Parisio and L. Glielmo, "Stochastic model predictive control for economic/environmental operation management of microgrids," in *2013 European Control Conference (ECC)*, 2013, pp. 2014-2019.
- [157] Y. Zhang, R. Wang, T. Zhang, Y. Liu, and B. Guo, "Model predictive control-based operation management for a residential microgrid with considering forecast uncertainties and demand response strategies," *IET Generation, Transmission & Distribution*, vol. 10, pp. 2367-2378, 2016.
- [158] L. Valverde, F. Rosa, A. Del Real, A. Arce, and C. Bordons, "Modeling, simulation and experimental set-up of a renewable hydrogen-based domestic microgrid," *International journal of hydrogen energy*, vol. 38, pp. 11672-11684, 2013.
- [159] F. Garcia-Torres, L. Valverde, and C. Bordons, "Optimal load sharing of hydrogen-based microgrids with hybrid storage using model-predictive control," *IEEE Transactions on Industrial Electronics*, vol. 63, pp. 4919-4928, 2016.
- [160] A. Mesbah, "Stochastic model predictive control: An overview and perspectives for future research," *IEEE Control Systems Magazine*, vol. 36, pp. 30-44, 2016.
- [161] R. Negenborn, M. Houwing, B. De Schutter, and J. Hellendoorn, "Model predictive control for residential energy resources using a mixed-logical dynamic model," in *2009 International Conference on Networking, Sensing and Control*, 2009, pp. 702-707.
- [162] M. D. Galus and G. Andersson, "Power system considerations of plug-in hybrid electric vehicles based on a multi energy carrier model," in *2009 IEEE Power & Energy Society General Meeting*, 2009, pp. 1-8.
- [163] A. Del Real, A. Arce, and C. Bordons, "Hybrid model predictive control of a two-generator power plant integrating photovoltaic panels and a fuel cell," in *2007 46th IEEE Conference on Decision and Control*, 2007.

- [164] L. Valverde, C. Bordons, and F. Rosa, "Power management using model predictive control in a hydrogen-based microgrid," in *IECON 2012-38th annual conference on IEEE industrial electronics society*, 2012, pp. 5669-5676.
- [165] D. P. Chassin, K. Schneider, and C. Gerkenmeyer, "GridLAB-D: An open-source power systems modeling and simulation environment," in *2008 IEEE/PES Transmission and Distribution Conference and Exposition*, 2008, pp. 1-5.
- [166] A. Argüello, W. L. Cunha, T. R. Ricciardi, R. Torquato, and W. Freitas, "Dynamic modeling in OpenDSS: An implementation sequence for object Pascal," in *2018 IEEE Power & Energy Society General Meeting (PESGM)*, 2018, pp. 1-5.
- [167] K. Thirugnanam, S. K. Kerk, C. Yuen, N. Liu, and M. Zhang, "Energy management for renewable microgrid in reducing diesel generators usage with multiple types of battery," *IEEE Transactions on Industrial Electronics*, vol. 65, pp. 6772-6786, 2018.
- [168] T. G. Paul, S. J. Hossain, S. Ghosh, P. Mandal, and S. Kamalasan, "A quadratic programming based optimal power and battery dispatch for grid-connected microgrid," *IEEE Transactions on Industry Applications*, vol. 54, pp. 1793-1805, 2017.
- [169] M. Elsieed, A. Oukaour, H. Gualous, and R. Hassan, "Energy management and optimization in microgrid system based on green energy," *Energy*, vol. 84, pp. 139-151, 2015.
- [170] E. C. Umeozor and M. Trifkovic, "Energy management of a microgrid via parametric programming," *IFAC-PapersOnLine*, vol. 49, pp. 272-277, 2016.
- [171] J. Almada, R. Leão, R. Sampaio, and G. Barroso, "A centralized and heuristic approach for energy management of an AC microgrid," *Renewable and Sustainable Energy Reviews*, vol. 60, pp. 1396-1404, 2016.
- [172] Y. A. Muñoz Maldonado, "Optimización de recursos energéticos en zonas aisladas mediante estrategias de suministro y consumo," Universitat Politècnica de València, 2012.
- [173] M.-C. Hu, S.-Y. Lu, and Y.-H. Chen, "Stochastic programming and market equilibrium analysis of microgrids energy management systems," *Energy*, vol. 113, pp. 662-670, 2016.
- [174] D. Rivola, A. Giusti, M. Salani, A. E. Rizzoli, R. Rudel, and L. M. Gambardella, "A decentralized approach to demand side load management: the Swiss2Grid project," in *IECON 2013-39th Annual Conference of the IEEE Industrial Electronics Society*, 2013, pp. 4704-4709.
- [175] R. S. Netto, G. R. Ramalho, B. D. Bonatto, O. A. Carpinteiro, A. Zambroni de Souza, D. Q. Oliveira, *et al.*, "Real-time framework for energy management system of a smart microgrid using multiagent systems," *energies*, vol. 11, p. 656, 2018.

- [176] Z. Chen, L. Wu, and Y. Fu, "Real-time price-based demand response management for residential appliances via stochastic optimization and robust optimization," *IEEE Transactions on Smart Grid*, vol. 3, pp. 1822-1831, 2012.
- [177] V. Jayadev and K. S. Swarup, "Optimization of microgrid with demand side management using Genetic Algorithm," 2013.
- [178] G. Wang, J. Zhao, F. Wen, Y. Xue, and G. Ledwich, "Dispatch strategy of PHEVs to mitigate selected patterns of seasonally varying outputs from renewable generation," *IEEE Transactions on Smart Grid*, vol. 6, pp. 627-639, 2014.
- [179] Y. Mou, H. Xing, Z. Lin, and M. Fu, "Decentralized optimal demand-side management for PHEV charging in a smart grid," *IEEE Transactions on Smart Grid*, vol. 6, pp. 726-736, 2014.
- [180] H. Mohsenian-Rad, "Optimal charging of electric vehicles with uncertain departure times: A closed-form solution," *IEEE Transactions on Smart Grid*, vol. 6, pp. 940-942, 2014.
- [181] W. Lee, L. Xiang, R. Schober, and V. W. Wong, "Electric vehicle charging stations with renewable power generators: A game theoretical analysis," *IEEE transactions on smart grid*, vol. 6, pp. 608-617, 2014.
- [182] M. H. Tushar, C. Assi, and M. Maier, "Distributed real-time electricity allocation mechanism for large residential microgrid," *IEEE Transactions on Smart Grid*, vol. 6, pp. 1353-1363, 2014.
- [183] F. Garcia-Torres, D. G. Vilaplana, C. Bordons, P. Roncero-Sanchez, and M. A. Ridao, "Optimal management of microgrids with external agents including battery/fuel cell electric vehicles," *IEEE Transactions on Smart Grid*, vol. 10, pp. 4299-4308, 2018.
- [184] P. Richardson, D. Flynn, and A. Keane, "Optimal charging of electric vehicles in low-voltage distribution systems," *IEEE Transactions on Power Systems*, vol. 27, pp. 268-279, 2011.
- [185] A. Di Giorgio, F. Liberati, and S. Canale, "Electric vehicles charging control in a smart grid: A model predictive control approach," *Control Engineering Practice*, vol. 22, pp. 147-162, 2014.
- [186] J. Pahasa and I. Ngamroo, "PHEVs bidirectional charging/discharging and SoC control for microgrid frequency stabilization using multiple MPC," *IEEE Transactions on Smart Grid*, vol. 6, pp. 526-533, 2014.
- [187] N. Z. Aitzhan and D. Svetinovic, "Security and privacy in decentralized energy trading through multi-signatures, blockchain and anonymous messaging streams," *IEEE Transactions on Dependable and Secure Computing*, vol. 15, pp. 840-852, 2016.
- [188] J. M. Guerrero, J. C. Vasquez, J. Matas, L. G. De Vicuña, and M. Castilla, "Hierarchical control of droop-controlled AC and DC microgrids—A general approach toward standardization," *IEEE Transactions on industrial electronics*, vol. 58, pp. 158-172, 2010.

- [189] A. M. Ersdal, L. Imsland, and K. Uhlen, "Model predictive load-frequency control," *IEEE Transactions on Power Systems*, vol. 31, pp. 777-785, 2015.
- [190] S. Panda and N. K. Yegireddy, "Automatic generation control of multi-area power system using multi-objective non-dominated sorting genetic algorithm-II," *International Journal of Electrical Power & Energy Systems*, vol. 53, pp. 54-63, 2013.
- [191] Y. Mi, Y. Fu, C. Wang, and P. Wang, "Decentralized sliding mode load frequency control for multi-area power systems," *IEEE Transactions on Power Systems*, vol. 28, pp. 4301-4309, 2013.
- [192] S. Saxena and Y. V. Hote, "Stabilization of perturbed system via IMC: An application to load frequency control," *Control Engineering Practice*, vol. 64, pp. 61-73, 2017.
- [193] K. Sabahi and M. Teshnehlab, "Recurrent fuzzy neural network by using feedback error learning approaches for LFC in interconnected power system," *Energy Conversion and Management*, vol. 50, pp. 938-946, 2009.
- [194] N. E. Y. Kouba, M. Mena, M. Hasni, and M. Boudour, "Optimal control of frequency and voltage variations using PID controller based on particle swarm optimization," in *2015 4th international conference on systems and control (ICSC)*, 2015, pp. 424-429.
- [195] R. K. Sahu, S. Panda, and U. K. Rout, "DE optimized parallel 2-DOF PID controller for load frequency control of power system with governor dead-band nonlinearity," *International Journal of Electrical Power & Energy Systems*, vol. 49, pp. 19-33, 2013.
- [196] S. Padhan, R. K. Sahu, and S. Panda, "Application of firefly algorithm for load frequency control of multi-area interconnected power system," *Electric power components and systems*, vol. 42, pp. 1419-1430, 2014.
- [197] H. Golpira and H. Bevrani, "Application of GA optimization for automatic generation control design in an interconnected power system," *Energy Conversion and Management*, vol. 52, pp. 2247-2255, 2011.
- [198] S. Panda, B. Mohanty, and P. Hota, "Hybrid BFOA-PSO algorithm for automatic generation control of linear and nonlinear interconnected power systems," *Applied Soft Computing*, vol. 13, pp. 4718-4730, 2013.
- [199] K. Naidu, H. Mokhlis, and A. A. Bakar, "Multiobjective optimization using weighted sum artificial bee colony algorithm for load frequency control," *International Journal of Electrical Power & Energy Systems*, vol. 55, pp. 657-667, 2014.
- [200] K. S. Parmar, S. Majhi, and D. Kothari, "Multi-area load frequency control in a power system using optimal output feedback method," in *2010 Joint International Conference on Power Electronics, Drives and Energy Systems & 2010 Power India*, 2010, pp. 1-5.

- [201] P. Kumar and D. P. Kothari, "Recent philosophies of automatic generation control strategies in power systems," *IEEE transactions on power systems*, vol. 20, pp. 346-357, 2005.
- [202] X. Su, M. Han, J. M. Guerrero, and H. Sun, "Microgrid stability controller based on adaptive robust total SMC," *Energies*, vol. 8, pp. 1784-1801, 2015.
- [203] Y. Han, P. M. Young, A. Jain, and D. Zimmerle, "Robust control for microgrid frequency deviation reduction with attached storage system," *IEEE Transactions on smart grid*, vol. 6, pp. 557-565, 2014.
- [204] T.-T. Nguyen, H.-J. Yoo, and H.-M. Kim, "Analyzing the impacts of system parameters on MPC-based frequency control for a stand-alone microgrid," *Energies*, vol. 10, p. 417, 2017.
- [205] S. Kayalvizhi and D. V. Kumar, "Load frequency control of an isolated micro grid using fuzzy adaptive model predictive control," *IEEE Access*, vol. 5, pp. 16241-16251, 2017.
- [206] M.-R. Chen, G.-Q. Zeng, and X.-Q. Xie, "Population extremal optimization-based extended distributed model predictive load frequency control of multi-area interconnected power systems," *Journal of the Franklin Institute*, vol. 355, pp. 8266-8295, 2018.
- [207] S. Z. Aljoaba, A. M. Cramer, and B. L. Walcott, "Thermoelectrical modeling of wavelength effects on photovoltaic module performance—Part I: Model," *IEEE Journal of Photovoltaics*, vol. 3, pp. 1027-1033, 2013.
- [208] S. Aljoaba, "Active optimal control strategies for increasing the efficiency of photovoltaic cells," 2013.
- [209] A. Jones and C. Underwood, "A thermal model for photovoltaic systems," *Solar energy*, vol. 70, pp. 349-359, 2001.
- [210] S. W. Churchill, "A comprehensive correlating equation for laminar, assisting, forced and free convection," *AIChE Journal*, vol. 23, pp. 10-16, 1977.
- [211] S. Armstrong and W. Hurley, "A thermal model for photovoltaic panels under varying atmospheric conditions," *Applied Thermal Engineering*, vol. 30, pp. 1488-1495, 2010.
- [212] A. J. Veldhuis, Andre M. Nobre, Ian M. Peters, Thomas Reindl, Ricardo Ruther, and Angele H. M. E. Reinders, "An Empirical Model for Rack-Mounted PV Module Temperatures for Southeast Asian Locations Evaluated for Minute Time Scales," *IEEE Journal of Photovoltaics*, 2015.
- [213] K. Uthaichana, R. DeCarlo, S. Benghea, M. Žefran, and S. Pekarek, "Hybrid optimal theory and predictive control for power management in hybrid electric vehicle," *arXiv preprint arXiv:1804.00757*, 2018.
- [214] K. Uthaichana, R. A. DeCarlo, S. C. Benghea, S. Pekarek, and M. Zefran, "Hybrid optimal theory and predictive control for power management in hybrid electric vehicle," *Journal of Nonlinear Systems and Applications*, vol. 2, pp. 96-110, 2011.

- [215] H. Wu, X. Liu, and M. Ding, "Dynamic economic dispatch of a microgrid: Mathematical models and solution algorithm," *International Journal of Electrical Power & Energy Systems*, vol. 63, pp. 336-346, 2014.
- [216] P. A. Gbadega and A. K. Saha, "Effects and Performance Indicators Evaluation of PV Array Topologies on PV Systems Operation Under Partial Shading Conditions," in *2019 Southern African Universities Power Engineering Conference/Robotics and Mechatronics/Pattern Recognition Association of South Africa (SAUPEC/RobMech/PRASA)*, 2019, pp. 322-327.
- [217] H. S. Rauschenbach, *Solar cell array design handbook: the principles and technology of photovoltaic energy conversion*: Springer Science & Business Media, 2012.
- [218] H. Wen and R. Yang, "Modeling and simulation of energy control strategies in AC Microgrid," in *2016 IEEE PES Asia-Pacific Power and Energy Engineering Conference (APPEEC)*, 2016, pp. 1469-1474.
- [219] S. Heier, *Grid integration of wind energy: onshore and offshore conversion systems*: John Wiley & Sons, 2014.
- [220] C. Bordons, F. Garcia-Torres, and M. A. Ridao, *Model Predictive Control of Microgrids*: Springer, 2020.
- [221] G. Migoni, P. Rullo, F. Bergero, and E. Kofman, "Efficient simulation of hybrid renewable energy systems," *international journal of hydrogen energy*, vol. 41, pp. 13934-13949, 2016.
- [222] D. Ipsakis, S. Voutetakis, P. Seferlis, F. Stergiopoulos, and C. Elmasides, "Power management strategies for a stand-alone power system using renewable energy sources and hydrogen storage," *International journal of hydrogen energy*, vol. 34, pp. 7081-7095, 2009.
- [223] P. A. Gbadega and A. K. Saha, "Model Predictive Controller Design of a Wavelength-Based Thermo-Electrical Model of a Photovoltaic (PV) Module for Optimal Output Power," *International Journal of Engineering Research in Africa*, vol. 48, pp. 133-148, 2020.
- [224] M. S. Taha, H. H. Abdeltawab, and Y. A.-R. I. Mohamed, "An online energy management system for a grid-connected hybrid energy source," *IEEE Journal of Emerging and Selected Topics in Power Electronics*, vol. 6, pp. 2015-2030, 2018.
- [225] P. J. Grbovic, P. Delarue, P. Le Moigne, and P. Bartholomeus, "Modeling and control of the ultracapacitor-based regenerative controlled electric drives," *IEEE Transactions on industrial electronics*, vol. 58, pp. 3471-3484, 2010.
- [226] P. J. Grbovic, P. Delarue, P. Le Moigne, and P. Bartholomeus, "The ultracapacitor-based regenerative controlled electric drives with power-smoothing capability," *IEEE Transactions on Industrial Electronics*, vol. 59, pp. 4511-4522, 2012.

- [227] B. E. Conway, *Electrochemical supercapacitors: scientific fundamentals and technological applications*: Springer Science & Business Media, 2013.
- [228] S. Mohammadshahi, E. M. Gray, and C. Webb, "A review of mathematical modelling of metal-hydride systems for hydrogen storage applications," *international journal of hydrogen energy*, vol. 41, pp. 3470-3484, 2016.
- [229] M. Mottus, M. Sulev, F. Baret, A. Reinart, and R. Lopez, "Photosynthetically Active Radiation: Measurement and Modeling," ed, 2011.
- [230] J. T. Pukrushpan, A. G. Stefanopoulou, and H. Peng, *Control of fuel cell power systems: principles, modeling, analysis and feedback design*: Springer Science & Business Media, 2004.
- [231] N. Amjady, F. Keynia, and H. Zareipour, "Short-term load forecast of microgrids by a new bilevel prediction strategy," *IEEE Transactions on smart grid*, vol. 1, pp. 286-294, 2010.
- [232] R. Weron, "Electricity price forecasting: A review of the state-of-the-art with a look into the future," *International journal of forecasting*, vol. 30, pp. 1030-1081, 2014.
- [233] L. Valverde, C. Bordons, and F. Rosa, "Integration of fuel cell technologies in renewable-energy-based microgrids optimizing operational costs and durability," *IEEE Transactions on Industrial Electronics*, vol. 63, pp. 167-177, 2015.
- [234] A. Ouammi, H. Dagdougui, L. Dessaint, and R. Sacile, "Coordinated model predictive-based power flows control in a cooperative network of smart microgrids," *IEEE Transactions on Smart grid*, vol. 6, pp. 2233-2244, 2015.
- [235] A. Bemporad and M. Morari, "Control of systems integrating logic, dynamics, and constraints," *Automatica*, vol. 35, pp. 407-427, 1999.
- [236] S. Anuphapharadorn, S. Sukchai, C. Sirisamphanwong, and N. Ketjoy, "Comparison the economic analysis of the battery between lithium-ion and lead-acid in PV stand-alone application," *Energy Procedia*, vol. 56, pp. 352-358, 2014.
- [237] P. Aliasghari, B. Mohammadi-Ivatloo, M. Alipour, M. Abapour, and K. Zare, "Optimal scheduling of plug-in electric vehicles and renewable micro-grid in energy and reserve markets considering demand response program," *Journal of Cleaner Production*, vol. 186, pp. 293-303, 2018.
- [238] M. Petrollese, L. Valverde, D. Cocco, G. Cau, and J. Guerra, "Real-time integration of optimal generation scheduling with MPC for the energy management of a renewable hydrogen-based microgrid," *Applied Energy*, vol. 166, pp. 96-106, 2016.
- [239] D. Bernardini and A. Bemporad, "Scenario-based model predictive control of stochastic constrained linear systems," in *Proceedings of the 48th IEEE Conference on Decision and Control (CDC) held jointly with 2009 28th Chinese Control Conference*, 2009, pp. 6333-6338.

- [240] A. A. Z. Diab and M. A. El-Sattar, "Adaptive model predictive based load frequency control in an interconnected power system," in *2018 IEEE Conference of Russian Young Researchers in Electrical and Electronic Engineering (EIConRus)*, 2018, pp. 604-610.
- [241] Y. S. P. K. H. Kwan, Y. C. Chu, and P. L. So, "Model Predictive Control of Unified Power Quality Conditioner for Power Quality Improvement," in *Proc. 16th IEEE Conf. on Control Applications*, Oct. 2007, pp. 916-921.
- [242] A. S. Mir and N. Senroy, "Adaptive model predictive control scheme for application of SMES for load frequency control," *IEEE Transactions on Power Systems*, 2017.
- [243] P. Chalupa, "Predictive control using self tuning model predictive controllers library," in *17th International Conference on Process Control 2009*, 2009, pp. 418-425.
- [244] X. Liu, Y. Zhang, and K. Y. Lee, "Robust distributed MPC for load frequency control of uncertain power systems," *Control Engineering Practice*, vol. 56, pp. 136-147, 2016.
- [245] G.-Q. Zeng, X.-Q. Xie, and M.-R. Chen, "An adaptive model predictive load frequency control method for multi-area interconnected power systems with photovoltaic generations," *Energies*, vol. 10, p. 1840, 2017.
- [246] C. G. M. Peters, P. Loper, B. Gross, J. Upping, F. Dimroth, B. Wehrspohn, and B. Blasi, "Spectrally-selective photonic structures for PV applications," *Energies*, vol. vol. 3, pp. pp. 171–193, Feb. 2010 2010.
- [247] S. Z. Aljoaba, A. M. Cramer, and B. L. Walcott, "Active optimal optical filtering of wavelengths for increasing the efficiency of photovoltaic modules," in *2014 IEEE 40th Photovoltaic Specialist Conference (PVSC)*, 2014, pp. 1329-1334.
- [248] J. Koo, D. Park, S. Ryu, G.-H. Kim, and Y.-W. Lee, "Design of a self-tuning adaptive model predictive controller using recursive model parameter estimation for real-time plasma variable control," *Computers & Chemical Engineering*, vol. 123, pp. 126-142, 2019.
- [249] M. Alizadeh, X. Li, Z. Wang, A. Scaglione, and R. Melton, "Demand-side management in the smart grid: Information processing for the power switch," *IEEE Signal Processing Magazine*, vol. 29, pp. 55-67, 2012.
- [250] A. K. Saha, S. Chowdhury, S. Chowdhury, and C. Gaunt, "Integration of wind turbine, SOFC and microturbine in distributed generation," in *2009 IEEE Power & Energy Society General Meeting*, 2009, pp. 1-8.
- [251] A. Adebisi, I. Lazarus, A. K. Saha, and E. Ojo, "Performance analysis of PV panels connected in various orientations under different climatic conditions," in *Proceedings of the 5th Southern African Solar Energy Conference (SASEC 2018)*, 2018, pp. 46-51.

- [252] A. K. Saha, S. Chowdhury, and S. Chowdhury, "PEM fuel cell as energy source using fuzzy logic controller," 2007.
- [253] A. K. Saha, S. Chowdhury, S. Chowdhury, and Y. Song, "Dynamic model of PEM fuel cell with fuzzy logic controller," in *2007 42nd International Universities Power Engineering Conference*, 2007, pp. 753-757.
- [254] R. C. Green II, L. Wang, and M. Alam, "The impact of plug-in hybrid electric vehicles on distribution networks: A review and outlook," *Renewable and sustainable energy reviews*, vol. 15, pp. 544-553, 2011.
- [255] A. K. Saha, "Grid-Connected PEM Fuel Cell with Multi-Pulse Multilevel Inverter," in *International Journal of Engineering Research in Africa*, 2020, pp. 54-67.
- [256] Y.-S. Kim, E.-S. Kim, and S.-I. Moon, "Frequency and voltage control strategy of standalone microgrids with high penetration of intermittent renewable generation systems," *IEEE Transactions on Power systems*, vol. 31, pp. 718-728, 2015.
- [257] Y.-S. Kim, C.-S. Hwang, E.-S. Kim, and C. Cho, "State of charge-based active power sharing method in a standalone microgrid with high penetration level of renewable energy sources," *energies*, vol. 9, p. 480, 2016.
- [258] S. Abd-Elazim and E. Ali, "Load frequency controller design of a two-area system composing of PV grid and thermal generator via firefly algorithm," *Neural Computing and Applications*, vol. 30, pp. 607-616, 2018.
- [259] P. A. Gbadega and K. T. Akindeji, "Linear Quadratic Regulator Technique for Optimal Load Frequency Controller Design of Interconnected Linear Power Systems," in *2020 IEEE PES/IAS PowerAfrica*, 2020, pp. 1-5.
- [260] H. Bevrani, F. Habibi, P. Babahajyani, M. Watanabe, and Y. Mitani, "Intelligent frequency control in an AC microgrid: Online PSO-based fuzzy tuning approach," *IEEE transactions on smart grid*, vol. 3, pp. 1935-1944, 2012.
- [261] T. Mohamed, H. Bevrani, A. Hassan, and T. Hiyama, "Decentralized model predictive based load frequency control in an interconnected power system," *Energy Conversion and Management*, vol. 52, pp. 1208-1214, 2011.
- [262] M. Ma, H. Chen, X. Liu, and F. Allgöwer, "Distributed model predictive load frequency control of multi-area interconnected power system," *International Journal of Electrical Power & Energy Systems*, vol. 62, pp. 289-298, 2014.
- [263] M. K. Debnath, T. Jena, and R. K. Mallick, "Optimal design of PD-Fuzzy-PID cascaded controller for automatic generation control," *Cogent Engineering*, vol. 4, p. 1416535, 2017.

- [264] J. Pahasa and I. Ngamroo, "Coordinated control of wind turbine blade pitch angle and PHEVs using MPCs for load frequency control of microgrid," *IEEE Systems Journal*, vol. 10, pp. 97-105, 2014.
- [265] T. Senjyu, R. Sakamoto, N. Urasaki, T. Funabashi, H. Fujita, and H. Sekine, "Output power leveling of wind turbine generator for all operating regions by pitch angle control," *IEEE Transactions on Energy conversion*, vol. 21, pp. 467-475, 2006.

APPENDICES

Appendix A

The mathematical descriptions of the matrix's forms of the SOC and LOH used in **chapters 5** are given as follows:

For a sampling time of $T_s = 60s$, the model in matrix form is expressed as [164]:

$$\begin{bmatrix} SOC(t+1) \\ LOH(t+1) \end{bmatrix} = \begin{bmatrix} SOC(t) \\ LOH(t) \end{bmatrix} + \begin{bmatrix} -\frac{\eta_{bat}T_s}{C_{max}} & \frac{\eta_{bat}T_s}{C_{max}} \\ \frac{\eta_{elz}T_s}{V_{max}} & 0 \end{bmatrix} \begin{bmatrix} P_{H_2} \\ P_{grid} \end{bmatrix} + \begin{bmatrix} -\frac{\eta_{bat}T_s}{C_{max}} \\ 0 \end{bmatrix} d(t) \quad (A-1)$$

Discretizing the overall continuous structure defined by Equation (A-1), the model in matrix form obtained for discrete-time is as follows:

$$\begin{bmatrix} SOC(k+1) \\ LOH(k+1) \end{bmatrix} = \begin{bmatrix} SOC(k) \\ LOH(k) \end{bmatrix} + \begin{bmatrix} -\frac{\eta_{bat}T_s}{C_{max}} & \frac{\eta_{bat}T_s}{C_{max}} \\ \frac{\eta_{elz}T_s}{V_{max}} & 0 \end{bmatrix} \begin{bmatrix} P_{H_2} \\ P_{grid} \end{bmatrix} + \begin{bmatrix} -\frac{\eta_{bat}T_s}{C_{max}} \\ 0 \end{bmatrix} d(k) \quad (A-2)$$

Evaluating the matrix expression of Eqn. (A-2) using the values given in the Table D-3, it results in Eqn. (A-3):

$$\begin{bmatrix} SOC(k+1) \\ LOH(k+1) \end{bmatrix} = \begin{bmatrix} SOC(k) \\ LOH(k) \end{bmatrix} + \begin{bmatrix} 1.564 \times 10^{-3} & 1.564 \times 10^{-3} \\ -5.667 \times 10^{-3} & 0 \end{bmatrix} \begin{bmatrix} P_{H_2}(k) \\ P_{grid}(k) \end{bmatrix} + \begin{bmatrix} 1.564 \times 10^{-3} \\ 0 \end{bmatrix} d(k) \quad (A-3)$$

Consequently, the system matrices admit expressions as:

$$A = I, \quad B = \begin{bmatrix} 1.564 \times 10^{-3} & 1.564 \times 10^{-3} \\ -5.667 \times 10^{-3} & 0 \end{bmatrix}, \quad B_d = \begin{bmatrix} 1.564 \times 10^{-3} \\ 0 \end{bmatrix}, \quad C = I \quad (A-4)$$

For the case of the integration of disturbance prediction in the AMPC algorithm, a sampling time of $T_s = 60s$, then the evaluation of the matrix expression of Eqn. (A-2) using the values given in Table D-3, it results in Eqn. (A-5):

$$\begin{bmatrix} SOC(k+1) \\ LOH(k+1) \end{bmatrix} = \begin{bmatrix} SOC(k) \\ LOH(k) \end{bmatrix} + \begin{bmatrix} 93.67 \times 10^{-3} & 93.67 \times 10^{-3} \\ -348 \times 10^{-3} & 0 \end{bmatrix} \begin{bmatrix} P_{H_2}(k) \\ P_{grid}(k) \end{bmatrix} + \begin{bmatrix} 93.67 \times 10^{-3} \\ 0 \end{bmatrix} d(k) \quad (A-5)$$

Consequently, the system matrices admit expressions as:

$$A = I, \quad B = \begin{bmatrix} 93.67 \times 10^{-3} & 93.67 \times 10^{-3} \\ -348 \times 10^{-3} & 0 \end{bmatrix}, \quad B_d = \begin{bmatrix} 93.67 \times 10^{-3} \\ 0 \end{bmatrix}, \quad C = I \quad (A-6)$$

During the micro-grid operation with hybrid energy storage (lithium and li-ion batteries), a new state variable is incorporated, $SOC_1(t)$, corresponding to the new li-ion battery, so the state vector is given by:

$$x(t) = [SOC_1(t) \quad SOC_2(t) \quad LOH(t)]^T \quad (A-7)$$

And the manipulated variables are given as:

$$u(t) = [P_{fc}(t) \quad P_{grid}(t) \quad P_{bat2}(t)]^T \quad (A-8)$$

The disturbance is similar to the preceding case:

$$d(t) = P_{gen}(t) - P_{load}(t) \quad (A-9)$$

This battery's SOC is constrained between 35 and 80%, with a maximum load/discharge capacity limited to 3000 W. The control-oriented model is given in this case as:

$$SOC_1(t+1) = SOC(t) - \frac{\eta_{bat1}T_s}{C_{1max}}(-P_{fc}(t) - P_{grid}(t) - d(t)) \quad (A-10)$$

$$LOH(t+1) = LOH(t) - \frac{T_s}{\eta_{fc}V_{max}}P_{fc}(t) \quad (A-11)$$

$$SOC_2(t+1) = SOC_2(t) - \frac{\eta_{bat2}T_s}{C_{2max}}P_{bat2}(t) \quad (A-12)$$

Then, for a sampling time of $T_s = 30s$, the model in matrix form is given as:

$$\begin{bmatrix} SOC_1(t+1) \\ LOH(t+1) \\ SOC_2(t+1) \end{bmatrix} = \begin{bmatrix} SOC_1(t) \\ LOH(t) \\ SOC_2(t) \end{bmatrix} + \begin{bmatrix} \frac{\eta_{bat1}T_s}{C_{1max}} & \frac{\eta_{bat1}T_s}{C_{1max}} & \frac{\eta_{bat1}T_s}{C_{1max}} \\ -\frac{T_s}{\eta_{fc}V_{max}} & 0 & 0 \\ 0 & 0 & \frac{\eta_{bat2}T_s}{C_{2max}} \end{bmatrix} \begin{bmatrix} P_{fc}(t) \\ P_{grid}(t) \\ P_{bat2}(t) \end{bmatrix} + \begin{bmatrix} \frac{\eta_{bat1}T_s}{C_{1max}} \\ 0 \end{bmatrix} d(t) \quad (A-13)$$

Discretizing the overall continuous structure defined by Equation (A-13), the model in matrix form obtained for discrete-time is as follows:

$$\begin{bmatrix} SOC_1(k+1) \\ LOH(k+1) \\ SOC_2(k+1) \end{bmatrix} = \begin{bmatrix} SOC_1(k) \\ LOH(k) \\ SOC_2(k) \end{bmatrix} + \begin{bmatrix} \frac{\eta_{bat1}T_s}{C_{1max}} & \frac{\eta_{bat1}T_s}{C_{1max}} & \frac{\eta_{bat1}T_s}{C_{1max}} \\ -\frac{T_s}{\eta_{fc}V_{max}} & 0 & 0 \\ 0 & 0 & \frac{\eta_{bat2}T_s}{C_{2max}} \end{bmatrix} \begin{bmatrix} P_{fc}(k) \\ P_{grid}(k) \\ P_{bat2}(k) \end{bmatrix} + \begin{bmatrix} \frac{\eta_{bat1}T_s}{C_{1max}} \\ 0 \end{bmatrix} d(k) \quad (A-14)$$

Evaluating the Matrix expression of Eqn. (A-14), it results in Eqn. (A-15):

$$\begin{bmatrix} SOC_1(k+1) \\ LOH(k+1) \\ SOC_2(k+1) \end{bmatrix} = \begin{bmatrix} SOC_1(k) \\ LOH(k) \\ SOC_2(k) \end{bmatrix} + \begin{bmatrix} 46.87 \times 10^{-3} & 46.87 \times 10^{-3} & 46.87 \times 10^{-3} \\ -225 \times 10^{-3} & 0 & 0 \\ 0 & 0 & -37.65 \times 10^{-3} \end{bmatrix} \begin{bmatrix} P_{fc}(k) \\ P_{grid}(k) \\ P_{bat2}(k) \end{bmatrix} + \begin{bmatrix} 46.87 \times 10^{-3} \\ 0 \\ 0 \end{bmatrix} d(k) \quad (A-15)$$

Consequently, the system matrices admit expressions as:

$$A = I, \quad B = \begin{bmatrix} 46.87 \times 10^{-3} & 46.87 \times 10^{-3} & 46.87 \times 10^{-3} \\ -225 \times 10^{-3} & 0 & 0 \\ 0 & 0 & -37.65 \times 10^{-3} \end{bmatrix}, \quad B_d = \begin{bmatrix} 46.87 \times 10^{-3} \\ 0 \\ 0 \end{bmatrix}, \quad C = I \quad (A-16)$$

Appendix B

The control-oriented model of the microgrid used in **chapter 5** of this thesis is modified by including the power demanded by the load, $P_{loadCurt-load}$, as a manipulated variable in **chapter 6** to solve EMS problem using DR technique. Then, for a sampling time of $T_s = 30s$, the model in matrix form is given as:

$$\begin{bmatrix} SOC(k+1) \\ LOH(k+1) \end{bmatrix} = \begin{bmatrix} SOC(k) \\ LOH(k) \end{bmatrix} + \begin{bmatrix} 0.046 & 0.046 & -0.046 \\ -0.169 & 0 & 0 \end{bmatrix} \begin{bmatrix} P_{H_2}(k) \\ P_{grid}(k) \\ P_{load}(k) \end{bmatrix} + \begin{bmatrix} 0.046 \\ 0 \end{bmatrix} P_{gen}(k) \quad (B-1)$$

Hence, to model the hydrogen storage dynamics, it is expedient to define the variable which is related to charging/discharging of the hydrogen storage used in **chapter 7** of this thesis:

$$z_{H_2}(t) = P_{H_2}(t) * \delta_{H_2}(t) \quad (B-2)$$

More so, different weights for purchase and sales were adopted to manage the purchase and sale of energy to the grid for the economical optimization.

$$z_{grid}(t) = P_{grid}(t) * \delta_{grid}(t) \quad (B-3)$$

Mixed logic dynamic (MLD) constraints in ref [18] were also introduced to solve the optimization problem.

It is expected that the microgrid battery has to balance the power at the bus, which needs to satisfies the power balance given in B-4:

$$P_{bat}(t) = P_{load}(t) + P_{elz}(t) - P_{fc}(t) - P_{grid}(t) - P_{gen}(t) + \sum_{i=1}^4 P_{evi}(t) \quad (B-4)$$

Where,

$$d(t) = P_{gen}(t) - P_{load}(t) \quad (B-5)$$

B-5 is the measurable disturbance. $P_{bat}(t)$ is a combination of the other variables but not a manipulated variable. Hence, the manipulated variable admits expression as:

$$u = [P_{grid} \ P_{H_2} \ P_{ev1} \ P_{ev2} \ P_{ev3} \ P_{ev4} \ P_{ev5} \ P_{ev6} \ \delta_{H_2} \ \delta_{grid} \ z_{H_2} \ z_{grid}] \quad (B-6)$$

Where the power supplied by the hydrogen storage system and the power that is charged into electric vehicle i are denoted by P_{H_2} and P_{evi} , respectively.

Hence, note that the state vector is composed of the SOC of the batteries (both for micro-grid storage and the EVs) and the LOH of the hydrogen storage:

$$x = [SOC \ LOH \ SOC_{ev1} \ SOC_{ev2} \ SOC_{ev3} \ SOC_{ev4} \ SOC_{ev5} \ SOC_{ev6}]^T \quad (B-7)$$

Therefore, the system matrices admit expressions as:

$$A = \begin{bmatrix} 1 & 0 & 0 & 0 & 0 & 0 & 0 & 0 \\ 0 & 1 & 0 & 0 & 0 & 0 & 0 & 0 \\ 0 & 0 & \epsilon_1 & 0 & 0 & 0 & 0 & 0 \\ 0 & 0 & 0 & \epsilon_2 & 0 & 0 & 0 & 0 \\ 0 & 0 & 0 & 0 & \epsilon_3 & 0 & 0 & 0 \\ 0 & 0 & 0 & 0 & 0 & \epsilon_4 & 0 & 0 \\ 0 & 0 & 0 & 0 & 0 & 0 & \epsilon_5 & 0 \\ 0 & 0 & 0 & 0 & 0 & 0 & 0 & \epsilon_6 \end{bmatrix} \quad B = \begin{bmatrix} \theta_1 & 0 & -\theta_1 & -\theta_1 & -\theta_1 & -\theta_1 & 0 & 0 & 0 & 0 \\ 0 & \mu_1 & 0 & 0 & 0 & 0 & 0 & 0 & \mu_2 & 0 \\ 0 & 0 & \tau_1 & 0 & 0 & 0 & 0 & 0 & 0 & 0 \\ 0 & 0 & 0 & \tau_2 & 0 & 0 & 0 & 0 & 0 & 0 \\ 0 & 0 & 0 & 0 & \tau_3 & 0 & 0 & 0 & 0 & 0 \\ 0 & 0 & 0 & 0 & 0 & \tau_4 & 0 & 0 & 0 & 0 \\ 0 & 0 & 0 & 0 & 0 & 0 & \tau_5 & 0 & 0 & 0 \\ 0 & 0 & 0 & 0 & 0 & 0 & 0 & \tau_6 & 0 & 0 \end{bmatrix}$$

$$B_d = \begin{bmatrix} \theta_1 \\ 0 \\ 0 \\ 0 \\ 0 \\ 0 \\ 0 \\ 0 \end{bmatrix}, \quad \theta_1 = \frac{\eta_{bat} T_s}{C_{max}}, \mu_1 = \frac{\eta_{elz} T_s}{V_{max}}, \mu_2 = \frac{\left(\frac{1}{\eta_{fc}} - \eta_{elz}\right)}{V_{max}}, \tau_i = \frac{\eta_{Bevi} T_s}{C_{max}^i} \quad (\text{B-8})$$

Where η is the charging/discharging efficiency of the storage unit, V_{max} and C_{max} are the maximum storage capacities, and T_s is the sampling time.

Appendix C

The state-space models of the stand-alone micro-grid system used in **chapter 8** are presented in this section. The state vector $x(t)$, the control vector $u(t)$, the disturbance vector $u_1(t)$ and the system output vector $y(t)$ are defined as follows:

$$x(t) = \begin{bmatrix} \Delta F_1(t) & \Delta F_2(t) & \Delta P_1(t) & \Delta P_{fc1}(t) & \Delta P_{f_{inv1}}(t) & \Delta P_{f_{ult1}}(t) \\ \Delta P_{bat1}(t) & \Delta P_{PV1}(t) & \Delta P_2(t) & \Delta P_3(t) & \Delta P_4(t) & \Delta P_{tie}(t) \end{bmatrix}^T \quad (\text{C-1})$$

$$u(t) = [\Delta P_{C1}(t) \quad \Delta P_{C2}(t)]^T, \quad (\text{C-2})$$

$$u_1(t) = [\Delta P_{L1}(t) \quad \Delta P_{L2}(t) \quad \Delta P_{L3}(t)]^T \quad (\text{C-3})$$

$$y(t) = [ACE_1(t) \quad ACE_2(t)]^T \quad (\text{C-4})$$

The following set of equations express the state-space model of the two-area interconnected power system with renewable generation sources (autonomous micro-grid):

$$\frac{dx(t)}{dt} = Ax(t) + Bu(t) + B_1 u_1(t), \quad (\text{C-5})$$

$$y(t) = Cx(t) + Du(t) \quad (\text{C-6})$$

Where A , B , B_1 , and C are the parameter matrices of $x(t)$, $u(t)$, $u_1(t)$, and $y(t)$, respectively. The discrete-time space model of Eqn. (C-5) is obtained mainly by discretization with sample time T_s , which is given by the following equation:

$$x(k+1) = A_d x(k) + B_d u(k) + B_{1d} u_1(k) \quad (\text{C-7})$$

$$y(k) = Cx(k) + Du(k) \quad (C-8)$$

Where $x(k+1)$, $x(k)$, $u(k)$, $u_1(k)$, and $y(k)$ are the discrete-time forms of $dx(t)/dt$, $x(t)$, $u(t)$, $u_1(t)$, and $y(t)$, respectively, $A_d = e^{AT_s}$, $B_d = \int_0^{T_s} e^{At} B dt$, $B_{1d} = \int_0^{T_s} e^{At} B_1 dt$. The incremental form of Eqns. (C-7) and (C-8) are expressed as follows:

$$\Delta x(k+1) = A_d \Delta x(k) + B_d \Delta u(k) + B_{1d} \Delta u_1(k) \quad (C-9)$$

$$\Delta y(k) = C \Delta x(k) + D \Delta u(k) \quad (C-10)$$

Where $\Delta x(k+1)$, $\Delta x(k)$, $\Delta u(k)$, $\Delta u_1(k)$ and $\Delta y(k)$ are the incremental forms of $x(k+1)$, $x(k)$, $u(k)$, $u_1(k)$, and $y(k)$, respectively.

The matrix's forms of the system model of Figure 8-2 admit expressions as:

$$A = \begin{bmatrix} \frac{D}{2H} & 0 & 0 & 0 & 0 & \frac{1}{2H} & -\frac{1}{2H} & 0 & 0 & 0 & \frac{1}{2H} & 0 \\ 0 & -\frac{1}{T_{P2}} & 0 & 0 & 0 & 0 & 0 & 0 & 0 & 0 & \frac{K_{P2}}{T_{P2}} & \frac{K_{P2}}{T_{P2}} \\ 0 & 0 & -a & 0 & 0 & 0 & 0 & 0 & 0 & 0 & 0 & 0 \\ 0 & 0 & 0 & -\frac{1}{T_{fc1}} & 0 & 0 & 0 & 0 & 0 & 0 & 0 & 0 \\ 0 & 0 & 0 & \frac{1}{T_{inv1}} & -\frac{1}{T_{inv1}} & 0 & 0 & 0 & 0 & 0 & 0 & 0 \\ 0 & 0 & 0 & 0 & \frac{1}{T_{filt1}} & -\frac{1}{T_{filt1}} & 0 & 0 & 0 & 0 & 0 & 0 \\ \frac{1}{T_b} & 0 & 0 & 0 & 0 & 0 & -\frac{1}{T_b} & 0 & 0 & 0 & 0 & 0 \\ 0 & 0 & (b_1 - a_1) & 0 & 0 & 0 & 0 & -c_1 & 0 & 0 & 0 & 0 \\ 0 & -\frac{R}{T_g} & 0 & 0 & 0 & 0 & 0 & 0 & -\frac{1}{T_g} & 0 & 0 & 0 \\ 0 & 0 & 0 & 0 & 0 & 0 & 0 & 0 & \frac{1}{T_t} & -\frac{1}{T_t} & 0 & 0 \\ 0 & 0 & 0 & 0 & 0 & 0 & 0 & 0 & \frac{K_r T_r}{T_t T_r} & \left(\frac{1}{T_r} - \frac{K_r T_r}{T_t T_r}\right) & -\frac{1}{T_r} & 0 \\ 0 & -\frac{1}{T_{UPFC1}} & 0 & 0 & 0 & \frac{2\pi T_{12}}{T_{UPFC1}} & -\frac{2\pi T_{12}}{T_{UPFC1}} & \frac{2\pi T_{12}}{T_{UPFC1}} & 0 & 0 & 0 & -\frac{1}{T_{UPFC1}} \end{bmatrix}$$

$$B = \begin{bmatrix} 0 & 0 \\ 0 & 0 \\ K_{P1} & 0 \\ 0 & 0 \\ 0 & 0 \\ 0 & 0 \\ 0 & 0 \\ 0 & 0 \\ K_{P1} & 0 \\ 0 & \frac{1}{T_g} \\ 0 & 0 \\ 0 & 0 \\ 0 & 0 \end{bmatrix}, \quad B_1 = \begin{bmatrix} -\frac{1}{2H} & 0 & 0 \\ 0 & -\frac{K_{P2}}{T_{P2}} & 0 \\ 0 & 0 & 0 \\ 0 & 0 & 0 \\ 0 & 0 & 0 \\ 0 & 0 & 0 \\ 0 & 0 & 0 \\ 0 & 0 & 0 \\ 0 & 0 & 0 \\ 0 & 0 & \frac{1}{T_g} \\ 0 & 0 & 0 \\ 0 & 0 & 0 \\ -\frac{2\pi T_{12}}{T_{UPFC1}} & 0 & 0 \end{bmatrix}, \quad C = \begin{bmatrix} 0 & 0 & 0 & 0 & 0 & 0 & 0 & 0 & 0 & 0 & 0 & -\frac{1}{T_{UPFC1}} \\ 0 & 0 & 0 & 0 & 0 & 0 & 0 & 0 & B & 0 & 0 & \frac{1}{T_{UPFC1}} \end{bmatrix}, \quad D = 0$$

Appendix D

Table D-1: System parameters used in chapter 4

Parameters	Values	Parameters	Values
Boltzmann constant, K	$1.38e^{-23} J/K$	Emissivity of the ground, ε_{grad}	0.95
Planck constant, h	$6.62617e^{-34} J.s$	Emissivity of the module, ε_m	0.94
Light speed, c	$3e8 m/s$	Open circuit voltage, V_{oc}	2.084 V
Electron charge, q	$1.60218e^{-19} J$	Short circuit current, I_{sc}	4.28 A
Area of cell, A_j	$148.25 cm^2$	Ideality factors, N_1, N_2	1.3812, 2.311
Number of cells in series, M	4	Series resistance, R_s	0.0377 Ω
Area of the PV module, A	$655.36 cm^2$	Short circuit voltage coefficient, K_v	$-123mV/^{\circ}C$
Tilt angle, $\beta_{surface}$	65°	Reference temperature, T_{mr}	$69.5^{\circ}C$
Stefan Boltzmann, σ	$5.669 \times 10^{-8} W / m^2 k^4$	Parallel resistance, R_p	2.630 Ω
Emissivity of the sky, ε_{sky}	0.95	Energy Bandgap, E_g	1.12
Reverse saturation current, I_{01}	$7.0125 \times 10^{-8} A$	Cell internal quantum efficiency, IQE	0.69005
Open circuit current coefficient, K_i	$3.18 mA/^{\circ}C$	Reverse saturation current, I_{02}	$2.1038 \times 10^{-3} A$

Table D-2: System parameters used in case 2 of chapter 4

Parameters	Values	Parameters	Values
δ_{ss}	0.04 %/hr	I_{sc}	8.21 A
η_{chrg}, η_{dis}	0.9	I_{mp}	55 A
τ_{ss}	0.1 sec	I_{pv}	8.23A
τ_d	0.3 sec	V_{mp}	250 V
$[E_{ss}^{min}, E_{ss}^{max}]$	[400, 800]kWh	V_{oc}	32.9 V
$[P_{ss}^{min}, P_{ss}^{max}]$	[-200, 200]kW	K_i	3.18mA/ $^{\circ}C$
$[P_d^{min}, P_d^{max}]$	[0, 150]kW	K_v	$-123mV/^{\circ}C$
N_s	30	A	1.6
R_s	0.34 Ω	R_p	168.5 Ω
Panel no	50	N_p	1
N_s	1	T_{pv}	300 $^{\circ}C$

Table D-3: Main components and the micro-grid characteristics used in chapter 5, 6 and 7

Datasheet and the estimated parameters of the two-diode model of the Photovoltaic system [Kyocera KG200GT].			
Parameters	Values	Parameters	Values
Panel peak power P_{mpp}	13.8 kW	I_{mp}, I_{sc}, I_{pv}	55 A, 8.21 A, 8.23 A, respectively
Efficiency	20%	K_i, K_v	$3.18mA/^{\circ}C, -123mV/^{\circ}C$ respectively
N_s, A_1, A_2	30, 1.6, 2.53	R_s, R_p	$0.34\Omega, 168.5\Omega$, respectively
Panel number	36	I_{O1}, I_{O2}	$7.012 \times 10^{-4} A, 2.103 \times 10^{-3} A$
V_{mp}, V_{oc}	250 V, 32.9 V	N_p, N_s, T_{pv}	1, 1, $300^{\circ}C$, respectively
The wind turbine system parameters and specifications			
Parameters	Values	Parameters	Values
Rated power	15 kW	Rated wind speed	12 m/s
Rated rotor speed	27.54 Rad/sec	Air density	$1.225 Kg/m^3$
Blade pitch angle	0°	Rotor diameter	3 m
Hub height	5.8 m	Configuration	3 blades, vertical axis
C_p	10	R	0.003873 m
Fuel Cell		Electrolyser	
Nominal power	1.5 KW	H_2 Net production rate	$1.05 Nm^3/h$
H_2 rated consumption	20 NI/min	Nominal power	1 KW
Nominal voltage	48 V	Number of cells	20
Nominal current	115 A	E_{elz}^0, K_{in}, PH_2	$1.25V, -0.9e^{-3}, 6.9$, respectively
$V_{fc,0}^{cell}, K_{1,act}$	0.93, 0.00295	PO_2, A_{elz} ,	$2.4, 212.35 cm^2$, respectively
$K_{2,act}, R_{ohm}$	0.0127, 0.292	$i_{a0,elz}, i_{c0,elz}$	$1.063e^{-6}, 1.0e^{-3} A/cm^2$, resp.
$K_{1,fc}^{conc}, K_{2,fc}^{conc}$	0.0284, 8.004	$T_{elz}^0, N_{elz}^{cell}, P_{elz}$	298K, 6, 3000W, respectively
$T_{fc}(t), T_{fc}^0$	296, 296 K		
A_{eff}, N_{fc}, I_{fc}	$65cm^2, 60, 100A$		
Batteries		Metal hydride tank	
Nominal voltage	12 V	Number	4
Rated capacity	270 Ah	Volume/tank	$7 Nm^3$ (storage capacity)
C_{max}, R_{Ω}	17.8 kWh, 0.08	Max. operating pressure	5 bar
Max. charge current	50 A	Ultracapacitor	
K_{bt}, A_{bt}	0.006215, 11.05 V	η_{ch}	0.97
$V_{bt,0}, C_{max,bt}$	52.56 V, 368 Ah	η_{ch}	0.99
B_{bt}	$2453 Ah_{-1}$		
Electronic power source		Electronic load (Critical and Curtailable)	

Rated supply	10 KW	Rated power	2.5 KW
Channel	2	Channel	2

Table D-4: Constraints imposed on the energy resources for safe operation used in chapter 5, 6 and 7

Variables	Power (W) $P_i^{min} \leq P_i(t) \leq P_i^{max}$	Power slew rate (W/s) $\Delta P_i^{min} \leq \Delta P_i(t) \leq \Delta P_i^{max}$	State of Charge (%) $SOC^{min} \leq SOC(t) \leq SOC^{max}$
Generation	0 - 6000	-2500 - 6000	-
Grid	0 - 2500	-1000 - 1000	-
Fuel cell	100 - 1200	-20 - 20	-
Electrolyser	100 - 900	-20 - 20	-
H_2 Storage	-	-	10 - 19
Battery	0 - 2500	$(-4.13 - 4.16)10^{-3}$	40 - 75

Table D-5: Weight values imposed on the multi-objective function to be solved by AMPC control Algorithm used in chapter 5, 6 and 7

Algorithm	Parameter Settings				
AMPC Control Algorithm	Power variables weights	α_1	α_2	α_3	α_4
		5×10^{-3}	5×10^{-3}	8×10^{-3}	100
	Power rate weights	β_1	β_2	β_3	β_4
		4	1.5	1×10^{-4}	1×10^{-4}
	Storage level weights	γ_1		γ_1	
		10		60	
	Time horizon N_p	60			
Control horizon N_c	2				
Sample time T_s	60 sec				
Conversion coefficients (Mean-Values)	Case 1	K_{bat1}	K_{elz1}	K_{fc1}	
		1.053×10^{-3}	3.205×10^{-3}	8.024×10^{-3}	
	Case 2	K_{bat2}	K_{fc2}	K_{H2}	
		1.245×10^{-3}	7.108×10^{-3}	-5.56×10^{-3}	

Table D-6: System model parameters used in chapter 8

Parameter	Value	Parameter	Value
T_g	0.08 sec	K_t	1 Hz/p. uMW
T_{12}	0.545 p. u	K_r	1 Hz/p. uMW
T_p	20 sec	B	0.08 p. uMW/Hz
T_t	0.3 sec	R	0.4 Hz/p. uMW
T_r	10 sec	K_{r1}	0.33 p. uMW

K_{P2}	120 Hz/p.uMW	a_1	99.5
K_g	1 Hz/p.uMW	b_1	-50
c_1	0.5	K_{P1}	-18
$2H$	0.1667sec	D	0.015p.u.MW/Hz
T_{fc}	0.26 sec	T_{inv}	0.04 sec
T_{fitt}	0.004 sec	T_b	0.1 sec

Table D-7: Characteristics of each battery types used in this research work [236].

Characteristics	Lead-Acid	Lithium-ion
Energy Density (Wh/L)	54 – 59	250–360
Specific Energy (Wh/kg)	30–40	110–175
Depth of Discharge (DOD)	50%	80%
Temperature Range of Charge	-40°C – 27°C	-20°C – 55°C
Efficiency	75%	97%
Replacement Timeframe (Year)	1.5 – 2	5 – 7
Maintenance Cost	SLA = 2%, VRLA = 10%	None
Battery Cost (\$/kWh)	120 (3,840baht)	600 (19,200baht)

Table D-8: Charging station management algorithms used in the EV integration

Charging Station Management Algorithm	
01	Input: $T_a, T_p, Ch_T, \epsilon, \text{Time}$
02	Output: $Q_x, Q_{Nf}, P_{Bev}^{max}$
03	For $i=1$ to N_{ev} do
04	If $\epsilon(i) = 1$ {Test if there is a parked vehicle} then
05	If $Ch_T(i) = 1$ {Fast Charge} then
06	If $\text{Time} \geq T_a + T_p - 30 \text{ minutes}$ then
07	Set $Q_x(i, i)$ to the fast charge value
08	Set $Q_{Nf}(i, i)$ to the fast charge value
09	Set P_{Bev}^{max} to the fast charge value
10	else {Use the battery as a grid storage}
11	Set $Q_x(i, i)$ to zero
12	Set $Q_{Nf}(i, i)$ to zero
13	end if
14	else {Slow Charge}
15	Set $Q_x(i, i)$ to the slow charge value
16	Set $Q_{Nf}(i, i)$ to the slow charge value
17	Set P_{Bev}^{max} to the slow charge value
18	end if

19 **end if**
20 **end for**

Manuscripts Acceptance Letters from ISI/SCOPUS/DoHET Accredited Journals

Journal 1:

IEEE Access - Decision on Manuscript ID Access-2020-39855

Yahoo/Inbox

IEEE Access <onbehalf@manuscriptcentral.com>

To: perosman4real1987@yahoo.com

Cc: hqzhao@home.swjtu.edu.cn, 217071302@stu.ukzn.ac.za, saha@stu.ukzn.ac.za

Tue, Sep 1, 2020 at 3:32 AM

31-Aug-2020

Dear Mr. GBADEGA:

Your manuscript entitled "Impact of Incorporating Disturbance Prediction on the Performance of Energy Management Systems in Micro-grid" has been accepted for publication in IEEE Access. The comments of the reviewers who reviewed your manuscript are included at the foot of this letter. We ask that you make changes to your manuscript based on those comments, before uploading final files.

However, NO CHANGES to the author list or the references will be permitted.

Finally, please improve the English grammar and check spelling, as it is only lightly edited before publication.

Once you have updated your article accordingly, please send all final versions of your files through the "Awaiting Final Files" queue in your Author Center on ScholarOne Manuscripts. Once you have completed the submission of your final files, you will not be able to make changes until you have received your page proofs from IEEE.

When submitting final files, you must submit all of the items in the list below. All files intended for publication need to be submitted during this step, even if some files are unchanged from initial submission. If you do not submit all files during this step, it will delay the publication of your article, or result in certain files not being published.

- 1) Manuscript in MS Word or LaTeX.
- 2) A PDF of the final manuscript in double column, single-spaced format named "FINAL Article.pdf".
- 3) Biographies and author photos in MS Word.
- 4) Figures/photos saved as separate PDF, Word, .eps, .ps, or .tiff files (if not embedded in the source file)
- 5) Video(s) included in peer review (if any)
- 6) A Graphical Abstract (GA) which provides a concise, visual summary of the findings of your article. The GA should be a figure or image from the accepted article. If you submitted a video with your article, the video will automatically become the GA and you will need to supply a still image to act as an overlay. For more information on the GA, please visit <https://ieeaccess.ieee.org/submitting-an-article/>
- 7) A Word file that indicates: a) the file name(s) of the GA and overlay (if applicable), b) a caption for the GA that should not exceed 60 words.

Copyright Information / APC instructions:

After you submit final files you will automatically be directed to the Electronic Copyright Form. Once the copyright information is completed, within a few business days you will receive an email from Copyright Clearance Center (CCC) to settle your balance by check, credit card, or wire transfer. If you need assistance with the site or payment process, please contact CCC Customer Service at IEEESupport@copyright.com.

Thank you for your fine contribution. On behalf of the Editors of IEEE Access, we look forward to your continued contributions to IEEE Access.

Sincerely,

Prof. Haiquan Zhao

Associate Editor, IEEE Access

hqzhao@home.swjtu.edu.cn

Reviewer(s)' Comments to Author:

Reviewer: 1

Recommendation: Accept (minor edits)

Comments:

Authors made necessary changes and the revised manuscript has been improved

Additional Questions:

Does the paper contribute to the body of knowledge?: yes- to a great extent

Is the paper technically sound?: yes

Is the subject matter presented in a comprehensive manner?: it has been improved

Are the references provided applicable and sufficient?: has been updated

Reviewer: 2

Recommendation: Accept (minor edits)

Comments:

Accept.

Additional Questions:

Does the paper contribute to the body of knowledge?: YES

Is the paper technically sound?: YES

Is the subject matter presented in a comprehensive manner?: YES

Are the references provided applicable and sufficient?: YES

If you have any questions, please contact article administrator: Ms. Ritika Gupta ritika.gupta@ieee.org

16

Journal 2:

Journal of Emerging and Selected Topics in Power Electronics - Decision on Manuscript ID JESTPE-2020-05-0528.R1

Yahoo/Inbox

Journal of Emerging and Selected Topics in Power

Electronics <onbehalf@manuscriptcentral.com>

To: perosman4real1987@yahoo.com

Cc: 217071302@stu.ukzn.ac.za, saha@stu.ukzn.ac.za

Thu, Jul 16, 2020 at 8:58 AM

16-Jul-2020

Dear Mr. GBADEGA,

It is a pleasure to accept your manuscript entitled "Load Frequency Control of a Two-Area Power System with a Stand-Alone Micro-grid based on Adaptive Model Predictive Control" in its current form for publication in the Journal of Emerging and Selected Topics in Power Electronics. The comments of the reviewer(s) who reviewed your manuscript are included at the foot of this letter. At this time, you must send all final versions of your files through the "Awaiting Final Files" queue in your Author Center on Scholar-One Manuscripts for publication. Please make sure your final package is correct and complete upon submission. Once you have completed the submission of your final files you will not be able to make changes until you have received your page proofs from IEEE. You must submit a full set of final files even if there are no changes from the accepted version, since only this final set of files will be passed to the publication team.

Please submit all of the following in the list below within 3 weeks from the date of this letter. Templates and additional details about acceptable formats for final submissions can be found at http://www.ieee.org/publications_standards/publications/authors/authors_journals.html.

Please note that missing items from this list may result in a delay of publication:

- * Manuscript without underlines in MS Word or LaTeX.
- * A PDF of the entire manuscript in double column, single-spaced format.
- * Figures/photos saved as separate pdf, Word, .eps, .ps, or .tiff files if not embedded in the source file above.
- * Biographies in MS Word as well as author photos.

If your paper exceeds the maximum number of pages allowed, you will receive a bill for the payment of the extra pages. Please make the payment as soon as possible to enable JESTPE pay the IEEE for those extra pages.

Thank you for your fine contribution. On behalf of the Editors of the Journal of Emerging and Selected Topics in Power Electronics, we look forward to your continued contributions to the Journal.

Sincerely,

Dr. Grain Philip Adam (GE)

Editor, Journal of Emerging and Selected Topics in Power Electronics

grain.adam@eee.strath.ac.uk

AE Comments to Author:

Associate Editor

Comments to the Author:

The paper is now acceptable for publication.

Reviewer(s)' Comments to Author:

Journal 3:

Your paper has been accepted for publication in International Journal of Engineering Research in Africa (IJERA)

Yahoo/Inbox

JERA <9780000018410@scientific.net>

To: perosman4real1987@yahoo.com

Cc: 217071302@stu.ukzn.ac.za, saha@stu.ukzn.ac.za

Mon, Dec 2, 2019 at 4:44 PM

Dear Mr. PETER GBADEGA,

Your article «Model Predictive Controller Design of a Wavelength-based Thermo-Electrical Model of a Photovoltaic (PV) Module for Optimal Output Power. » has been preliminary accepted for publication in the «JERA». Although no further action is required, you can verify the status of your article by logging in to the publisher's website:

Please go to <https://www.scientific.net> and log in using the credentials below.

Username: XXXXXXXXX

Password: XXXXXXXXX

After you log in, please select « Author » role near the top of the screen.

If any further changes in your article become necessary you must notify and obtain a permission from an Editor via E-mail PRIOR to uploading a new version.

The final acceptance notice you will receive after publisher's internal check. Thank you very much.

Best regards,

TTP Reviewer

Journal 4:

Your paper has been accepted for publication in International Journal of Engineering Research in Africa (IJERA)

Yahoo/Inbox

JERA <9780000018410@scientific.net>

To: perosman4real1987@yahoo.com

Cc: 217071302@stu.ukzn.ac.za, saha@stu.ukzn.ac.za

Thu, Sep 3, 2020 at 5:44 PM

Dear Mr. Peter Anuoluwapo Gbadega,

Your article « Dynamic Tuning of the Controller Parameters in a Two-Area Multi-Source Power System for Optimal Load Frequency Control Performance» has been preliminary accepted for publication in the «JERA». Although no further action is required, you can verify the status of your article by logging in to the publisher's website:

Please go to <https://www.scientific.net> and log in using the credentials below.

Username: XXXXXXXXX

Password: XXXXXXXXX

After you log in, please select « Author » role near the top of the screen.

If any further changes in your article become necessary you must notify and obtain a permission from an Editor via E-mail PRIOR to uploading a new version.

The final acceptance notice you will receive after publisher's internal check. Thank you very much.

Best regards,

Dr. Lina Kieush

Managing Editor Scientific.net
